



**ENLARGED STOPPING DISTANCE TO  
IMPROVE VEHICLE DISCHARGE AT  
URBAN SIGNALISED INTERSECTIONS**

**Shuai Yang**

**B.Arch, MDes (UrbDes)**

**Submitted in fulfilment of the requirements for the degree of**

**Doctor of Philosophy**

**Civil Engineering and Built Environment School**

**Science and Engineering Faculty**

**Queensland University of Technology**

**2013**



## **Keywords**

Enlarged Stopping Distance (ESD), Urban signalised intersections, Departure model, Vehicle trajectory, Discharge pattern, Discharge headway, Driver response time, Saturation flow rate, Start-up lost time, Traffic management, Signal timing, 'Keep Clear' road making, NGSIM Peachtree Street data, Gold Coast Nerang Street data.



## Abstract

In recent years, the urbanisation process has led to huge social and economic benefits, but it has also brought significant challenges. Transportation technical problems are common in urban areas, particularly the problem of road congestion (Heanue & Salzberg, 2011). Furthermore, the escalating price of oil, the imperative to reduce greenhouse gas emissions and governments facing increasing demands for investment from all sectors have led to a great amount of research on better urban traffic management (Edwards & Smith, 2008). The development of trajectory data collection and traffic analysis techniques has enabled researchers to develop more accurate departure models for signal control improvement to facilitate traffic flow. However, there are two questions that still need investigation. First, the issue of start-up lost time which refers to the first four queuing vehicles consuming additional time beyond the saturation headway owing to reaction to the initiation of the green phase (TRB, 2010). Second, the second vehicle delay phenomenon which emphasizes the second vehicle in queue using more time than other first four queuing vehicles that cause the start-up lost time at signalised intersections.

Technically, few solutions can reduce the start-up lost time. In addition, despite Medelska noting the second vehicle delay phenomenon as far back as 1972, contemporary research that seeks to characterise vehicle departure still ignore the relation between the second vehicle delay problem and the start-up lost time problem. Consequently, these two questions still cause inefficiencies at urban signalised intersections. This highlights the need for an innovative method of dealing with the start-up lost time problem and the second vehicle delay phenomenon. Research presented in this thesis demonstrates an approach that could potentially reduce the start-up loss and also the second vehicle delay by educating drivers about the concept of the Enlarged Stopping Distance (ESD). This research collects data at two intersections on Nerang Street (Gold Coast ) to generate vehicle trajectories as a means of better understanding the second vehicle delay phenomenon. Through the collection and analysis of further data from the American Next Generation

Simulation program - Peachtree Street Datasets, this research separately characterises the first five leading queuing vehicles departure patterns. The limitation of the applicable queue discharge samples data causes this research to use the Intelligent Driver Model (IDM) to replicate discharge time based on the queuing position through the simulation method.

This research significantly demonstrates that ESD method creates more efficient queuing vehicle departure at signalised intersections, and therefore reduces the start-up lost time. However, there is a trade-off between the shortened start-up lost time and the enlarged leading five vehicles' storage space if we consider the application of ESD in urban areas. The simulation results show, that evenly enlarging the first five leading queuing vehicles stopping distance will optimally reduce the start-up lost time by about one second, but this requires a longer storage space for the queuing vehicles. The application of ESD between the second and the third vehicles in queue can better balance the obtained benefit with the lost storage space for the queuing vehicles. It requires a distance of 10 metres ESD between the first and the second vehicles to reduce the start-up loss by more than 0.6 seconds. Ultimately, this research provides guidelines for the implementation of the ESD and proposes further research of this concept.

# Table of Contents

Keywords .....	i
Abstract .....	iii
Table of Contents .....	v
List of Figures .....	ix
List of Tables .....	xi
List of Symbols .....	xiii
Glossary .....	xvii
Statement of Original Authorship .....	xix
Acknowledgments.....	xxi
<b>CHAPTER 1: INTRODUCTION .....</b>	<b>1</b>
1.1 Overview.....	1
1.2 Background.....	1
1.3 Research problems .....	2
1.4 Research hypothesis.....	4
1.5 Research aim and objectives .....	5
1.6 Thesis scope.....	6
1.7 Research plan .....	6
1.8 Thesis outline .....	7
<b>CHAPTER 2: LITERATURE REVIEW .....</b>	<b>9</b>
2.1 Introduction.....	9
2.2 Start-up lost time & second vehicle delay.....	9
2.2.1 Start-up lost time problem .....	9
2.2.2 Second vehicle delay phenomenon.....	10
2.3 Countdown timers .....	11
2.3.1 Different types of countdown timers .....	12
2.3.2 Real effects of the countdown timers.....	12
2.4 Signalised intersections.....	14
2.4.1 Signalised intersection development.....	14
2.4.2 Signal timing algorithm .....	15
2.4.3 Signal-controlled roundabouts .....	17
2.4.4 Case study of signal control of left turn.....	18
2.5 Driver behaviour & vehicle length.....	21
2.5.1 Human psychological elements in car following .....	21
2.5.2 Driver behaviour and traffic capacity in queue discharge .....	22
2.5.3 Vehicle length factors .....	24
2.6 Vehicle dynamic models.....	24
2.6.1 Vehicle departure model.....	25
2.6.2 Vehicle-following model .....	26
2.6.3 Vehicle clearance model.....	32

2.6.4	Micro simulation models .....	33
2.7	Various understandings of the traffic discharge problem .....	34
2.7.1	Queuing vehicle discharge.....	35
2.7.2	Innovative traffic control approaches .....	37
2.7.3	Related research.....	38
2.8	Conclusions.....	43
<b>CHAPTER 3: DATA COLLECTION .....</b>		<b>45</b>
3.1	Introduction.....	45
3.2	Nerang Data .....	45
3.2.1	Nerang data background .....	46
3.2.2	Video record preparation .....	48
3.2.3	Video recording .....	50
3.2.4	Nerang video tracking .....	51
3.2.5	Nerang data extraction.....	53
3.3	NGSIM Peachtree Data .....	59
3.3.1	NGSIM data background.....	59
3.3.2	Known issues of NGSIM data and Mitigation.....	59
3.3.3	Peachtree data extraction .....	62
3.4	Chapters' contributions.....	67
<b>CHAPTER 4: MODELLING OF VEHICLE DEPARTURE .....</b>		<b>69</b>
4.1	Introduction.....	69
4.2	Exploration of the second vehicle delay .....	69
4.2.1	Video record survey of queue discharge.....	69
4.2.2	Data analysis of second vehicle delay .....	71
4.3	Nerang discharge patterns.....	73
4.4	The 'Keep Clear' road marking effects.....	75
4.4.1	Effect on driver behaviour .....	76
4.4.2	Effect on velocity .....	79
4.5	Peachtree discharge patterns .....	80
4.5.1	Five leading vehicle average discharge pattern .....	80
4.5.2	Three categories of discharge patterns.....	82
4.6	Findings within local Data .....	85
4.7	Peachtree findings.....	87
4.8	Simulation.....	90
4.8.1	The IDM model .....	91
4.8.2	Model calibration.....	92
4.8.3	Optimization with genetic algorithm .....	93
4.8.4	Calibration results.....	94
4.9	Data synthesis and results .....	95
4.9.1	Experiment setup .....	96
4.9.2	Results .....	96
4.10	Chapters' contributions.....	98
<b>CHAPTER 5: CONCLUSIONS &amp; RECOMMENDATIONS .....</b>		<b>99</b>
5.1	Introduction.....	99
5.2	Benefits of the ESD .....	99
5.2.1	Tradeoff of the ESD .....	100



5.3	Proposed approaches for the ESD implementation .....	101
5.4	Conclusions.....	101
5.5	Recommendations for future work.....	102
<b>CITATIONS .....</b>		<b>105</b>
<b>APPENDICES .....</b>		<b>110</b>
	Appendix A: Nerang Data collection application .....	110
	Appendix B: Nerang Data collection official permission .....	111
	Appendix C: Nerang Data site I raw trajectory velocity & acceleration samples .....	111
	Appendix D: Nerang Data site II raw trajectory velocity & acceleration samples .....	125
	Appendix E: Nerang Site I data parameters .....	148
	Appendix F: Nerang Site II data parameters .....	150
	Appendix G: Nerang Data average vehicle length.....	152
	Appendix H: NGSIM Peachtree Data 21 discharge samples .....	153
	Appendix I: Peachtree Data parameters .....	158
	Appendix J: Peachtree Data raw vehicle length (m) .....	161
	Appendix K: Peachtree Data categories “Fast” “Normal” “Slow” trajectories.....	161
	Appendix L: Peachtree data original & calibration of three group trajectories.....	163
	Appendix M: The 20 <sup>th</sup> percentile Clearance & Velocity.....	165
	Appendix N: Peachtree Data velocity acceleration & clearance analysis .....	166
	Appendix O: Peachtree data five leading vehicle velocity variation with clearance .....	192
	Appendix P: Peachtree Data five leading vehicles’ time & acceleration .....	194
	Appendix Q: Peachtree Data each sample velocity & clearance .....	195
	Appendix R: Peachtree data 20 percentile safety distance.....	201
	Appendix S: Peachtree Data median safety distance .....	202
	Appendix T: Peachtree Data average safety distance .....	204
	Appendix U: Peachtree Data minimum safety distance .....	205



# List of Figures

Figure 1: Recorded by Shuai YANG on 21 August, 2008, Southbank, Brisbane .....	3
Figure 2: Recorded by Shuai YANG on 16 November 2010, Southbank, Brisbane .....	3
Figure 3: (A) Normal discharge and (B) Hypothesis of Enlarged Stopping Distance discharge .....	5
Figure 4: Dowling College, New York: A prototype CFI was built at a T intersection <a href="http://teexwebtest.tamu.edu/eu/documents/04_01-02.pdf">http://teexwebtest.tamu.edu/eu/documents/04_01-02.pdf</a> .....	19
Figure 5: The tandem intersection concept: (a) full tandem; (b) partial tandem; (c) general case. ....	20
Figure 6: Scattered Points of Speed Difference and Time Headway .....	39
Figure 7: Scattered Points of Speed Difference and Headway Distance .....	39
Figure 8: Gamma distribution for desired time gap ( $T_x$ ) .....	40
Figure 9: Lognormal Distribution for Time Headway (T) .....	40
Figure 10: Development of professional driver adjustment factors for the capacity analysis of signalised intersections .....	41
Figure 11: Crossing Stop Line Headway Analysis (Kobari Intersection) Drawn by Shuai YANG .....	42
Figure 12: Nerang study area schematic .....	47
Figure 13: Nerang site map measurement and equipment .....	49
Figure 14: Super high tripod and battery supported ground monitor .....	49
Figure 15: Nerang study area and camera recorder coverage.....	50
Figure 16: Sample frames from Nerang each site video sequences .....	51
Figure 17: Nerang data camcorder recording signal timing and traffic flow .....	51
Figure 18: Expectations of the Nerang Data extraction .....	53
Figure 19: Nerang Site I; 18 sets of vehicle trajectory samples .....	54
Figure 20: Nerang Site II; 31 sets of vehicle trajectory samples .....	55
Figure 21: Nerang Site I and Site II raw average trajectories.....	56
Figure 22: Limitation of the Nerang Data .....	57
Figure 23: Error sequence sample .....	60
Figure 24: Using AutoCAD to test the data accuracy .....	61
Figure 25: Time-Space graph sample 04.....	65
Figure 26: Peachtree Data; 21 sets of vehicle trajectory samples .....	66
Figure 27: Relationship $z_i$ & $k_i$ with $h_i$ .....	71
Figure 28: Nerang data raw average five leading vehicle discharge patterns.....	73
Figure 29: Nerang Data II clips .....	76
Figure 30: “Keep Clear” effects on drivers’ “catching up” .....	77
Figure 31: Comparative analysis of Nerang Data Site I and Site II .....	79
Figure 32: Peachtree data average five leading cars discharge patterns.....	81
Figure 33: Driver response time relative to stopping spacing .....	86

Figure 34: Response time of drivers in different positions in the queue at Nerang I - without 'keep clear' .....	86
Figure 35: Response time of drivers in different queue positions at Nerang II - with 'keep clear'.....	87
Figure 36: Example of trajectories with automatically identified times of starting and reaching free flow speed .....	88
Figure 37: Relative time to free flow depending on queue position and distance .....	88
Figure 38: Regression tree considering the first vehicle's speed and spacing between first and second vehicle. The predicted time to free flow is reported on the leaves of the tree. ....	89
Figure 39: Regression tree considering additionally the second vehicles discharge speed and spacing of the second and third vehicle .....	90
Figure 40: Relative response time depending on the queue position .....	91
Figure 41: Screenshot of simulated results, using the IDM car following model .....	91
Figure 42: Comparison of relative discharge speed between real data and simulation. (a) Box plot generated from the observed Peachtree data. (b) Results from the IDM trajectories produced by the numerically optimum solution, in which the parameter $a$ is close to 2. (c) Results from the IDM model, whose parameters are identical to that of (b), except for the decreased acceleration factor, $a=1$ . ....	95
Figure 43: Simulation results showing plots for evenly spaced vehicles, and for platoons with increased spacing between certain cars .....	97
Figure 44: Minimal discharge times with different platoon structures .....	97
Figure 46: Capacity increase by green phase time for different start up lost .....	100
Figure 47: (A) Normal discharge and (B) Enlarged Stopping Distance discharge .....	102

# List of Tables

Table 1: Effects of the countdown times .....	13
Table 2: Summary of optimal parameter combinations for the GHR equations* .....	27
Table 3: Most reliable estimates of parameters within the GHR model <sup>a</sup> .....	28
Table 4: Summary of optimal combinations for the Helly equation <sup>a</sup> .....	30
Table 5: Nerang Data collection timeline.....	47
Table 6: Video record survey of the second vehicle delay phenomenon .....	70
Table 7: Peachtree Street data set yield time $z_i$ & $k_i$ .....	72
Table 8: Two methods to obtain the time of vehicles crossing the stop line .....	74
Table 9: Nerang Site I data average five leading vehicle discharge patterns .....	75
Table 10: Nerang Site II data average five leading vehicle discharge patterns .....	75
Table 11: Peachtree data average five leading vehicle discharge patterns .....	81
Table 12: Categorisation of trajectories .....	82
Table 13: Peachtree data “Fast” group average five leading vehicle discharge patterns.....	83
Table 14: Peachtree data “Normal” group average five leading vehicle discharge patterns .....	84
Table 15: Peachtree data “Slow” group average five leading vehicle discharge patterns .....	84
Table 16: Numerically optimum parameter set .....	94



## List of Symbols

$a_i$	Deceleration of the driver
$a_n$	The acceleration of vehicle $n$ implemented at time $t$
$c$	Clearance, m; cycle times, s
$c_0$	Approximate optimum cycle time, s
$d_a$	Acceleration delay, s
$D_p$	Preferred following distance, m
$D_{(t)}$	Desired following distance, m
$E_s$	Enlarged stopping distance, m
ESD	Enlarged Stopping Distance, m
$F_i$	Change time for the $i$ th phase
$g$	Effective green time, s
$h$	Saturation headway, s
$h_d$	Headway, s
$H_{D_i^{(w)}}$	The membership function of consequent $D_i$ after the input is given
$h_s$	Queue discharge (saturation) headway, s
$h_n$	Minimum queue discharge headway, s
$k$	Stop penalty parameter
$L$	Intersection lost time, s
$l$	Inter-green time of phase; lost time for the movement in question
$l_a$	the A vehicle length, m
$l_h$	the spacing of the A and B at time $T_{rb}$ , m
$l_{h-l}$	the spacing of the A and B at time $T_{ra}$ , m
$L_h$	Spacing, m
$L_{hj}$	Queue space per vehicle (jam spacing), m
$L_{hs}$	Vehicle spacing, m/veh
$L_p$	Detection zone length, m
$L_v$	Average vehicle length, m
$L_v$	Vehicle length, m
$m_v$	A parameter in the queue discharge model
$m_q$	A parameter in the queue discharge flow rate model

$n_s$ .....	Cumulative queue discharge flow at time t
$Q$ .....	Traffic stream capacity, veh/h
$q_s$ .....	Queue discharge flow rate at time t, veh/h
$q_n$ .....	Maximum queue discharge flow rate, veh/h
$Rs$ .....	Revised spacing portion, m
$S$ .....	Saturation flow rate, veh/h
$s$ .....	Saturation flow rate, veh/h
$S_{dab}$ .....	safety distance that B's driver perceived from $V_a$ , m
$S_{tab}$ .....	the A and B vehicles' stopping distance, m
$Sv$ .....	Platoon speed of queuing vehicles in departure process, m/s
$T$ .....	Driver response time, s; time lag of the car K with (K+1), also as reaction time
$T_{ra}$ .....	the A's driver response time, s
$T_{rb}$ .....	the B's driver response time, s
$t$ .....	Time since the start of the display green period, s; Duration of analysis period, s
$t_c$ .....	Gap, s
$t_f$ .....	Follow-up headway, s
$t_{os}$ .....	Occupancy time, s
$t_p$ .....	Time headway, s
$t_r$ .....	Start response time, s
$t_s$ .....	Start loss, s
$t_{ss}$ .....	Space time, s
$U$ .....	Intersection green time ratio
$u$ .....	Movement; green time ratio
$V_a$ .....	the A's velocity at the time when the B's driver make response to move forward, m/s
$V_s$ .....	Saturation speed, m/s
$v$ .....	Speed of the $n^{\text{th}}$ vehicle at time t
$v_i$ .....	Speed of the driver's vehicle, m/s
$v_s$ .....	Queue discharge speed at time t, km/h
$v_x$ .....	Queue clearance wave speed, m/s
$Y$ .....	Intersection flow ratio
$\Delta x$ .....	Relative spacing



$\Delta v$ ..... Relative speeds  
 $\varepsilon$ ..... Random error term



## Glossary

Clearance - The distance between the rear bumper of the leading vehicle and the front bumper of the following vehicle. The clearance is equivalent to the spacing minus the length of the leading vehicle (AECPortico, August 2003).

ESD - The hypothesis of this research which assumes that an enlarged stopping distance between the lead vehicle and the successive vehicle could shorten the start-up lost time.

Gap - The space or time between two vehicles, measured from rear bumper of the front vehicle to the front bumper of the second vehicle (TRB, 2010).

Headway - The time between two successive vehicles as they pass a point on the roadway, measured from the same common feature of both vehicles (TRB, 2010).

Spacing - The distance between two successive vehicles in a traffic lane, measured from the same common feature of the vehicles (TRB, 2010).

Start-up Lost Time - The additional time consumed by the first few vehicles in a queue at a signalised intersection above and beyond the saturation headway because of the need to react to the initiation of the green phase and to accelerate (TRB, 2010).



## Statement of Original Authorship

The work contained in this thesis has not been previously submitted to meet requirements for an award at this or any other higher education institution. To the best of my knowledge and belief, the thesis contains no material previously published or written by another person except where due reference is made.

Signature:

A handwritten signature in black ink, appearing to be 'J. J. J.', written in a cursive style.

Date: 12 June 2013



## **Acknowledgments**

I am grateful to my parents, my wife Yi Yang, and my loving children Hansen and Kailin. I am also heartily thankful to my principal supervisor Edward Chung, whose encouragement, guidance and support from the initial to the final stages enabled me to develop an understanding of the Enlarged Stopping Distance. I would like to show my gratitude to my associate supervisors Marc Philipp Miska and Glen D'este, and to the Research Portfolio officers Elaine Reyes and Professor Kunle Oloyede. This thesis would not have been completed without their help.

Furthermore, I am grateful to the NGSIM Program for the availability of the Peachtree Street Data and appreciate Dr K.S.Tang's help in providing the Kobari field data for this research. I would like to thank Cho Kopong, Ashish Bhaskar, Alfredo Nantes, David Ryan, Simon Denman, Clinton Fookes and Sridha Sridharan for their help in the data collection, extraction and analysis process.

Finally, I offer my regards and blessings to all those who supported me in any respect during the completion of this project. I also thank QUT and the SEF (BEE) Faculty for the scholarships that allowed me to focus full time on this research. It is my hope that the ESD can be implemented to save people's travel time on roads. It is my wish that this work can be my thanks to Australia and its people for their help and support.





# Chapter 1: Introduction

---

## 1.1 OVERVIEW

This chapter gives a brief outline of the background to the study (Section 1.2), the research problems (Section 1.3), and the research hypothesis (Section 1.4). It then describes the research aim and objectives (Section 1.5). Subsequent sections describe the scope of this research (Section 1.6) and the research plan (Section 1.7). The thesis outline is introduced in the last section (Section 1.8).

## 1.2 BACKGROUND

Concentrated populations in urban areas have resulted in traffic congestion common to major cities around the world. Many capital cities suffer urban congestion that carries a social cost (BTRE, 2007). Innovative methods are required to develop traffic management for urban streets and intersections to ease traffic congestion problems. Worldwide research of traffic management indicates that if urban signalised intersections were made more efficient, there would be a substantial reduction in traffic congestion, with resulting benefits for the economy and environment (EPA, 2011).

Since people first used signals to control traffic at urban street intersections in 1868, traffic management has undergone enormous development (Philpot, 2005). Departure models (i.e. models describing queues departing from signalised intersections), for example, are essential tools used to characterise dynamic traffic flow performance at urban signalised intersections as they directly contribute to signal timing setup. The saturation flow rate, which is an important component of the departure model, is used to estimate lane and intersection capacity. Highway Capacity Manual 2010 (TRB, 2010) shows that start-up time is lost because it takes three to five vehicles to pass the intersection before a full saturation flow rate can be realised (see Glossary, Start-up Lost Time). If the start-up lost time at every signal phase could be reduced, it would utilise the green signal phase more efficiently. However, there are currently few solutions to reduce this lost start-up time for better

traffic flow at urban signalised intersections. Countdown timers are one effective method that is widely implemented to shorten driver's response time at signalised intersections in some countries. However, literature from some countries has reported increase of crashes especially when applied during green phase. Hence, further opportunity exists for developing initiatives to decrease start-up lost time.

In 2008, I observed the vehicle delay phenomenon at Brisbane and Melbourne urban intersections. These observations aroused my curiosity to investigate the phenomenon and to understand the factors that slow driver's response to green onset. The driver's slow response time causes a reductive in the number of queuing vehicles able to achieve saturation flow rate and consequently large start-up lost time. For this reason, it is imperative implemented to reduce driver's response time?

In 1972, Medelska found that when a signal changed to green, the second queuing vehicle needed more time because the second driver could only react after the movement of the first vehicle, and the successive vehicles in the queue kept equal intervals after the fifth vehicle (Jan et al., 2009). Although Medelska identified the second vehicle delay problem forty years ago, no research has been carried out in this area. In terms of finding acceptable solutions, particularly with respect to explore the relationship of the second vehicle delay phenomenon to the start-up lost time problem in the queuing vehicle discharge process at urban signalised intersections.

### **1.3 RESEARCH PROBLEMS**

The second vehicle delay phenomenon is a longstanding traffic problem. However, previous researchers have not widely studied this problem with negative effects on the dynamic performance of the queuing vehicle discharge process. The second vehicle delay phenomenon is illustrated in the two visual clips below; these were recorded in different years at the signalised intersection of Vulture Street and Grey Street, Southbank, Brisbane, Australia.

On 21 August 2008, the second vehicle delay phenomenon was recorded, as shown in Figure 1. Two years later, an analogous delay phenomenon was recorded at the

same place on 16 November 2010, as shown in Figure 2. This visual evidence indicates that the second vehicle delay phenomenon exists. In Figure 1, the green signal onset on the time 00:49 (see left image) and then the second vehicle starts to move on the time 00:59 (see right image). It takes 10 seconds from the onset of the green light for the rear bumper of the first white car to pass over the stop line. By contrast, the second red 4×4 SUV just reacted to the green signal and blocks the passage of the following vehicles in the queue for 10 seconds.



Figure 1: Recorded by Shuai YANG on 21 August, 2008, Southbank, Brisbane



Figure 2: Recorded by Shuai YANG on 16 November 2010, Southbank, Brisbane

In Figure 2, the first black car uses 3 seconds to cross over the stop line from its queuing position. However, the second car only moves forward a small distance. Thus, the second car lost start-up time is longer than those for leading vehicles in the queue. In short, the second vehicle delay problem is that the second queuing vehicle generally will start to accelerate a few seconds later than the first vehicle, leaving the following vehicles a relatively shorter time to respond in the queue discharge process. As a result, fewer cars discharge per green phase.

Since the second vehicle delay phenomenon occurs at every traffic signal cycle, time and fuel are wasted at signalised intersections in urban centres. For example, Australian Bureau of Statistics (1996) indicated that, “Cars are the most common form of transport in Australia. In 1992, 71% of Australians used cars on an average day. These people spent, on average, 1 hour 27 minutes per day on car travel. Transport is necessary for many basic aspects of everyday living such as shopping and working, as well as participating in community activities. The efficiency of transport systems affects daily life. Every day, people undertake millions of individual journeys. The time people spend on transport affects the amount of time they have available for other activities.” Therefore, the second vehicle delay problem needs to be addressed and explored and an effective solution found to eliminate negative effects on signalised intersection traffic flow efficiency.

#### **1.4 RESEARCH HYPOTHESIS**

Second vehicle delay phenomenon may be caused by the short stopping distance behind the lead vehicle, which inhibits the second vehicle to accelerate at the same time as the lead vehicle. Drivers need a significant clearance distance (distance between rear bumper of lead vehicle and front bumper of following vehicle) to accelerate safely. If the second driver clearance distance between the first and second vehicles obtained ideal distance, the vehicle response time should be equal. Hence, the hypothesis of this research assumes that an Enlarged Stopping Distance (ESD) between the lead vehicle and the successive vehicle could shorten the start-up lost time (see Figure 3). If successive vehicles have an ideal clearance distance in which to accelerate, it will shorten the successive vehicle’s driver response time so as to improve the start-up lost time problem. A parallel example can be drawn from motor vehicle racing such as Formula 1 Grand Prix where vehicles are kept some queuing distance apart and staggered to allow simultaneous start. If all racing drivers were positioned with no distance apart, all drivers would have to wait till their respective lead vehicle to depart before they could depart themselves.

In terms of practical applications, three approaches are proposed which may contribute to improve the start-up lost time problem by reducing leading queuing

vehicles' driver response time. Countdown timers have already been integrated with intelligent transport signal systems at some urban intersections. Furthermore, IBM has already made a substantial investment in a vehicle engine control system that can automatically respond to traffic light systems (Bristow, 2010). However, these two applications do not address the second vehicle delay problem due to the fact that countdown timers shorten the first driver's response time and the IBM method requires remodelling the vehicle engine's control system. In contrast, Enlarged Stopping Distance (ESD) may have potential to increase intersection efficiency by addressing the second vehicle delay problem and resulting in queuing vehicles obtaining ideal clearance distance.

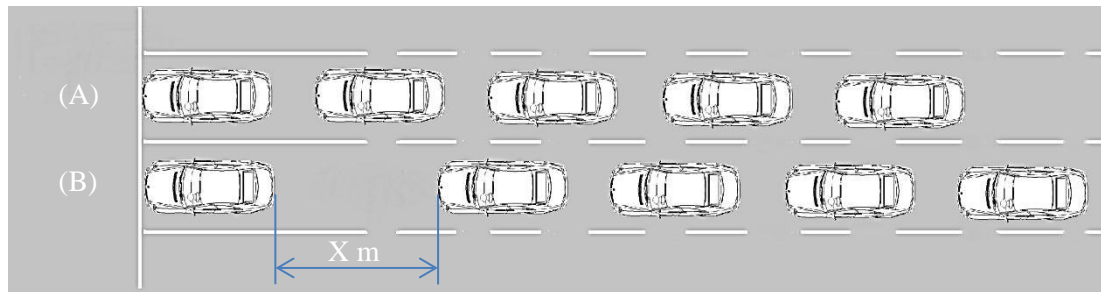


Figure 3: (A) Normal discharge and (B) Hypothesis of Enlarged Stopping Distance discharge

## 1.5 RESEARCH AIM AND OBJECTIVES

The Start-up Lost Time is one of the well-known problems in vehicle discharge process. Second vehicle delay undoubtedly appertains to the start-up lost time problem issue. This research, therefore, explores whether the second vehicle delay phenomenon exists, what factors contribute to the phenomenon, and whether ESD improves intersection performance. To that end, this research project is to addresses the following question:

### **Does ESD improve vehicle discharge start-up time?**

In order to achieve this aim, additional objectives are defined as follows:

- Objective 1: Explore the second vehicle delay phenomenon
- Objective 2: Characterise vehicle dynamic performance in discharge
- Objective 3: Create scenarios and simulate the ESD

#### Objective 4: Test the ESD hypothesis

In summary, the outcomes of this research are to demonstrate that ESD improves the start-up lost time problem and especially for the second queuing vehicle delay in urban areas.

## 1.6 THESIS SCOPE

Following the above hypothesis of the second vehicle delay, this research aims to test the hypothesis that the ESD has the potential to reduce the start-up lost time of the queuing vehicle discharge and improve the efficiency of urban signalised intersections. Therefore, this research focuses on the first five leading vehicles dynamic performance in the discharge process at urban signalised intersections because after the fifth vehicle, saturation flow rate is achieved and therefore has no impact on the start-up lost.

## 1.7 RESEARCH PLAN

This research plan adopted for this thesis can be divided into four parts:

- a) Literature review;
- b) Data collection;
- c) Data analysis; and
- d) Modelling.

The first part of this research is a comprehensive review of literature pertinent to start-up lost and driver response time at signalised intersection (see Chapter 2). To collect quantitative evidence of the second vehicle delay phenomenon, traffic surveys were conducted in Nerang, Queensland. This research also uses traffic survey data from the American Next Generation Simulation (NGSIM) program for analysis of drivers' behaviour at signalised intersection (see Chapter 3). Third part of this research analyses the data collected to give insights and to provide evidence of the second vehicle delay phenomenon. Understanding of drivers' behaviour and parameter values obtained from part three, are used to calibrate the simulation model used in this research (see Chapter 3). The calibrated simulation model (Intelligent

Driver Model) is then applied to simulate different scenarios to demonstrate the potential benefit that ESD could have on minimising start-up lost at urban signalised intersections and to determine the best ESD configuration to maximise the benefit of ESD (see Chapter 4).

## **1.8 THESIS OUTLINE**

The five chapters of this thesis are:

### Chapter 1: Introduction

This chapter includes: research background, research problems, research hypothesis, research aim and objectives, scope of this thesis, research plan and a brief outline of the thesis structure.

### Chapter 2: Literature Review

This chapter introduces research results that are related to the vehicle discharge research. Specifically, it explores the research into urban intersection signal control development, driver behaviour and vehicle dynamic models relevant. Using the ESD as a possible approach to improve the start-up lost time problem, there are few studies directly linked with this research hypothesis. However, the literature review offers some background for this research and demonstrate the value of this research.

### Chapter 3: Data Collection

To collect quantitative evidence of the second vehicle delay phenomenon, traffic surveys were conducted in Nerang, Queensland. This research also uses traffic data from the American Next Generation Simulation (NGSIM) program to analyse drivers' behaviour at signalised intersection. Raw discharge samples are obtained after finished the data collection. And also some relative parameters are extracted in this step for the further study.

### Chapter 4: Modelling of Vehicle Departure

This part of research explores the second vehicle delay phenomenon through video survey analyses. The data collected in the previous step give an insight view of the second vehicle delay phenomenon. To understand the drivers' behaviour under the

“Keep Clear” road markings condition, the discharge samples obtained from the Nerang Data are used to reveal the effects on the drivers’ behaviour changing by the “Keep Clear” road marking. The Intelligent Driver Model (IDM) is then applied to simulate different scenarios to demonstrate the potential benefit that ESD could have on minimising start-up lost at urban signalised intersections and to determine the best ESD configuration to maximise the benefit of ESD.

#### Chapter 5: Recommendations & Conclusions

The last chapter discusses how to realise the benefit of the ESD and also introduces the contribution and limitation of this research. A short recommendation for future work is mentioned and concludes this thesis.



# Chapter 2: Literature Review

---

## 2.1 INTRODUCTION

This chapter provides an overview of the current civil engineering literature on traffic management research, focusing specifically on concepts relating to the leading role of queuing vehicle dynamic performance in the discharge process at urban intersections. Section 2.2 reviews the start-up lost time and second vehicle delay. Section 2.3 introduces current research about the countdown timers' effects on vehicle discharge. Section 2.4 shows the development of approaches to the signalised control of urban intersections and explores some innovative approaches in the vehicular signal management field. Section 2.5 introduces the effects of human factors on some parameters of traffic performance analysis models. Section 2.6 reviews traditional vehicle dynamic models of departure, following, left-turn clearance, and micro simulation models. The discussion in Section 2.7 covers different theoretical perspectives such as saturation flow headway, queue discharge flow pattern and intelligent traffic control. This study seeks to address the lack of research on solutions to the start-up lost time problem at signalised intersection due to the observed second vehicle delay phenomenon.

## 2.2 START-UP LOST TIME & SECOND VEHICLE DELAY

This literature review reveals that: second vehicle delay belongs to the start-up lost time issue. However, descriptions of second vehicle headway shorter than the first vehicle in the traditional departure model (i.e. HCM 2010) assumption is contradicted by the observed second vehicle delay phenomenon. Therefore, it is necessary to confirm the second vehicle delay problem. This research not only seeks a solution for second vehicle delay but also to improve the start-up lost time problem.

### 2.2.1 Start-up lost time problem

This research begins with the conventional assumption about the departure model of the Highway Capacity Manual 2010 to review the start-up lost time problem. The

authors state that: “The driver of the first vehicle in the queue must observe the signal change to green and react to the change by releasing the break and accelerating through the intersection. As a result, the first headway will be comparatively long. The second vehicle in the queue follows a similar process, except that the reaction and acceleration period can occur while the first vehicle is beginning to move. The second vehicle will be moving faster than the first as it crosses the stop line, because it has a greater distance over which to accelerate. Its headway will generally be less than that of the first vehicle. The third and fourth vehicles follow a similar procedure, each achieving a slightly lower headway than the preceding vehicle. After four vehicles, the effect of the start-up reaction and acceleration has typically dissipated. Successive vehicles then move past the stop line at a more constant headway until the last vehicle in the original queue has passed the stop line.” (TRB, 2010)

In summary, the headway time (See Glossary, Headway) or driver response time tends to decrease from the first to the fourth vehicle and then remains constant when the delayed start-up reaction has dissipated. Therefore, saturation flow is achieved and maintained after approximately 10 seconds from green onset or after the fourth vehicle in the queue crosses the stop-line. The authors (TRB, 2010) give the definition of the start-up lost time as follows: “The additional time consumed by the first few vehicles in a queue at a signalised intersection above and beyond the saturation headway because of the need to react to the initiation of the green phase and to accelerate”.

### **2.2.2 Second vehicle delay phenomenon**

The above description summarises the leading vehicle discharge process and the start-up lost time problem in detail. However, its conclusion about the second vehicle’s headway is less than the first vehicle’s headway is contradicted by the observed second vehicle delay phenomenon. Greenshield is a respected scholar who has contributed to departure model research. In their vehicle discharge process research, Greenshield et al. (1947) indicated that the first queuing vehicle’s response time to the signal change and the response time of successive vehicles should be separately considered. In their report, the average starting response time varied from

0.63 to 2.86 seconds, with a corresponding range from 4% to 30% of drivers who participate in the signal change. Their investigation also indicated that the response time between successive vehicles ranges from 1 second to 1.75 seconds.

In contrast with the second vehicle delay phenomenon addressed in this thesis, Greenshield et al. (1947) stated that the second vehicle can start as soon as the first if the second vehicle queue position is not too close the first vehicle. Greenshield et al. (1947) explained that to achieve the (impractical) zero response time, the second driver would need to react to the green signal rather than to the movement of the first vehicle. This characterization of the second vehicle discharge process was generated based on the analysis of the field data that were collected in New Haven and Hartford, Connecticut, America in 1947. However, the departure model keeps changing as the dynamic of vehicle trajectory has already changed as a result of powerful combustion engines and automatic transmission development.

In 1972, Medelska identified the three following characteristics of vehicle departure. Firstly, the second queuing vehicle needs more time to cross because its driver could only react following the movement of the first vehicle. Secondly, successive vehicles in the row keep equal intervals after the fifth vehicle. Thirdly, during the green signal phase, vehicles cross the intersection randomly after the queuing vehicles clear (Jan, et al., 2009). These characteristics are classified as start-up lost time, saturation flow rate and end gain. The first characteristic contradicts Greenshield's conclusion (above). Significantly, however, Medelska has identified the second vehicle delay phenomenon.

### **2.3 COUNTDOWN TIMERS**

Some research indicates that countdown timers are an effective approach to shorten driver response time at signalised intersections. This section presents literature that analyses the real effects and understanding of countdown timers.

### **2.3.1 Different types of countdown timers**

In recent years, progressively more intersections have been equipped with countdown timers to assist drivers or pedestrian in perceiving the remaining time in signal time phases. A countdown timer (CDT) can work together with standard pedestrian signal heads (PSHs) to help pedestrians acknowledge the remaining time before the end of the safe walking phase, thus deploying a countermeasure to improve pedestrian safety (Brandon, 2007; Pulugurtha et al., 2010). Normally, three types of countdown timers operate in conjunction with traffic signals for drivers: timers for the green signal phase, red signal phase, or full signal cycle phase. As this thesis focuses on the second vehicle queuing discharge delay problem and the start-up lost time issue, only a subset of literature on the vehicular countdown timer is reviewed.

The green-phase countdown timer (GSCD) displays the right of way time to assist drivers in making the decision to stop or accelerate. The original purpose of the GSCD was to reduce the potential conflict caused by an approaching vehicle's red light running violations; however, current research findings even question this intention. A countdown timer that only serves the red-signal phase (RSCD) can predict the time of the red signal changing to green; however, this potentially lowers the start-up loss in queue discharge (Chiou & Chang, 2010; Long et al., 2011). Full signal cycle countdown timers are increasingly used in traffic-congested Asian cities. These devices can continuously display different signal phase timing (Limanond et al., 2010).

### **2.3.2 Real effects of the countdown timers**

From a theoretical perspective, countdown timers can potentially increase capacity and reduce right-angle crashes. However, current research findings reveal that these desired effects are not always achieved, especially with regard to safety. Furthermore, because traffic conditions and driver behaviours differ from country to country, and even from city to city in the same country, there are various and sometimes conflicting research studies of the timers. From a practice perspective, there is still limited unified scientific knowledge about the device and no unified

global manufacture standard or appearance. This also causes varying performance of the device being reported in various studies. Table 1 presents some recent studies and evaluation of the countdown timer's effectiveness.

Table 1: Effects of the countdown times

Research Sites	Evaluate the countdown timer's effects	Source
Taiwan	Driver tendency to stop is lower, dilemma zone lengthened by 28m; higher red light-running violation end green phase rear-end crash rates; reduced start-up lost time and saturated headway but no significant safety improvement	(Chiou & Chang, 2010)
Thailand	Reduced the start-up lost time at the beginning of the green phase by 22% and reduced the number of red light-running violations during the beginning of the red phase by 50%; relieved the driver frustration caused by stopping during uncertain red phase, but slightly reduced the saturation flow rate during the green phase	(Limanond, et al., 2010)
China	Encourages decision to accelerate to enter intersection during the amber time so can increased capacity of the intersection approach, smooth the driver's response and prevent sudden speeds changing, effectively solving the dilemma zone problem; significantly reduced red light-running violations, but increased the possibility of collisions	(Ma et al., 2010)
Malaysia	Amber onset stopping ratio is lower but amber phase longer; can reduce red light-running violation; no effect on dilemma zone problem	(Puan & Ismail, 2010)
Thailand	Reduced average start-up lost time by about 1 -1.92 seconds per cycle; trivial impact on saturation flow rate	(Limanond et al., 2009)
India	Installation of the timers decreased start-up lost time and transition lost time	(Sharma et al., 2009)
China	Influenced drivers' behaviour decision-making significantly	(Wu et al., 2009)
Malaysia	Little effect on initial delay but significant effect on discharge headway; more red light-running violation observed than none countdown timer	(Ibrahim et al., 2008)
Taiwan	Accidents rate decreased about 50% in red phase but increased about 100% during green phase	(Chen et al., 2007)
Singapore	Reduced red light-running violation by about 65% but effectiveness tended to dissipate after 1.5-month; amber stopping significant increased 6.2 times; red stopping increased under heavy traffic flow	(Lum & Halim, 2006)
Malaysia	Little effect on the capacity but reduce about 50%	(Kidwai et al., 2005)

In summary, the installation of the countdown timer undoubtedly received widely enthusiastic receptions from drivers as it significantly relieves tension during the

uncertain red phase at intersections. The timers can significantly decrease the start-up lost time; however, its optimistic goal to decrease red light-running violations is difficult to achieve in practice. Also, the red signal countdown timer is less controversial and more beneficial than the green signal countdown timer.

## **2.4 SIGNALISED INTERSECTIONS**

The more centralised, urbanised and motorized a society becomes, the more it depends on the knowledge obtained from traffic signal controls at urban intersections to inform contemporary traffic management theories. Correspondingly, the stop line is setup as a traffic road marking to indicate the need for vehicles to stop in the red signal phase. This section addresses the gap between this research hypothesis and the traditional traffic control knowledge for urban signalised intersections. First, this section reviews traffic signal development history and Akcelick's signal timing algorithm. It then uses a case study of a signalised roundabout to show the recent expansion in the use of signalised control. Next, this section reviews the Continuous Flow Intersection (CFI) and Pre-timed signal left turn to show how these approaches effects for the improvement of the start-up lost time.

### **2.4.1 Signalised intersection development**

On 10 December 1868, the railway engineer J. P. Knight erected the first manual switch traffic light in London (Philpot, 2005). People used this red and green device to open up an entirely new way of perceiving and understanding traffic management in urban areas. After the traffic light was invented, adding a yellow light to the red and green traffic signal was firstly used in Great Britain in 1918 (Sobey, 2006). As early traffic lights only included red and green lights, the red, green and yellow light was considered to be the first definitive version of modern traffic lights. The traffic control signal system had reached a significant milestone. Today, the three-coloured traffic lights system is still the most favoured means of traffic control at urban junctions.

Interestingly, after the introduction of traffic signals, traffic management research increased. Traffic management covers aspects, such as research of traffic signal systems and traffic stream characteristics. In the 1930s, Greenshield conducted pioneering research into traffic dynamic performance at urban junctions at the Yale Bureau of Highway Traffic. Greenshield's traffic flow study was the first to apply probability theory to the description of urban road traffic dynamic performance (Lieu, 1999). In recent years, with the help of computers, intelligent transportation light systems (ITS) are drawing more attention in the traffic management research field. In addition to progress made in traffic light control technology, research on driver behaviours has also opened a new frontier for traffic management in recent years.

In "Optimal traffic control: urban intersections" (Guberinić et al., 2008), traffic streams or traffic flows are defined by their volume, speed, density, headway or spacing interval, composition, the percentage of straight-through or left-turning and right-turning volume, and the paths they use to cross an intersection. This differentiation reflects the direction taken by many researchers in the traffic management research area.

#### **2.4.2 Signal timing algorithm**

The pre-timed signal control system is still widely used by signal controllers; even the most recent research has focused on updating the systems to adaptive signal control systems. However, due to the high costs of implementing these new systems, they need to perform significantly better than the present pre-timed signal systems (Smith et al., 2002; Yin, 2008). Therefore, this section only reviews the signal timing solution algorithm for the pre-timed signal system and uses Akcelik's method as an example.

In 1995, Akcelik published his transport research report, "Traffic signals: capacity and timing analysis." This report introduced a basic theory of traffic flow at signalised intersections and detailed the signal timing setting process. Akcelik explained the process for the calculation of the signal timings as follows. The first

step is calculation of the cycle time by using approximate optimum or practical methods. The algorithms are expressed as follows:

$$c_0 = \frac{(1.4+k)L+6}{1-Y} \quad \text{Equation 1}$$

where  $c_0$  is approximate optimum cycle time;  $L$  is intersection lost time in seconds;  $Y$  is intersection flow ratio and  $k$  is equal to  $K / 100$ , the stop penalty parameter. Meanwhile, the typical stop penalty values  $K$  is set as  $k = 0.4$  for minimum fuel consumption,  $k = 0.2$  for minimum cost and  $k = 0$  for minimum delay. On the other hand, the practical cycle time, is also considered the minimum cycle time; this ensures that the degrees of saturation of all movements are below the specified maximum acceptable degrees of saturation ( $x < x_p$ ). The equation is:

$$c_p = L / (1 - U) \quad \text{Equation 2}$$

where  $L$  is intersection lost time in seconds and  $U$  is intersection green time ratio.

After calculation of the cycle times, the next process is the calculation of the green times for a chosen cycle time through the following steps.

Calculation of the critical movement green time:

$$g = \left( \frac{c-L}{U} \right) u \quad \text{Equation 3}$$

where  $u$  is the movement and  $U$  is intersection green time ratio.

Calculation of the non-critical movement green times:

$$g = (g_c + l_c) - l \quad \text{Equation 4}$$

where  $l$  is the lost time for the movement in question.

Determine the green phase times:

$$G = (g + l) - l \quad \text{Equation 5}$$

where  $(g+l)$  is the time allocated to a movement that receives right of way during that phase only and  $l$  is the inter-green time of that phase.

The followed process is a calculation of the phase change times and is expressed as the following equation:

$$F_i = F_{i-1} + (I + G)_{i-1} \quad \text{Equation 6}$$

where  $F_i$  is change time for the  $i$  th phase;  $F_{i-1}$  is change time for the previous phase and  $(I+G)_{i-1}$  is the sum of the inter-green and green times of the previous phase.

Considering the above equations and practical perspectives, if lower the intersection lost time, it will significantly decrease the approximate optimum cycle time.



Additionally, these times can be shortened, while still ensuring acceptable degrees of saturation. In other words, the number of cycles per day can be increased to allow more vehicles to access and cross an intersection.

### **2.4.3 Signal-controlled roundabouts**

This subsection provides an overview of the current literature on signal-controlled roundabouts. As an effective form of traffic control, modern signal-controlled roundabouts relieve congestion during daily peak hours and afford safety for pedestrians and cyclists (Stevens, 2005). Azhar and Svante (2011) summarise the findings of previous research into the advantages of signal control of roundabouts, different types of signal control, the criteria for using signals at roundabouts, the number of signal lenses at the crosswalks, and the distance to the circular roadway.

Azhar and Svante (2011) state that using signals to manage roundabout traffic can handle queued vehicle flow and prevent vehicles blocking nearby intersections. Therefore, utilisation of signals can have the advantage of balancing roundabout delays and can also decrease delays in coordinated networks. There are two types of signal control: direct control and indirect control. Indirect control covers control of internal roundabout links while direct control also involves control of external links. Furthermore, the roundabout can be partially or fully signal controlled and controlled either permanently or at certain times only.

Different countries use special criteria for using signals at roundabouts. For example, a signal-controlled roundabout is constructed in the Netherlands if the circular roadway has enough space for queued vehicles and a traditional signalised intersection cannot offer sufficient capacity. However, the UK only uses signals for pedestrian crossings to improve traffic flow at roundabouts. The number of signal lenses at roundabouts varies in different countries. The UK for example, uses three-lens signals, while Australia uses two lenses only so as to avoid confusion for drivers. The distance from signal to the circular roadway, upstream of the yield line is different too. The FHWA guide recommends 20 to 50 metres (Robinson et al., 2000). In the UK, 7 to 10 metres is considered the norm, while, at least 15 metres in France (Azhar & Svante, 2011).

The signalised roundabout is still a new approach in most countries. It will take a long time for drivers to accustom themselves to the new signalised roundabout policy and regulation; nevertheless, it is of great benefits to the traffic flow.

#### **2.4.4 Case study of signal control of left turn**

Where there is a heavy demands on left turn, a signalised intersection often utilises a separate left turn phase. However, it wastes capacity on the approach because the vehicles in the opposite through lane cannot discharge during the same signal phase. This problem has already been addressed by some researchers and the following left turn case studies illustrate that innovative approach can contribute to better traffic management.

Improta and Cantarella (1984) propose a grouping of streams into phases using mathematical programming to maximize capacity. Their method uses a Binary-Mixed-Integer-Linear-Programming model to allow incorporation of the variables. However, this mathematical programming technique indirectly uses traffic signal settings to reduce left turn delay. The following literature introduces two other direct control methods: the CFI and the Pre-timed signal which both use better intersection design as a means of improving the left turn process.

Francisco D. Mier with Belisario H. Romo obtained their United States Patent on 17 September 1991 (see one practical case of CFI in Figure 4 follow). According to Google Patent records, the CFI is the use of a separate left lane before an intersection to better manage large left turn traffic flow (for driving on the right). Hutchinson (1995) summarised the CFI as: “A triple conflict between traffic streams - for instance, an appreciable right-turning flow, as well as heavy straight-through flows - is often the key factor leading to limited capacity and high delay at a junction, either three-legged T or four-legged crossroads. It is possible to design a junction so that such a conflict is replaced by three lesser conflicts, each between only a pair of flows. This leads to higher capacity and less delay for a given amount of road space.”

The CFI was successfully implemented to better manage traffic. As Pitaksringkarn (2005) wrote: “An unconventional intersection so called Continuous Flow

Intersection (CFI) is new in the United States, but in recent years, many jurisdictions have begun considering using the CFI intersection as an alternative means of improving traffic flow and reducing congestion at major intersections. The CFI has proven to facilitate left turn movement and decrease congestion at a major intersection”. The CFI has been an important development for traffic management since the introduction of traffic signals (Hutchinson, 1995). As Inman (2009) states, the CFI can support a large volume of left turning traffic. Berkowitz, Bragdon and Mier (1996) noted that: “The Continuous flow intersection (CFI) provides an at-grade spatial solution that improves traffic operation beyond the capacity of a conventional intersection”.



Figure 4: Dowling College, New York: A prototype CFI was built at a T intersection  
[http://teexwebtest.tamu.edu/eu/documents/04\\_01-02.pdf](http://teexwebtest.tamu.edu/eu/documents/04_01-02.pdf)

Apart from the CFI, another valuable solution for the left turn delay problem is the Pre-timed signal traffic management method. Xuan, et al. (2011) introduce a Pre-timed signal to enable all lanes to fully discharge during both the left turn and sub-phase. This method aims to dynamically re-organise traffic upstream of the intersection with a pre-signal and to allocate the area in front of the pre-signal as the sorting area. The operation of pre-signal includes three phases. Firstly, the pre-signal allows left turn vehicles to enter the sorting area while the intersection signal is red. Significantly, it prepares all lanes for the left turn vehicles to use when the signal changes to green. The aim is to increase the capacity through effectively utilising all traffic lanes for both left turn and through vehicles. Secondly, the pre-signal changes to green for through vehicles to precede at the same time as the left turn vehicles. Finally, intersection signal can be set only one single phase for all

queuing vehicles to pass through the intersections. The basic idea is depicted in Figure 5.

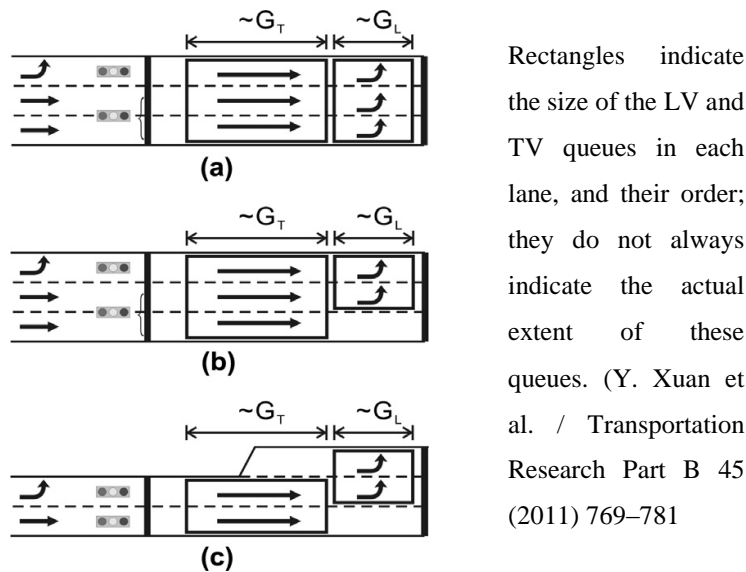


Figure 5: The tandem intersection concept: (a) full tandem; (b) partial tandem; (c) general case.

Compared with the CFI which separates the left turn bays from the main traffic lanes, the Pre-timed signal is simpler and can be easily implemented at normal intersections. However, both the CFI and the Pre-timed signal aim to decrease the left turn delay, so as to improve the capacity of the through lanes. Additionally, both approaches illustrate that design methods can be applied to traffic management to solve particular problems.

In summary, the above literature review indicates the viability of the enlarged stopping distance method for better traffic management by showing its similarity to the CFI and the Pre-timed signal control measure, i.e. through changing signalised intersection appearance to reorganise vehicle queue in approach. To solve a traffic problem by using the innovative approach is one of the most practical applications in the traffic management research area. The new method, integrated with traditional transport research approaches, has the potential to generate simple answers to historical longstanding traffic management problems. From a practice perspective, J.P.Night's erection of traffic lights at a London intersection in 1868 is an early case in traffic management history that illustrates a new method serving to improve vehicle safety. Another case which adopted an innovative method to solve red light-

running violations at signalised intersections was the introduction of countdown times in the 1990s.

## 2.5 DRIVER BEHAVIOUR & VEHICLE LENGTH

Driver behaviour can affect traffic performance for signalised intersections. For example, follow-up headway, gap-acceptance situations and saturation flow rate. To amend micro simulation models of traffic performance, it is valuable to explore the relationship between the basic parameter in traffic performance analytical models and various driver behaviour characteristics. Therefore, the human psychological factors in the car following, the relationship between capacity and driver behaviour, and vehicle length factors are introduced in this section.

### 2.5.1 Human psychological elements in car following

Substantial evidence already confirms that drivers maintain their following distance based on time headway. Individual drivers follow time headway that is independent of vehicle speed (Wim, 1999; Wim & Heino, 1996). Therefore, a driver's attempt to maintain the car following distance  $D_p$  can be express as:

$$D_p = t_p v_i \quad \text{Equation 7}$$

where  $D_p$  is the preferred following distance (m);  $t_p$  is time headway (s);  $v_i$  is the speed of the driver's vehicle (m/s). The  $t_p$  is associated with driver's skills and general state (for example, ability to see, mental effort, and attention paid to the leading vehicle). Van Winsum (1999) reports: "The rationale behind this rule is that drivers use time headway as a safety margin. Controlling the distance to the lead vehicle then basically consists of controlling available time in case the lead vehicle decelerates. Drivers who are less skilled in adjusting the braking response to the Time-to-Collision (TTC) with the lead vehicle generally choose to drive at large time headway".

Therefore, to avoid collision, drivers always make their decision to accelerate or decelerate based on the  $D_p$ . If the distance to the lead vehicle is larger than  $D_p$ , some drivers are encouraged to increase their speed. By contrast, drivers must decelerate

the vehicle if the distance to the lead vehicle is smaller than  $D_p$  for safety-related reason. Van Winsum (1999) introduces this relationship as follows:

$$a_i = cTTC_{est} + d + \varepsilon \quad \text{Equation 8}$$

where  $a_i$  is the deceleration of the driver;  $TTC_{est}$  is the TTC as estimated by the driver;  $c$  is a constant;  $d$  is a constant ( $<0$ ) and  $\varepsilon$  is a random error term.

For this research, when setting up simulation scenarios, it is necessary to extract corresponding car following distance patterns which are based on the preceding vehicle's velocity. Meanwhile, the vehicles' dynamic trajectories also need to be tested for safety related issue. Furthermore, a consideration of human psychological elements in the micro-simulation test is important in this research. Therefore, this research categorised the driver behaviours into "Fast", "Normal" and "Slow" groups to simulate possible scenarios.

### 2.5.2 Driver behaviour and traffic capacity in queue discharge

The traffic stream capacity is a basic parameter of traffic performance simulation models. For vehicle dynamic analysis in intersections, Akcelik (2008) provides a general analytical model to reveal the relationship between capacity and parameters representing driver behaviour. These parameters are: driver response time during queue discharge, spacing between vehicles in the queue (jam spacing) and saturation (queue discharge) speed. For signalised intersections, the basic traffic stream capacity formulation is expressed as:

$$Q = us \quad \text{Equation 9}$$

where  $Q$  is capacity (veh/h);  $u$  is the green time ration and  $u = g/c$ , where  $g$  is effective green time (s) and  $c =$  cycle time (s);  $s$  is saturation (queue discharge) flow rate (veh/h). The saturation flow rate is also known as the 'queue discharge flow rate'; this, in turn, corresponds to queue discharge headway and can be shown as follows:

$$h_s = 3600/s \quad \text{Equation 10}$$

where  $h_s$  is queue discharge (saturation) headway (seconds);  $s$  is saturation flow rate (veh/h). As the follow-up headway ( $t_f$ ) can equal the queue discharge headway ( $h_s$ ), the following equation results:

$$s = 3600/t_f \quad \text{Equation 11}$$

where  $t_f$  is follow-up headway as a queue discharge (saturation) headway (seconds). Akcelik (2008) states that: “the queue discharge headway is a key parameter that determines capacity”.

Akcelik and Besley (2002) describe that the  $h_s$  saturation (queue discharge) headway (seconds) can be expressed as a function of the  $t_r$  driver response time during queue discharge (seconds),  $L_{hj}$  queue space per vehicle (jam spacing) which includes the vehicle length, adds the gap distance between vehicles in the queue (metres), and the  $v_s$  saturation speed (m/s). This relationship is shown as following equation:

$$h_s = t_r + L_{hj} / v_s \quad \text{Equation 12}$$

This equation also can be represented as  $t_r = h_s - L_{hj} / v_s$ . Therefore, Akcelik (2008) points out that the vehicle length and driver alertness can affect both the driver response time, the queue discharge speed, and the queue vehicles' gap distance. Akcelik also describes the relationship among driver behaviour, the queue clearance wave speed, and average acceleration delay as the following two equations:

$$v_x = L_{hj} / (h_s - L_{hj} / v_s) \quad \text{Equation 13}$$

$$d_a = t_s + h_s - t_r = t_s + L_{hj} / v_s \quad \text{Equation 14}$$

where  $v_x$  is queue clearance wave speed (m/s);  $d_a$  is acceleration delay (seconds);  $t_s$  is start loss (seconds).

Equation 13 above reveals that the queue clearance wave speed is determined by the saturation headway and saturation speed. However, even if it can characterise most driver behaviour in the queue clearance, the leading vehicles start-up lost time is oversimplified. Therefore, Equation 14 expresses the start-up loss separately. However, while the start-up delay still represents saturation flow speed, it also oversimplifies the role of the characteristic the four leading driver behaviours. Therefore, it is necessary to separately extract each of the four leading vehicle driver behaviours in the queue discharge process for this research.

### **2.5.3 Vehicle length factors**

The separation of driver behaviour and vehicle length is essential for the vehicle dynamic simulation test because the car and driver are two close characters in the research into queue discharge. For the scenarios simulation test, it is also necessary to extract the average vehicle length and the driver response time as two separate parameters. This is particularly necessary given that the vehicle length varies for specific time periods in different countries, and even in different cities in the same country.

Car length and car storage length are two vehicle-related dimensions in queue vehicle discharge research. Through comprehensive surveys undertaken in Melbourne and Sydney from 1996 to 1998, Akcelik (2000) determined the related queue vehicle discharge parameters for these two dimensions. Firstly, for the Australian car length, Akcelik confirmed Taylor, et al.'s (1996) finding: "In Australia, the 85<sup>th</sup> percentile car length is 4.7 m and the width is 1.9 m". Secondly, Akcelik amended Taylor, et al.'s statement of storage length for cars. Akcelik (2000) stated that: "Usually allow 6 to 7 m per vehicle storage length for a queue of cars (light vehicles) and 9 to 14 m for a queue of heavy vehicles. It may be appropriate to use 7.0 m per car (11.5 m for heavy vehicles for through traffic lanes, and 6.5 m per car (10.0 m for heavy vehicles) for turning lanes". However, Ewing (2011) notes that with fuel prices spiralling, smaller and more fuel-efficient cars are enjoying ever increasing popularity in Australia. Therefore, for this study, car length and storage length for cars need to be investigated.

## **2.6 VEHICLE DYNAMIC MODELS**

This section reviews the traditional vehicle dynamic models for departure, following, and clearance. However, as this research focuses on the queuing vehicle discharge process, discussion of the clearance model is limited to discussion of the left-turn clearance time aspect of the model. The review of these three models reveals the significant potential effects of the enlarged stopping distance approach on traditional vehicle dynamic models.



### 2.6.1 Vehicle departure model

The departure model is one of the models that assist in characterising the dynamics of the traffic flow at a signalised intersection. Other examples of such models are the arrival model or the model of vehicle movement at an intersection. Research into the departure model is useful to determine the number of vehicles that can pass through an intersection during the signal phase. This, in turn, enables people to determine the capacity of the intersection. This model can be directly used for the traffic signal timing set process. Departure model research and mathematical applications of the departure model are reviewed below.

In Australia, Akcelik (2002) summarised a previous queue discharge model as a model to: “express the queue discharge speed, flow rate and headway as a function of the time since the start of green”.

$$V_s = V_n [1 - e^{-m_v(t-t_r)}] \quad \text{Equation 15}$$

$$q_s = q_n [1 - e^{-m_q(t-t_r)}] \quad \text{Equation 16}$$

$$h_s = h_n / [1 - e^{-m_q(t-t_r)}] \quad \text{Equation 17}$$

where  $t$  is time since the start of the displayed green period (seconds);  $t_r$  is start response time (a constant value) related to an average driver response time for the first vehicle to start moving at the start of the displayed green period (seconds);  $v_s$  is queue discharge speed at time  $t$  (km/h);  $v_n$  is maximum queue discharge speed (km/h);  $m_v$  is a parameter in the queue discharge speed model;  $q_s$  is queue discharge flow rate at time  $t$  (veh/h);  $q_n$  is maximum queue discharge flow rate (veh/h);  $m_q$  is a parameter in the queue discharge flow rate model;  $h_s$  = queue discharge headway at time  $t$  (seconds);  $h_s$  is  $3600/q_s$ , and  $h_n$  is minimum queue discharge headway (seconds),  $h_n = 3600/q_n$ .

Therefore, the vehicle spacing,  $L_{hs}$  (m/veh), occupancy time  $t_{os}$  (seconds), space time  $t_{ss}$  (seconds) and the cumulative queue discharge flow  $n_s$  (vehicles), at time  $t$  during queue discharge can be determined from:

$$L_{hs} = v_s h_s / 3.6 = 1000 v_s / q_s \quad \text{Equation 18}$$

$$t_{os} = 3.6(L_p + L_v) / v_s \quad \text{Equation 19}$$

$$t_{ss} = h_s - t_{os} \quad \text{Equation 20}$$

$$n_s = \int_{t_r}^t \frac{q_s}{3600} dt \quad \text{for } t > t_r$$

$$= \frac{q_n}{3600} \left[ (t - t_r) - \frac{1 - e^{-m_q(t-t_r)}}{m_q} \right] \quad \text{Equation 21}$$

where  $v_s$  (km/h),  $h_s$  (seconds),  $q_s$  and  $q_n$  (veh/h) are the same as for Equation 15 and 16 above;  $L_p$  is the detection zone length (m) and  $L_v$  is the average vehicle length (m). This model can already refine most dynamic characteristics to suit each instance; various driver response times are simple to average and this average is presented as a constant value. Therefore, it is necessary to characterize each leading vehicle discharge pattern to explore the solution to the second vehicle delay phenomenon. Unlike traditional departure model, this exploration belongs specifically to the field of micro-simulation.

For easy understanding of Akcelik's model, equation 15 is used as an example and its expression form is changed as follow:

$$V_s = V_n [1 - e^{-m_v(t-t_r)}] = V_n - \frac{V_n}{e^{m_v(t-t_r)}} \quad \text{Equation 22}$$

As  $e^{m_v(t-t_r)}$  is a positive number, its value maybe less or over the  $e$  value. The result is that  $v_s$  may be less or over  $v_n$ . This equation can cover most situations, but, it still considers queuing vehicles as a group. The differentials between the first five leading vehicle are ignored since the important parameter  $t_r$  is considered as a constant value. Compare with Akcelik's model, this research tries to express the difference of the first five leading vehicles dynamic performance; therefore, this research extracted each queue position vehicle trajectory samples. This research develops five leading vehicles queue discharge pattern as the function of the queue position so as to express the difference of the leading vehicle driver response time.

## 2.6.2 Vehicle-following model

In the 1990s, car-following models were highlighted in traffic management research and in the study of traffic flow safety. The review of the historical development of car-following models below shows how far work has already processed in the area (Brackstone & McDonald, 1999). This review first introduces car-following models

according to a historical time-line, and then summarises recent experimental car-following models. This car-following research could contribute to create scenarios and driving safety studies for this research simulation step.

### ***Gazis-Herman-Rothery models (GHR) model***

During the late 1950s to the early 1960s, the GHR model was a famous car-following model which attracted most researchers in the area (Brackstone & McDonald, 1999).

Its formulation is:

$$a_n(t) = c v_n^m(t) \frac{\Delta v(t-T)}{\Delta x^l(t-T)} \quad \text{Equation 23}$$

where  $a_n$  is the acceleration of vehicle  $n$  implemented at time  $t$  by a driver and is proportional to;  $v$  is the speed of the  $n^{\text{th}}$  vehicle;  $\Delta x$  and  $\Delta v$  are relative spacing and speed respectively between the  $n^{\text{th}}$  and  $(n-1)^{\text{th}}$  vehicle (the vehicle immediately in front), assessed at an earlier time  $t-T$ , where  $T$  is the driver response time, and  $m$ ,  $l$  and  $c$  are the constants to be determined.

Brackstone and McDonald (1999) summarised some research contributions to the GHR model as follows. The important contributors were Chandler, Herman, Montroll (1958) in Detroit in the late 1950s. Through data analysis, these researchers determined that  $\Delta x$  contributes little to the car-following relationship and needs to be discarded when GHR model produces a case where  $l=m=0$ . Meanwhile, the scaling constant appears to have a high variation between subjects (0.17-0.74 s), as does  $T$  (1.0-2.2 s). Subsequently, Gazis, Heman and Potts (1959) concluded that the GHR model should be amended by introducing a  $(1/\Delta x)$  term into the sensitivity constant ( $c \rightarrow c/\Delta x$ ) to minimise the discrepancy between the two approaches. Brackstone and McDonald's (1999) table (Table 2) below summarizes many other engineers' contributions to the GHR model.

Table 2: Summary of optimal parameter combinations for the GHR equations\*

Source	$m$	$l$	Approach
Chandler et al. (1958)	0	0	Micro
Gazis, Herman and Potts (1959)	0	1	Macro

Herman and Potts (1959)	0	1	Micro
Helly (1959)	1	1	Macro
Gazis et al. (1961)	0-2	1-2	Macro
May and Keller (1967)	0.8	2.8	Macro
Heyes and Ashworth (1972)	-0.8	1.2	Macro
Hoefs (1972) (dcn no brk/dcn brk/acn)	1.5/0.2/0.6	0.9/0.9/3.2	Micro
Treiterer and Myers (1974) (dcn/can)	0.7/0.2	2.5/1.6	Micro
Ceder and May (1976) (Single regime)	0.6	2.4	Macro
Ceder (1976) (uncgd/cgd)	0/0	3/0-1	Macro
Aron (1988) (dcn/ss/can)	2.5/2.7/2.5	0.7/0.3/0.1	Micro
Ozaki (1993) (dcn/can)	0.9/-0.2	1/0.2	Micro
* Key: dcn/acn: deceleration/acceleration; brk/no brk: deceleration with and without the use of brakes; uncgd/cgd: uncongested/congested; ss: steady state.			

Table 3: Most reliable estimates of parameters within the GHR model <sup>a</sup>

Source	$m$	$l$	Approach
Chandler et al. (1958)	0	0	Micro
Herman and Potts (1959)	0	1	Micro
Hoefs (1972) (dcn no brk/dcn brk/acn)	1.5/0.2/0.6	0.9/0.9/3.2	Micro
Treiterer and Myers (1974) (dcn/can)	0.7/0.2	2.5/1.6	Micro
Ozaki (1993) (dcn/can)	0.9/-0.2	1/0.2	Micro
<sup>a</sup> Key: dcn/acn: deceleration/acceleration; brk/no brk: deceleration with and without the use of brakes.			

The GHR model offers a basic simulation method for this research demonstration step. When queuing vehicles have completed the departure process in green signal phase, vehicles will convert to the pattern of the car-following model. The vehicle dynamic performance is determined by the preceding vehicle's velocity and by safety distance. Thus, it is necessary to extract the relative spacing and speed from the data analysis to examine the accuracy of the scenarios simulation.

### *Safety distance or collision avoidance models (CA) model*

In 1959, Kometani and Sasaki (1959) determined this differentiating equation to express the car space as a linear function of velocities:

$$v_k(t - T) - v_{k+1}(t - T) = -mTv_k(t - T) + nTv_{k+1}(t) \quad \text{Equation 24}$$

where  $T$  is the time lag of the car  $k$ , with  $(k+1)$  as the response time.  $V$  is the speed of car at time  $t$ . The  $m$  and  $n$  are the constants to be determined. Then, based on the above mode, and through mathematical derivation, Kometani and Sasaki (1959) defined a safety index for the traffic flow as follows:

$$\text{safety index} = \Pr[t; \text{equation(4)}] \quad \text{Equation 25}$$

$$(n - m - 1)v_0 + l_0 - l + A(\Delta_1 \cos \omega t + \Delta_2 \sin \omega t) + \mu_1'[v_0 - A \sin \omega t]^2 - \mu_2'[v_0 - A(\theta_1 \cos \omega t + \theta_2 \sin \omega t)]^2 > 0 \quad \text{Equation 26}$$

$$\text{where } \Delta_1 = W \sin(1/2 \omega T + \varphi) - |U| \cos(\arg U),$$

$$\Delta_2 = W \cos(1/2 \omega T + \varphi) + |U| \sin(\arg U),$$

$$\theta_1 = |E| \sin(\omega T + \varphi),$$

$$\theta_2 = |E| \cos(\omega T + \varphi),$$

and here  $\Delta_1, \Delta_2, \theta_1, \theta_2$  are all the function of  $\omega T$  and have the following properties:

$$\lim_{\omega T \rightarrow 0} (\Delta_1, \theta_1) = 0, \quad \lim_{\omega T} \theta_2 = 1,$$

$$\lim_{\omega T \rightarrow 0} \Delta_2 = n - m + 1, \quad \lim_{\omega T \rightarrow \infty} (\Delta_1, \Delta_2, \theta_1, \theta_2) = 0.$$

Brackstone and McDonald (1999) claim that the CA model was trying to determine a safe following distance and that it is different to the GHR model which describes a stimulus-response type function. The CA model can be dated from Kometani and Sasaki's model and is as follows:

$$\Delta_x(t - T) = \alpha v_{n-1}^2(t - T) + \beta_1 v_n^2(t) + \beta v_n(t) + b_0 \quad \text{Equation 27}$$

Brackstone and McDonald (1999) summarise the CA model's advantages thus: "Part of the attractiveness of this model is that it may be calibrated using common sense assumptions about driver behaviour, needing (in the most part) only the maximal braking rates that a driver will wish to use, and predicts other drivers will use, to allow it to fully function".

For this research, demonstration scenario's setup process needs to test the safety distance between vehicle trajectories. Although the CA model can better describe the safety distance with corresponding vehicle velocity, its complex parameters also limits its application in this research data analysis. This suggests that a suitable safety distance pattern should be extracted for this research.

**Linear models (Helly) model**

Brackstone and McDonald (1999) introduced the linear model as follows:

$$a_n(t) = C_1 \Delta v(t - T) + (\Delta x(t - T) - D_n(t)), D_n(t) = \alpha + \beta v(t - T) + \gamma \alpha_n(t - T), \quad \text{Equation 28}$$

where  $D(t)$  is a desired following distance and  $T$  is the driver response time. Helly (1959) found that the best fit parameters were almost all being produced at  $\gamma^2 > 0.8$  and ranged from  $T= 0.5-2.2$  and  $C_1= 0.17-1.3$ , with an average of 0.75 and 0.5 respectively. Hence, Helly produced the final equation as follows:

$$\begin{aligned} \alpha &= 0.5 \Delta v(t - 0.5) + 0.125 (\Delta x(t - 0.5) - D_n(t)), D_n(t) \\ &= 20 + v(t - 0.5) \end{aligned} \quad \text{Equation 29}$$

Brackstone and McDonald (1999) summarised the various research results of combinative optimal parameters for the Helly equation in the following table (see Table 4).

Table 4: Summary of optimal combinations for the Helly equation<sup>a</sup>

Source	$C_1(\Delta v)$	$C_2(\Delta x)$
Helly (1959)	0.5	0.125
Hanken and Rockwell (1967)	0.5	0.06
Bekey, Burnham and Seo (1977)	0.5	1.64
Aron (1988) (dcn/ss/can)	0.36/ 1.1/ 0.29	0.03/ 0.03/ 0/ 0.3
Xing (1995)	0.5	
aKey: dcn/can: deceleration/ acceleration; ss: steady state.		

Helly’s model, which indicates that the desired safety distance is  $20+v(t-0.5)$ , offers a potential option for testing the safety distance. However, as difference in queue position affects vehicle velocity and travel time, it is necessary to separately consider each leading vehicle’s required safety distance pattern.

### *Psychophysical or action point models (AP) model*

Michaels was the first to state the concept that drivers normally approach the front vehicle according to their perception of its relative velocity which they have determined through their observation of the apparent change in its size. This threshold of perception is known as “ $d/dt(\sim\Delta v/\Delta\chi^2)\sim 6 \times 10^{-4}$ ”. If this threshold is exceeded, drivers will decelerate until they do not perceive any relative velocity. Subsequently, the threshold will not be exceeded again that is based on drivers’ actions will not be exceeded again, and whether there is any changes in spacing could be perceived (Almond, 1965; Brackstone & McDonald, 1999).

Even though others have produced similar models, the validity of the AP model has still not been determined. These models seem to offer suitable simulation of driving behaviour but are unsuccessful in the calibration of the individual elements and thresholds (Brackstone & McDonald, 1999). Also, in this research, it is not practically possible to precisely determine the variations in the visual size of vehicles.

### *Fuzzy logic-based models*

These models used fuzzy logic to input overlapping ‘fuzzy sets’ to describe a ‘term’ within car-following models. For instance, for describing driving behaviour, less than 0.5 s is defined as ‘too close’ and named as Membership 1; 2 s is not close and given Membership 2. Hence, a fuzzy example output set can be shown as IF ‘close’ AND ‘closing’ THEN ‘break’. Using this method, fuzzy logic can be used to describe actual cases of traffic flow and to calculate all potential results (Brackstone & McDonald, 1999).

One example of the fuzzy logic-based model is proposed by Chakroorty and Kikuchi (1999). Their model fuzzy inference rules were set up as: “If at time  $t$ , Distance Headway DS is  $A_i$  AND Relative Speed RS is  $B_j$  AND Acceleration of LV is  $C$ ; Then at time  $t+\Delta t$  Accel./Decel. Of FV should be  $D_t$ . Three fuzzy sets,  $A_i$ ,  $B_j$ , and  $C_k$ ” (Chakroorty & Kikuchi, 1999). This process can be mathematically expressed as:

$$h_{D_{l'}}(w) = \min \{h_{A_i}(x), h_{B_j}(y), h_{C_k}(z), h_{D_l}(w)\} \quad \text{Equation 30}$$

where  $h_{D_l}(w)$  is the membership function of notion of consequent  $D_{l'}$  after the input is given. Details can be seen in their paper.

Although a Fuzzy logic-based model cannot be used for this research scenario's test process, it can still be used to determine the vehicle's performance for the term "Stop" and "Move". This is because the data shows that most vehicles do not absolutely stop and wait for the signal to change to green.

In summary, this thesis assumes that the first leading vehicle drivers could actively enlarge their stopping distance; but after accomplishment of the discharge process, these vehicles will convert from the discharge process to the car-following process. As a result, the car-following research could directly contribute to create scenarios and driving safety studies for this research scenario's simulation. Additionally, the Fuzzy logic-based research method can be used to extract driver response time from the raw vehicle trajectories in this research.

### **2.6.3 Vehicle clearance model**

Comprehensive studies for qualifying end lost time generate various clearance models which present vehicle-driver performance when using the yellow interval before the signal changes to red. This end lost time includes lost through lane clearance and the separate left-turn lane loss which is based on the assumption that drivers will choose to stop at the end of the green signal phase. However, once the signal change is perceived, clearing vehicle's drivers tend to use the yellow interval if they do not have a sufficient comfortable stopping distance (James A. Bonneson, 1992). Driver behaviours differ between countries and even cities; however, clearing vehicle drivers present various options in the dilemma zone. This research only focuses on the leading vehicle's start-up lost time issue; hence, the clearance for the through lane is introduced with saturation flow headway in Section 2.7.1. This opposing left-turn clearance model is addressed in this section as if it provides potential opportunity to improve the fore mentioned research into start-up lost time.



In the HCM2000, the blocked time for the left-turn (driving on the right) clearance model was earmarked for the opposing traffic queue clearance time. The left-turn queue clearance time assumed that the permitted left-turn vehicles could not find acceptable gaps before the opposing queue cleared (Wang, 2008). In Appendix C left-turn worksheet, Chapter 16 estimated the queue clearance time for a left-turn lane group with multilane opposing approaches from the Equation C16-6 in the finding  $g_q$  as:

$$g_q = \frac{v_{o/c}qr_o}{0.5 - [v_{o/c}(1 - qr_o)/g_o]} - t_L \quad \text{Equation 31}$$

where  $v_{o/c}$  is adjusted opposing flow rate per lane per cycle;  $qr_o$  is opposing queue ratio that is a proportion of the opposing flow rate originating in opposing queues;  $g_o$  is effective green for opposing flow (s); and  $t_L$  is lost time for the opposing lane group (s). Also  $v_{o/c}$  and  $qr_o$  are computed as

$$v_{o/c} = \frac{v_o C}{3600 N_o f_{LU_o}} \quad \text{Equation 32}$$

$$1 - R_{po}(g_o/C), qr_o \geq 0 \quad \text{Equation 33}$$

where  $v_o$  is adjusted opposing flow rate (veh/h);  $f_{LU_o}$  is lane utilization factor for opposing flow;  $N_o$  is the number of opposing lanes;  $R_{po}$  is platoon ratio for opposing flow, based on opposing arrival type (TRB, 2000).

Foil and Qureshi (2005) documented their research results in the paper, “Accuracy of the HCM 2000 Queue Clearance Model: Case of Multiple Approach Lanes with Shared Left Turns and Multiple Opposing Lanes”. They selected five intersections for field data collection and compared the observed queue clearance time with the predicted queue clearance time from the HCM2000 queue clearance model. They stated that the HCM2000 clearance model underestimated the observed clearance time on average by 5.8 seconds. Although more comprehensive studies are necessary before amending the HCM2000 clearance model, the improvement of the through lane vehicles’ start-up lost time has the potential benefit of decreasing the left-turn blocked time; this is because the opposing lane group lost time  $t_L$  could be shortened.

#### 2.6.4 Micro simulation models

In recent years, traffic micro-simulation models have been widely applied in studying driver performance and behaviour at the micro level. With the continuous

development of computer power, civil engineers are widely using microscopic simulation models for modelling of the real applications. Several microscopic simulation models are presently available from academic and commercial sources, and new models are continually being developed (Krogscheepers & Kacir, 2001). For instance, Ossen (2008) used real trajectories data for calibration of micro-simulation model to perform the extensive empirical analyses on interactions between drivers moving on the same lane, a so-called longitudinal driving task. Ossen also summarised some widely used micro-simulation tools, such as TSSTransport Simulation Systems (2006), PTV (2006) and SIAS (SIAS Limited, 2005). This research will use Intelligent Driver Model (IDM) to generate data for simulation purposes. Therefore, this part introduces the IDM model in details.

The Intelligent Driver Model (IDM) is a time-continuous car-following model for simulating freeway and urban traffic which was developed by Treiber, Hennecke and Helbing (2000). The IDM model improved upon results provided by other "intelligent" driver models such as the Gipps' Model, which fail to account for realistic parameters. For a simplified version of the IDM model, the dynamics of vehicle  $\alpha$  are then described by the following two ordinary differential equations:

$$\dot{x} = \frac{dx_\alpha}{dt} = v_\alpha = \alpha \left( 1 - \left(\frac{v_\alpha}{v_0}\right)^\delta - \left(\frac{s^*(v_\alpha, \Delta v_\alpha)}{s_\alpha}\right)^2 \right) \dots \dots \dots \text{Equation 34}$$

$$\text{with } s^*(v_\alpha, \Delta v_\alpha) = s_0 + v_\alpha T + \frac{v_\alpha \Delta v_\alpha}{2\sqrt{ab}} \dots \dots \dots \text{Equation 35}$$

where:  $v_0, s_0, T, a,$  and  $b$  are model parameters. As a car-following model, the IDM describes the dynamics of the positions and velocities of single vehicles.

**2.7 VARIOUS UNDERSTANDINGS OF THE TRAFFIC DISCHARGE PROBLEM**

This part of the literature review reveals the gap between the existing discharge patterns with the second vehicle discharge delay phenomenon and also offers some practical research methods for this research.

### 2.7.1 Queuing vehicle discharge

Saturation flow rate is a major determinant of signalised intersection design and operations. According to Highway Capacity Manual 2010 (TRB, 2010), “saturation flow rate is defined as the flow rate per lane at which vehicles can pass through a signalised intersection. It is computed by equation:  $S=3600/h$ . “S” is saturation flow rate (vehicle/ hour) and “h” is saturation headway. The saturation flow rate represents the number of vehicles per hour per lane that can pass through a signalised intersection if the green signal was available for the full hour, the flow of vehicles was never halted, and there were no large headways.” Highway Capacity Manual 2010 assumes that saturation flow will be achieved and maintained after the fourth vehicle is discharged.

However, some studies presented different understanding of the process of saturation flow rate based on the research of queue discharge patterns (Tang & Nakamura, 2007). Lee and Chen (1986) found that drivers queuing in the last part of a queue are more aggressive and may compress the saturation headways. This means that the saturation headways tend to decrease after the tenth queue position. Therefore, Lee and Chen suggest that the calculation of saturation flow rate should exclude the last vehicles in the queue as the headways are smaller than saturation headways.

On the contrary, some researchers claim that there was a gradual increase in saturation headway in the last part of a queue. In Israel, researchers found that saturation headways tended to increase after around the twenty-third to twenty-eighth vehicle at signalised intersections with extraordinary long cycle lengths (Mahalel et al., 1991). Bonneson (1992) found there was a negative relationship between saturation headways of the first 12 discharging vehicles and traffic pressure measured by lane volume, degree of saturation at the lane and queue length per cycle. Whether saturation headways increase or decrease in the last part of the queued vehicles discharge process has not been conclusive. In contrast to the studies reported above, this research is investigating start-up lost time of initial queuing vehicles. The reduction of the start-up lost time will enable earlier realisation of saturation flow for a traffic stream. Hence, there is the opportunity for more vehicle to safely cross an intersection that can be achieved irrespective of the end lost factor.

The literature review above indicates that the discharge pattern of queuing is inconstant when vehicles cross the stop line at signalised intersections. As this research focuses on the leading vehicle discharge process, the following literature will review the first part of the queuing vehicles discharge pattern.

Nguyen and Montgomery (2006) explored the HCM2000 discharge flow pattern and compared their research results on the variability of the discharge rate over the green phase time with results from other researchers. Through investigation of ten approaches in Hanoi (Vietnam), Nguyen and Montgomery suggested that the discharge pattern at signalised intersections is reliant on the degree of saturation, traffic composition, and type of operating signal control. The authors also stated that the period of time from the onset of green to the moment the discharge rate reached a temporary stability or maximum value, largely depended on the proportion and manoeuvrability of the predominant type of vehicle at the head of the queue. In short, traffic across the stop-line of signalised intersections is not constant.

Lin, Tseng and Su (2004) studied other researchers' data that were collected from Florida and Hawaii and found that queue discharge might not reach a steady maximum rate until after the fourth vehicle. For comparison, they collected data at five intersections in Taiwan. Their research results revealed that there is a relatively stable discharge rate from queue position six to twelve and a greater rate for preceding vehicles in the queue. Their data analysis also suggested that the drivers in the back of a long queue tend to shorten headways to get opportunities to cross the intersection before the green interval expires. Lin, Tseng and Su (2004) wrote: "Field data provide ample evidence to show that queue discharge often does not conform to the notion of a quick rise to a steady state. In some cases, it is not clear whether a steady-state queue discharge exists at all. Under these conditions, saturation flow can become an ambiguous parameter." However, their research only mentions that the vehicles in the preceding position appeared to have a greater discharge rate. They did not offer more details about the leading vehicles discharge patterns.

In conclusion, various researchers have demonstrated that there are differences between observed discharge patterns and those described in the HCM2010 and HCM2000. This research field data collection process will focus on the first part of

the queuing vehicle discharge pattern – that is, on the first four to five vehicles. Data analysis of each vehicle's response time and its headway time to cross the stop line will generate new evidence to enhance the second queuing vehicle's discharge delay problem. Also, the leading vehicle's traffic trajectories can be used to generate micro-simulation discharge patterns.

### **2.7.2 Innovative traffic control approaches**

Besides using the traditional traffic lights to manage traffic flow at intersections, many traffic departments adopt new technologies in traffic management, such as use of intelligent traffic signals systems, vehicle engine intelligent control systems and global position systems. Based on the development of computer technology, applied artificial intelligence is popularly used in the traffic control field. Meanwhile, intelligent traffic control is also using better algorithm, better sensors, better use of data, and so on. Rosaci (1998) wrote that: "A main problem in transportation engineering is the following: given the topology of an urban transportation network and the transportation demand, determine the saturation level of each row". This suggests that each discharge model needs to simulate real traffic situations, and then use an equation to control traffic signals in smart traffic systems. The result was that adoption of intelligent traffic signals needed considerable investment.

As Bristow (2010) stated, on 20 May 1984, IBM successfully obtained a patent for future traffic management. This was known as the "System and Method for Controlling Vehicle Engine Running State at Busy Intersections for Increased Fuel Consumption Efficiency". This system allowed vehicles to control vehicle engine power and torque output at traffic signals so as to save fuel. However, the system has been discarded because application of this IBM technology needed an enormous budget. This example reveals the flaws of utilizing high technology in the traffic management process.

There is, however, one example of successful application of high technology in traffic management, the Global Position System which has helped drivers with planning their route (Dia, 2002). Furthermore, in recent years, the use of the driving simulators in driver behaviour research has also been successful in recent years.

Malik and Rakotonirainy (2008) outlined a vision for future research in the area of intelligent driver training systems for enhancing road safety and they also present preliminary implementations with a great deal of attention is being paid to contemporary driving behaviour.

In short, as the smart traffic systems require discharge model to accurately simulate the real traffic situation; the leading vehicle discharge patterns that are extracted from this research can be used to calibrate the traditional departure models. Therefore, this research has potential benefits for the control of the traffic signals in smart traffic systems.

### **2.7.3 Related research**

The research is relevant to vehicle departure model for signalised intersections. As traffic flow at a signalised intersection is complex and its observation difficult, there has been little detailed studies of leading vehicle discharge pattern criteria in the traffic management research area. However, the following researcher's methods can be used in this research in the field data collection and data analysis stages.

Yu with his research team members (Yu et al., 2008) used a close-range photogrammetry method to collect car-following data at a signalised intersection in Beijing, China. They stated that: "By speed difference analysis, the critical headway of 3 seconds and the headway distance of 30m are identified. With 3 seconds headway, the capacity of a through lane in a signalised intersection is  $3600/3=1200$  vehicles". They used the following graphs (Figure 6, Figure 7) to describe the vehicle following data that resulted from their field work.

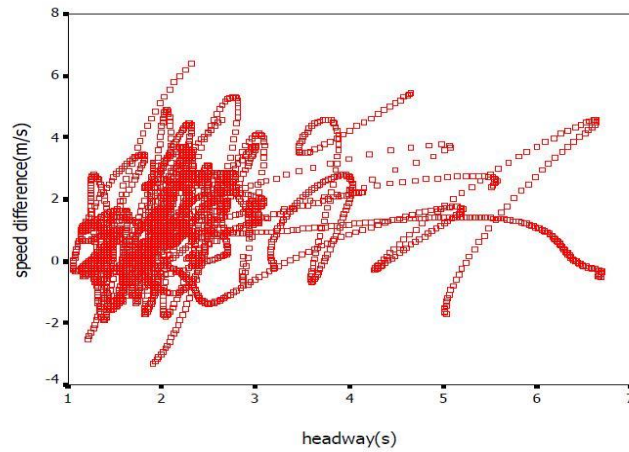


Figure 6: Scattered Points of Speed Difference and Time Headway

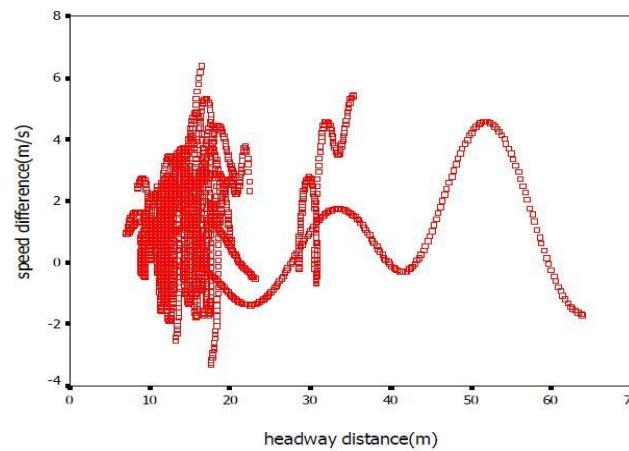


Figure 7: Scattered Points of Speed Difference and Headway Distance

Dey and Chandra used two continuous statistical distribution models, gamma and lognormal, to fit a desired time gap ( $T_X$ ) (Figure 8) and time headway ( $T$ ) (Figure 9) of drivers in a steady car-following state on two-lane roads under mixed traffic conditions. Headway data obtained from simulation runs were analysed to develop a relationship between the desired time gap ( $T_X$ ) and the speed of the vehicles for five categories of vehicles; namely: car, heavy vehicle, motorized two-wheeler, three-wheeler, and tractor. Their research results contribute to developing the micro-simulation models of traffic flow on two-lane highways (Dey & Chandra, 2009). If driver response time could be decreased, the slope of the observed line with the theoretical line will decrease in the following lognormal distribution for the time headway diagram. It means that the car flow rate can reach the theoretical saturation faster and the time gap will become smaller.

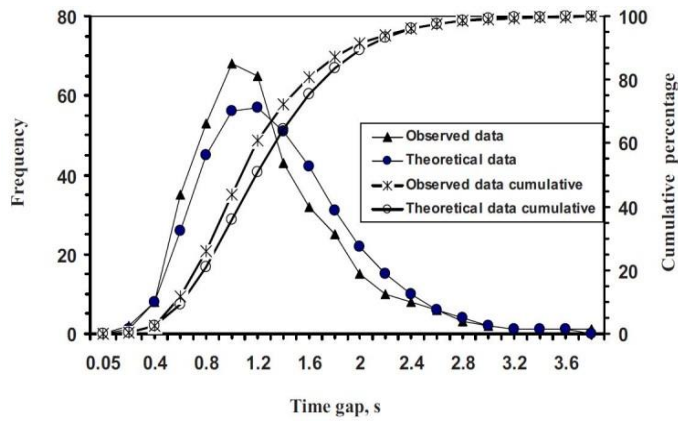


Figure 8: Gamma distribution for desired time gap ( $T_X$ )

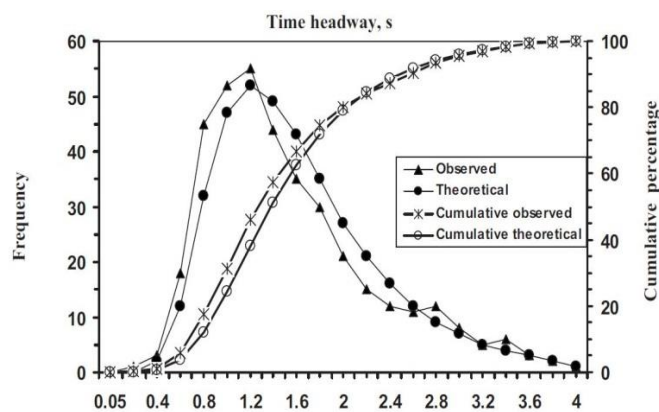
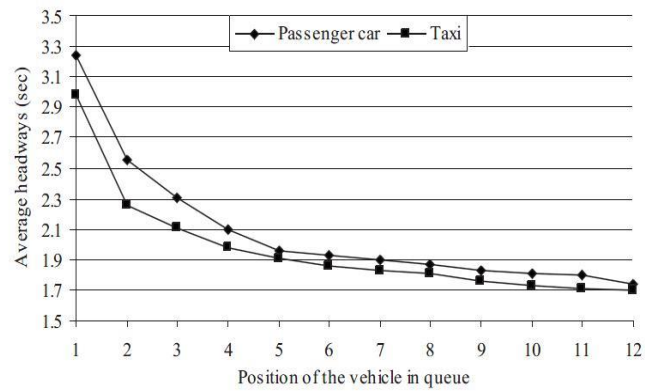


Figure 9: Lognormal Distribution for Time Headway (T)

If the start-lost time could be shortened, it will also adjust the base saturation flow rate for capacity analysis. Rahman, Hasan and Nakamura (2008) state that drivers' behaviour can influence the time that flow rate reaches saturation at signalised intersections. They collected data in Yokohama City, Japan, for a study aimed at developing professional driver adjustment factors for capacity analysis of signalised intersections. As shown in Figure 10, their research results indicate that professional drivers had a significant impact on the saturation flow rate. The researchers wrote that, "The saturation flow rate as well as the capacity could be increased by 20%, which corresponded to a professional driver adjustment factor as high as 1.20" (Rahman, et al., 2008).





Effects of taxi on the headways of queued vehicles

Results of Headway Analysis

Queue position	$H_{TT}$ (s)	$H_{PT}$ (s)	$H_{PP}$ (s)	$H_{TP}$ (s)
2	2.26	2.32	2.55	2.42
3	2.11	2.16	2.31	2.23
4	1.98	2.04	2.10	2.08
5	1.91	1.94	1.96	1.95
6	1.86	1.88	1.93	1.89
7	1.83	1.85	1.90	1.87
8	1.81	1.86	1.87	1.85
9	1.76	1.79	1.83	1.81
10	1.73	1.76	1.81	1.78

Note:  $H_{TT}$ =headway of a taxi following a taxi;  $H_{PT}$ =headway of a taxi following a passenger car;  $H_{PP}$ =headway of a passenger car following a passenger taxi; and  $H_{TP}$ =headway of a passenger car following a taxi.

Figure 10: Development of professional driver adjustment factors for the capacity analysis of signalised intersections

This part of the research uses Japanese data to determine driver response time and to illustrate the second vehicle delay phenomenon. Tang and Nakamura (2007) investigated the discharge patterns at signalised intersections and explored the causes of those patterns using field data collected at 10 intersections in Aichi Prefecture, Japan. In 2010, Tang offered the field data of one intersection (Kobari) to this research. This Kobari field data is given in the following diagram (see Figure 11).

Through the use of countdown timers and other methods, the study of first vehicle response time has already had successful results. This research area, however, focuses on the response and crossing time of the first five leading vehicles in queue at a signalised intersection. The following diagram shows that the first two vehicles cannot reach average flow rate. To counteract this problem, if there can be a decrease driver response time for the second vehicle, consequently the time for the first 4 to 5

vehicles to cross the stop line will be shorter; this will generate an observable impact on the saturation flow rate. This means the slope of the cumulative plot shown in Figure 11 will be steeper.

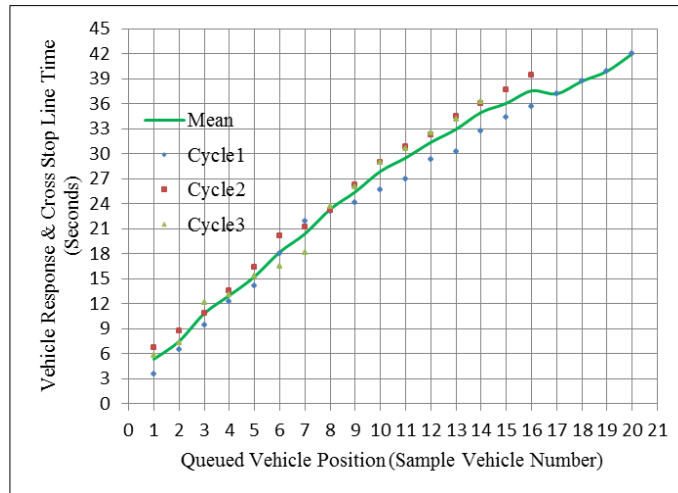


Figure 11: Crossing Stop Line Headway Analysis (Kobari Intersection) Drawn by Shuai YANG

To support the hypothesis of this research, a prediction of the suitable enlarged stopping distance is necessary. Akcelik (2000) recommends that traffic planners: "allow six to seven metres per vehicle storage length for a queue of cars (light vehicles) and nine to fourteen metres for a queue of heavy vehicles. It may be appropriate to use seven metres per car (eleven and a half metres for heavy vehicles) for through traffic lanes and six and a half metres per car (ten metres for heavy vehicles) for turning lanes". Therefore, it is suggested that the second queuing vehicles stopping distance should be eight metres behind the first vehicle to solve the second vehicle delay problem. This distance is recommended as contemporary cars are more powerful than they were historically. This distance will ensure that the second car has enough space to quickly accelerate at the same time as the first car, while still having a good view of the traffic signals. This research examines the efficacy of this suggested distance.

## 2.8 CONCLUSIONS

The core finding from the literature is that there is no current research regarding the enlarged stopping distance assumption, even though the start-up lost time and the second vehicle discharge delay are historic traffic problems. Nevertheless, some of the literature explored above does help in the clarification of this research aim, plan and methodology. Furthermore, the gap between the research assumptions and current queue discharge findings reveals the significant value of conducting this research. The results of this research will enhance the knowledge of the micro-simulation of leading queuing vehicle traffic performance. Several aspects of the literature review's findings are explored below.

From a practical perspective, if we can reduce start-up lost time, the approximate optimum traffic cycle time can also be significantly decreased. Furthermore, this can be done while still ensuring acceptable degrees of saturation. In other words, the number of traffic signal cycle per day can be increased to allow more vehicles to access and pass through an intersection. This is the remarkable value of this research.

From a research methodology perspective, innovative method is one of the most practical applications in the traffic management research area that can be used to solve a traffic problem. Some innovative methods, integrated with traditional transport research approaches, have already been used to generate simple answers to transport management problems. The CFI and Pre-timed signals for the left-turn, for example, have been discussed in this chapter.

With respect to the current research plan, existing departure models oversimplify the characteristics of the four leading drivers' dynamic performance in discharge. Therefore, it is necessary to separately extract each leading vehicle driver's behaviour in the queue discharge process for this research. The separation of driver behaviour and vehicle length is essential for the vehicle dynamic simulation test because the car and driver are two closely related players in the research of queue discharge.

With regard to existing knowledge of discharge patterns, the HCM2010 descriptions state that the second vehicle headway is less than the first vehicle's headway; however, the observed second vehicle delay phenomenon contradicts this. Therefore, using data to confirm the negative performance of various second vehicle drivers in the queue discharge is crucial to the demonstration step. Thus, the demonstration scenarios setup process needs to test the safety distance between each vehicle trajectory and its corresponding velocity. The existing safety-distance models include complex parameters and this limits their application to this research demonstration process. This suggests that a suitable safety distance pattern should be extracted for this research to separately consider each driver's performance at different leading queue positions after perception of a signal change.

From the data analysis perspective, the literature review contributed the GHR model which provides a basic simulation method for this research demonstration plan. After a queuing vehicle's departure converts to car-following, the vehicle's dynamic performances are determined by the preceding vehicle's velocity and safety distance. Thus, extraction of the relative spacing and speed from the data enable checking of the accuracy of this research scenarios simulation. Also, as the data shows, most vehicles do not come to an absolute stop in queue. To address this phenomenon, Fuzzy logic-based model method can be used for the vehicles' safety distance test to determine the vehicle's performance for the terms "Stop" and "Move".

The literature review has illustrated the gap in the current queue vehicle dynamic characteristics research of consideration of the vehicle delay problem in queue discharge. The review of the research into the HCM2010 clearance model reveals that the reduction of the start-up lost time will enable earlier realisation of the saturation flow for a traffic stream. As a result, there is potential to decrease the left-turn blocked time if the opposing lane group lost time  $t_L$  could be shortened. This research demonstration seeks to confirm the accuracy of the hypothesis of this research by traffic simulation. The methodology for this demonstration is introduced in the next chapter.

## **Chapter 3: Data Collection**

---

### **3.1 INTRODUCTION**

The previous chapter introduced the observation of enlarged headways between the first and second vehicle in a platoon, departing from an intersection approach. To investigate this phenomenon further, data has been collected to see if further evidence could be found to support the observation. This chapter gives an overview of the data sources, the data collection, and the data preparation needed to allow for a later analysis. First, data which was chosen due to its specific layout was collection from a local site and was described by a widely used data set in traffic engineering analysis from Georgia, United States. The sections give a background of the data sets, provide details on the collection and demonstrate how the data was prepared to extract the required information.

### **3.2 NERANG DATA**

This research hypothesis can be summarised as that if successive vehicles have ideal clearance distance in which to accelerate, it will shorten the successive vehicle's driver response time so as to improve the start-up lost time problem. Therefore, if there was an existing intersection which has an enlarged stopping distance for the leading queuing vehicles, it will contribute to exploring the changes of the drivers' behaviour that caused by the enlarged stopping distance. In addition, characterise the driver behaviour changes in an enlarged stopping distance situation can express the value to do this research and the reasons are indicated as following.

There are two possible situations would happen if the queuing vehicles' stopping distance were enlarged. First, there is no change to the driver behaviour so the queuing vehicles will use more time to cruise the enlarged stopping distance. Hence, the ESD will negatively effects on the vehicle departure. On the other hand, if driver behaviour changed and driver response time on traffic signal change were shortened, vehicles will use shorter time to achieve saturation flow which means the start-up lost time problem could be improved. Therefore, to find an intersection where has

existing enlarged stopping distance for the leading vehicles in queue will benefit to obtain knowledge of the ESD to the driver behaviour change. The existing “Keep Clear” road marking can force drivers to keep an enlarged clearance distance.

A signalised intersection in Nerang Street on Gold Coast was selected for data collection for two reasons. First, it is a main road intersection in an urban area and one side of the intersection has a “Keep Clear” road marking, while the other side does not. Second, the second reason is that there are no buildings at the surrounding area of the intersection, so the impacts of external factors on drivers’ behaviour are small. The “Keep Clear” site can be used to investigate how an enlarged stopping distance affects the queuing vehicles discharge for an actual traffic lane. This specific discharge sample can then be compared with the data collected from the site on the other side of the intersection. This subsection introduces the background of the Nerang Data, methodologies and process to obtain the data, the cooperation with the staff of the video laboratory of QUT for the raw data extraction, and the Nerang data extraction.

### **3.2.1 Nerang data background**

The Nerang data collection site was found on 28 October, 2010. It is located in Southport, Gold Coast, Queensland, Australia. The study area schematic is shown in Figure 12. The Nerang Data represent traffic flow in Nerang Street and Southport-Nerang Road, an arterial running primarily east-west. The field data collection site is a four directional intersection; the eastern part of the site is Nerang Street, the western part is the Southport-Nerang Road, and the north and south sections constitute Wardoo Street.

This research simply calls the streets going from east to west as Nerang Street, and their data sets are labelled as “Nerang Data”. The speed limit on the Nerang Street and Southport-Nerang Road is 60 kilometre per hour. This field data collection site includes two sections. The east site is labelled “Site I” which has a typical queuing discharge situation; its opposite side is labelled as “Site II” and has a “Keep Clear” road marking.

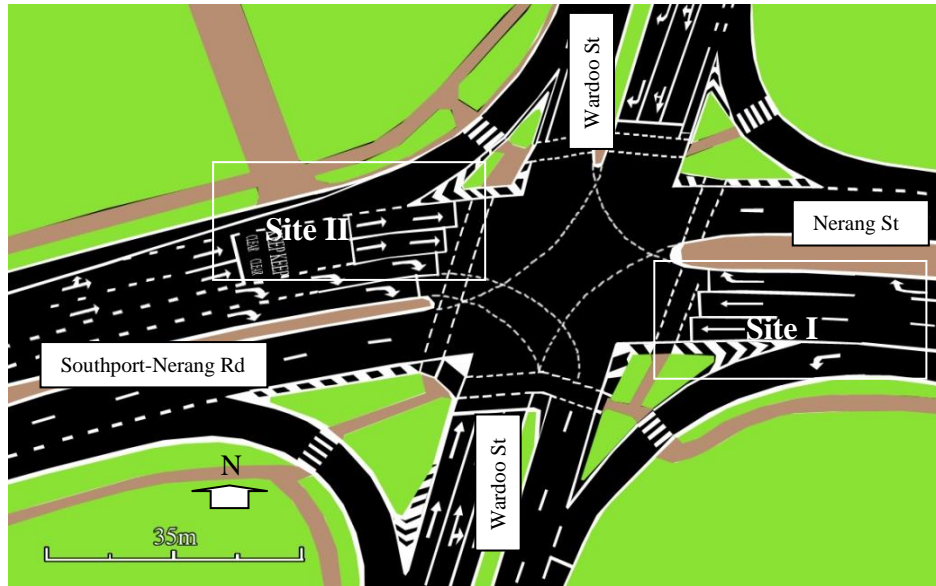
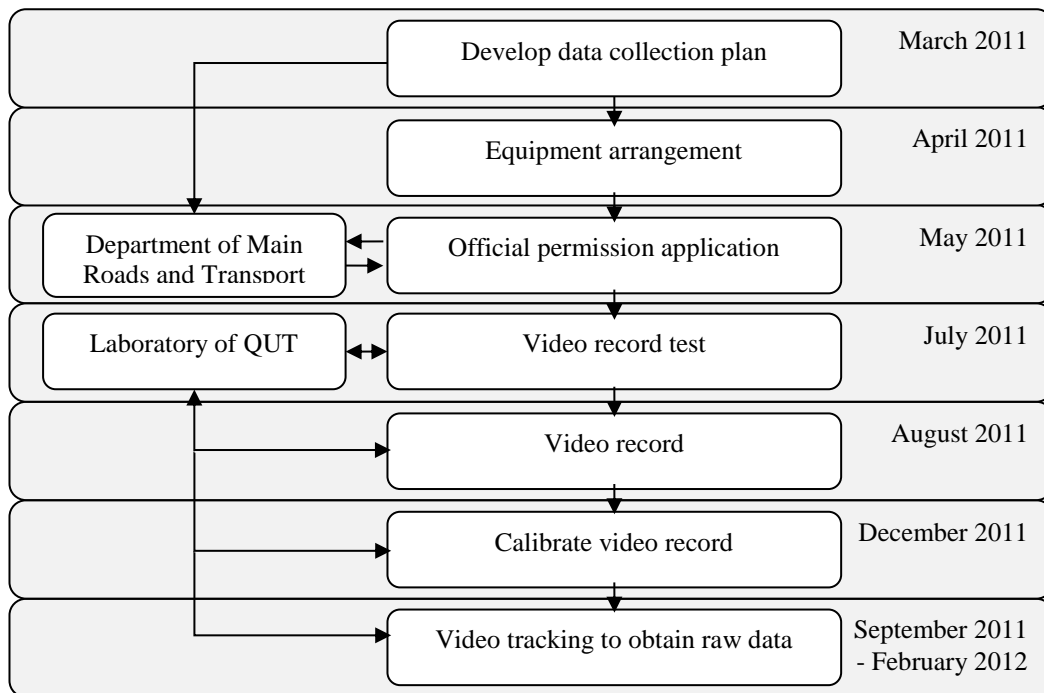


Figure 12: Nerang study area schematic

Table 5: Nerang Data collection timeline



The process of data collection includes seven stages. They are: data collection planning, equipment arrangement, official permission application (see Appendix B), videorecording test, videorecording, calibration of the video recording, and extraction of data from the video (see

Table 5). QUT laboratory staff extracted datasets from the raw videos. However, wind has affected the quality of some raw videos, rendering them unsuitable for data extraction. Therefore, a video data recording calibration step is necessary to annul the negative effect of the wind on the results extracted from the data. The action in calibration step is changing the material of the wind lace for the super height tripod from nylon line to steel wire to avoid the camcorder shaking by wind. Therefore, the video quality can meet the requirement for the tracking process.

### **3.2.2 Video record preparation**

There are various methods widely used for the data survey. These include the manual recording of vehicle dynamic performance, sound recording to identify the traffic flow, and the combination of a stop watch with a camera to generate time space images. In 1947, Greenshields introduced the use of video and a projector to manually extract data for the purpose of conducting traffic performance research at urban signalised intersections (D.Greenshields, et al., 1947). Modern advances in computer vision technology, such as object tracking, have enabled us to automate a large portion of this procedure so that vehicle data can be extracted efficiently from raw video footage. Hence, this research chose a video recording method to collect raw video and then used object tracking methods to extract vehicle dynamic performance data.

The equipment preparation includes four steps: camcorder and lens test, data collection site examination, equipment purchase and construction, and equipment field testing. A wide angle lens is used so that the camcorder can capture five leading vehicles together within the ‘Keep Clear’ area. Therefore, it is necessary to measure the data collection site before purchasing the camcorder and wide angle lens. To avoid distracting drivers, an aluminium camcorder cover is made; this cover can also be used to adjust the pitch angle of the camcorder on the ground. The camcorder is Canon LEGRIA HFM31 and the wide angle lens is Raynox HD-3035PRO (see Figure 13).





Figure 13: Nerang site map measurement and equipment

To avoid the left turn vehicles blocking the nearest through lane vehicles, suitable height for raw video capture is over seven metres after calculation by trigonometric functions from the site map. This height is beyond the capacity of ordinary tripods and to hire a jib crane or articulating booms is costly and inflexible. Therefore, a super high tripod was custom-built for this video survey. This super high tripod is made from a spectrum speaker stands, a paint roller extension pole and a tent pole. A ground battery support monitor is made from a vehicle's electronic rear view monitor (see Figure 14).



Figure 14: Super high tripod and battery supported ground monitor

In May 2011, this field video record survey was approved by the Gold Coast Department of Transport and Main Roads (see Appendix A). After that, the first video record test was carried out and staff of the QUT laboratory examined the quality of the raw video. The videorecording was completed in August 2011. However, unforeseen circumstances occurred: strong winter wind affected the quality of the video. After changing the wind lace of the tripod, a calibrated videorecording was carried out before the end of 2011.

### 3.2.3 Video recording

The Nerang raw videos are collected by using a camcorder which is mounted on a seven metres super high tripod on open land on the roadside. Figure 15 presents a map image of the location with the video camera coverage. Figure 16 presents sample images from the Site I and Site II video sequences. The Site I road has an approximately 10% slope from east to west, but the Site II road is almost flat. Although the criteria for queuing discharge samples extraction are that queuing vehicles should completely stop and that the five leading vehicles' queue length is relatively short, the Site I road slope effects on the dynamic performance is obvious. The times of conducting videorecording were: Site II- 10:30 a.m. to 13:47 p.m. on 12 August 2011; Site I- 11:22 a.m. to 13:19 p.m. on 19 August 2011; and Site II (after calibrated the wind effects) – 8:22 a.m. to 11:29 a.m. on 19 December 2011.



Figure 15: Nerang study area and camera recorder coverage



(a) Nerang Site I.



(b) Nerang Site II.

Figure 16: Sample frames from Nerang each site video sequences

The first time of the raw videorecording test was carried out (in July 2011 and after consultation with QUT teacher Dr Clinton), the second camcorder was used to record the traffic signal timing; hand waves were used as signs in both videos (see Figure 17). The raw videos were uploaded to the service computer in a QUT laboratory on 5 September 2011. Unfortunately, the wind caused negative effects on the Site II video, so another recording was needed. To strengthen the stiffness of the super high tripods, and to decrease the negative effect of the wind, the wind lace material was changed from nylon rope to iron wire. After successfully addressing the wind effects, the Site II video was sent to the laboratory at the end of 2011.



Figure 17: Nerang data camcorder recording signal timing and traffic flow

### 3.2.4 Nerang video tracking

The staff of the QUT laboratory helped to extract the raw data from the raw video using the KLT Tracker approach (Lucas & Kanade, 1981) approach. The video tracking process was completed in February 2012. The Gold Coast video survey took one year and successfully obtained vehicle trajectory data sets for this research. The Site I raw data extraction (extracted from video by the staff of QUT video laboratory

through using KLT method) was completed on 29 January 2012 and after calibrating some errors, the final version was obtained on 17 February 2012; the Site II raw data extraction was completed on 27 February 2012. It was already one year since the preparation work for the Gold Coast data collection had started (7 March 2011). Problems in this data collection stage caused it to run beyond the anticipate time frame, and led to a change in the total research time plan. Therefore, for future work, outside factors (especially human labour factors) need to be carefully considered.

The Nerang data extraction items include:

- Frame ID
- Vehicle ID
- Vehicle Length (m)
- Position (m)
- Velocity (m/s)
- Acceleration (m/s<sup>2</sup>)
- Preceding vehicle
- Following Vehicle ID
- Space Headway (m)
- Time Headway (s)

The time frame ratio is 1/25 second in the Nerang Data; this is more accurate than the Peachtree Data's 1/10 second frame ratio. It means each second includes 25 frames to generate more accurate data than the 1/10 frame ratio. The higher frame ratio can effectively reduce the difference between the estimating trajectories and the real trajectories as the vehicle path is not always straight.

The Site I data sets has five file folds - named as Track1, Track2, Track3, Track4, Track5 - and each file fold has some sequences. The Site II data sets include 52 separate sequences. The front of the car is  $x + (L/2)$ , where  $x$  is the position of the car's centroid, and  $L$  is the car's length. The frame ID of the first frame of each sequence is 0 in the Excel spread sheet. Also, there is a file which includes a signal timing corresponding with the frame number. In the Site I data, each pixel represents 0.03262 metres horizontally. Distances are measured from the right hand side of the

image ( $x=0$  corresponds to the rightmost pixel, and  $x=50.85\text{m}$  corresponds to the leftmost pixel). The stop line is at approximately  $x=44.98\text{m}$  (pixel 180 from the left). The Site II data, each pixel represents  $0.05103$  metres horizontally. Distances are measured from the right hand side of the image ( $x=0$  corresponds to the rightmost pixel and  $x=48.94\text{m}$  corresponds to the leftmost pixel). The stop line is at approximately  $x=42.56\text{m}$  (pixel 125 from the left). In short, this research stage successfully extracts the necessary components for the raw Nerang Data.

### 3.2.5 Nerang data extraction

After obtaining the raw Nerang Data, this step extracted required information for the next research strategies. This subsection starts with a short introduction of the expectations of this stage and follows with an overview of the methodologies and steps of the Nerang Data extraction. A short summary of the data extraction results is given in the last part.

#### *Expectations*

In order to characterise recent vehicle dynamic performance in discharge process, the main aim of this stage is to extract five leading vehicles discharge samples from the raw Nerang Data. After understanding data limitation problem, this step calibrates the raw average discharge patterns. Additionally, this step obtains the Nerang Data vehicle dynamic parameters such as vehicle queue spacing, driver response time, vehicle velocity, and so on. Figure 18 summarises the three steps of the Nerang data extraction.

- a) Obtain raw discharge data
- b) Understand data limitation & formulate average discharge trajectories
- c) Extract vehicle dynamic parameters

Figure 18: Expectations of the Nerang Data extraction

### *Raw discharge samples*

This step extracts raw discharge samples for the listed first aim. The Site I obtain 18 sets of vehicle trajectories and the Site II obtain 31 sets of raw vehicle trajectories. The method employed in this research to obtain the discharge samples is simpler than that employed for the Peachtree data which needs thorough and complex mathematical calculation (introduce in the next subsection). In the Nerang Data extraction process, it is only necessary to convert the Position item data into the distance to the stop line. The formula is the Position data plus the half vehicle length minus the stop line position value.

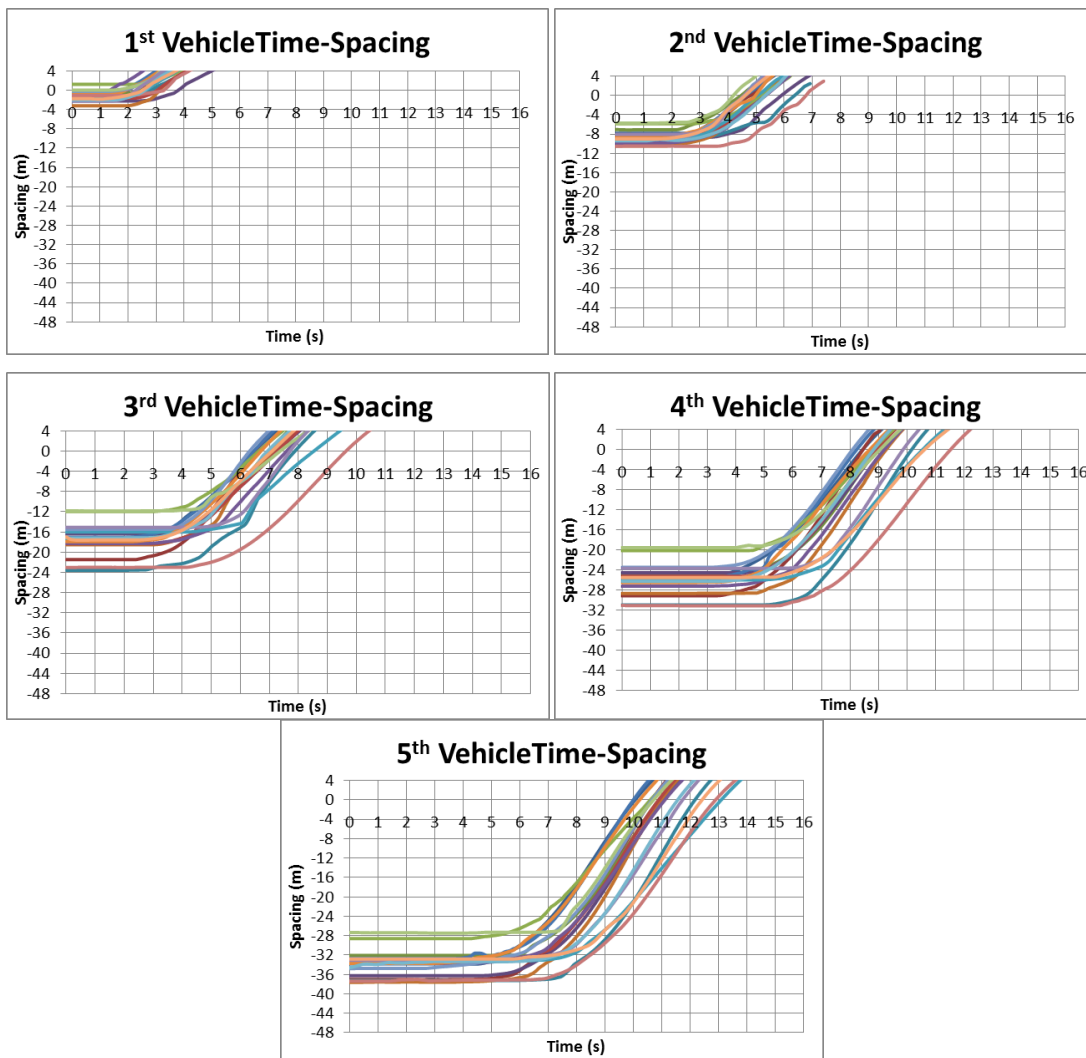


Figure 19: Nerang Site I; 18 sets of vehicle trajectory samples

The criterion for the discharge samples is that only the sequences which include more than five queuing vehicles can achieve the requirement. Results from the raw data yield 18 discharge samples from Site I, and 31 discharge samples from Site II. The results are presented in Appendix C (Nerang Data Site I raw trajectory samples) and Appendix D (Nerang Data Site II raw trajectory samples). The Figure 19 and Figure 20 present the Nerang Data Site I's common queuing discharge samples and Site II's specific queuing discharge samples.

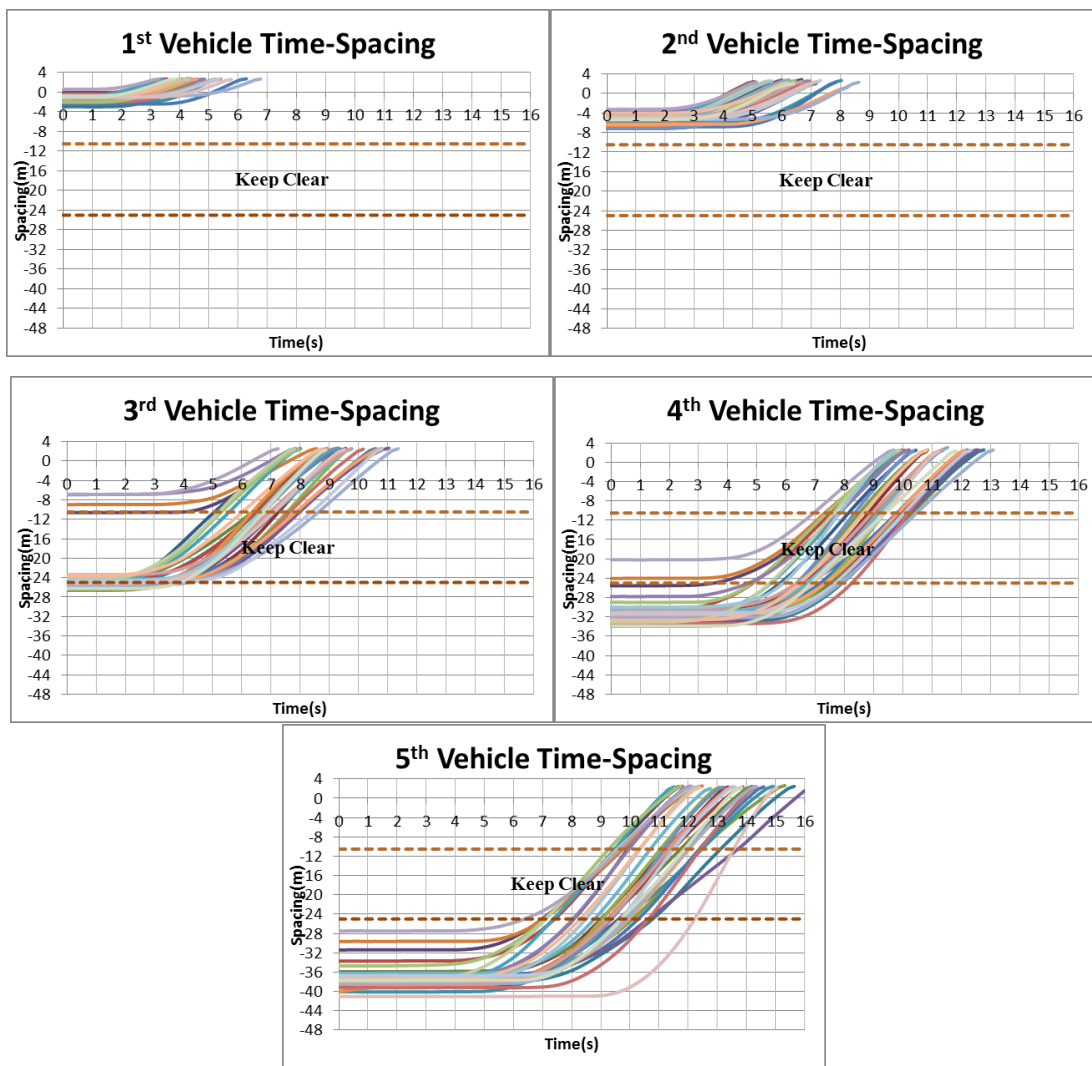


Figure 20: Nerang Site II; 31 sets of vehicle trajectory samples

In each time-spacing graph, the X axis represents the time in seconds and the Y axis shows the distance to the stop line. Green signal onset at  $x=0$  and the stop line at  $y=0$ . For example,  $y = -10$  metres means the vehicle at 10 metres upstream of the stop

line;  $x=5$  seconds means 5 seconds after the green signal onset. Hence, the variation of the Y axis value of two succeeding trajectory curves represents the spacing value. The variable on the X axis at same Y value represents the time headway of two succeeding vehicles.

**Methods and limitation**

To achieve the aim b), this step uses average method to extract raw average vehicle trajectories from the obtained Site I (18 sets) and Site II (31 sets) vehicles discharge samples (see Figure 21). Each sets of vehicles discharge sample is labelled as “E number”. The labelled E05, E09, and E14 samples of the Site I discharge samples include vehicle pulling trailer or truck in queue. Also the Site II discharge samples, the labelled E04, E09, E12, E14, E30, E05, E07, E08, E16, E20, E22, and E25 sets of samples include motor bikes, vehicle pulling trailer, trucks or motorhome in queue. Furthermore, there happen to be three vehicles in the part of the leading queue that is ahead of the “Keep Clear” road marking in the labelled E04, E10, E20 and E26 discharge samples of the Nerang site II Data (see Figure 20 for the third vehicle’s trajectories). By contrast, there are only two vehicles in the part of leading queue that is ahead of the “Keep clear” road marking. Thus, in the average trajectory extraction process, these sets of discharge samples are excluded.

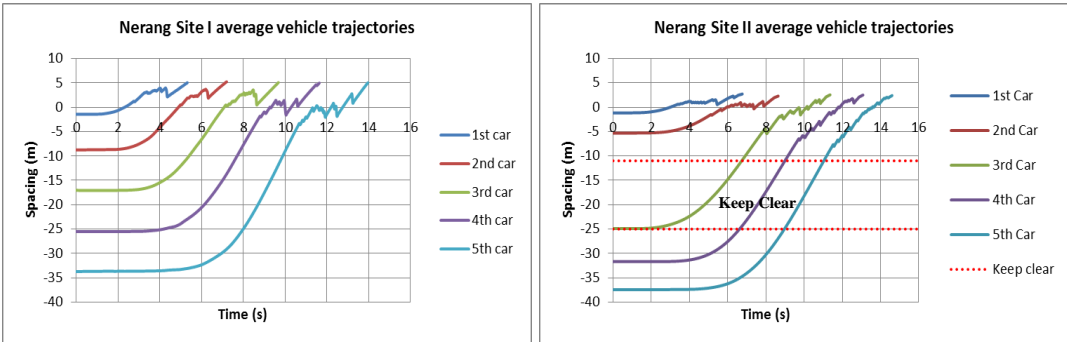


Figure 21: Nerang Site I and Site II raw average trajectories



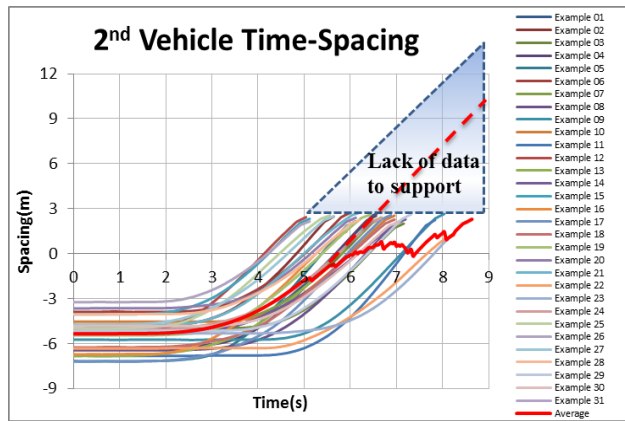


Figure 22: Limitation of the Nerang Data

One limitation of the average method is that the end part of each vehicle's queuing position discharge trajectory appears to wave (see Figure 22). The raw samples data widely vary because the amount of trajectory data suddenly drops as the time line increases. Also, because the raw video only covers the five leading vehicles' queue stream area, only a small part of the intersection beyond the stop line is recorded. This directly means that the data can only include a short time period after each vehicle passes through the stop line. This limitation strongly suggests that future research should use more camcorders to obtain a greater coverage of the site. This would enable vehicle trajectory data to include the time since the vehicle crosses the stop line. This greater time coverage in the data can counteract the variation in the end part of the trajectory.

### *Extract vehicle dynamic parameters*

The process to achieve the aim: c) extract Nerang Data vehicle dynamic parameters is introduced as follows. To avoid the deviation of the raw velocity and acceleration, this step uses time difference distance formula to calculate the velocity. This step extracted eight parameters items: queuing vehicles distance from the stop line (m), driver response time since the green signal onset (s), two successive vehicles' queue clearance (m), two successive vehicles' queue spacing (m), delay in response time (s), two successive vehicles' spacing when the follow vehicle make response to the green signal onset (m) (labelled as spacing') and the preceding vehicle's speed (m/s) (see Appendix E & Appendix F). And then, this step summarises the average vehicle length of the Nerang Data.

For the Nerang Site I data, this step extracts five leading vehicles dynamic parameters according to vehicles' queue position. Driver response time and the corresponding queue clearance are linked together into one graph. Furthermore, two successive vehicles' spacing and the preceding car's speed, at the time when the following vehicle make response to the green signal, are joined into one graph. For the Nerang Site II data, the samples E10 and E26 are different to other samples. There is one more vehicle joined into the leading platoon which followed by the "Keep Clear" road making; while other samples there are only two vehicles in the leading platoon. Therefore, in the Nerang Site II data parameters extraction process, the samples E10 and E26 are put into one category.

On the other hand, different times and locations lead to researchers using various vehicles length data in their research. For instance, Akcelik (2000) recommends allowing 6 to 7 metres per vehicle storage length for a queue of cars. However, with fuel prices increasing, more and more smaller cars are now being used on the roads. Thus, the average car length keeps changing. Therefore, this step calculates the average vehicle length in the applicable trajectory samples from the Nerang Data and the result is 4.15 metres. Details of each sample vehicles' length see Appendix G. This result confirms that it is necessary to keep this vehicle length parameter updated. It also indicates the problems that can arise when each research case uses different data.

### *Summary*

This subsection describes the methodologies and process to achieve the aims for the Nerang Data collection and extraction. Four aims are achieved that: a) from the Nerang Site I Data obtains 18 sets of vehicle trajectories and from the Site II data obtains 31 sets of raw vehicle trajectories; b) the limitation of the Nerang Data is introduced and the raw average discharge vehicle trajectories are extracted from the obtained raw trajectories for the Site I and Site II; c) obtained the Nerang Data vehicle dynamic parameters.

### **3.3 NGSIM PEACHTREE DATA**

The Peachtree Street Datasets are an open access data source and are widely being used in traffic research. According to the NGSIM Community website description ("Peachtree Meta Data," 2007), Peachtree Street Data Set is developed by Cambridge Systematics Inc. as part of the Federal Highway Administration's Next Generation Simulation project. This data characterizes a thirty minute video that consists of two time periods. Registered members have free access to these data sets.

#### **3.3.1 NGSIM data background**

As an important part of the Federal Highway Administration's (FHWA) Next Generation Simulation (NGSIM) project, Peachtree Data provides datasets of arterial vehicle trajectories on a segment of Peachtree Street in Atlanta, Georgia. The Peachtree Data includes two components which separately present vehicle trajectories during 12:45 p.m. to 1:00 p.m. and 4:00 p.m. to 4:15 p.m. on November 8, 2006. The raw data offer detailed trajectory data, wide-area detector data and supporting data. Two data analysis report indicate the aggregate summaries of flow and vehicles' velocities, number of lane changes, and analysis of the headway and gap.

The researcher registered as a member of the Next Generation SIMulation (NGSIM) Community website on 20 July 2010. The members of this website can obtain basic access to the documents, data and research which are created by the NGSIM Program and Community. Therefore, the Peachtree Data collection process is simple that directly download the data files from the Next Generation SIMulation (NGSIM) Community website. After completed data collection, this research starts to do data extraction process.

#### **3.3.2 Known issues of NGSIM data and Mitigation**

Since this data set was published, many authors have reported its shortcomings. For instance, Dixon et al. (2010) announced that some errors in the NGSIM Peachtree Street data lead to it being difficult to obtain the location of the stop bar. Vincenzo et

al. (2009) also stated that this dataset included many mistakes in data items; for example, vehicle velocity continued appeared as zero even when raw video showed the vehicle was accelerating. These limitations of the Peachtree Data mean that this research applies rigorous and practical caution to its using.

There are 25 samples generated in the previous steps of the data extraction process; however, some of them have errors and need to be removed. The method is to use a Time-Spacing graph to compare the samples with the raw video clips. The results show that four samples have errors which may have been caused by the movement of the tracking boxes. Hence, there are only 21 samples that reach the required standards of this research. Indeed, the main limitation of the Peachtree Data with respect to this research is that it cannot offer more discharge sequences for the departure model research work.

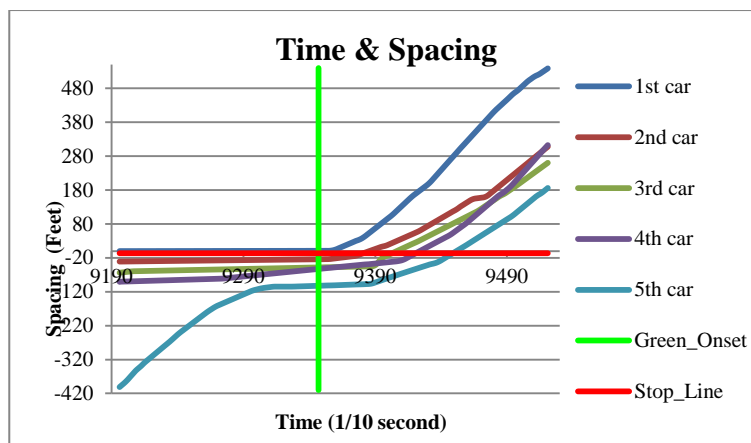


Figure 23: Error sequence sample

Figure 23 presents an error example which was recorded at the intersection of N-Peachtree Street and 11<sup>th</sup> Street, on the 10<sup>th</sup> traffic timing cycle. The Time and Spacing graph of the raw data shows that a collision occurred between the 2<sup>nd</sup>, the 3<sup>rd</sup>, and the 4<sup>th</sup> cars; this is represented by these cars' trajectories curves crossing over each other. However, the raw video record is completely different to this presented data.

This step introduces a method to identify the stop line location and explains the procedure employed to obtain this important component. For example, the lack of stop line location information led to Dixon’s (2010) research in the area being unsuccessful. It also causes confusion in the early stage of the Peachtree Data analysis. It is a significant challenge to find the stop line location when first time confronted by the mass of Peachtree data. The important point is that the Peachtree Data uses an AutoCAD file to show the whole site map and this has stop lines (the NGSIM data offered stop line location to user using Peachtree-Main-Data/ cad-diagram/ Atlanta-Peachtree.dwg). To check the accuracy of the stop line location, the AutoCAD software is used to import the Peachtree image into the CAD map and the stop line location accuracy is then confirmed. The stop lines on the CAD file drawings are the same to the stop lines are shown in the whole site photo.

The following step determines the method for matching the time frame number with the vehicle crossing the stop line at the time. The authors of the Peachtree Data used the change of the “section” item number to justify the vehicle entering and exiting each “intersection”. (The Peachtree Data study area includes five intersections which are numbered from 1 to 5 in the “Intersection” data item; Peachtree Street is further divided into six sections between neighbouring intersections which are named from 1 to 6.) Hence, it is necessary to examine whether the vehicle time location change corresponds to the section item change to intersection item when the vehicle is crossing over the stop line.

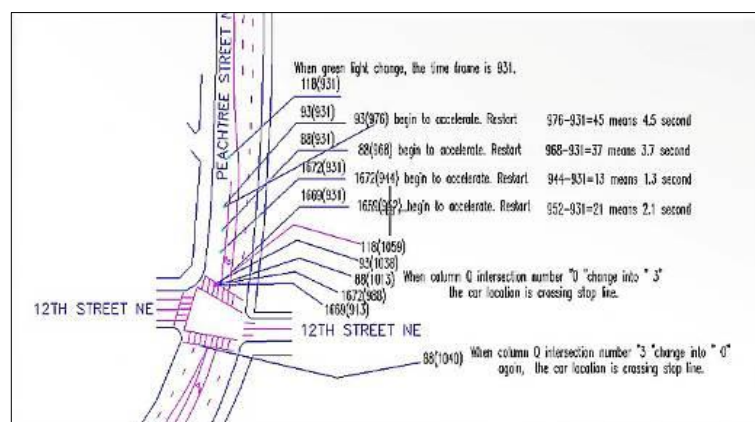


Figure 24: Using AutoCAD to test the data accuracy

The AutoCAD software is again used to import one vehicle each time location point into the Peachtree Data CAD site map. The significant finding is that the vehicle location exactly corresponds with the section item number change as the vehicle cross over the stop line. Thus, the challenge question has been solved by the time frame number when the section number change is the accurate time of the vehicle crossing the stop line. Detail is illustrated in Figure 24.

When putting two succeeding vehicles' time location points into the CAD map in the step above, the distance between these points presents the spacing between these two vehicles. However, the Peachtree Data headway (m) data have various errors, as indicated in Vincenzo et al. (2009). This step also confirms that the Global location data item are accurate. This is easy to understand because the Peachtree Data provides its GIS system file. The shortcoming of the Peachtree Data is that it does not directly use its accurate Global Location Data to calculate and obtain its headway (m) data (The spacing is labelled as headway (m) in the Peachtree Data).

Overall, this research uses the Global Location Data item, using raw Global X and Global Y data in terms of trigonometric function, to calculate spacing between each vehicle, and to then extract each vehicle's accurate trajectory. This step is different to Dixon's method, which only used Local Y data as vehicle spacing to generate vehicle trajectory.

### **3.3.3 Peachtree data extraction**

This subsection starts with a short introduction of the expectations of this stage and follows with an overview of the methodologies and steps of the Peachtree Data extraction. A short summary of the data extraction results is given in the last part.

#### ***Expectations***

To characterise Peachtree Data vehicle dynamic performance in discharge process, the main aim of this stage is: a) extract five leading vehicles discharge samples from the raw data. After get discharge samples, this step: b) obtains the Peachtree Data

vehicle dynamic parameters such as vehicle queue spacing, driver response time, vehicle velocity.

### *Methods and steps*

The scope of this research is using the first five leading queuing vehicles, because queue clearance achieves saturation flow rate after five vehicles. Therefore, only the sequences which include more than five queuing vehicles can be used for this research.

A check of the raw videos of all five intersections shows that only the datasets collected on the Peachtree Street and 11<sup>th</sup>, 12<sup>th</sup>, and 14<sup>th</sup> Street from 4:00 p.m. to 4:15 p.m. are suitable for data extraction requirements. The reason is that there were not many vehicles passing through Peachtree Street when the data were collected at noon. Also, the fact that many vehicles changed direction also made other intersection data unsuitable for this research.

Moreover, the objects of this research are limited to passenger cars. From raw data column of vehicle classes, only the data belonging to the “class 2 auto” are extracted. Hence, the first step- to identify the suitable date from the datasets- is accomplished. The result of this step was that only 25 sequences could be selected. However, in confirmation of other researchers’ claim that the Peachtree Data included many mistakes, four sequences have clear error after compared with raw video records. Hence, there are only 21 discharge samples achieving the requirement.

The second step needs to re-establish each sequence through review of the raw video clips. The Peachtree Data raw video offers a tracking box with the vehicles’ ID numbers. Separate items of the raw data are categorised under a vehicle’s ID. Therefore, in terms of samples extraction, it necessary to put every sequence of five cars together in real queuing orders and to remove unnecessary data items.

For example, there is a discharge sample labelled as ‘E02’ in this research which presents the car’s departure at the intersection of Peachtree Street and 11<sup>th</sup> Street during the traffic timing Cycle 4. The raw video presents the first five leading cars

labelled as 399, 419, 420,443, and 449. This step extracts the data belonging to the section item number changed from 2 to 3 for each car. This means that the data was recorded at this intersection. These data are then combined as the raw data for the sample 'E02'. Moreover, the units of measure are also changed from feet to metres.

The next step is to generate each vehicle's trajectory and to present it in a time-spacing graph. From the green time document, it is easy to identify the frame number according to the green signal onset time. Therefore, it is possible to obtain the trajectories based on the items in the frame number and the spacing data. Dixon et al. (2010) believe that the headway data include many errors and that the data do not offer the information about the stop line location. While Dixon's former statement is confirmed by this research data test, this research also makes detection with respect to the stop line location. It does this by showing the right way to obtain the stop line location from the Peachtree Data. This step also confirms the accuracy of the variation in the Global location X and Y data and the Section data item. Consequently, by following trigonometric function to calculate the Global X and Y data from the Peachtree Data extraction, this research obtains 25 queuing car discharge samples.

### ***Raw discharge samples***

This sub-step achieves the first aim of the data extraction of obtaining vehicles discharge samples. The methods discussed above lead to the successful extraction of 21 applicable queuing vehicle discharge samples from the Peachtree Data. All of these samples use Time-Spacing graphs to present in the last chapter Appendix H: Raw discharge samples. Figure 25 below uses Sample 04 to illustrate and explain the graphs.



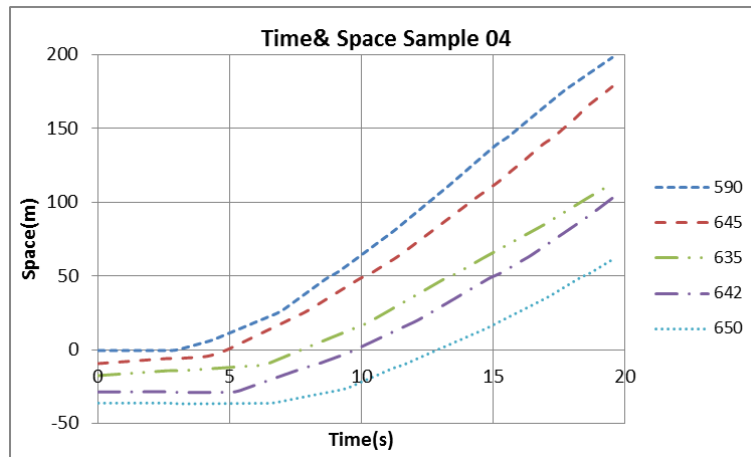
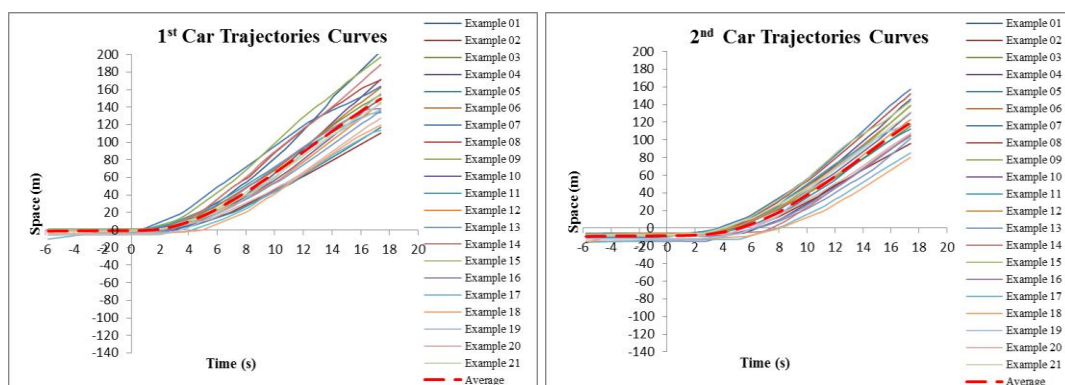


Figure 25: Time-Space graph sample 04

First, there are five curves, named as 590, 645, 635, 642, and 650. Each number corresponds with a car's ID number in the Peachtree Data, and each curve separately illustrates the traffic trajectory of each car. The X axis represents the time in seconds and the Y axis shows the distance to the stop line. Green signal onset at  $x=0$  and the stop line at  $y=0$ . For example,  $y=-10$  metres means the vehicle at 10 metres upstream of the stop line;  $x=5$  seconds means 5 seconds after the green signal onset. Hence, the variation of the Y axis value of two succeeding trajectory curves represents the spacing value. Figure 26 presents 21 sets of Peachtree data five leading vehicles discharge samples and the red dash line indicates the average trajectory.



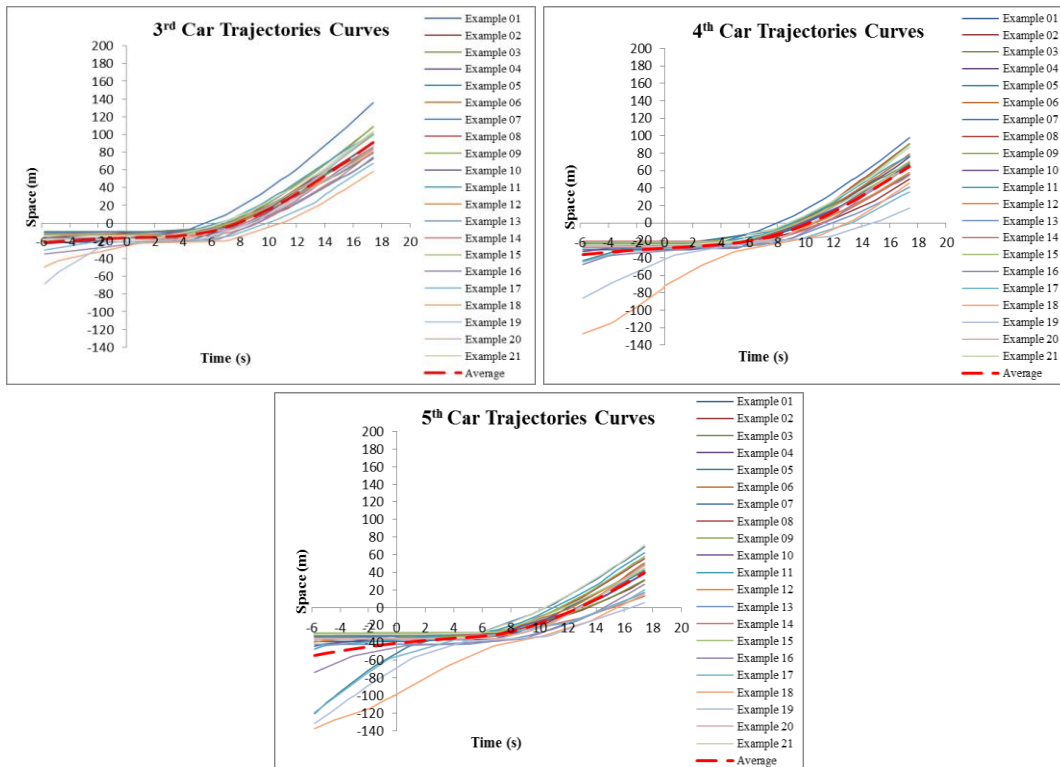


Figure 26: Peachtree Data; 21 sets of vehicle trajectory samples

***Extract vehicle dynamic parameters***

This step achieved the second aim of extracting Peachtree Data vehicle dynamic parameters. This step extracted eight parameters items: queuing vehicles distance from the stop line (m), driver response time since the green signal onset (s), two successive vehicles’ queue clearance (m), two successive vehicles’ queue spacing (m), delay in response time (s), two successive vehicles’ spacing when the follow vehicle make response to the green signal onset (m) (labelled as spacing’) and the preceding vehicle’s speed (m/s) (see Appendix I). This step summarises the average vehicle length of the Peachtree Data.

In the obtained 21 sets of vehicle trajectories, some samples are not suitable for the parameters extraction. This is due to that some vehicles are in an unsaturated situation where they are simply decreasing speed and preparing to stop when the signal changes to green. These cars then accelerate after obtaining enough safety distance corresponding to the preceding vehicle’s velocity. These cars’ trajectories are clearly unreasonable to use them to describe ordinary queuing vehicles departure

which assumes that all vehicles waiting for the green signal onset are in a saturated situation. Therefore, some vehicle discharge samples need to be removed. Hence, the labelled as E16, E17, E18, and E19 samples are not included in this parameters extraction process.

This research then yields average vehicle length for determination of the queue discharge performance. An important factor is that this average vehicle length parameter is appropriate to the Peachtree Data. This research acknowledges that vehicle average length is not a constant value and needs to be determined for varying research purposes. In the 21 sets of Peachtree Data vehicles trajectories, the average car length is 4.93 metres. For quality purposes, this step also manually calibrates each vehicle length item data for comparison with the raw video. Appendix J presents the results.

### *Summary*

This subsection describes the methodologies and process to achieve the aims in the Peachtree Data extraction step for this research. The two predetermined aims are successfully achieved is that there are 21 applicable discharge samples are extracted from the Peachtree Data which are labelled as E01 – E21 and five leading vehicles discharge dynamic parameters are obtained.

## **3.4 CHAPTERS' CONTRIBUTIONS**

### Outcomes

- Achieved raw data collection and extraction process aims for the research plan b) data collection and c) data extraction.

### Key findings

- Obtained five leading vehicles discharge samples from the Nerang Site I, Site II Data and Peachtree Data
- Extracted vehicles dynamic parameters from the above datasets

### Limitations

- The limitation of the Nerang Site I and Site II Data collection led to these datasets not being able to provide the vehicle trajectories after crossing over the stop line.
- The Peachtree Data include many errors as many researchers have reported. Hence, extracted raw data needs to be adjusted to obtain more accurate vehicle trajectories.

# **Chapter 4: Modelling of Vehicle Departure**

---

## **4.1 INTRODUCTION**

The previous chapter described the data sources and data collection performed for this study. The local data from Nerang, at intersections with and without a “Keep Clear” road marking, and the data from NGSIM’s Peachtree arterial are processed to extract all necessary parameters to create vehicle trajectories that can be used in further analysis. This chapter starts with an exploration of the second vehicle delay phenomenon. The chapter then explores the “Keep Clear” road marking effects in driver behaviour and vehicle discharge. The data analyses attempts to identify the mechanisms that are behind the observed phenomenon on the second driver’s delay. The chapter also offers analysis of the discharge pattern from the Peachtree data. Finally, the chapter summarises the findings from Nerang data and Peachtree data separately, and uses the Intelligent Driver Model (IDM) to simulate the ESD scenarios to complete the demonstration process.






## **4.2 EXPLORATION OF THE SECOND VEHICLE DELAY**

The aim of this subsection is to reveal the relation between the second vehicle delay phenomenon and the traditional start-up lost time problem in the queuing vehicle discharge process.

### **4.2.1 Video record survey of queue discharge**

In Section 1.3 research problem introduction, evidence for the second vehicle delay only uses data from Brisbane. To offer more visual evidence for the second vehicle delay phenomenon in queue discharge, further video recording of the queuing vehicle departures at urban signalised intersections was conducted in Brisbane, Melbourne and Sydney (Australia).

Table 6: Video record survey of the second vehicle delay phenomenon

Video clips	Record date & place	Aim
	21 August 2008, Vulture Street and Grey Street, Southbank, Brisbane. Recorded by Shuai Yang	Different time but same location
	16 November 2010, Vulture Street and Grey Street, Southbank, Brisbane. Recorded by Shuai Yang	Different time but same location
	20 September 2008, Nicholson Street and Victoria Street, Melbourne. Recorded by Shuai Yang	In the same city and same day but different location
	20 September 2008, Brunswick Street and Victoria Parade, Fitzroy, Melbourne. Recorded by Shuai Yang	In the same city and same day but at different location
	26 July 2010, Broadway and Abercrombie Street, Ultimo, Sydney. Recorded by Haoyao Zhang	Different time and different location

To ensure the accuracy of this survey, the video recording is based on the following three criteria: different time and different location, different time but same location, in the same city on the same day but different location. To avoid affecting drivers, this survey used a mobile phone to record the video clips which only captured the vehicle discharge process during one signal phase when the researcher arrived at the intersection. Some clips are recorded in Melbourne in 2008, and the Sydney video is recorded by a friend Haoyao Zhang. For future consideration, one limitation of this research is that it only focuses on exploring the second vehicle delay phenomenon in Australia. Hence, it is proposed to widely conduct this research in other countries in the future.

Table 6 indicates that the second vehicle in the queue generally starts to accelerate a few seconds after the first vehicle, while the third vehicle accelerates almost at the same time as the second. Therefore, the second driver response time is longer than that of other drivers. In the Brisbane case, the problem still exists, even two years on.

The video in the Sydney case indicates that the second taxi driver, a professional driver, starts to accelerate only when the first vehicle has crossed the stop line. However, the survey only offers visual evidence, so it is necessary to conduct quantitative measurements and analysis to support this research. The research problems of this study are again strengthened.

#### 4.2.2 Data analysis of second vehicle delay

Traditional methods use headway to measure queuing vehicle dynamic performance at signalised intersections (J A Bonneson, 1992; Fairclough et al., 1997; Jin et al., 2009; Lee & Chen, 1986). Greenshield et al. (1947) stated that driver response time to signal change and response time between successive vehicles should be calculated independently in discharge process research. Therefore, this research explores each queuing vehicle's dynamic performance in the discharge process by considering two aspects: the time it takes the driver to perceive a signal change (or obtain safety distance to accelerate) and react, and the time it takes the vehicle to start to move and crosses the stop line.

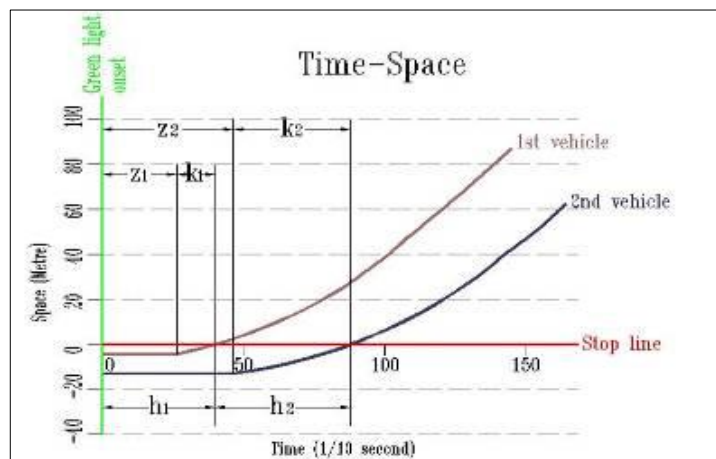


Figure 27: Relationship  $z_i$  &  $k_i$  with  $h_i$

These two components are separately symbolised as  $z_i$  and  $k_i$  in this thesis. This research also uses  $h_i$  to represent the time for the  $i^{\text{th}}$  vehicle to cross the stop line from the queuing position from the onset of the green signal. Thus, the time of  $z_i$

added to  $k_i$  equals the time  $h_i$ . The headway at the stop line will be  $h_i$  minus  $h_{i-1}$ . Figure 27 presents the relationship between  $z_i$ ,  $k_i$  and  $h_i$  (Yang & Chung, 2012).

To characterise the leading vehicles' dynamic performance in the discharge process, this stage uses the obtained Peachtree Data five leading vehicles' dynamic parameters to explore the second vehicle delay phenomenon. Typically, most departure models use average methods to obtain driver response time, mainly because the variation of driver response time is presumed to be small. Thus, the definition of the term "Stop" (less than 5 km/h) criterion is used to extract the driver response time. Table 7 presents the five leading queuing vehicles' average response time  $z_i$  and the headway. This stage uses average times to measure the time that the vehicle spends in moving from queuing position to the stop line (the time  $k_i$ ). Using average time for this research can cover most common samples because, with the exception of the first vehicle, each queuing vehicle needs to have a safety distance before it can accelerate.

Table 7: Peachtree Street data set yield time  $z_i$  &  $k_i$

Vehicle position	Response time $z_i$ (Second)	Time to cross the stop line $k_i$ (Second)	Total time (Second)	Headway (Second)
The first five queued vehicles at signalised intersections	The time the vehicle starts to move from green onset	The time the vehicle takes to cross the stop line from queue position	The total time the vehicle takes to cross the stop line from green onset	The headway between each vehicle
1 <sup>st</sup> vehicle	1.5	0	1.5	1.5
2 <sup>nd</sup> vehicle	2.7	2.0	4.7	<b>3.2</b>
3 <sup>rd</sup> vehicle	3.3	4.2	7.5	2.8
4 <sup>th</sup> vehicle	4.3	5.5	9.8	2.3
5 <sup>th</sup> vehicle	6	6.3	12.3	2.5

In this step, the Peachtree Data study reveals that the time  $z_i$  and the average time  $k_i$  are regressed to generate the headway time. The waving trend in driver response time ( $z_i$ ) in the above analyses reveals that the driver response time is not a constant parameter, and a significant headway exists between the first and the second vehicle. This fits the observed visual display (see Section 4.2.1, Table 6).



### 4.3 NERANG DISCHARGE PATTERNS

The main aim here is to obtain five leading vehicle discharge patterns through the following steps. Each driver response time is extracted from the raw data, using 5 km/h as the definitions for the terms “stop” and “move”. As the Nerang Data time ratio is 1/25 second, the 5 km/h is equal to 0.0556 m per 1/25 second. This criterion is used to extract the driver response time. Consequently, each vehicle’s trajectory can be divided into queue waiting and acceleration phases. The Nerang Data Site I and Site II five leading queuing vehicle discharge patterns are generated by using the Excel Trendline Options from the average five leading vehicle trajectories which have excluded the end waving parts of the trajectory curve (see Figure 28).

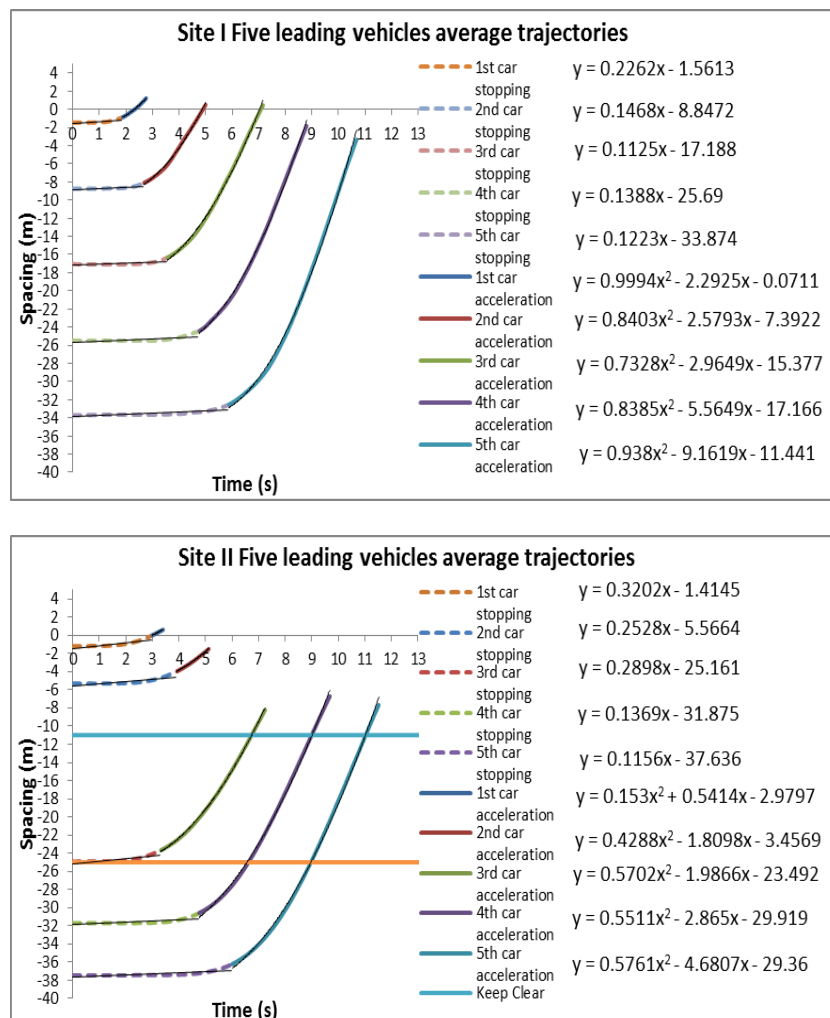


Figure 28: Nerang data raw average five leading vehicle discharge patterns

As there is limitation of the Nerang Data, this step calibrates the obtained vehicles average discharge patterns. The average time of the vehicles crossing the stop line can be calculated by using the obtained discharge patterns and also can be directly averaged out from each discharge sample. The second method is accurate and the deviations from these two methods are used to evaluate the accuracy of the Nerang Data five leading vehicles average discharge patterns (see Table 8).

Table 8: Two methods to obtain the time of vehicles crossing the stop line

Nerang data	Time for vehicle crossing the stop line (s)					
	Queue position	1 <sup>st</sup> Car	2 <sup>nd</sup> Car	3 <sup>rd</sup> Car	4 <sup>th</sup> Car	5 <sup>th</sup> Car
Site I	Calculated by discharge patterns	2.32	4.87	7.03	8.93	10.89
	Averaged from data	2.37	4.91	7.09	9.03	11.04
	Deviation	<b>0.05</b>	<b>0.04</b>	<b>0.06</b>	<b>0.1</b>	<b>0.15</b>
	Calibrated discharge patterns	2.37	4.91	7.09	9.03	11.04
Site II	Calculated by discharge patterns	2.99	5.65	8.39	10.41	12.28
	Averaged from data	3.16	5.69	8.49	10.76	12.67
	Deviation	<b>0.17</b>	<b>0.04</b>	<b>0.1</b>	<b>0.35</b>	<b>0.39</b>
	Calibrated discharge patterns	3.16	5.69	8.49	10.76	12.67

Note: the discharge patterns are vehicle acceleration equations in Figure 28; the calibrated discharge patterns are equations in Table 9 and Table 10.

Furthermore, the deviations are used to manually calibrate those parameters of the obtained vehicle discharge patterns in Figure 28 to make them more accurate. Consequently, Nerang Data Site I and Site II first five leading queuing vehicle discharge patterns are accurately expressed (see Table 9 and Table 10). A limitation of these obtained discharge patterns is that they only accurately indicate queue dissipation up until the point where the vehicles are just over the stop line.

For example, the acceleration phase of the Site I the first car discharge pattern is  $y=0.9994x^2-2.2925x-0.0711$  in the raw discharge patterns (see Figure 28) and if  $y=0$ ,  $x=2.32$ . This means the first car crosses the stop line at a time of 2.32 seconds. In contrast, the average time of the first car to cross over the stop line from each of the car discharge sample is 2.37 seconds. Moreover, the above equation is manually calibrated as  $f(x) = 0.9794x^2 - 2.2925x - 0.0711$ , so as to make its calculation result consistent with the averaged method result. Using this method, Site I and Site II five leading vehicle discharge patterns are calibrated. The Nerang Site I data five leading

vehicle discharge patterns are labelled as B1, B2, B3, B4 and B5, while the Site II patterns are labelled as C1, C2, C3, C4 and C5 in this thesis.

Table 9: Nerang Site I data average five leading vehicle discharge patterns

Patterns ID	Queue position	Time x in seconds with distance to the stop line f(x) in metres. Green onset at time x=0 and stop line located at f(x) =0.	Conditions
B1	1 <sup>st</sup>	$f(x) = 0.2262x - 1.5613$	$x \leq 1.9s$
		$f(x) = 0.9794x^2 - 2.2925x - 0.0711$	$x > 1.9s$
B2	2 <sup>nd</sup>	$f(x) = 0.1468x - 8.8472$	$x \leq 2.7s$
		$f(x) = 0.8323x^2 - 2.5793x - 7.3922$	$x > 2.7s$
B3	3 <sup>rd</sup>	$f(x) = 0.1125x - 17.188$	$x \leq 3.6s$
		$f(x) = 0.7238x^2 - 2.9649x - 15.377$	$x > 3.6s$
B4	4 <sup>th</sup>	$f(x) = 0.1388x - 25.69$	$x \leq 4.8s$
		$f(x) = 0.8265x^2 - 5.5649x - 17.166$	$x > 4.8s$
B5	5 <sup>th</sup>	$f(x) = 0.1223x - 33.874$	$x \leq 5.9s$
		$f(x) = 0.924x^2 - 9.1619x - 11.441$	$x > 5.9s$
Note: If speed is <5 km/h, the car is looked as 'stop', otherwise the car is 'moving'.			

Table 10: Nerang Site II data average five leading vehicle discharge patterns

Patterns ID	Queue position	Time x in seconds with distance to the stop line f(x) in metres. Green onset at time x=0 and stop line located at f(x) =0.	Conditions
C1	1 <sup>st</sup>	$f(x) = 0.3202x - 1.4145$	$x \leq 3.0s$
		$f(x) = 0.127x^2 + 0.5414x - 2.9797$	$x > 3.0s$
C2	2 <sup>nd</sup>	$f(x) = 0.2528x - 5.5664$	$x \leq 3.9s$
		$f(x) = 0.425x^2 - 1.8098x - 3.4569$	$x > 3.9s$
C3	3 <sup>rd</sup>	$f(x) = 0.2898x - 25.161$	$x \leq 3.3s$
		$f(x) = 0.5602x^2 - 1.9866x - 23.492$	$x > 3.3s$
C4	4 <sup>th</sup>	$f(x) = 0.1369x - 31.875$	$x \leq 4.8s$
		$f(x) = 0.5248x^2 - 2.865x - 29.919$	$x > 4.8s$
C5	5 <sup>th</sup>	$f(x) = 0.1156x - 37.636$	$x \leq 6.0s$
		$f(x) = 0.5521x^2 - 4.6807x - 29.36$	$x > 6.0s$
Note: If speed is <5 km/h, the car is looked as 'stop', otherwise the car is 'moving'.			

#### 4.4 THE 'KEEP CLEAR' ROAD MARKING EFFECTS

The "Keep Clear" pavement markings are predominantly used to improve access from side roads onto a main road in Australia (DTEI, 2010; Office of Legislative Drafting, 2009). If a 'Keep Clear' road marking is positioned close to a signalised

intersection, the enlarged stopping distance created by this road marking can be used to reveal the effects on those vehicles queuing behind the marking. Therefore, this research used the “Keep Clear” pavement markings as a case study to investigate the ESD effects in a real situation. This subsection introduces how the “Keep Clear” road markings, change a driver’s behaviour whose queuing position is located behind this road marking. It also uses discharge samples to introduce the effects of this road marking on the vehicle velocity and explores the effects in the vehicle discharge process.

#### 4.4.1 Effect on driver behaviour

To personally experience the “Keep Clear” road marking, the researcher drove a car many times to cross the intersection of Nerang Street and Wardoo Street on the Gold Coast. As this measure depended on the occasional opportunity to stop behind the “Keep Clear” road marking, the rate of successfully capturing the discharge process was very low. There were only a few videos that were recorded from the driver’s position using a mobile phone video function. Two clips were obtained on 01 November 2010, another two (separately) on 04 November 2010 and 17 November 2010. Here are two clips that can be used to show the queuing vehicles discharge process. Two images from one video clip illustrate how the “Keep Clear” road marking work to reduce the start-up loss; or, in other words, how the ESD is working. The Figure 29 clips show that the third car in the left through-lane only takes 8 seconds to pass through the stop line after the signal changing to green, while on the right through-lane, the green “mini” uses only 6 seconds.

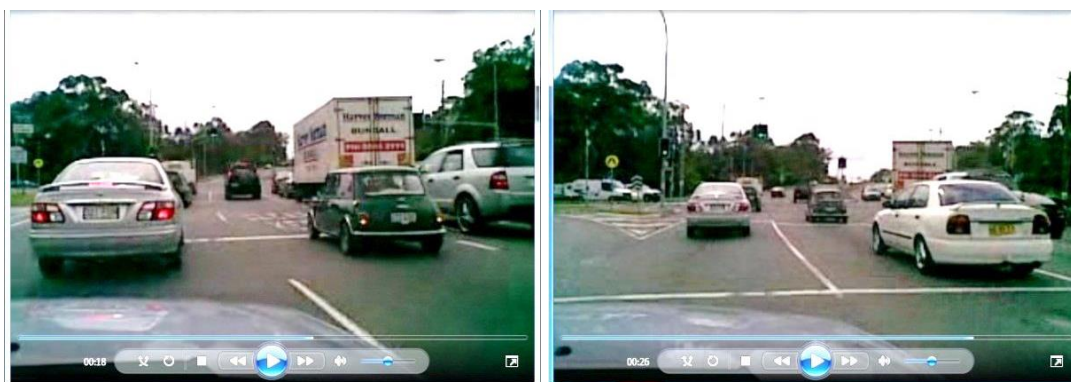


Figure 29: Nerang Data II clips

The above visual image shows that a “Keep Clear” road marking does not present negative effects on the queuing vehicle discharge process. Contemporary departure models assume that queuing vehicle drivers almost always exhibit the same driving behaviour. As a result, vehicle trajectories will present as parallel curves. Hence, if a “Keep Clear” road marking causes the clearance (in metres) to be increased, the spacing (in metres) will also be enlarged. The result will be that a “Keep Clear” road marking will cause an increase in the clearance time of all the queuing vehicles. This issue is vital for the ESD hypothesis; unless the ESD can work for changing driver-vehicle performance, the ESD will not work to improve the start-up lost time problem either.

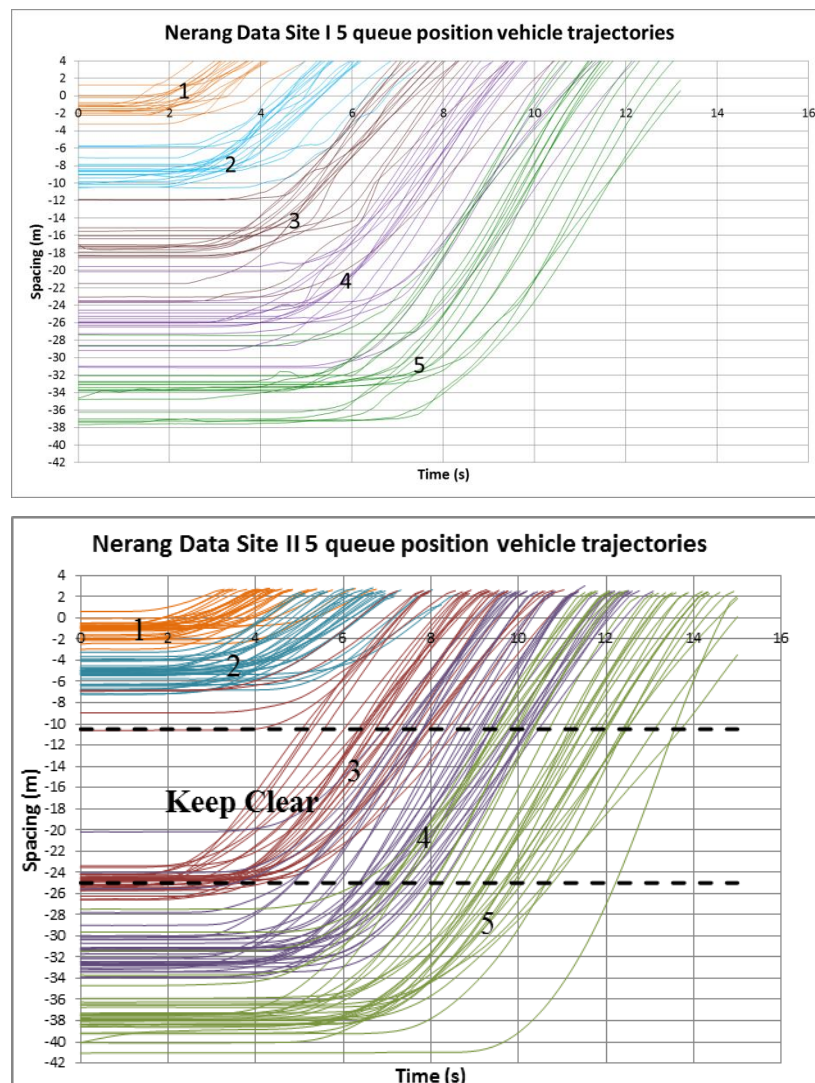


Figure 30: “Keep Clear” effects on drivers’ “catching up”

The Nerang Site II Data raw five leading vehicles discharge samples analysis results confirm that the “Keep Clear” road marking can change driver behaviour. The data show that the sequenced vehicles located behind the “Keep Clear” road marking try to keep up with the leading vehicles in the discharge process (when compared to the Site I the third vehicle trajectories and the Site II the third vehicle trajectories) until the process reverts to the typical following model (see Figure 30). This evidence vitally supports that the “Keep Clear” road marking changes driver-vehicle performance, the basis of the ESD hypothesis. This is contribution to the traffic management research field and this finding can be used to calibrate the traditional departure model.

The next issue reveals that the driver’s ability to comply with the road rules of the “Keep Clear” road marking. The raw videos of the Nerang Site II show that: the follow vehicle slowly approaches to the end side of the “Keep Clear” road marking and then its driver makes judgement whether they should move forward or stop behind the “Keep Clear” road marking. There are two situations that could happen: if the following driver adjusting to the front site (located in front of the “Keep Clear” road marking) can offer one more queuing position, this following vehicle will be moved forward to join the leading queuing vehicles; by contrast, if there are no more queuing positions left, this following vehicle will completely stop behind the “Keep Clear” road marking. Additionally, few samples are detected that the following vehicle do not slow down when it approaches the “Keep Clear” road marking and the vehicle stops in the “Keep Clear” area.

The Gold Coast Nerang Data analysis results show that the percentage for drivers who strictly observe the “Keep Clear” road markings. Examination of the third vehicle trajectories shows that, of the total 31 samples, there are 22 samples (71%) where the 3<sup>rd</sup> queue position drivers obey the “Keep Clear” road marking. Moreover, of the remaining 9 samples, 8 samples are just over the line by a few metres, and only one driver completely ignores the line.

#### 4.4.2 Effect on velocity

The following Figure 31 uses Nerang Site I/ Sample 01 and Nerang Site II/ Sample 01 to illustrate how the “Keep Clear” road marking affects the queuing vehicles behind this road mark in terms of their traffic performance in the discharge process. The time spacing graphs show that the third driver behind the “Keep Clear” road marking tries to keep up with the preceding vehicle, and this behaviour directly changes the traffic trajectory performance. The Site II 3<sup>rd</sup> vehicle’s speed in the time-velocity graph changes more frequently than the preceding vehicle’s speed when compared with the normal discharge. These results make an original contribution to the micro-simulation departure model research area. This research conclusion is also an innovative outcome for traffic management research. It can also directly benefit the calibration of other departure models. In short, the “Keep Clear” road marking can make a positive change in vehicle-driver discharge performance.

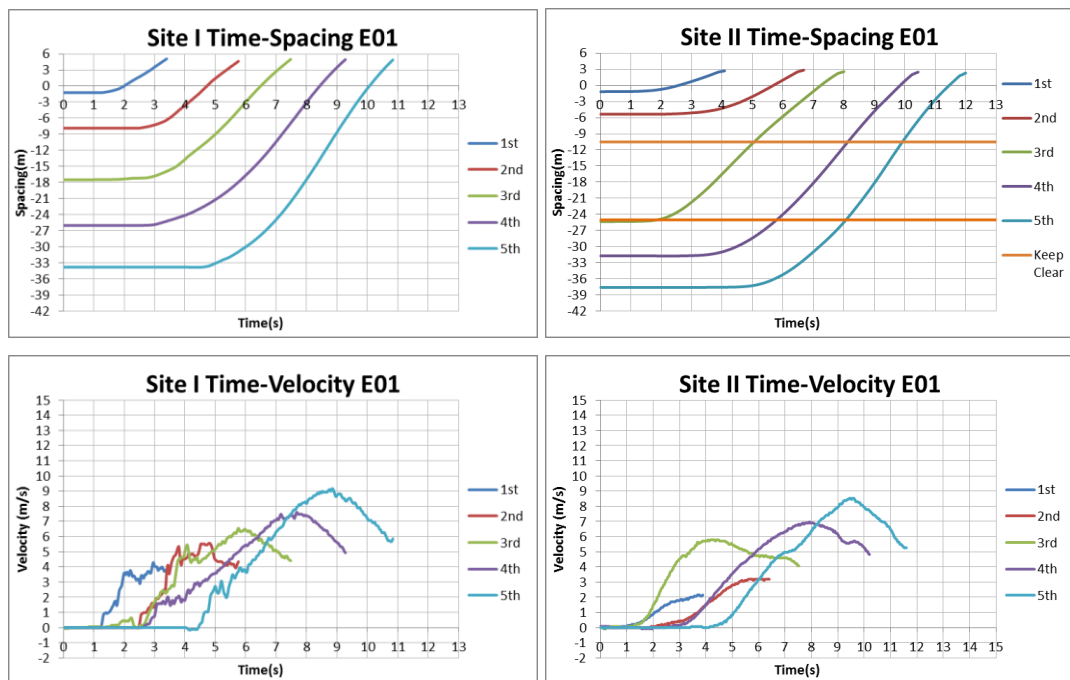


Figure 31: Comparative analysis of Nerang Data Site I and Site II

## **4.5 PEACHTREE DISCHARGE PATTERNS**

This section introduces the methodologies and the process to obtain the Peachtree Data five leading vehicle average discharge patterns and then those applicable platoons are set into “Fast”, “Normal” and “Slow” three categories.

### **4.5.1 Five leading vehicle average discharge pattern**

This sub-step obtains average leading vehicle discharge patterns from the obtained 21 applicable discharge samples. Although the raw samples can be used for the characterisation vehicle dynamic performance in departure, some of them are not suitable to analysis discharge patterns. The reason is that some sample vehicles are in an unsaturated situation where they are simply decreasing speed and preparing to stop when the signal changes to green. These cars then accelerate after obtaining enough safety distance. These cars' trajectories are suitable for the driver response time analysis. However, it is clearly unreasonable to use them to describe ordinary queuing vehicles departure which assumes that all vehicles waiting for the green signal onset are in a saturated situation. Therefore, some vehicle traffic trajectory curves need to be removed from the Time-Space graphs as they would negatively affect the results of the average trajectories. The meaning of this step is very clear if all 21 samples are combined to separately obtain the five car trajectory Time-Space graphs (for details see Appendix I).

As shown in Figure 26 (Section 3.3.3), for the 4<sup>th</sup> and 5<sup>th</sup> car trajectories, the samples E05, E16, E17, E18, and E19 are under unsaturated situation. Hence, these sample car trajectories are excluded so as to make the average trajectory results more accurate (16 samples remain). Furthermore, although the accuracy of the relevant Peachtree Street Data items has been confirmed, outside factors still have negative effects on some data items. For instance, the wind makes the camcorder vibrate and, thus, the value of the velocity appears positive and negative alternately. Also, the number zero does not appear in the velocity data because most queuing vehicles keep sliding forward.



Therefore, it is necessary to define the term “Stop”; this research defines “Stop” that is more rigid and refers to a speed slower than 5 km/h (equal to about 1.39 m/s). This criterion is used to extract the driver response time. Consequently, each vehicle’s trajectory can be divided into queue waiting and acceleration phases. The first five leading queuing vehicle discharge patterns are expressed as the following equations (see Table 11), and are used to study appropriate ESD distance. They are generated by using the Excel Trendline Options from the average five leading vehicle trajectories (see Figure 32). In this thesis, these patterns are labelled as A1, A2, A3, A4 and A5.

Table 11: Peachtree data average five leading vehicle discharge patterns

Patterns ID	Queue position	Time x in seconds with distance to the stop line f(x) in metres. Green onset at time x=0 and stop line located at f(x)=0.	Conditions
A1	1 <sup>st</sup>	$f(x) = 0.6296x - 0.0881$	$x \leq 1.5s$
		$f(x) = -0.0261x^3 + 0.9932x^2 - 0.4485x - 0.9562$	$x > 1.5s$
A2	2 <sup>nd</sup>	$f(x) = 0.588x - 7.751$	$x \leq 2.7s$
		$f(x) = -0.0254x^3 + 1.1065x^2 - 4.2814x - 1.8539$	$x > 2.7s$
A3	3 <sup>rd</sup>	$f(x) = 0.5174x - 15.461$	$x \leq 3.3s$
		$f(x) = -0.0201x^3 + 1.0158x^2 - 6.0284x - 3.2215$	$x > 3.3s$
A4	4 <sup>th</sup>	$f(x) = 0.4889x - 25.553$	$x \leq 4.3s$
		$f(x) = -0.0175x^3 + 0.9407x^2 - 6.3878x - 11.302$	$x > 4.3s$
A5	5 <sup>th</sup>	$f(x) = 0.524x - 34.422$	$x \leq 6s$
		$f(x) = -0.0141x^3 + 0.8423x^2 - 6.752x - 18.195$	$x > 6s$

Note: If speed is <5 km/h, the car is looked as ‘stop’, otherwise the car is ‘moving’.

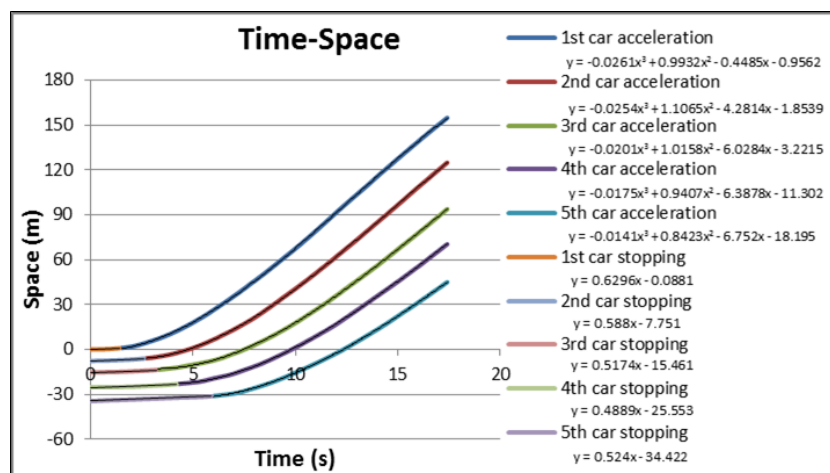


Figure 32: Peachtree data average five leading cars discharge patterns

#### 4.5.2 Three categories of discharge patterns

This subsection introduces the methodology to categorise the obtained applicable discharge samples into “Fast”, “Normal”, and “Slow” groups to simulate different driver behaviour so as to setup possible combinations for the scenarios for the ESD simulation. There are 15 discharge patterns generated in this step to simulate these three categories of driver behaviour at each queuing position in the discharge process.

The standard to qualify the trajectories as “Fast”, “Normal”, and “Slow” is based on the value of the acute angle between the trajectory curves and the X axis. If the angle degree is larger, the velocity is higher (see Appendix K). Moreover, this step also excludes the samples E05, E16, E17, E18, and E19 for the trajectories of the 4<sup>th</sup> and the 5<sup>th</sup> car convoys (as explained in the previous subsection). As a result, the 1<sup>st</sup>, the 2<sup>nd</sup> and the 3<sup>rd</sup> car convoys have 21 samples, while the 4<sup>th</sup> and the 5<sup>th</sup> only obtain 16 sets of samples. Subsequently, the trajectories of each convoy are equally divided into three groups.

Table 12: Categorisation of trajectories

Queue Position	1 <sup>st</sup>	2 <sup>nd</sup>	3 <sup>rd</sup>	4 <sup>th</sup>	5 <sup>th</sup>
“Fast” group	E01, E06, E07, E08, E09, E11, E14	E04, E06, E07, E08, E09, E11, E15	E07, E08, E09, E11, E15, E19, E21	E07, E08, E09, E11, E21	E07, E08, E09, E11, E21
“Normal” group	E03, E04, E10, E15, E16, E19, E21	E03, E05, E10, E12, E14, E19, E21	E01, E03, E04, E06, E10, E12, E16	E01, E03, E04, E06, E15, E20	E01, E04, E06, E12, E15, E20
“Slow” group	E02, E05, E12, E13, E17, E18, E20	E01, E02, E13, E16, E17, E18, E20	E02, E05, E13, E14, E17, E18, E20	E02, E10, E12, E13, E14	E02, E03, E10, E13, E14

In the next step, each group of trajectories generates average trajectories separately, and Excel Trendline extracts the following discharge patterns. Table 12 above shows how these trajectories are categorised, and the item “E number” refers to the 21

sample trajectories' ID numbers. In this step, there is an important action to calibrate the average trajectories. After separately putting the above trajectories into the three groups, the average trajectory shows a continual shaking if the average trajectories are directly calculated from the raw data. Hence, it is necessary to manually use Excel Trendline to calibrate and smooth the trajectories. Moreover, in some trajectory curves, the "Stop" parts are not exactly connected with their "Accelerate" parts after the "Stop" term (less than 5 km/h) is applied to these trajectories. All these factors need to be manually calibrated (see Appendix L).

The trajectories of vehicles with fast driver behaviour are averaged separately, and simulated as F1, F2, F3, F4 and F5; the numbers 1<sup>st</sup>, 2<sup>nd</sup>, 3<sup>rd</sup>, 4<sup>th</sup>, 5<sup>th</sup> present the vehicles' queue position;  $f(x)$  is the distance to the stop line (metre); and  $x$  is duration of analysis period (second).

Table 13: Peachtree data "Fast" group average five leading vehicle discharge patterns

Patterns ID	Queue position	Time $x$ in seconds with distance to the stop line $f(x)$ in metres. Green onset at time $x=0$ and stop line located at $f(x)=0$ .	Conditions
F1	1 <sup>st</sup>	$f(x) = 0.301$	$x \leq 0.8s$
		$f(x) = 1.0517x^2 - 0.0788x - 0.309$	$x > 0.8s$
F2	2 <sup>nd</sup>	$f(x) = -6.4562$	$x \leq 2s$
		$f(x) = 0.8477x^2 - 2.4671x - 4.9128$	$x > 2s$
F3	3 <sup>rd</sup>	$f(x) = -14.79$	$x \leq 2.9s$
		$f(x) = 0.576x^2 - 2.0693x - 13.633$	$x > 2.9s$
F4	4 <sup>th</sup>	$f(x) = -24.364$	$x \leq 3.6s$
		$f(x) = 0.4685x^2 - 1.1897x - 26.153$	$x > 3.6s$
F5	5 <sup>th</sup>	$f(x) = -30.516$	$x \leq 5.5s$
		$f(x) = 0.4353x^2 - 1.6583x - 34.563$	$x > 5.5s$
Note: If speed is $< 5$ km/h, the car is looked as 'stop', otherwise the car is 'moving'.			

The average trajectories of the convoy vehicles experiencing normal driver behaviour are separately simulated as N1, N2, N3, N4 and N5; the numbers 1<sup>st</sup>, 2<sup>nd</sup>, 3<sup>rd</sup>, 4<sup>th</sup>, 5<sup>th</sup> present the vehicles' queue positions;  $f(x)$  is the distance to the stop line (metre); and  $x$  is duration of analysis period (second).

Table 14: Peachtree data “Normal” group average five leading vehicle discharge patterns

Patterns ID	Queue position	Time $x$ in seconds with distance to the stop line $f(x)$ in metres. Green onset at time $x=0$ and stop line located at $f(x)=0$ .	Conditions
N1	1 <sup>st</sup>	$f(x) = 0.3735$	$x \leq 2s$
		$f(x) = 0.7492x^2 - 0.2214x - 2.9275$	$x > 2s$
N2	2 <sup>nd</sup>	$f(x) = -5.9537$	$x \leq 2.8s$
		$f(x) = 0.6638x^2 - 2.4195x - 4.3833$	$x > 2.8s$
N3	3 <sup>rd</sup>	$f(x) = -14.51$	$x \leq 4.2s$
		$f(x) = 0.6102x^2 - 3.4759x - 10.675$	$x > 4.2s$
N4	4 <sup>th</sup>	$f(x) = -23.013$	$x \leq 5s$
		$f(x) = 0.4849x^2 - 2.3519x - 23.376$	$x > 5s$
N5	5 <sup>th</sup>	$f(x) = -32.436$	$x \leq 7.1s$
		$f(x) = 0.3912x^2 - 1.6595x - 40.374$	$x > 7.1s$
Note: If speed is $<5$ km/h, the car is looked as ‘stop’, otherwise the car is ‘moving’.			

The average trajectories of the convoy vehicles are experiencing slow driver behaviour are separately simulated as S1, S2, S3, S4 and S5; the number 1<sup>st</sup>, 2<sup>nd</sup>, 3<sup>rd</sup>, 4<sup>th</sup>, 5<sup>th</sup> present the vehicles’ queue positions;  $f(x)$  is the distance to the stop line (metre); and  $x$  is duration of analysis period (second).

Table 15: Peachtree data “Slow” group average five leading vehicle discharge patterns

Patterns ID	Queue position	Time $x$ in seconds with distance to the stop line $f(x)$ in metres. Green onset at time $x=0$ and stop line located at $f(x)=0$ .	Conditions
S1	1 <sup>st</sup>	$f(x) = -0.1253$	$x \leq 2s$
		$f(x) = 0.6764x^2 - 1.8215x + 0.8121$	$x > 2s$
S2	2 <sup>nd</sup>	$f(x) = -8.4921$	$x \leq 3.8s$
		$f(x) = 0.5963x^2 - 3.0476x - 5.5218$	$x > 3.8s$
S3	3 <sup>rd</sup>	$f(x) = -13.387$	$x \leq 5.6s$
		$f(x) = 0.4942x^2 - 3.269x - 10.579$	$x > 5.6s$
S4	4 <sup>th</sup>	$f(x) = -24.843$	$x \leq 5.4s$
		$f(x) = 0.3753x^2 - 1.6738x - 26.748$	$x > 5.4s$
S5	5 <sup>th</sup>	$f(x) = -30.731$	$x \leq 6.9s$
		$f(x) = 0.2748x^2 - 1.2645x - 35.089$	$x > 6.9s$
Note: If speed is $<5$ km/h, the car is looked as ‘stop’, otherwise the car is ‘moving’.			

The obtained three categories discharge patterns indicate that the 1<sup>st</sup> vehicle's stopping positions of the "Fast" and "Normal" groups have passed over the stop line. The main reason to keep these cases includes two aspects. Firstly, these discharge patterns are extracted from the average vehicle trajectory. This does not mean that all of the 1<sup>st</sup> queuing vehicles are stopped over the stop line. Secondly, all of these discharge patterns use the stop line as reference line, if revised the "Fast" and "Normal" 1<sup>st</sup> vehicle stopping position back to the stop line, the "Slow" 1<sup>st</sup> vehicle will need be revised more distance. This will result in the "Slow" group discharge patterns cannot accurately reflect its actual occurrence in the discharge process.

Furthermore, to explore the safety distance corresponding to preceding vehicle speed in discharge, this research yields the 20<sup>th</sup> percentile clearance and velocity pattern (see Appendix M). The physics constant acceleration formula  $d=v_0t+(at^2)/2$  is used in this step to obtain each point of the trajectory speed and to then obtain the corresponding following vehicle velocity at the same time point. This method differs from previous studies, such as Vincenzo et al. (2009), that directly used the velocity and acceleration data offered by the Peachtree Data. The next approach is to determine the following vehicles' clearance values (from each trajectory sample) that correspond with this speed and to combine them. Some other parameters also extracted from the raw discharge samples; such as, velocity variation with clearance, time and acceleration, velocity with clearance and so on (see Appendix N, O, P, Q). The median safety distance, average safety distance and the minimum safety distance are also explored in this research (see Appendix S, T, U).

## **4.6 FINDINGS WITHIN LOCAL DATA**

As the local data sources from Nerang are the only data available with a forced "keep clear" area, this data is checked first to find indications to explain the second drivers delay during discharge at an intersection. Figure 33 shows the response time of drivers depending on the stopping distance – the space between the cars from front-bumper to front-bumper. Response time is the time that it takes a driver to accelerate after the leading vehicle has started to move.

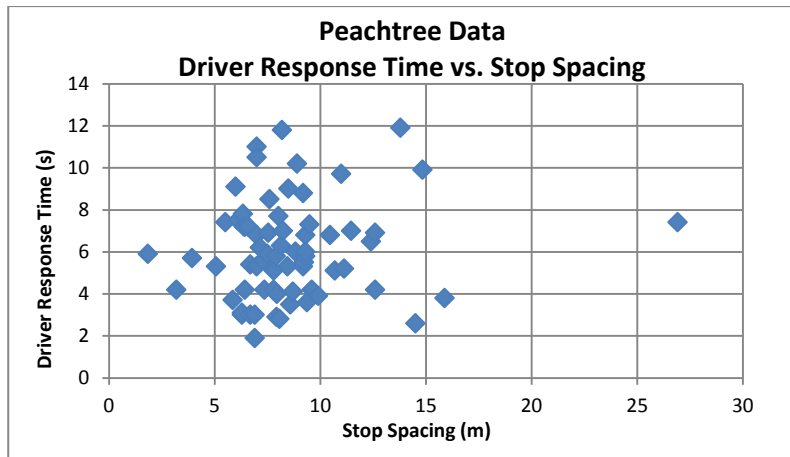


Figure 33: Driver response time relative to stopping spacing

While no relationship between response time and spacing is visible, one can see that the majority of points are in the area of 5.5 – 10 metres spacing. Given an average vehicle length of 4.5m, indicates that vehicles choose a gap between 1.0 metre and 5.5 metres most often. This indicates that a stopping distance up to 10 metres has no effect on the driver response.

Figure 34 shows data for Nerang Site I only, but instead of a stopping distance, it plots the response time which is based on the position in the queue.

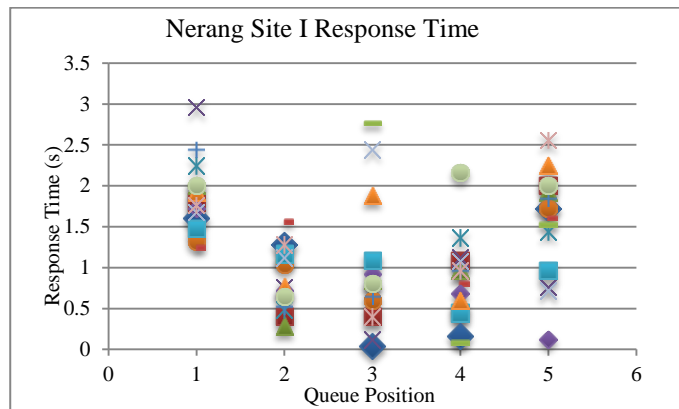


Figure 34: Response time of drivers in different positions in the queue at Nerang I - without 'keep clear'

The plot indicates that drivers respond within normally assumed human reaction time with some noise. Interestingly, Figure 35 of the Nerang Site II data set has a very crisp respond time for queue position 3, the vehicle with the 'keep clear' in front.

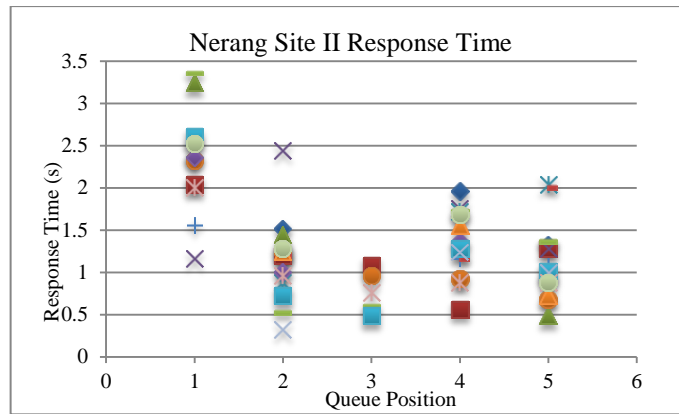


Figure 35: Response time of drivers in different queue positions at Nerang II - with 'keep clear'

This shows that the noise around the response time of the driver is related to the leading vehicle clearance distance, starting speed, or a combination of both. To investigate this further, the time a car needs from starting to move to reaching cruising speed is examined. Due to the limitations in the data collection behind the stop line, Peachtree Data has been used for this.

#### 4.7 PEACHTREE FINDINGS

To have a consistent method of determining the timings of a vehicle starting to move and reaching cruising speed, the polynomial approximations of the trajectories have been used. Thresholds then determine the time a vehicle starts to move, and when it reaches the desired speed. To this end, the first derivative of position (i.e. speed) is considered. The starting point, in time, corresponds to the time at which the derivative of the polynomial is than 0.1 m/s. Similarly, the cruise speed is assumed to be reached when the derivative is at its maximum. An example of this approach is shown in Figure 36.

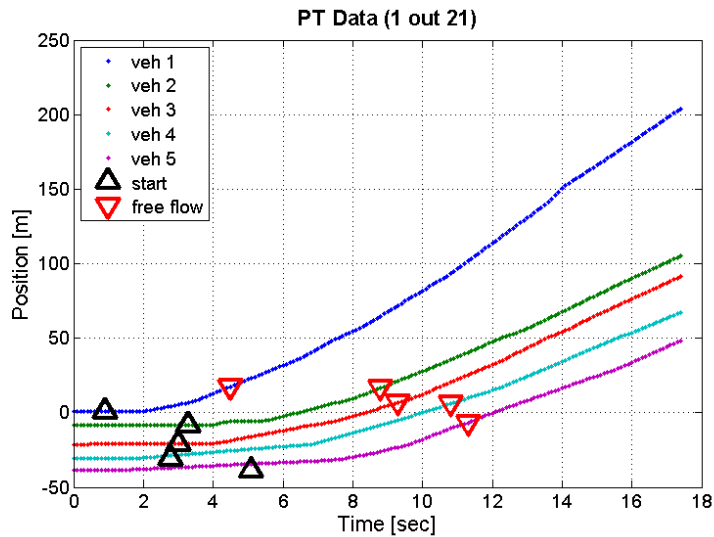


Figure 36: Example of trajectories with automatically identified times of starting and reaching free flow speed

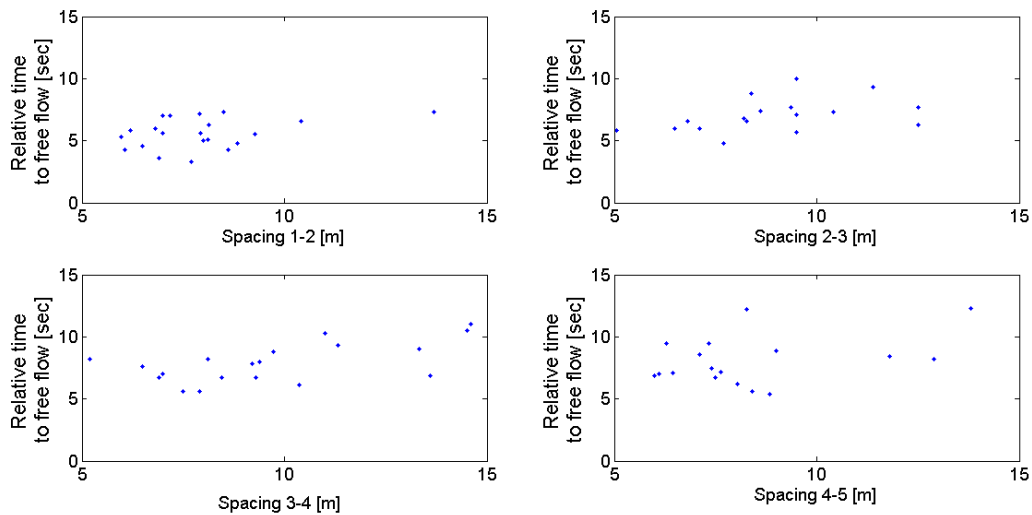


Figure 37: Relative time to free flow depending on queue position and distance

With this preparation it is possible to calculate the relative time needed before free flow speed is reached. This relative time to free-flow is computed as a difference between absolute times to free-flow of consecutive vehicles. With reference to Figure 36, a relative time to free flow is the difference between the time of two consecutive downward triangle. The relationship between time to free-flow and queue position and spacing is displayed in Figure 37. Although no visible trends can be identified from the figure, a simple analysis of the data through regression trees



showed that the spacing between vehicles has little influence on the platoon discharge, only if certain conditions are satisfied.

Two regression trees were trained, which were named as RT2 and RT3, to predict the time to free flow of vehicle 2 and 3, respectively. For RT2, the independent variables chosen were:

- Time to free flow speed of the first vehicle, T1
- Spacing between first and second vehicle, S1-2.

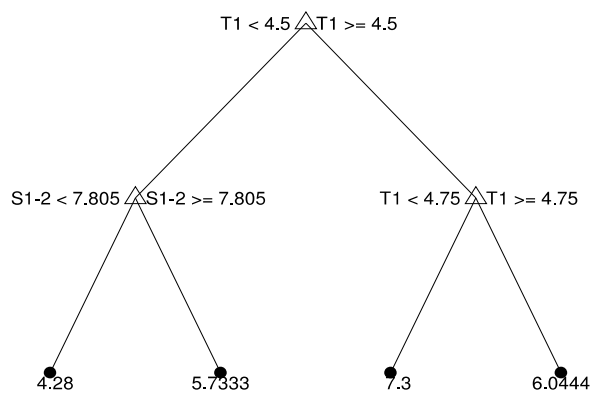


Figure 38: Regression tree considering the first vehicle's speed and spacing between first and second vehicle. The predicted time to free flow is reported on the leaves of the tree.

The results indicated that the spacing of vehicles has no influence on the platoon discharge when the first vehicle is a slow starter. This indicates that all data where the first vehicle is moving slower than a threshold (i.e. T1 is smaller than 4.5) should be neglected when looking for a relationship between spacing and discharge.

For RT3, we used the predictors:

- time to free flow speed of first vehicle, T1
- time to free flow speed of second vehicle, T2
- spacing between vehicles 1-2, S1-2
- spacing between vehicle 2-3, S2-3

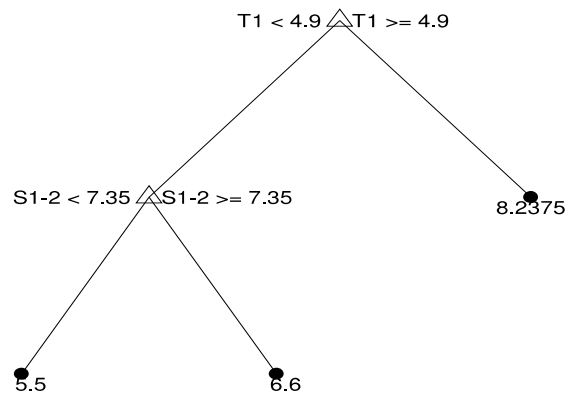


Figure 39: Regression tree considering additionally the second vehicles discharge speed and spacing of the second and third vehicle

Again, it can be seen that the discharge speed of the first vehicle is dominant and that only for fast discharge of the first vehicle; the spacing plays a role in the total platoon discharge behaviour.

A natural step forward for the analysis would then involve the removal, from the datasets, of those samples for which the times  $T1$ , of the first vehicles, were below the related threshold. Unfortunately, cleansing a dataset containing a relatively small number of samples, involves shrinking the dataset even further. As a result, any machine learning algorithm trained on such an impoverished dataset is unlikely to learn the underpinning cause of the observed phenomena. In fact, data mining techniques work better upon richer datasets. In order to perform a more accurate analysis, this research therefore needs to synthesize large amount of traffic data, by using an established, realistic car following model.

## 4.8 SIMULATION

With queue discharge time being the value of interest, a realistic simulation needs to produce trajectories whose discharge time is close to the one observed. When plotting the relative discharge time based on the queue position, a clear trend becomes visible (see Figure 40). Vehicles starting from behind a ‘keep clear’ area have a crisp relative discharge time.

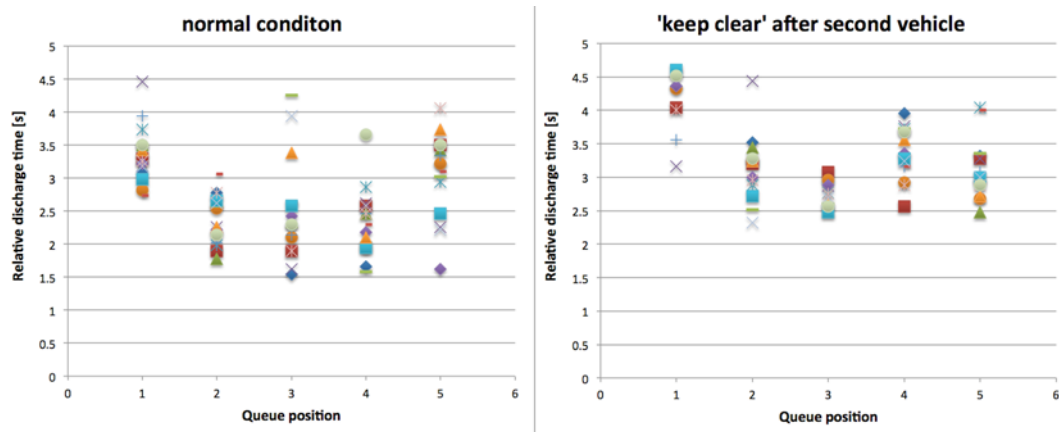


Figure 40: Relative response time depending on the queue position

As it turns out, such a pattern can be observed in the trajectories produced by the Intelligent Driver Model (IDM), as depicted in Figure 40.

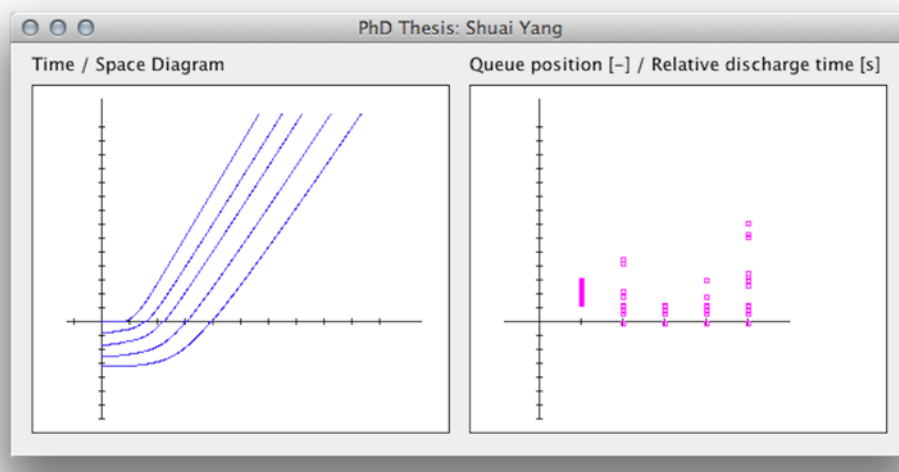


Figure 41: Screenshot of simulated results, using the IDM car following model

The purpose of this section is threefold: introducing the IDM model, explaining how such a model was calibrated upon the observational data; and showing how the data from the calibrated model show aggregate properties that are also observed in the Nerang and Peachtree datasets.

#### 4.8.1 The IDM model

The IDM model describes the dynamics of the positions and velocities of single vehicles. For vehicle  $\alpha$ ,  $x_\alpha$  denotes its position at time  $t$ , and  $v_\alpha$  its velocity.

Furthermore,  $l_\alpha$  gives the length of the vehicle. To simplify the notation, this research defines the *net distance*  $s_\alpha = x_{\alpha-1} - x_\alpha - l_{\alpha-1}$ , where  $\alpha-1$  refers to the vehicle directly in front of vehicle  $\alpha$ , and the velocity difference, or *approaching rate*,  $\Delta v_\alpha = v_\alpha - v_{\alpha-1}$ . For a simplified version of the model, the dynamics of vehicle  $\alpha$  are then described by the following two ordinary differential equations:

$$\dot{x} = \frac{dx_\alpha}{dt} = v_\alpha = \alpha \left( 1 - \left( \frac{v_\alpha}{v_0} \right)^\delta - \left( \frac{s^*(v_\alpha, \Delta v_\alpha)}{s_\alpha} \right)^2 \right) \quad \text{Equation 36}$$

$$\text{with } s^*(v_\alpha, \Delta v_\alpha) = s_0 + v_\alpha T + \frac{v_\alpha \Delta v_\alpha}{2\sqrt{ab}} \quad \text{Equation 37}$$

where:  $v_0, s_0, T, a$ , and  $b$  are model parameters which have the following meaning:

*Desired velocity*  $v_0$ : the velocity the vehicle would drive at in free traffic

*Minimum spacing*  $s_0$ : a minimum net distance that is kept even at a complete standstill in a traffic jam

*Desired time headway*  $T$ : the desired time headway to the vehicle in front

*Acceleration*:  $a$

*Comfortable braking deceleration*:  $b$

The exponent  $\delta$  is usually set to 4.

A parameter calibration was performed to find the best fit. Figure 42 (see page 95) shows comparisons between the real data and simulation with varying values for 'normal' acceleration.

#### 4.8.2 Model calibration

The calibration of the IDM model was addressed as an optimization problem, that is, the parameter set of the model was determined in such a way as to minimize an error function that penalized non-realistic model. In this case, a good error function would need to produce large values for simulated trajectories that are greatly different from the observed trajectories. The objective function that used for this research was the mixed error measure, introduced by (Kesting & Treiber, 2008). This error reads:

$$E = \sqrt{\frac{1}{\langle s_{\text{data}} \rangle} \left\langle \frac{(s_{\text{sim}} - s_{\text{data}})^2}{s_{\text{data}}} \right\rangle}, \quad \text{Equation 38}$$

where  $s_{sim}$  and  $s_{data}$  are the simulated and observed trajectory, and the expression  $\langle \cdot \rangle$  is the temporal average across the entire simulation. More precisely, the temporal average of the time series considered in Eq. 36 is computed as:

$$\langle z \rangle = \frac{1}{N} \sum_{n=1}^N \left( \frac{1}{T-T_n} \sum_{t=T_n}^{T_n+T} z_n(t) \right), \quad \text{Equation 39}$$

where  $N$  is the number of observed vehicles – four in the research case, from vehicle 2 to 5;  $T$  the entire duration of the observation – 20 seconds in the experiments;  $T_n$  the time at which the first vehicle starts moving. As it can be easily verified, the mixed error measure produces large values if the difference ( $s_{sim} - s_{data}$ ) is large, that is, if the simulated trajectories are largely different from the observed trajectories. Therefore, the objective of the calibration is to find a parameter set for the IDM model so as to keep the differences between simulated and the actual trajectories to a minimum.

### 4.8.3 Optimization with genetic algorithm

The objective function  $E$  is a function of trajectories, generated by the IDM model. Because the IDM model is non-linear, the solution that minimizes  $E$  (i.e. the optimum parameter set) needs to be found numerically. To achieve this, a generic algorithm (GA) was used, as suggested by Kesting and Treiber (2008). In the implementation process, an individual of the GA population was a parameter set of the IDM model, that is, a vector  $(T, s_0, a, b)$  representing the desired time headway to the leading vehicle; the minimum spacing in traffic jam situations; the acceleration term; and the breaking deceleration, respectively. The desired velocity  $v_0$  was set to the speed limit of the road section (16.6 m/s in the experiments), and the exponent  $\delta$  was set 4.

Each iteration of the GA algorithm consisted in randomly selecting pairs of individuals (two sets of parameters of the IDM) from the population, according to their fitness score, and recombining them to form new individuals. Once a new individual (parameter set) was generated, it was used as an input for the IDM which, in turn, would produce a new simulated set of trajectories. A ‘population’ consisted

of  $N$  such sets. Finally, each new set of trajectories,  $s_{sim}$  was used to estimate the error function introduced earlier and thus to determine the fitness of each of the individuals. The fittest individual amongst the current population was then passed on to the next generation without any modification. All individuals, but the fittest, underwent mutation through random variations of the model parameters. The termination criterion implemented was based on fitness convergence. The parameters  $T$ ,  $s_0$ ,  $a$  and  $b$  were restricted to the intervals  $[1,2]$ ,  $[1.5,2.5]$ ,  $[1,3]$  and  $[2,4]$  respectively. Those choices were motivated by physical considerations.

#### 4.8.4 Calibration results

Table 16 reports the results from the calibration process. As can be observed, the acceleration parameter from the best fit had value close to 2. This result is plausible, as long as it is assumed that the majority of vehicles at the stop line stand to perform sharp acceleration maneuvers as the light turn green.

Table 16: Numerically optimum parameter set

Parameter	Calibrated value
$T$	1.6723
$s_0$	1.9032
$a$	1.9855
$b$	2.7067

In order to ensure that the trajectory data from the IDM showed realistic discharge patterns, we analyzed the real and synthetic data through boxplots (Figure 42). To this end, we first clustered the relative discharge time of vehicles according to their position in the queue. Then, for each cluster, a box plot was generated.

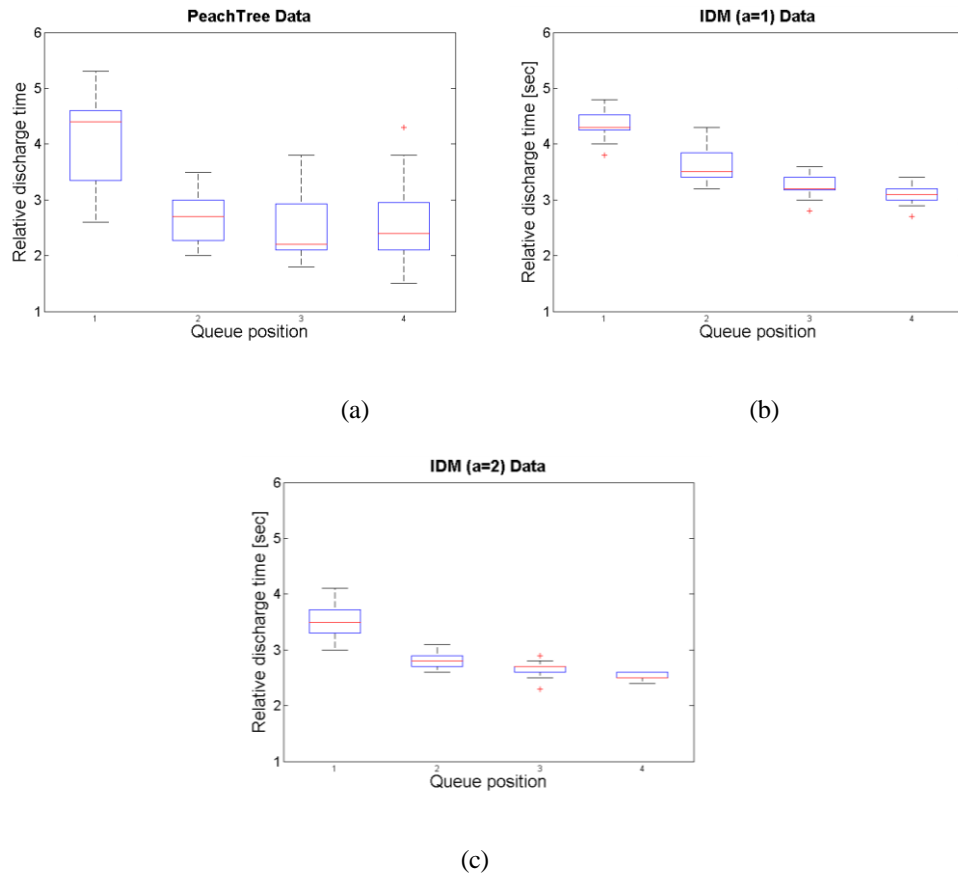


Figure 42: Comparison of relative discharge speed between real data and simulation. (a) Box plot generated from the observed Peachtree data. (b) Results from the IDM trajectories produced by the numerically optimum solution, in which the parameter  $a$  is close to 2. (c) Results from the IDM model, whose parameters are identical to that of (b), except for the decreased acceleration factor,  $a=1$ .

As it can be noted, both the non-linear, decreasing trend of the median relative discharge time (red segments within the boxes), and the values of the median itself of actual and synthetic data are close to each other. The reduced variance in the synthetic data (involving shorter whiskers in the plots) is due to both a larger set of data, and the absence of noise from the mathematical mode. As an example, Figure 42 shows that a parameter set slightly different from the numerically optimum solution produces results that do not resemble as well as those from the actual data.

## 4.9 DATA SYNTHESIS AND RESULTS

Once established that the IDM model can be effectively used to replicate the discharge-time patterns observed in Nerang dataset, observed through boxplots, this step will now turn attention to the quantitative analysis of the ESD phenomena.

### **4.9.1 Experiment setup**

In order to measure the effect of vehicle spacing on the discharge time of the entire platoon – or time to full discharge – this step set up five experiments. Each experiment, aimed at measuring the effect of spacing of a specific pair of adjacent vehicles in the queue. Accordingly, experiment 1 measured the effect of spacing between vehicle 1 and 2, on the time to full discharge. Similarly, experiments 2, 3 and 4, concerned the effect of spacing between vehicles, 2-3, 3-4 and 4-5 on time to full discharge, respectively. Finally, experiment 5 measured the effect of vehicle spacing, across the entire platoon. Under this latter hypothesis, cars were all evenly spaced across the entire queue.

To generate the data for the five experiments, the next step then used the IDM model, calibrated as explained in the previous sections. The initial spacing between cars in the platoon, that is, the initial position of vehicles, varied according to the experiment. For example, in experiment 1, the initial spacing between vehicles 2, 3 and 4 was kept constant, while the initial distance between car 1 and 2 was allowed to change, within some range. Analogously, in experiment 2, the initial spacing between cars 1 and 2 and between 3, 4 and 5 were kept unchanged, whereas the spacing between car 2 and 3 varied.

Each of the five experiments involved running the IDM simulation several times. Each run produced a ‘point’, in the space defined by platoon length versus time to full discharge. By varying the spacing between two target vehicles we therefore generated a set of points, for the experiment at hand. This set of points, was then used to quantitatively define the effect of spacing on the time to full discharge (Figure 43, left).

### **4.9.2 Results**

The simulation results in Figure 43 show that evenly spaced platoons (experiment 5) discharge fastest when spread out over a total distance of 72 metres with a saving of



about 1 second, with respect to a queue out of 30 metres. Added gaps between certain vehicle pairs influence the total discharge time.

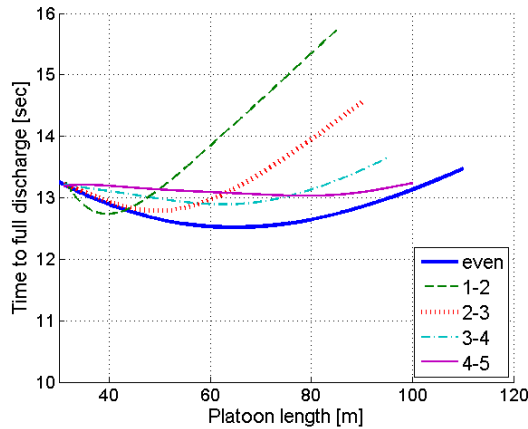


Figure 43: Simulation results showing plots for evenly spaced vehicles, and for platoons with increased spacing between certain cars

When looking at the minimal discharge times (see Figure 44), obtained from the curves in Figure 43, the result shows that an evenly spread out platoon has the lowest overall discharge time.

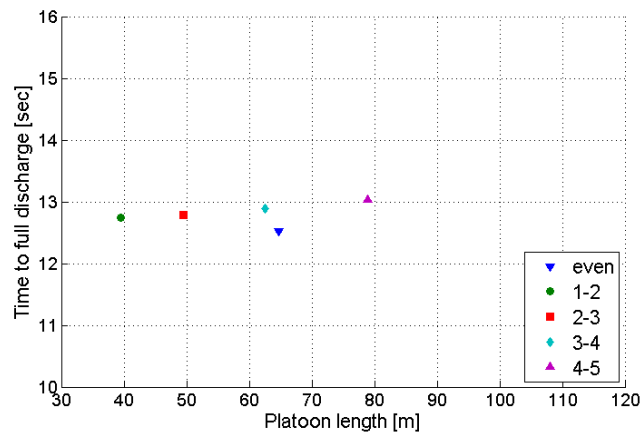


Figure 44: Minimal discharge times with different platoon structures

However, along with any theoretically optimum solution, practical considerations must be taken into account. There clearly is a trade-off between space and time, and as space is important in urban environments, any optimisation should take space and time evenly into account. Further, to educate drivers to stop evenly spaced with a

certain distance requires a high level of compliance. On the other hand, an increased distance of only 10 metres between the first and second vehicle (which means the stopping distance or the queue clearance be increased to about 6 metres when the average vehicle length is 4 metres) would reduce the average discharge time and only requires the change of behaviour of a single vehicle.

## **4.10 CHAPTERS' CONTRIBUTIONS**

### **Outcomes**

- Achieved predicted research objectives:
  - 1) Explore the second vehicle delay phenomenon
  - 2) Characterise vehicle dynamic performance in discharge
  - 3) Create scenarios and simulate the ESD
  - 4) Demonstrate the ESD hypothesis

### **Key findings**

- Enlarged Stopping Distance between the second and the first vehicle shortened the discharge time of the platoon.

### **Recommendation**

- The ESD implementation requires a real road test.

# Chapter 5: Conclusions & Recommendations

---

## 5.1 INTRODUCTION

This chapter provides the benefits, recommendations and conclusions of this research. The benefit of ESD is discussed in the first subsection and this is followed by recommendations on how ESD could be applied. The research conclusions and recommendations for further research are given in the last two subsections respectively.

## 5.2 BENEFITS OF THE ESD

The main benefit of the ESD is its potential to get a platoon of queued vehicles at a signalised intersection to cross the stop line more quickly by up to 1 second. This means higher throughput, i.e. more vehicles clearing the green phase or a shorter green time per cycle is needed to discharge the same number of vehicles. In the traffic engineering term, ESD could result in lower start-up lost time.

In practice, when calculating capacity at signalised intersection, start-up lost and end gains are assumed to be equal at 3 seconds (see Equation 40). However, suppose ESD reduced start up lost from 3 to 2 seconds, the capacity would increase by 5% for short green phase of 15 seconds and by 2% for longer green phase of 45 seconds (see Figure 45). The benefit in terms of throughput per hour for cycle length of 90 and 180 seconds is an increase of 20 and 10 vehicles per hour respectively. Whilst ESD would increase capacity for any length of green phase and cycle length, greater gain could be realised from shorter green phase for example at a right turn phase.

$$Q = \frac{s(G+I-l_a+l_b)}{c} \quad \text{Equation 40}$$

where

Q is the capacity (veh/hr),

s is the saturation flow rate (veh/hr),

$G$  is the display green time (sec),  
 $c$  is the cycle time (sec),  
 $I$  is the intergreen time (sec),  
 $l_a$  is the start-up lost time (sec), and  
 $l_b$  is the end gain time (sec).

The Bureau of Infrastructure, Transport and Regional Economics (BITRE) estimated the cost of congestion to Australia in 2020 to be \$20 billion per annum. Imagine the cost savings ESD could deliver with a conservative 2% increase in capacity at urban signalised intersections. The ESD concept also illustrates the positive effect of “Keep Clear” road marking has on driver behaviour and this research could be used to enhance the knowledge of road designers with respect to the road marking design.

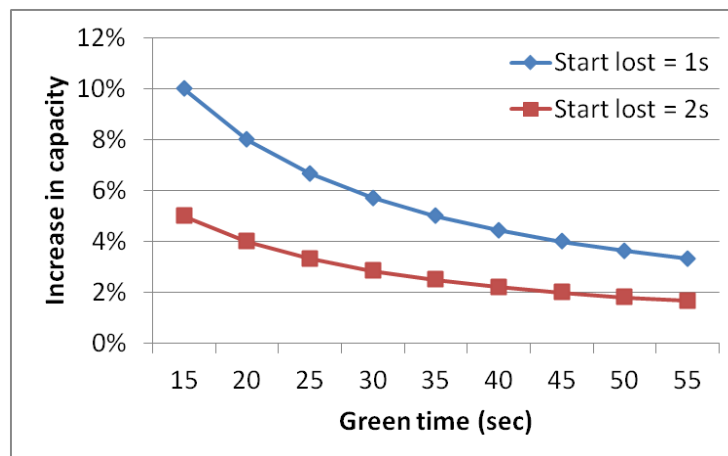


Figure 45: Capacity increase by green phase time for different start up lost

### 5.2.1 Tradeoff of the ESD

The tradeoff in the gain in lower response time from ESD is the longer storage space required for queued vehicles. Is an increase in short lane length by one vehicle length worth the saving of one second per green phase? This is the question practitioner would have to contemplate each time. This question arises only when there is space limitation. Another way of looking at the tradeoff is to ask the question whether there is any other measure that could help increase capacity without sacrificing space? It is important to note that when there is slow 1<sup>st</sup> vehicle, the benefit of the ESD will be erased because the following vehicles will have to slow down. The reason is that the

following vehicles will catch up with the lead vehicles and pick-up velocity. The ideal scenario is to implement count down timer during red phase to reduce reaction time, ESD for increase throughput, and a proactive adaptive traffic signal control system.

### **5.3 PROPOSED APPROACHES FOR THE ESD IMPLEMENTATION**

From the practical perspective, this research seeks to use an ESD to reduce the negative effects caused by the second vehicle discharge delay phenomenon. The ESD method can potentially be applied to most urban signalised intersections. To implement the ESD at signalised intersections, this research proposed through the education, publicity and training approaches to quickly realise the efficacy of the ESD. There are three steps as follow. First, education will inform more people about the ESD and its benefits. Second, publicity to make more drivers change driver's behaviour to actively enlarge the stopping distance at signalised intersections. Third, training system, such as driving school, new drivers can be trained actively to enlarge the stopping distance.

### **5.4 CONCLUSIONS**

From a knowledge perspective, this research identifies the second queuing vehicle delay phenomenon occurring at urban signalised intersections and demonstrates the feasibility of using the ESD as an innovative solution to the problem. Data from Nerang, Queensland and Peachtree, California were collected and analysed to provide evidence of the second vehicle delay phenomenon. Unfortunately, due to limited data sets, no conclusive evidence could be drawn.

Further analysis using regression tree were performed and the results indicate that the first vehicle's discharge speed is dominant. In addition, it is only for fast discharge of the first vehicle that the spacing plays a role in the total platoon discharge behaviour. Therefore, the limitation number of the Peachtree discharge samples leads to this research using the IDM model to for further simulation. The results show that evenly spaced platoons discharge fastest when spread out over a total distance of 64 metres

with a saving of about 1 second. Splitting the platoon into two sets of evenly spaced cars also decreases the discharge time. In particular, an enlarged stopping distance of 10 metres between the first vehicle and the rest of the platoon reduces the discharge time by half a second. Splitting the platoon at any other position still positively affects the time to full discharge, however, to a lesser extent. Splits after the fourth vehicle, have negligible effects on the discharge time and require a poor utilization of the road infrastructure.

Educating the drivers to adapt to an enlarged stopping distance may be very beneficial, as far as network efficiency is concerned. From a practical perspective, however, a good compromise between efficiency and capacity can be achieved if the second driver stops at a distance of about 10 metres from the leader (see Figure 46).

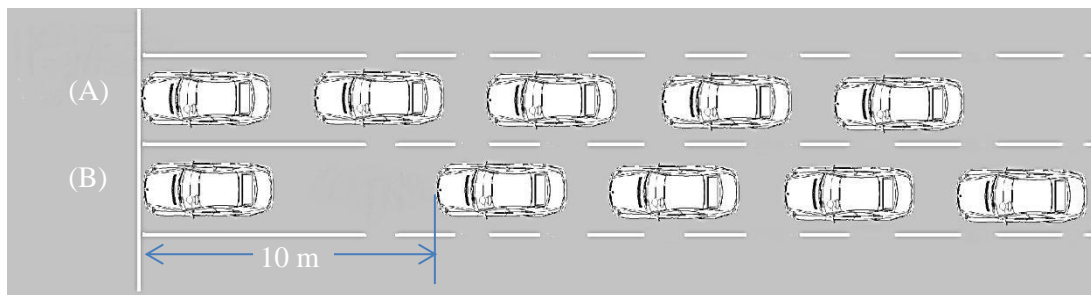


Figure 46: (A) Normal discharge and (B) Enlarged Stopping Distance discharge

In summary, this research followed through an intuition of the second vehicle delay phenomenon caused by the close spacing between vehicles which prevents drivers from responding quicker; and used field data, data analysis, and traffic simulation to demonstrate that indeed enlarge spacing distance between vehicles especially between first and second vehicles could increase throughput. The benefit of ESD is not only limited to increase signalised intersection capacity but also its simplicity to implement in Australian urban cities through education, publicity and training.

## 5.5 RECOMMENDATIONS FOR FUTURE WORK

Further research study and practical work are recommended before the ESD can be realised and can contribute to better traffic flow in Australia and abroad. This

research uses NGSIM Peachtree Street Data and the Gold Coast Nerang Street Data for simulation purposes. However, more traffic data analyses will be needed to provide concrete evidence of the positive effects of the ESD. Also, driving test of ESD at real signalised intersections will benefit the calibrations of the ESD simulation results.





# Citations

---

- ABS. (1996). *Australian Social Trends 1996*.
- AECPortico. (August 2003). Transportation Engineering Online Lab Manual. *Traffic flow theory* Retrieved January 20, 2012, from [http://www.webs1.uidaho.edu/niatt\\_labmanual/Chapters/trafficflowtheory/theoryandconcepts/TrafficFlowParameters.htm](http://www.webs1.uidaho.edu/niatt_labmanual/Chapters/trafficflowtheory/theoryandconcepts/TrafficFlowParameters.htm)
- Akcelik, R. (2008). *The relationship between Capacity and Driver Behaviour*. Paper presented at the The TRB National Roundabout Conference. Retrieved from [http://www.teachamerica.com/rab08/RAB08\\_Papers/RAB08S2AAkcelik.pdf](http://www.teachamerica.com/rab08/RAB08_Papers/RAB08S2AAkcelik.pdf)
- Akçelik, R. (2000). *On the Validity of Some Traffic Engineering Folklore*. Paper presented at the 22nd Conference of Australian Institutes of Transport Research (CAITR 2000),.
- Akcelik, R., & Besley, M. (2002). *Queue Discharge Flow and Speed Models for Signalised Intersections*. Paper presented at the 15th International Symposium on Transportation and Theory. Retrieved from [http://www.sidrasolutions.com/Documents/Akcelik\\_ISTTT15\\_2002\\_Paper.pdf](http://www.sidrasolutions.com/Documents/Akcelik_ISTTT15_2002_Paper.pdf)
- Almond, J. (1965). *Proceedings of the second international symposium on the theory of road traffic flow: (25-27 June) 1963, London, England: O.E.C.D.*
- Aron, M. (1988). Car following in an urban network: simulation and experiments. *PLANNING AND TRANSPORT RESEARCH AND COMPUTATION*, 27-39.
- Azhar, A.-M., & Svante, B. (2011). Signal Control of Roundabouts. *Procedia - Social and Behavioral Sciences*, 16(0), 729-738.
- Bekey, G. A., Burnham, G. O., & Seo, a. J. (1977). Control theoretic models of human drivers in car following. *Human Factors*, 19(4), 399-413.
- Berkowitz, C. M., Bragdon, C. R., & Mier, F. (1996). *Continuous flow intersection*. Paper presented at the Proceedings of Meeting on Global Networks for Environmental Information: Bridging the Gap Between Knowledge and Application, 4-7 Nov. 1996, Ann Arbor, MI, USA.
- Bonneson, J. A. (1992). Change Intervals and Lost Time at Single-Point Urban Interchanges. *Journal of Transportation Engineering*, 118(5), 631-650.
- Bonneson, J. A. (1992). Study of Headway and Lost Time at Single-Point Urban Interchanges. *Transportation Research Record*(1365), 30-39.
- Brackstone, M., & McDonald, M. (1999). Car-following: a historical review. *Transportation Research Part F: Traffic Psychology and Behaviour*, 2(4), 181-196.
- Brandon, B. (2007). *Modification of driver behavior based on information from pedestrian countdown timers*. University of Kansas, Lawrence.
- Bristow, N. (2010). IBM wants to control your car at stoplights - 1984, here we come. Retrieved 3rd, June, 2010, from <http://green.autoblog.com/2010/05/26/ibm-wants-to-control-your-car-at-stoplights-1984-here-we-come/>
- BTRE. (2007). *Estimating Urban Traffic and Congestion Cost Trends for Australian Cities*. Canberra: Elect Printing.
- Ceder, A. (1976). A deterministic traffic flow model for the two regime approach. *Transportation Research Record*, 567, 16-30.
- Ceder, A., & May, A. D. (1976). Further evaluation of single and two regime traffic flow models. *Transportation Research Record*, 567, 1-30.
- Chakroorty, P., & Kikuchi, S. (1999). Evaluation of the General Motors based car-following models and a proposed fuzzy inference model. *Transportation Research Part C: Emerging Technologies*, 7(4), 209-235.
- Chandler, R. E., Herman, R., & Montroll, E. W. (1958). Traffic Dynamics: Studies in Car Following. *Operations Research*, 6(2), 165-184.
- Chen, I. C., Chang, K. K., Chang, C. C., & Lai, C. H. (2007). *The Impact Evaluation of Vehicular Signal Countdown Displays*. Taiwan: Institute of Transportation, Ministry of Transportation and Communications.

- Chiou, Y.-C., & Chang, C.-H. (2010). Driver responses to green and red vehicular signal countdown displays: Safety and efficiency aspects. *Accident Analysis & Prevention*, 42(4), 1057-1065.
- D.Greenshields, B., Schapiro, D., & L.Ericksen, E. (1947). *Traffic Performance at Urban Street Intersections*. New Haven: Bureau of Highway Traffic Yale University.
- Denos C. Gazis, Robert Herman, & Rothery, R. W. (1961). Nonlinear follow the leader models of traffic flow. *Operations Research*, 9(4), 545-567.
- Dey, P. P., & Chandra, S. (2009). Desired Time Gap and Time Headway in Steady-State Car-Following on Two-Lane Roads. *Journal of Transportation Engineering*, 135(10), 687-693.
- Dia, H. (2002). An agent-based approach to modelling driver route choice behaviour under the influence of real-time information. *Transportation Research Part C (Emerging Technologies)*, 10C(Copyright 2003, IEE), 331-349.
- Dixon, M., Abdel-Rahim, A., & Kyte, M. (2010). *Improved Simulation of Stop Bar Driver Behaviour at Signalized Intersections*. Moscow: National Institute for Advanced Transportation Technology, University of Idaho.
- DTEI. (2010). *KEEP CLEAR Pavement Markings - Operational Instruction 2.23*. Retrieved from [http://www.dpti.sa.gov.au/\\_data/assets/pdf\\_file/0015/40155/1585750-v4-Traffic\\_Management\\_-\\_AS1742\\_2\\_-\\_Keep\\_Clear\\_Pavement\\_Markings\\_-\\_Operational\\_Instruction\\_.pdf](http://www.dpti.sa.gov.au/_data/assets/pdf_file/0015/40155/1585750-v4-Traffic_Management_-_AS1742_2_-_Keep_Clear_Pavement_Markings_-_Operational_Instruction_.pdf).
- Edwards, T., & Smith, S. (2008). *Transport Problems Facing Large Cities*. Retrieved from [http://www.parliament.nsw.gov.au/prod/parlment/publications.nsf/key/TransportProblemsFacingLargeCities/\\$File/TransportFINALindex.pdf](http://www.parliament.nsw.gov.au/prod/parlment/publications.nsf/key/TransportProblemsFacingLargeCities/$File/TransportFINALindex.pdf).
- EPA. (2011). *Transportation Control Measures*. Retrieved from <http://www.epa.gov/otaq/stateresources/policy/430r09040.pdf>.
- Ewing, J. (2011). Toyota Yaris, 2005-2010. *The Road Ahead*, 64.
- Fairclough, S. H., May, A. J., & Carter, C. (1997). The effect of time headway feedback on following behaviour. *Accident Analysis & Prevention*, 29(3), 387-397.
- Foil, S. L., & Qureshi, M. A. (2005). Accuracy of the HCM 2000 Queue Clearance Model: Case of Multiple Approach Lanes with Shared Left Turns and Multiple Opposing Lanes. *Journal of Transportation Engineering*, 131(12), 912-916.
- Gazis, D. C., Herman, R., & Potts, R. B. (1959). Car-Following Theory of Steady-State Traffic Flow. *Operations Research*, 7(4), 499-505.
- Guberinić, S., Šenborn, G., & Lazić, B. (2008). *Optimal traffic control: urban intersections*. Boca Raton: CRC Press.
- Heanue, K., & Salzberg, A. (2011). *Metropolitan Transportation Institutions; Six Case Studies Australia, Brazil, Canada, France, Germany and the United States*. Retrieved from <http://siteresources.worldbank.org/INTURBANTRANSPORT/Resources/Heanue-Salzberg-MTA-for-India-9Mar2011.pdf>.
- Helly, W. (1959). Simulation of Bottlenecks in Single Lane Traffic Flow *Proceedings of the Symposium on the Theory of Traffic Flow* (pp. 207-238). New York: Elsevier Publishing.
- Herman, R., Montroll, E. W., Potts, R. B., & Rothery, R. W. (1959). Traffic Dynamics: Analysis of Stability in Car Following. *Operations Research*, 7(1), 86-106.
- Heyes, M. P., & Ashworth, R. (1972). Further research on car following models. *Transportation Research*, 6, 287-291.
- Hutchinson, T. (1995). The continuous flow intersection - the greatest new development in traffic engineering since the traffic signal? . [Journal Article]. *Traffic Engineering and Control*, 36, 156-157
- Ibrahim, M. R., Karim, M. R., & Kidwai, F. A. (2008). The effect of digital count-down display on signalized junction performance. *Am J Appl Sci.*, 5, 479.
- Improta, G., & Cantarella, G. E. (1984). Control system design for an individual signalized junction. *Transportation Research Part B: Methodological*, 18(2), 147-167.
- Inman, V. W. (2009). Evaluation of signs and markings for partial continuous flow intersection. *Transportation Research Record(Compendex)*, 66-74.


- Jan, K., Ivan, N., & Michal, J. (2009). *Mathematical application for departure model*. Paper presented at the Proceedings of the 2009 Euro American Conference on Telematics and Information Systems: New Opportunities to increase Digital Citizenship.
- Jin, X., Zhang, Y., Wang, F., Li, L., Yao, D., Su, C.-W., et al. (2009). Departure headways at signalized intersections: A log-normal distribution model approach. *Transportation Research Part C: Emerging Technologies*, 17(3), 318-327.
- Kesting, A., & Treiber, M. (2008). Calibrating Car-Following Models by Using Trajectory Data: Methodological Study. *Transportation Research Record: Journal of the Transportation Research Board*, 2088(-1), 148-156.
- Kidwai, F. A., Karim, M. R., & Ibrahim, M. R. (2005). Traffic flow analysis of digital countdown signalized urban intersection. *Eastern Asia Society for Transportation Studies*, 5, 1301.
- Kometani, E., & Sasaki, T. (1959). A Safety Index for Traffic with Linear Spacing. *Operations Research*, 7(6), 704-720.
- Krogscheepers, C., & Kacir, K. (2001). *Latest Trends in Micro Simulation: An Application of the Paramics Model*. Paper presented at the 20th South African Transport Conference. Retrieved from <http://repository.up.ac.za/bitstream/handle/2263/8186/4g5.pdf?sequence=1>
- Lee, J. J., & Chen, R. L. (1986). Entering Headway at Signalized Intersections in a Small Metropolitan Area. *Transportation Research Record* (1091), 117-126.
- Lieu, H. (1999). Traffic-flow theory (Vol. 62(4), Available from <http://search.proquest.com/docview/205374923?accountid=13380>
- Limanond, T., Chookerd, S., & Roubtonglang, N. (2009). Effects of countdown timers on queue discharge characteristics of through movement at a signalized intersection. *Transportation Research Part C: Emerging Technologies*, 17(6), 662-671.
- Limanond, T., Prabjabok, P., & Tippayawong, K. (2010). Exploring impacts of countdown timers on traffic operations and driver behavior at a signalized intersection in Bangkok. *Transport Policy*, 17(6), 420-427.
- Lin, F.-B., Tseng, P.-Y., & Su, C.-W. (2004). Variations in Queue Discharge Patterns and Their Implications in Analysis of Signalized Intersections. [10.3141/1883-22]. *Transportation Research Record: Journal of the Transportation Research Board*, 1883(-1), 192-197.
- Long, K., Han, L. D., & Yang, Q. (2011). Effects of Countdown Timers on Driver Behavior After the Yellow Onset at Chinese Intersections. *Traffic Injury Prevention*, 12(5), 538-544.
- Lucas, B. D., & Kanade, T. (1981). *An iterative image registration technique with an application to stereo vision*. Paper presented at the Proceedings of the 7th international joint conference on Artificial intelligence.
- Lum, K. M., & Halim, H. (2006). A before-and-after study on green signal countdown device installation. *Transportation Research Part F: Traffic Psychology and Behaviour*, 9(1), 29-41.
- Ma, W., Liu, Y., & Yang, X. (2010). Investigating the Impacts of Green Signal Countdown Devices: Empirical Approach and Case Study in China. *Journal of Transportation Engineering*, 136(11), 1049-1055.
- Mahalel, D., Gur, Y., & Shiftan, Y. (1991). Manual versus automatic operation of traffic signals. *Transportation Research Part A: General*, 25(2-3), 121-127.
- Malik, H., & Rakotonirainy, A. (2008, 19-21 Aug. 2008). *The Need of Intelligent Driver Training Systems for Road Safety*. Paper presented at the Systems Engineering, 2008. ICSENG '08. 19th International Conference on.
- May, A. D., & Harmut, E. M. (1967). Non integer car following models. *Highway Research Record*, 199, 19-32.
- Nguyen, H. Q., & Montgomery, F. (2006). *Comparison of Discharge Patterns at Traffic Signals*. Paper presented at the Transportation Research Board 85th Annual Meeting.
- Office of Legislative Drafting (2009). *Australian Road Rules*. A. T. Council. Melbourne, National Road Transport Commission.

- Ossen, S. (2008). *Longitudinal Driving Behavior: Theory and Empirics*. Delft University of Technology, The Netherlands.
- Ozaki, H. (1993). *Reaction and anticipation in the car following behaviour*. Paper presented at the 13th International Symposium on Traffic and Transportation Theory.
- Peachtree Meta Data. (2007). Retrieved from [http://ngsim-community.org/index.php?option=com\\_docman&task=cat\\_view&gid=29&dir=DESC&order=name&Itemid=34&limit=15&limitstart=0](http://ngsim-community.org/index.php?option=com_docman&task=cat_view&gid=29&dir=DESC&order=name&Itemid=34&limit=15&limitstart=0)
- Philpot, F. (2005). Blasted lights. [Article]. *Professional Engineering*, 18(21), 48-48.
- Pitaksringkarn, J. (2005). *Measures of effectiveness for continuous flow intersection: a Maryland intersection case study* Paper presented at the Institute of Transportation Engineers (ITE) Annual Meeting.
- PTV. (2006). *VISSIM 4.20 User Manual*. Karlsruhe.
- Puan, O. C., & Ismail, C. R. (2010). Dilemma zone conflicts at isolated intersections controlled with fixed-time and vehicle actuated traffic signal systems. *International Journal of Civil & Environmental Engineering*, 10(3), 19.
- Pulugurtha, S. S., Desai, A., & Pulugurtha, N. M. (2010). Are Pedestrian Countdown Signals Effective in Reducing Crashes? *Traffic Injury Prevention*, 11(6), 632-641.
- Punzo, V., Borzacchiello, M. T., & Ciuffo, B. F. (2009). *Estimation of Vehicle Trajectories from Observed Discrete Positions and Next-Generation Simulation Program (NGSIM) Data*. Paper presented at the Transportation Research Board 88th Annual Meeting. Retrieved from <http://pubsindex.trb.org/orderform.html>
- Rahman, M. M., Hasan, T., & Nakamura, F. (2008). Development of Professional Driver Adjustment Factors for the Capacity Analysis of Signalized Intersections. *Journal of Transportation Engineering*, 134(12), 532-536.
- Robinson, B. W., Rodegerdts, L., Scarborough, W., Kittelson, W., Troutbeck, R., Brilon, W., et al. (2000). *Roundabouts: An Informational Guide* (No. FHWA-RD-00-067).
- Rosaci, D. (1998). STOCHASTIC NEURAL NETWORKS FOR TRANSPORTATION SYSTEMS MODELING. *Applied Artificial Intelligence: An International Journal*, 12(6), 491 - 500.
- Sharma, A., Vanajakshi, L., & Rao, N. (2009). Effect of Phase Countdown Timers on Queue Discharge Characteristics Under Heterogeneous Traffic Conditions. *Transportation Research Record: Journal of the Transportation Research Board*, 2130(-1), 93-100.
- SIAS Limited. (2005). *S-Paramics 2005 reference manual*. Edinburgh.
- Smith, B. L., Scherer, W. T., Hauser, T. A., & Park, B. B. (2002). Data-Driven Methodology for Signal Timing Plan Development: A Computational Approach. *Computer-Aided Civil and Infrastructure Engineering*, 17(6), 387-395.
- Sobey, E. J. C. (2006). *A Field Guide to Roadside Technology* (Vol. 1). Chicago: Chicago Review Press.
- Stevens, C. R. (2005). *Signals and Meters at Roundabouts*. Paper presented at the 2005 Mid-Continent Transportation Research Symposium, Ames, Iowa.
- Tang, K., & Nakamura, H. (2007). *An Analysis on Saturation Flow Rate and Its Variability*. Paper presented at the The 11th World Conference on Transportation Research.
- Taylor, S., Bennett, D., & Ogden, K. (1996). *Traffic Engineering Folklore*. Melbourne: Monash University.
- TRB. (2000). *Highway Capacity Manual*. Washington, D.C.: Transportation Research Board, National Research Council.
- TRB. (2010). *HCM2010 Highway Capacity Manual*. Washington, DC: Transportation Research Board of the National Academies.
- Treiber, M. H., Ansgar; Helbing, Dirk. (2000). Congested traffic states in empirical observations and microscopic simulations. *Physical Review E*, 62(2), 1805-1824.
- Treiterer, J., & Myers, J. A. (1974). *The hysteresis phenomenon in traffic flow*. Paper presented at the 6th International Symposium on Transportation and Traffic Theory
- TSS-Transport Simulation Systems. (2006). *AIMSUN 5.1 Microsimulator user's manual, version 5.1.2*. Barcelona.

- Wang, M.-H. (2008). *Development of Arrival/departure Based Uniform Delay Model for Left-turn Traffic at Signalized Intersections*. University of Illinois at Urbana-Champaign.
- Wim, V. W. (1999). The human element in car following models. *Transportation Research Part F: Traffic Psychology and Behaviour*, 2(4), 207-211.
- Wim, v. W., & Heino, A. (1996). Choice of time-headway in car-following and the role of time-to-collision information in braking. [Article]. *Ergonomics*, 39(4), 579-592.
- Wu, W.-j., Juan, Z.-c., & Jia, H.-f. (2009). Drivers' Behavioral Decision-Making at Signalized Intersection with Countdown Display Unit. *Systems Engineering - Theory & Practice*, 29(7), 160-165.
- Xing, J. (1995). *A parameter identification of a car following model*. Paper presented at the Second World Congress on ATT.
- Xuan, Y., Daganzo, C. F., & Cassidy, M. J. (2011). Increasing the capacity of signalized intersections with separate left turn phases. *Transportation Research Part B: Methodological*, 45(5), 769-781.
- Yang, S., & Chung, E. (2012). Driver Response Time of Queuing Vehicles at Urban Signalized Intersections. *Procedia - Social and Behavioral Sciences*, 43(0), 169-177.
- Yin, Y. (2008). Robust optimal traffic signal timing. *Transportation Research Part B: Methodological*, 42(10), 911-924.
- Yu, Q., Li, L., & Rong, J. (2008). *Car Following Criterion Research in Signalized Intersection*.

# Appendices

## Appendix A: Nerang Data collection application



Queensland Government

### Road Corridor Permit Application

The form may be used to apply for works, structures and activities for which approval is required under the Transport Infrastructure Act 1994. This approval includes the construction, maintenance, upgrading or consulting of those works, structures and activities characterised as auxiliary works and encroachments under the Transport Infrastructure Act 1994. The form may also be used for the renewal of existing permits.

Essential information on Road Corridor Permits and the application processes can be found on the Road Corridor Permit information sheet (available on [www.tmr.qld.gov.au](http://www.tmr.qld.gov.au)).

**1. Applicant Details**

Note: The applicant is the person who holds the permit and is legally responsible for complying with the applicable conditions. A business name is not applicable and should not be entered in this field as the applicant. Where a person or company operates a business, the applicant is the person or company.

Name/Company Name:

Position (in company if applicable):

Contact Name (if different to above):

Postal Address:

Residential Address:

Phone Number:

Fax Number:

Mobile Number:

Email:

**2. Are you seeking to renew an existing Road Corridor Permit?**

2a)  Yes  No  Continue to 3

2b) Existing Road Corridor Permit No.:

**3. Duration of approval sought**

Please give details of dates (the times if applicable) your Road Corridor Permit is required

Baseline: From 30 May 2011 to 3 June 2011, need 5 sunny day, Times 9:00-18:00

**4. Description of works, structures or activities you intend to carry out**

e.g. authorised signs, benches, construction activity etc., or if road works, the nature of the road works e.g. roadworks, median strip etc.

A 7 metres tripod will be erected on temporary grade in front of the gate way of the Wood Concrete factory

A 1V cantilever will be installed on above tripod

**5. Location**

Please give a location of the activity, works or structure, including:

- road names
- road name(s)
- direction of travel (with another road)
- direction to points of the compass (i.e. north, south, east, west)
- GPS coordinates
- adjacent property description (or registered plan) if known

At the intersection of Nelson Street and Southport Esplanade Road

At the above intersection, the tripod will be erected on an empty space

GPS coordinates: 27°46'02.589"S, 153°02'07.8"E (Retrieved from Google Earth)

Adjacent with the Wood Concrete, Concrete Pipe Manufacturer, Southport

Nelson Concrete, 217, 3 Southport Esplanade Rd, QLD 4215, Ph: (07) 5531 4163

**6. Details of how you plan to carry out the works, structures or activities**

Please attach copies of, plans and diagrams of works, structures or activities where appropriate, showing how they will be implemented.

Note: The study is an academic sign, to assess the propagation, including ambient, emission origin and appropriate measures during existing local long or any nearby superfund, to be included.

**7. Who the applicant(s)**

a. requires approval / approval of approval to carry out works, structures or activities as specified in the Transport Infrastructure Act 1994

b. warrant that the information contained within and/or attached to this application is true and accurate to the best of my/our knowledge.

**For Individual Applicants**

Signature:

Date:

**or Corporate Applicant**

Executed in accordance with Corporations Act 2001 (CA) section 127 by:

Company name and ACN:

Name in full:

Business Director:

Date:

Name in full:

Signed Director/Secretary:

Date:

**Please forward completed application to your local regional office.**

Privacy Statement: The Department of Transport and Main Roads is seeking the information or system for the purposes of applying for a Road Corridor Permit in accordance with the Transport Infrastructure Act 1994. The Department of Transport and Main Roads will only use the information for the purposes of processing your application. Your personal data will not be disclosed to any other government department or agency. You may request access to your personal data, or request that your personal data is deleted, by contacting the Information Management Unit on 1300 737 737.

## Appendix B: Nerang Data collection official permission

**Road Corridor Permit**  
Transport Infrastructure Act 1994, Chapter 6 Part 5

Permit Number: CM02559      Start Date: 03/06/11      Expiry Date: 03/06/11

**Permit Holder's Details**  
Name/Company Name: Shuai Yang  
Position in company (if applicable): Postgraduate Student

Postal Address: U1/117 Eugene Street, Southport Qld 4215  
Residential Address: U1/117 Eugene Street, Southport Qld 4215

Phone Number:      Fax Number:      Mobile Number: 0423 635 112  
Email: Shuai.yang@student.qut.edu.au

**Description of works, structure or activity**  
Location (e.g. street name, road name/number, T-Post, GPS coordinates): At signalled intersection of Warwood Street and Southport-Nerang Road.  
Exact location shown on email attachment dated 15 April 2011.

Suburb: Southport      Regional or City Council Reference: Gold Coast City Council

Additional details: Use a camcorder to record traffic departure trajectory for research data collection. A 7 metre tripod will be erected on an open space in front of the gate way of the Nucor concrete factory. A DV camcorder will be mounted on the tripod.

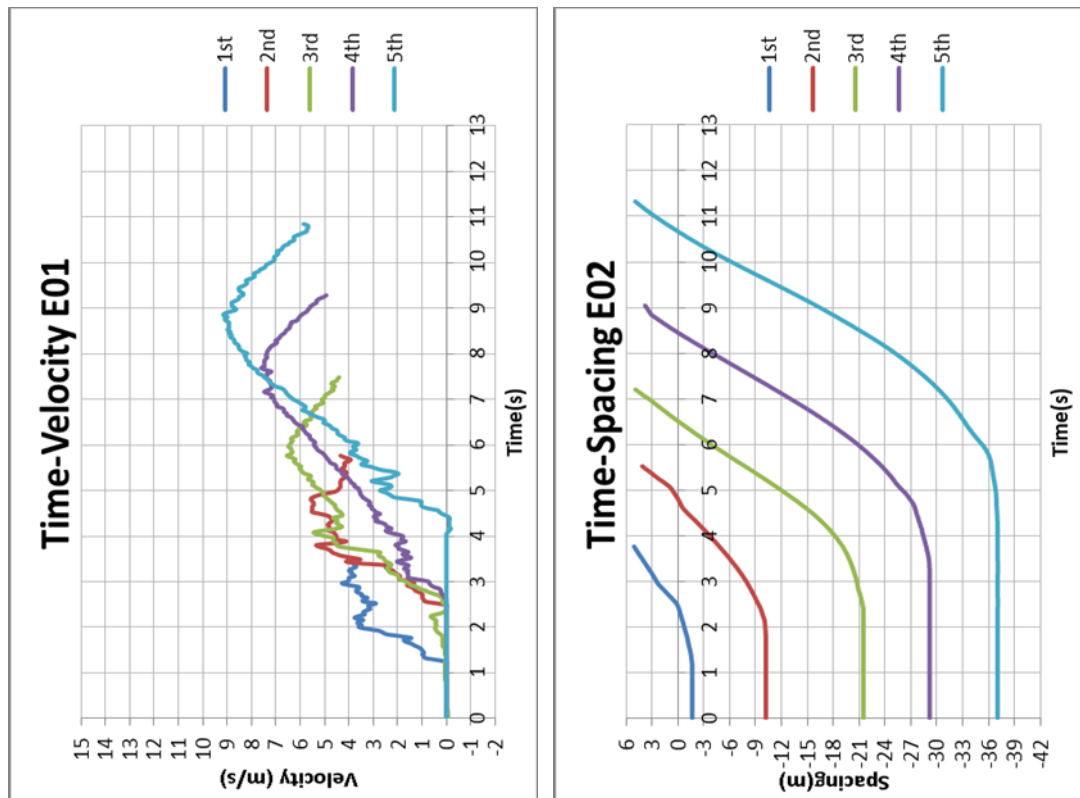
**Issuing Region/Office**  
South Coast Region / Gold Coast Office

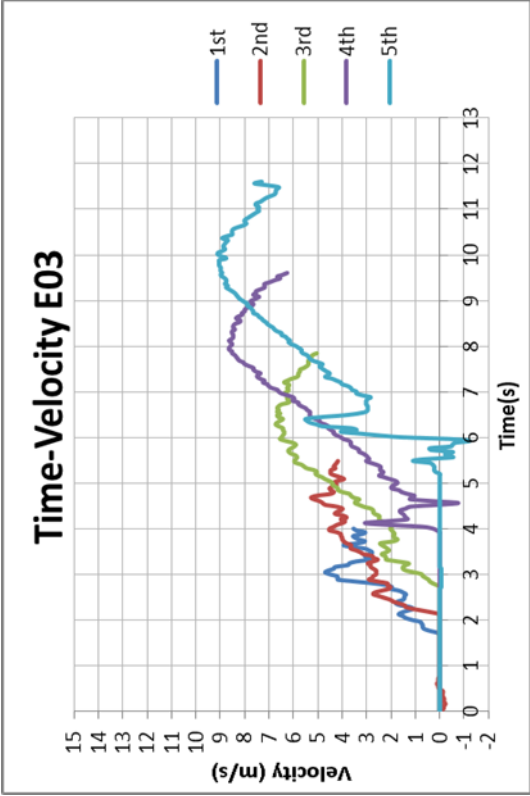
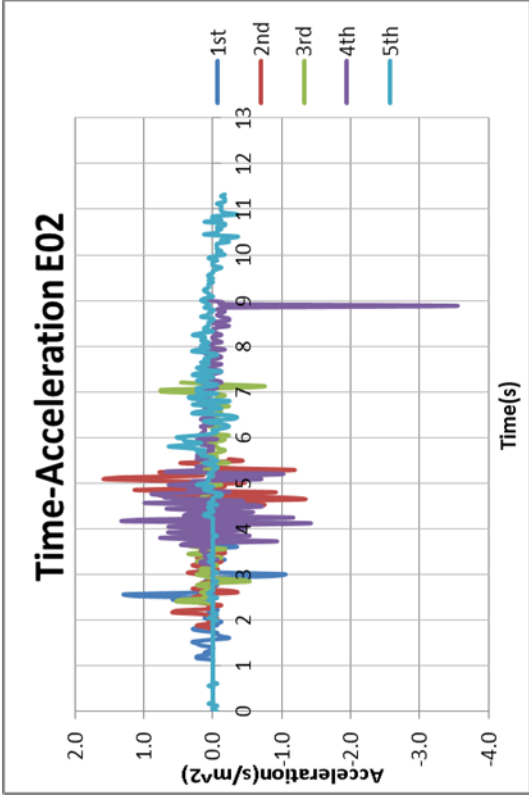
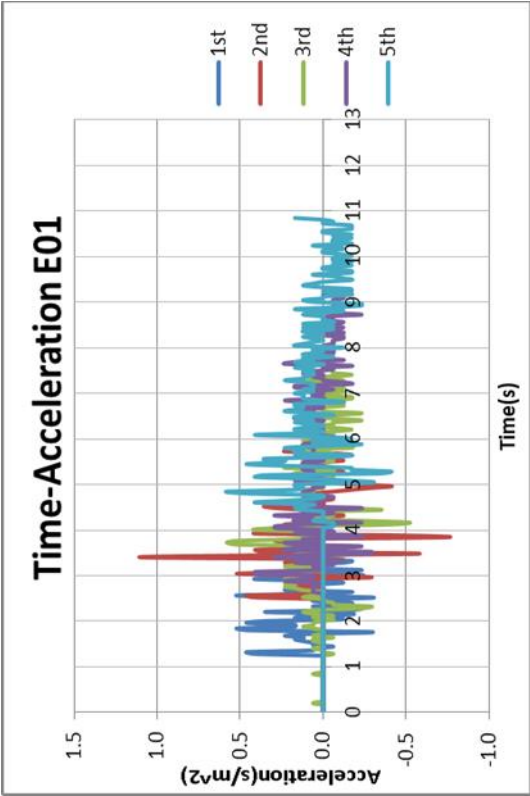
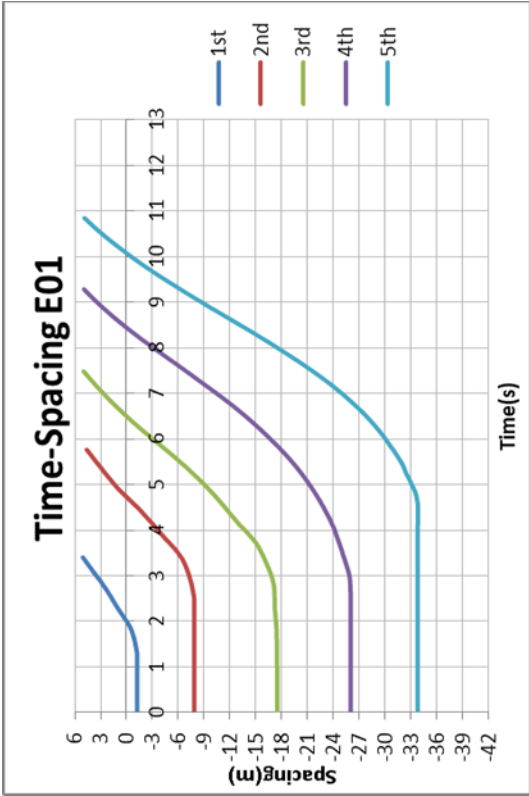
Signature: *Ken Jernan*  
Name: Ken Jernan      Date: 03 / 06 / 2011  
Position: Senior Engineer      Office Use Only

Privacy Statement: The Department of Transport and Main Roads has collected this information in its role for the purposes of a Road Corridor Permit in accordance with the Road Corridor Permit Act 2009. This information is held by the Department of Transport and Main Roads, Queensland State Government. Your personal details will not be disclosed to any other third party without your consent unless required to do so by law.

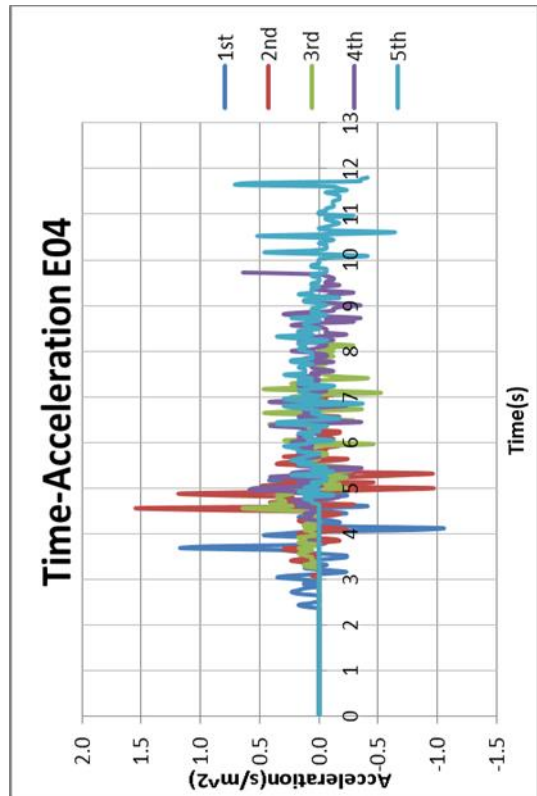
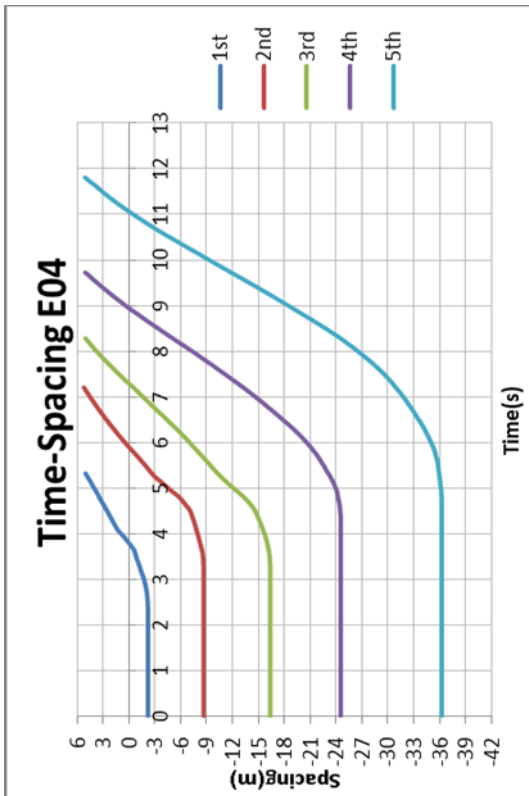
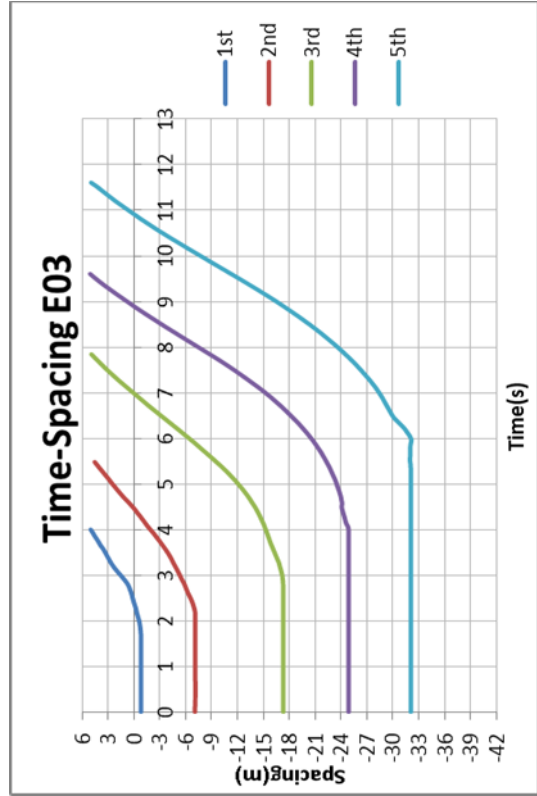
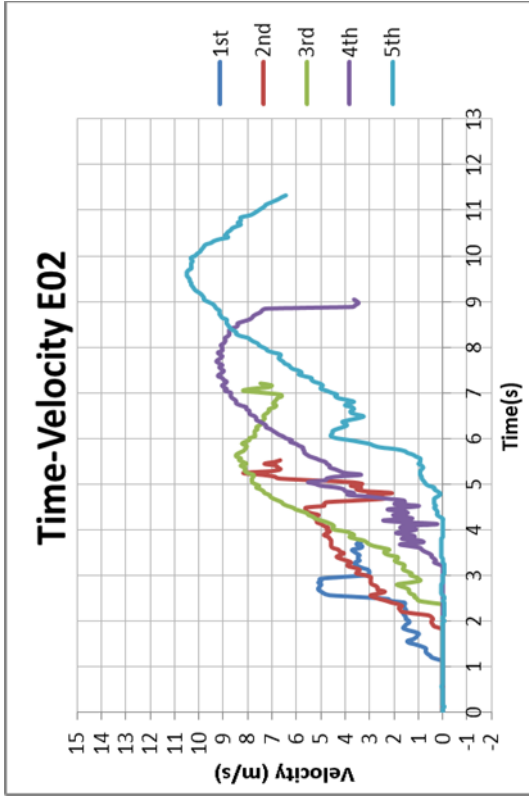
Page 1 of 2 IM771 ES V02 Aug 2010

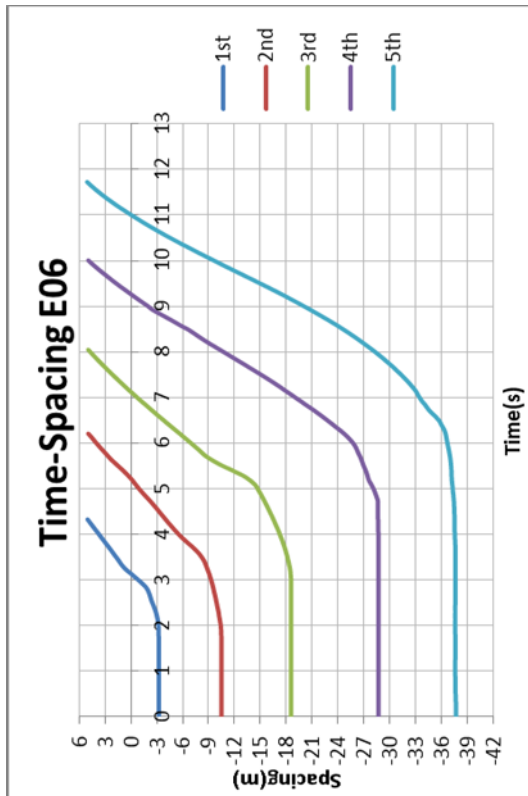
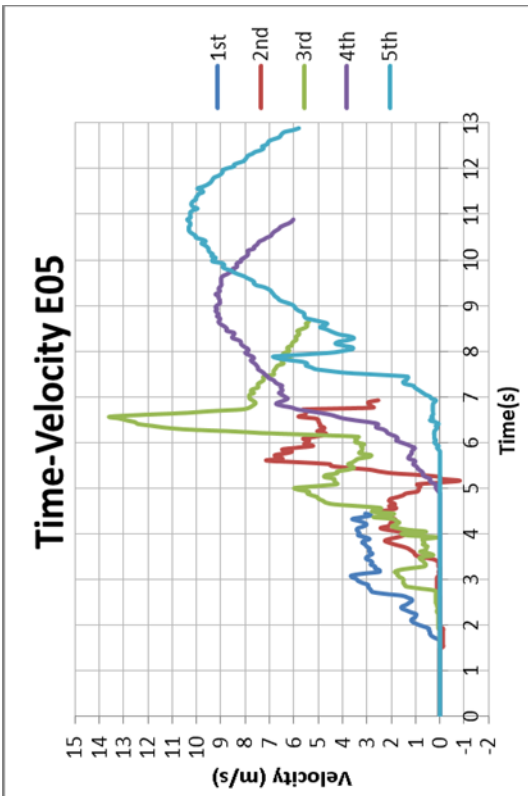
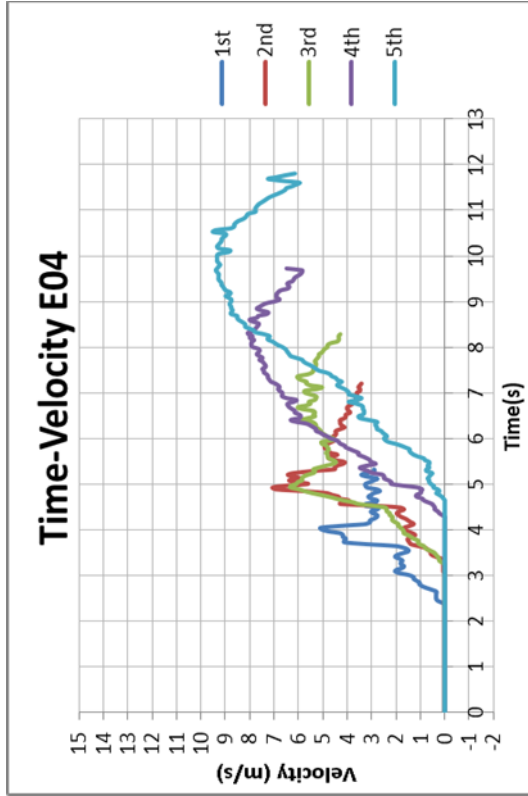
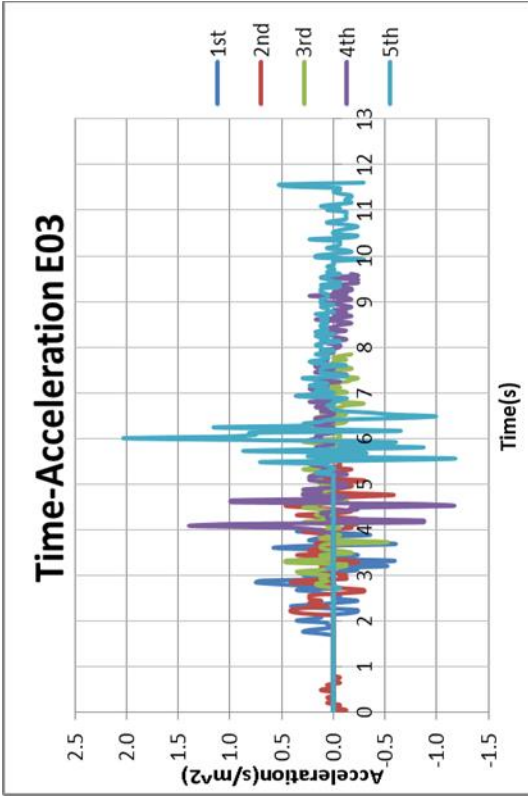
## Appendix C: Nerang Data site I raw trajectory velocity & acceleration samples

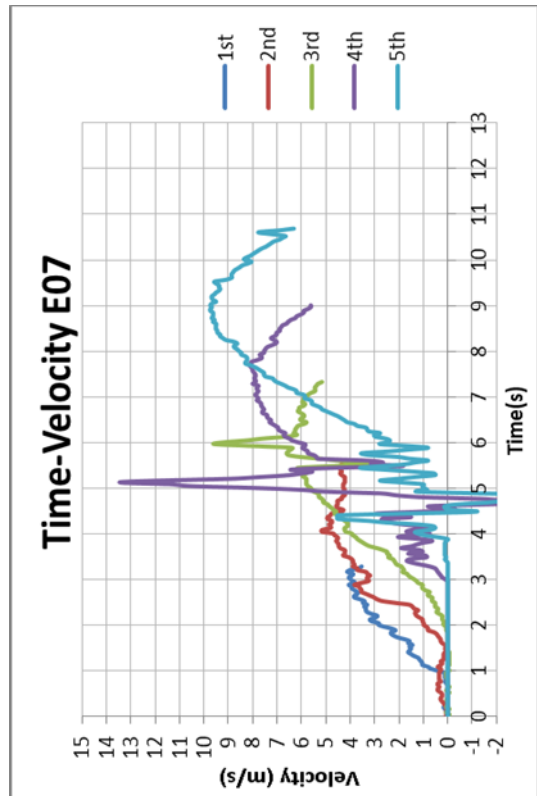
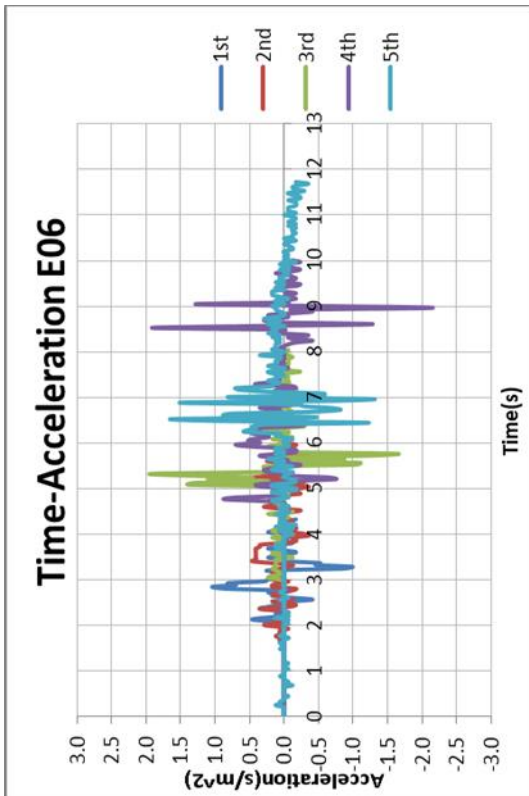
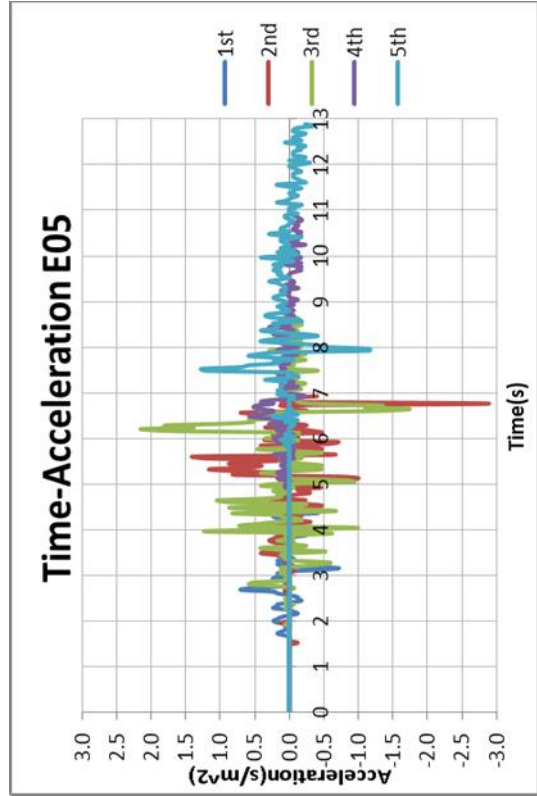
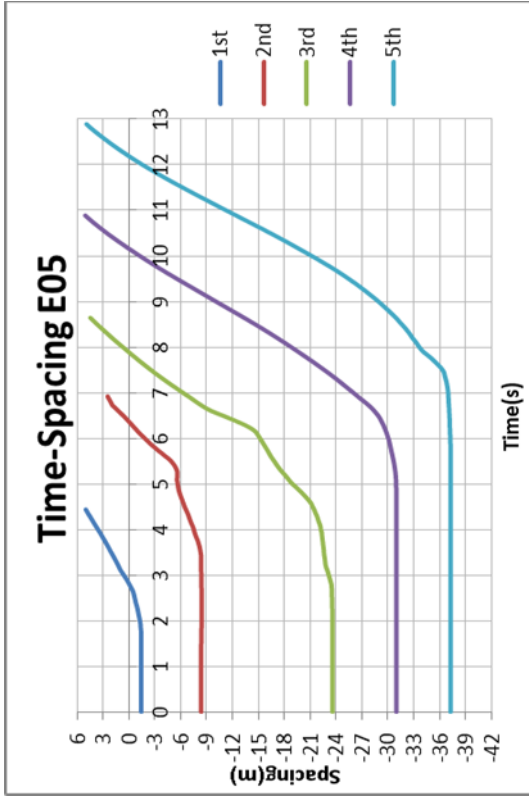


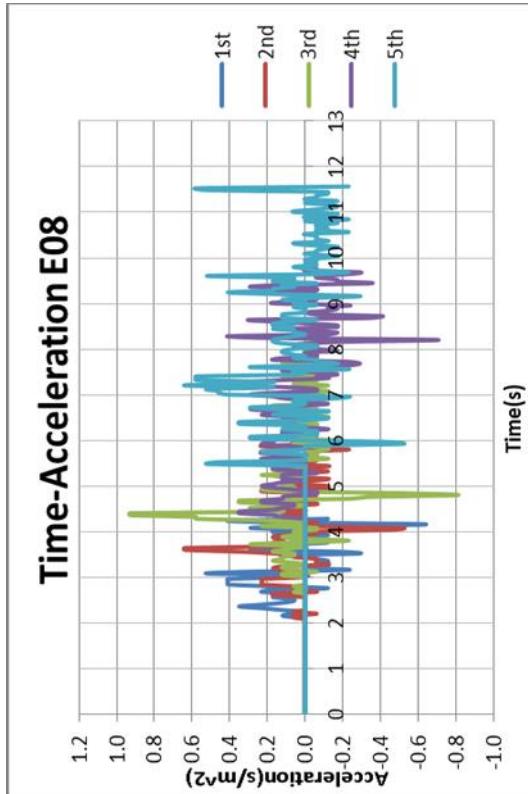
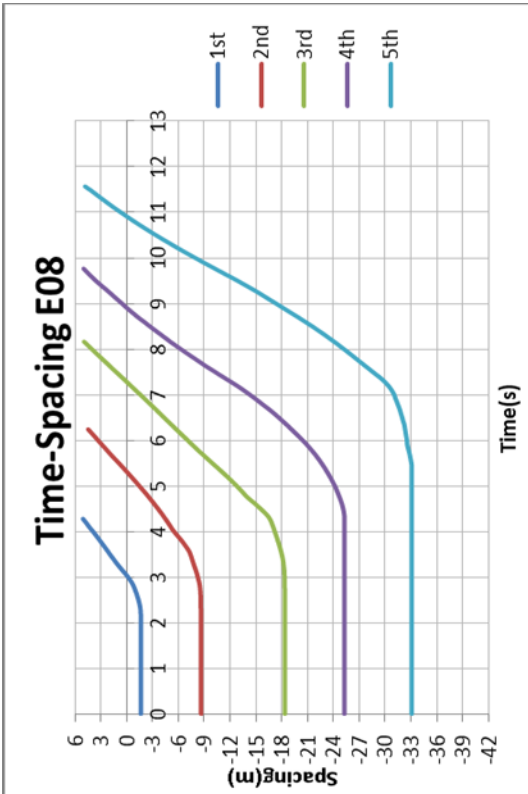
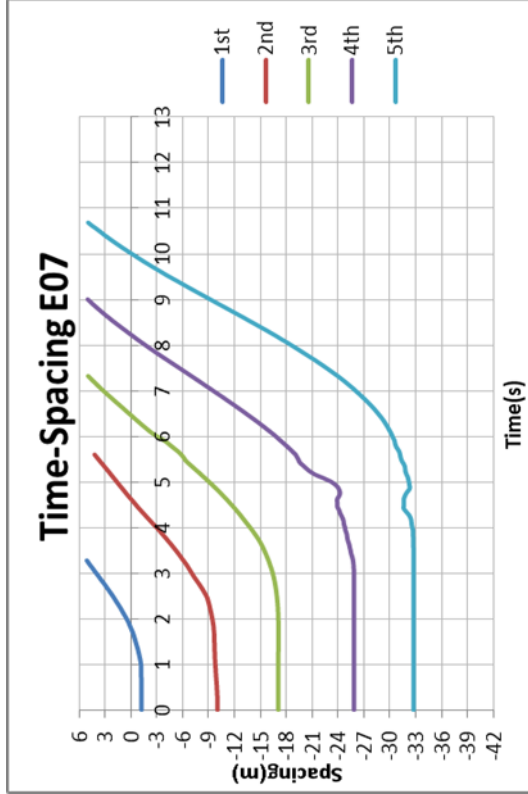
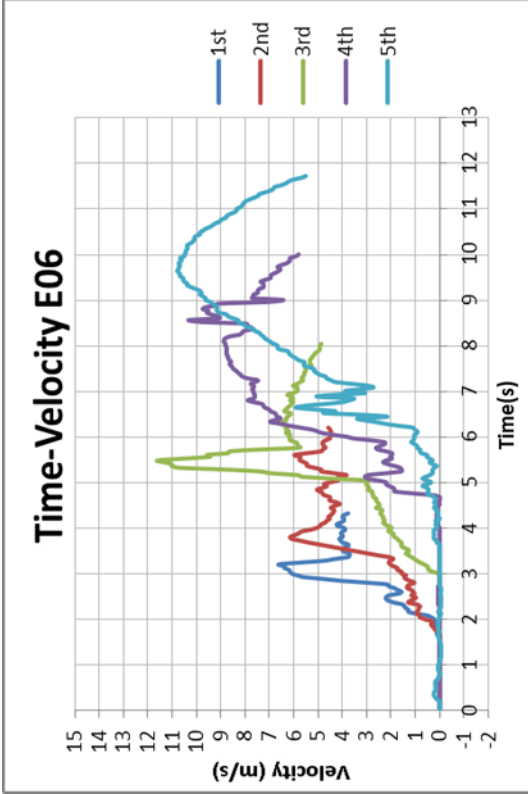


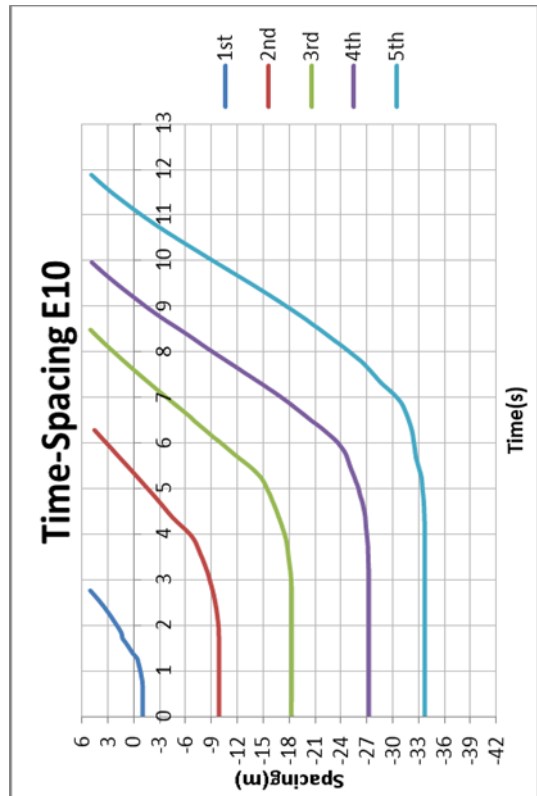
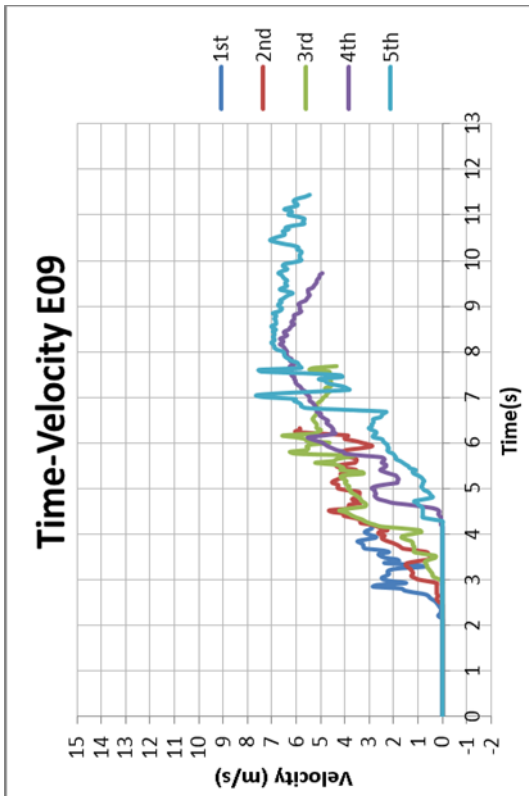
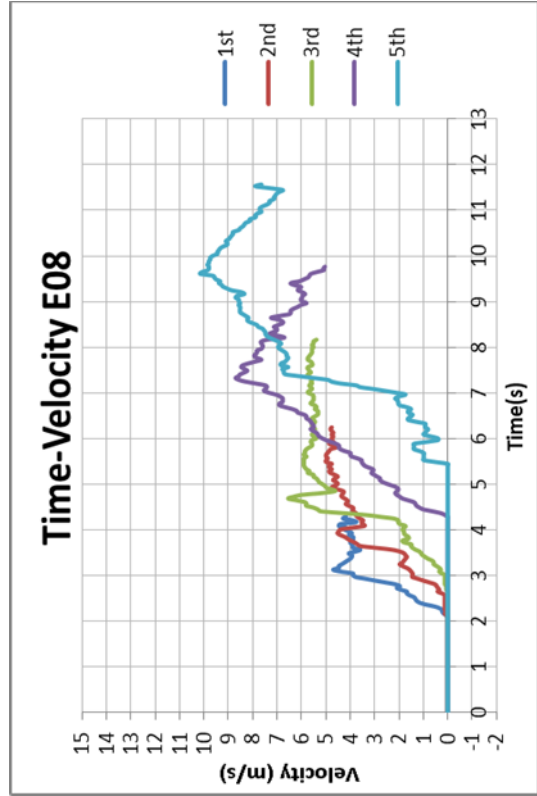
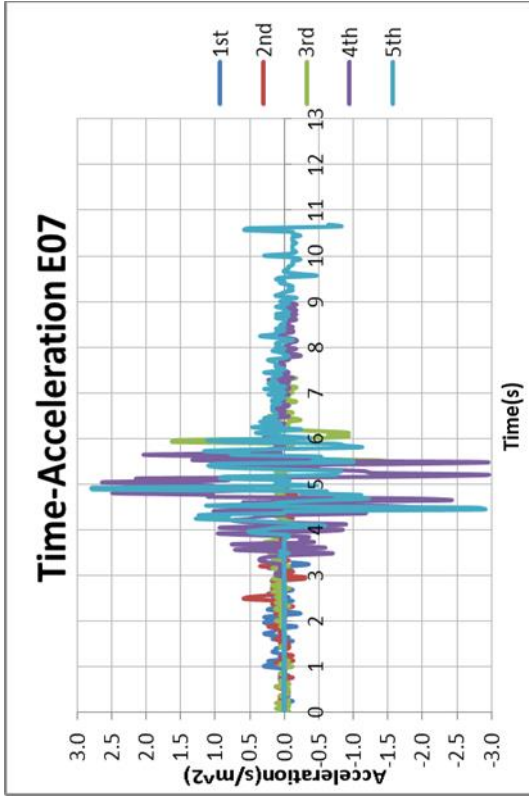


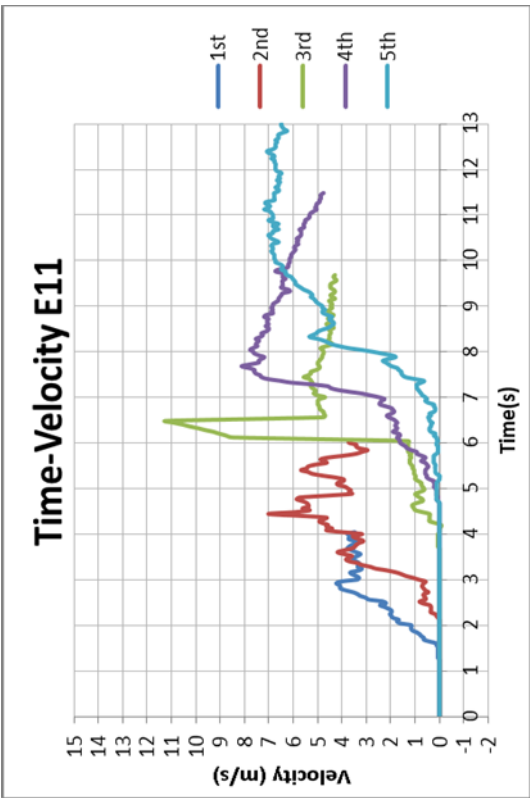
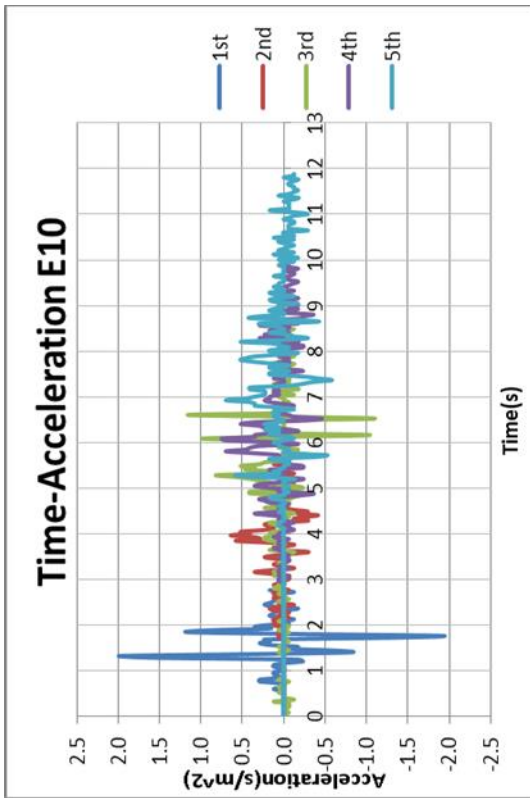
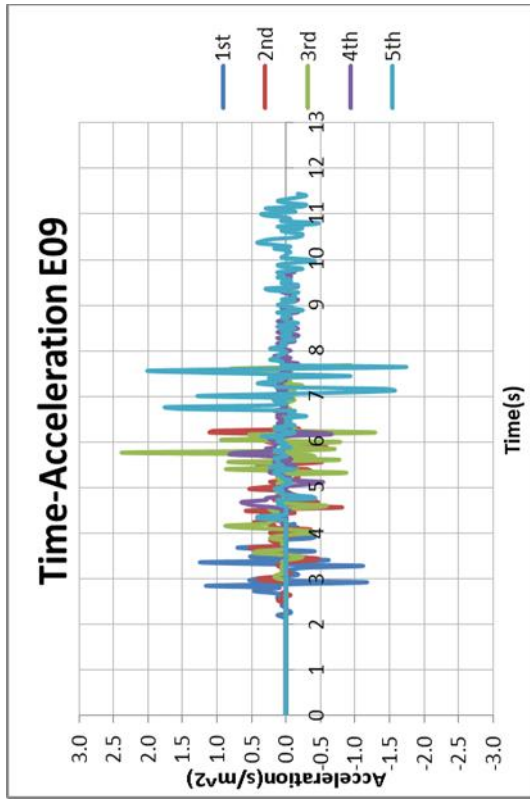
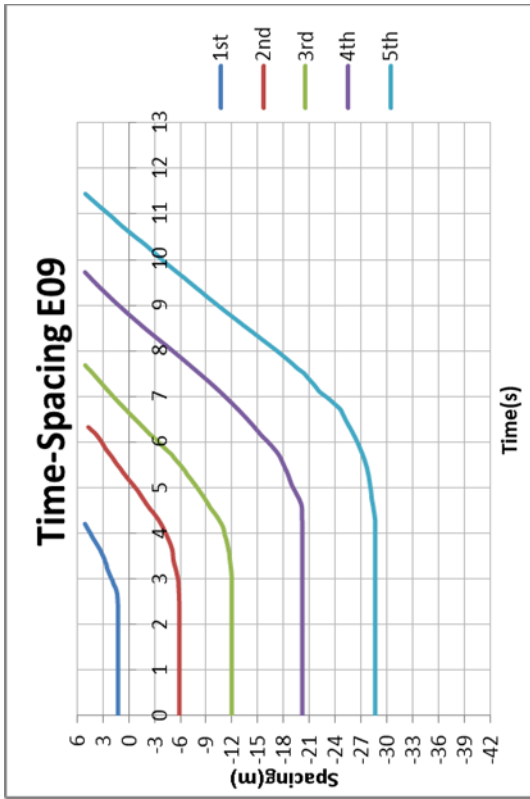


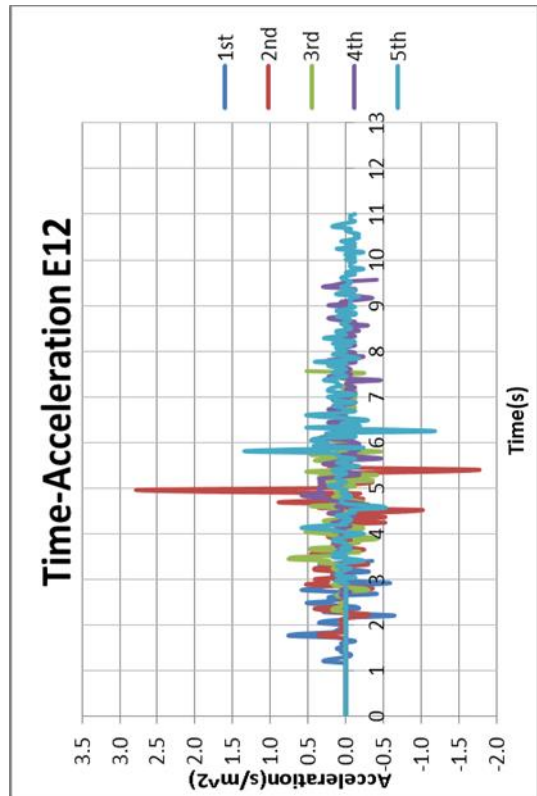
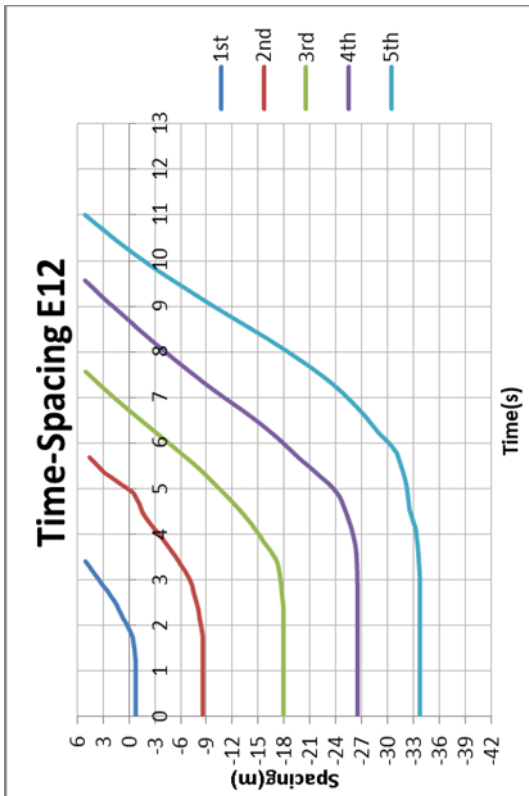
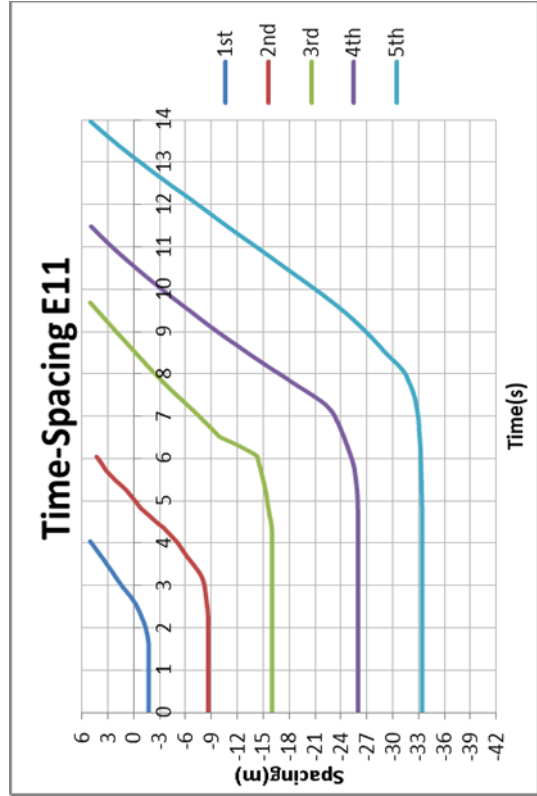
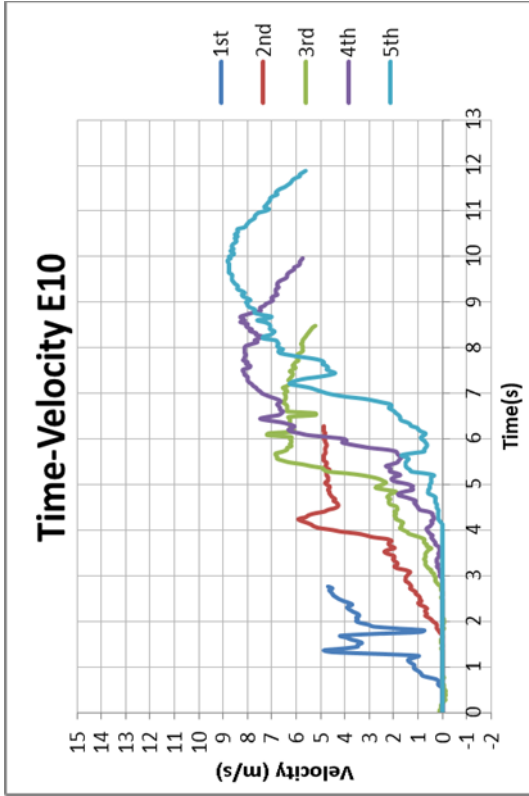


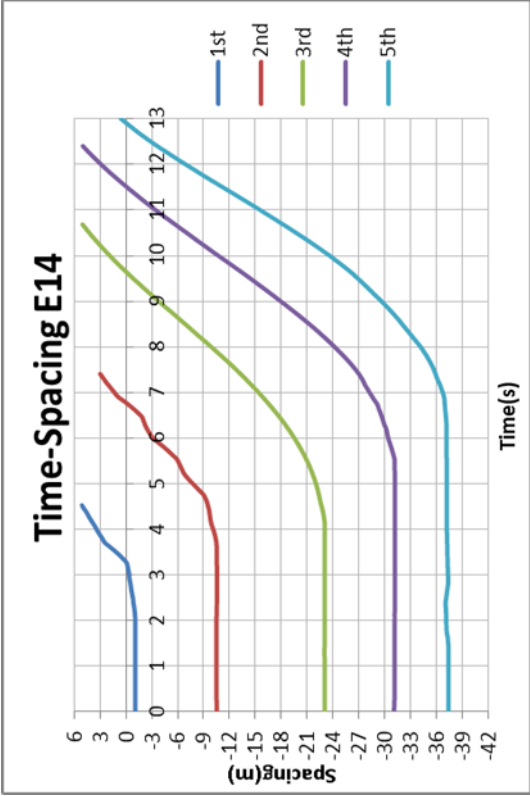
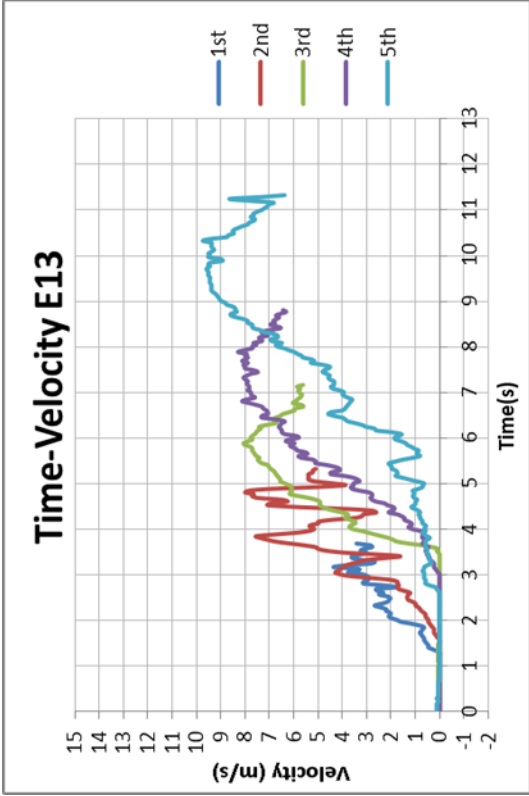
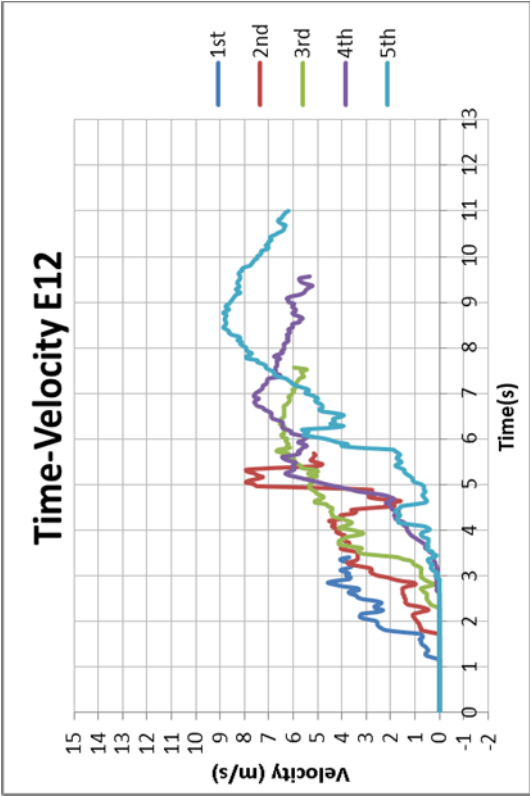
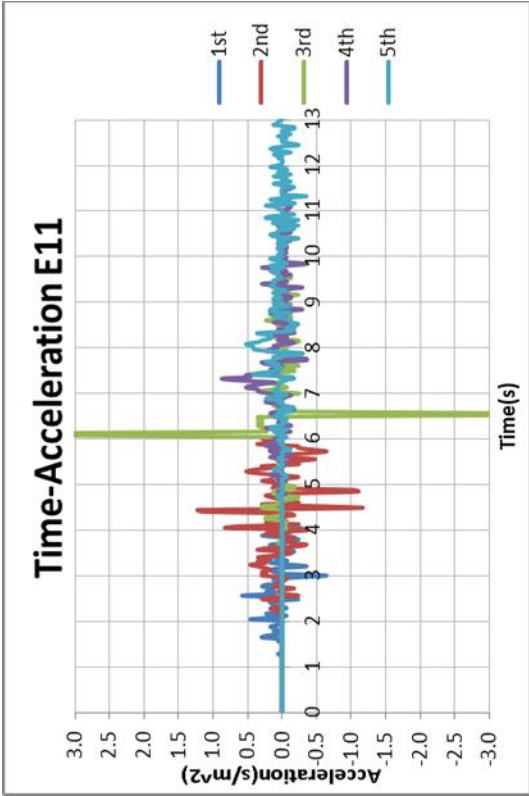




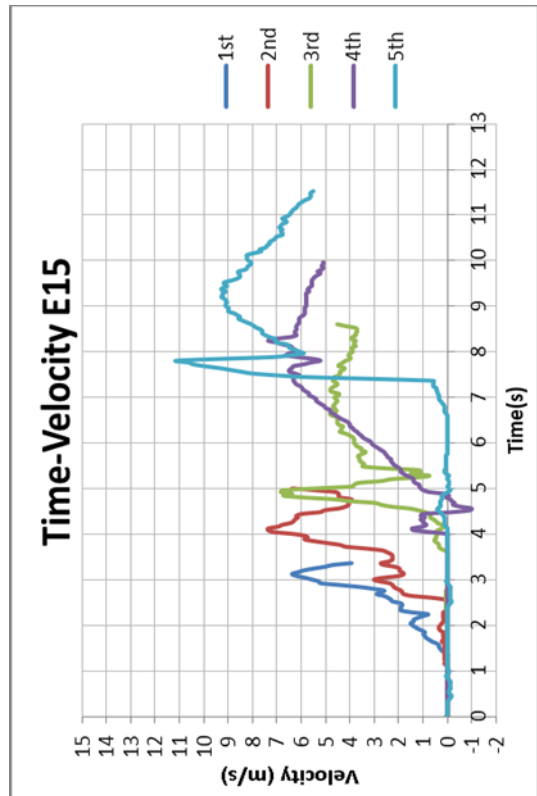
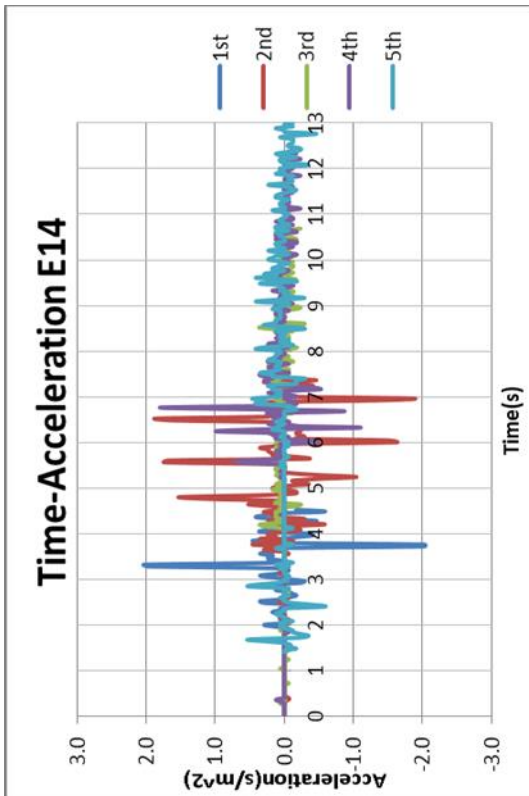
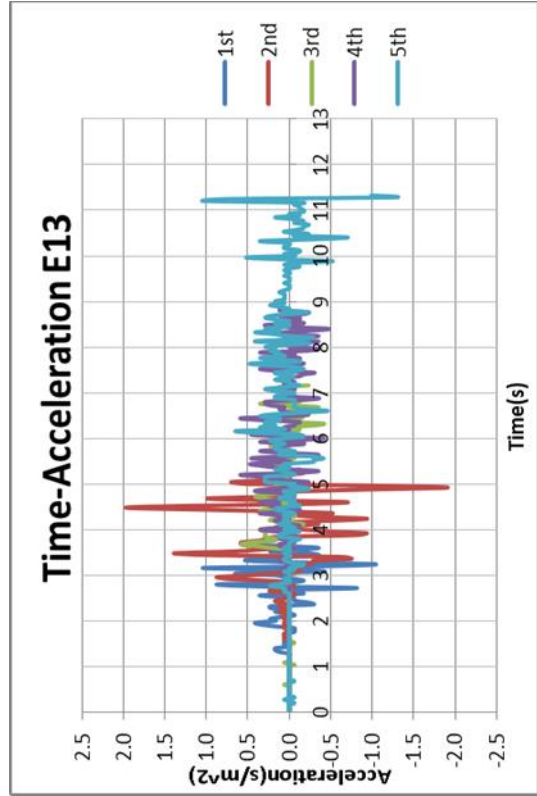
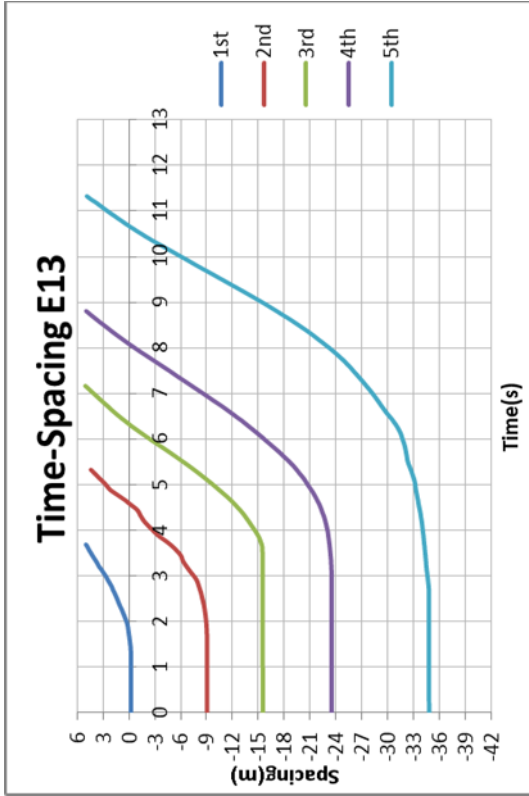


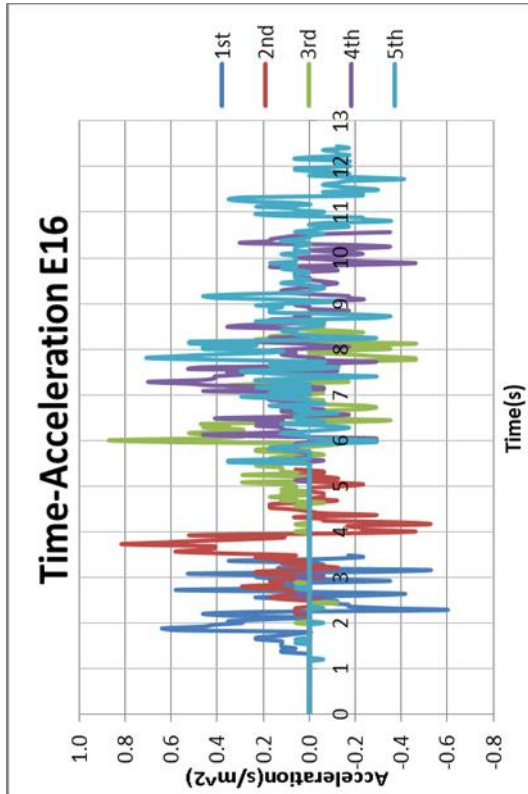
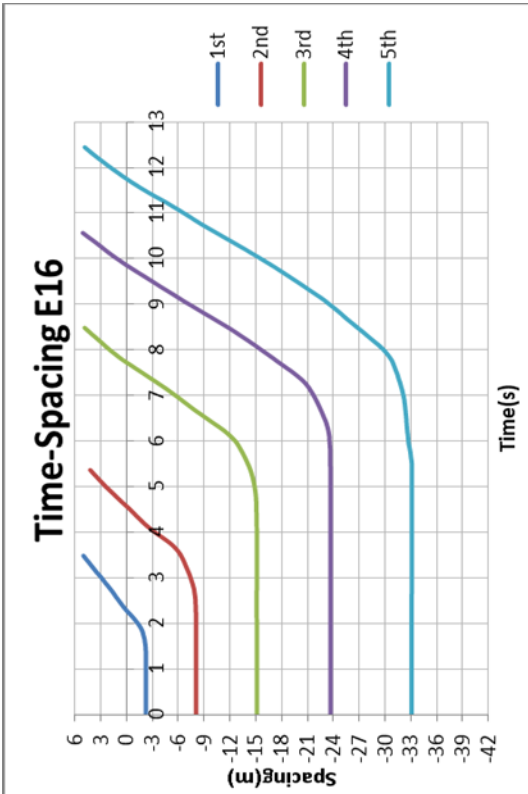
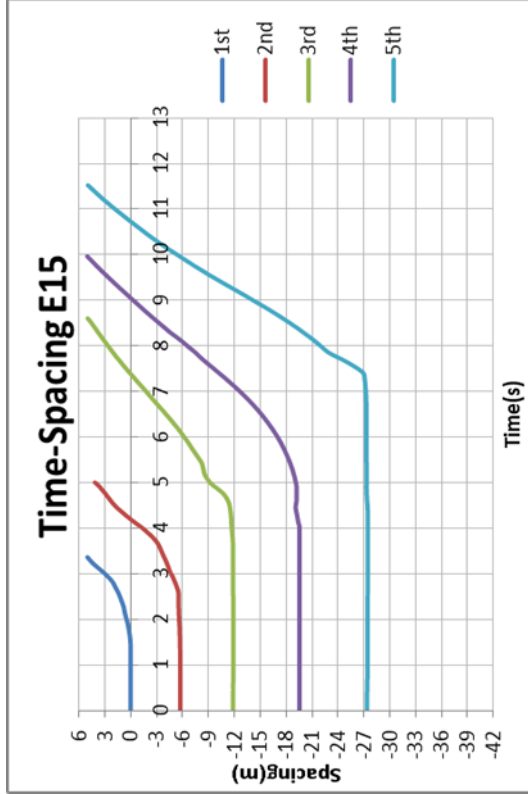
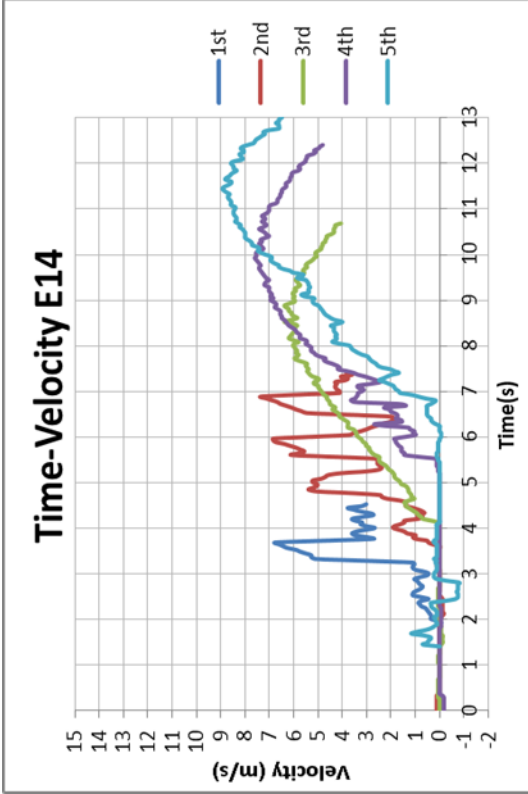


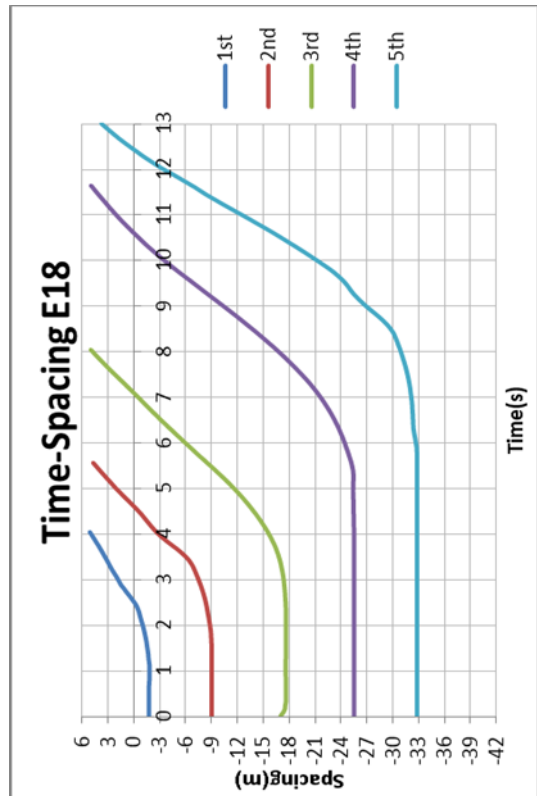
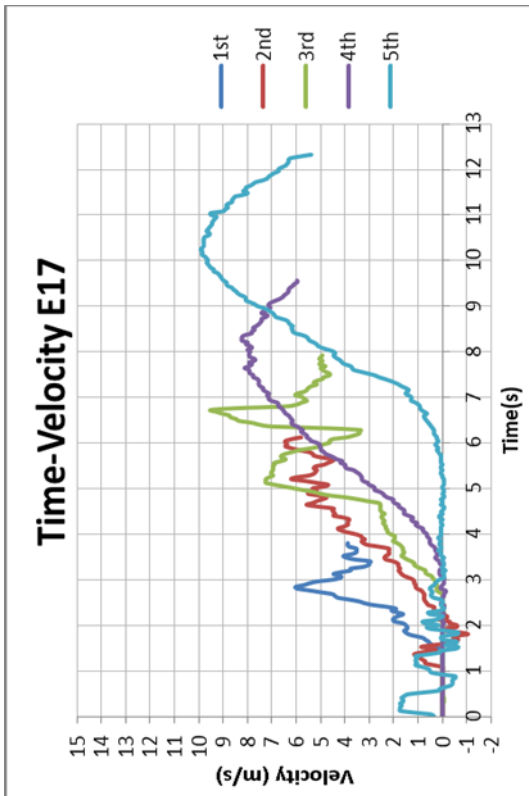
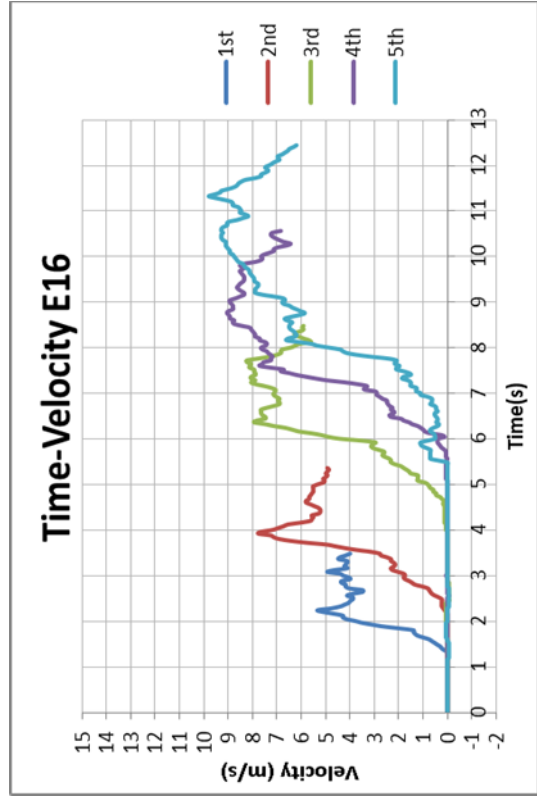
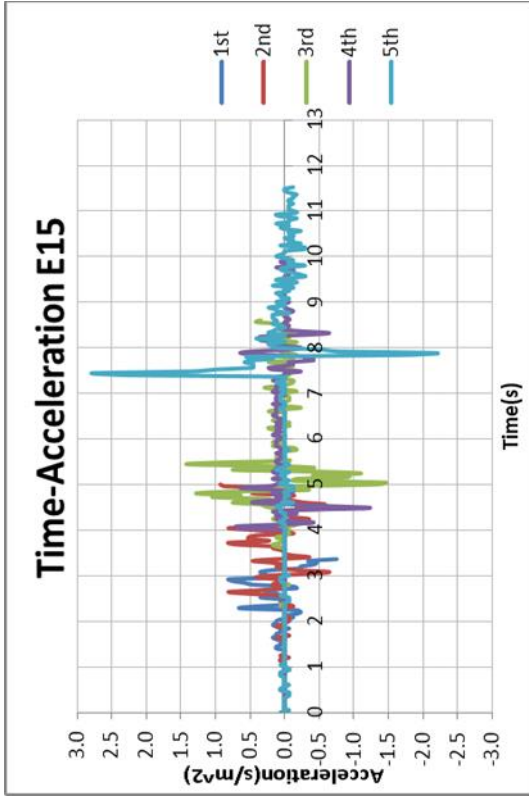


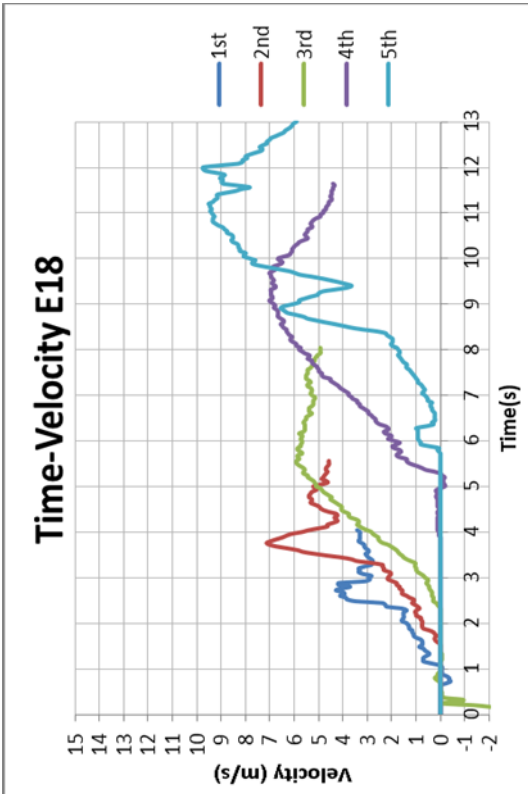
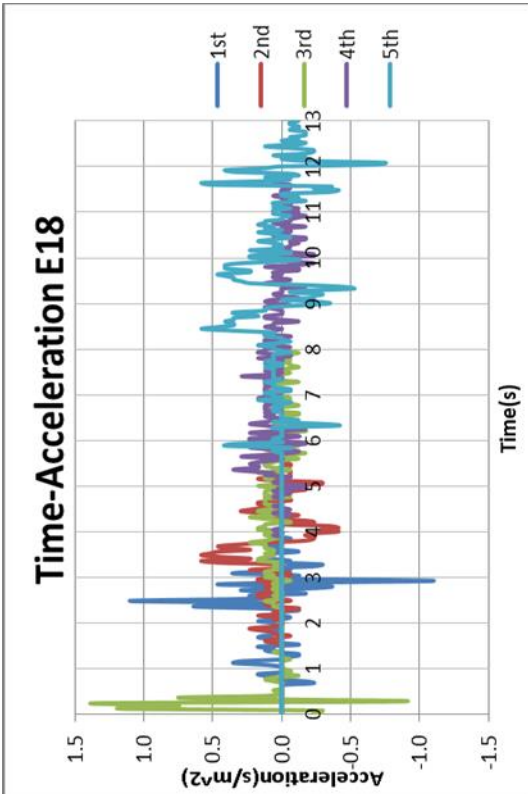
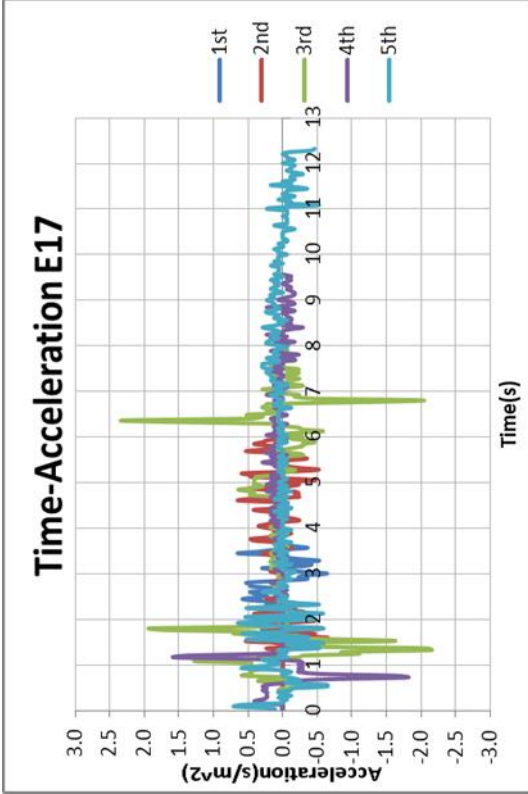
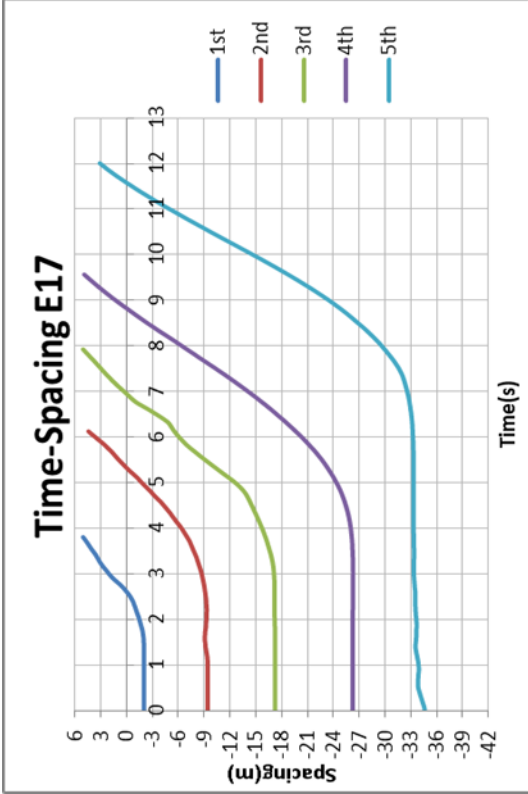




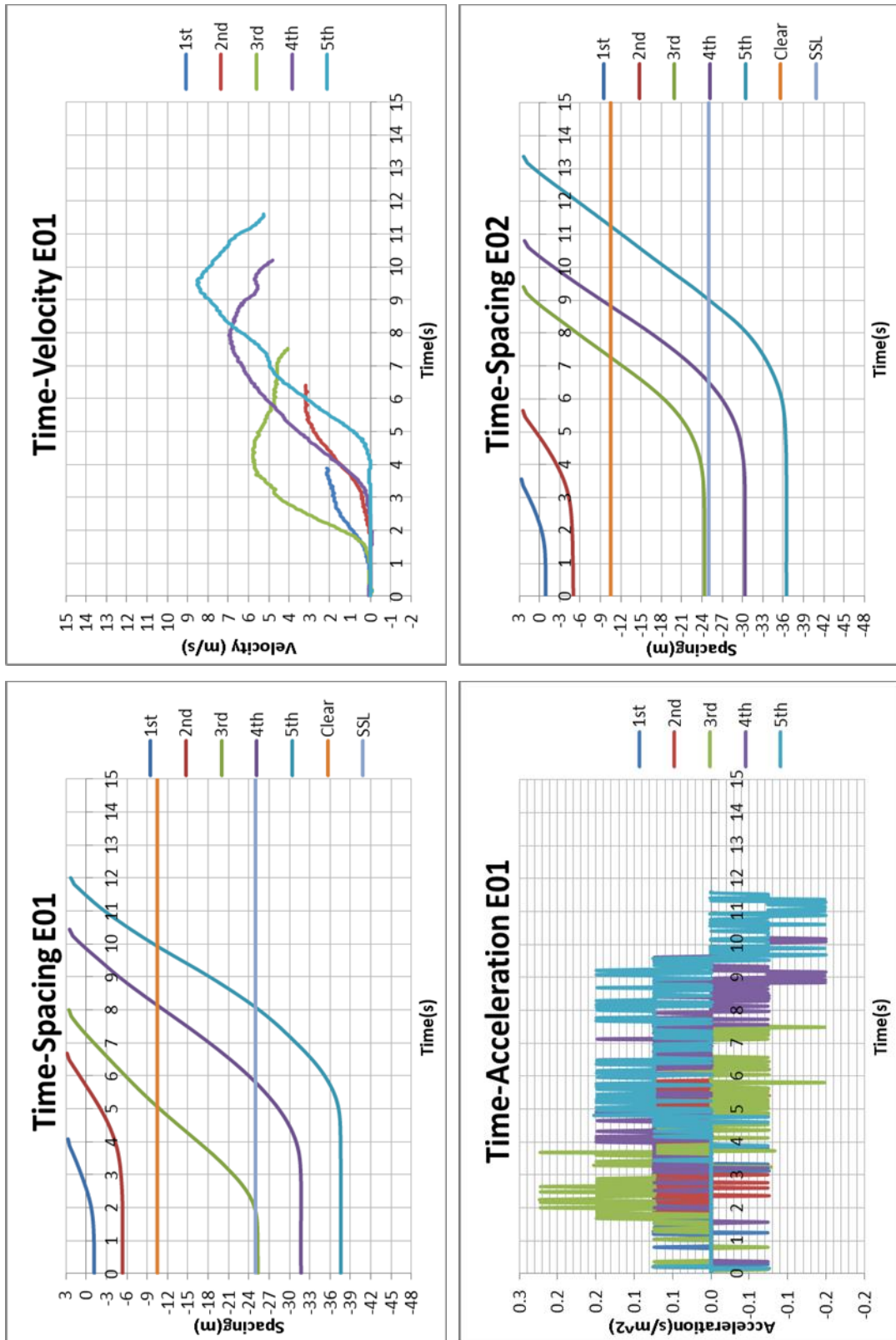


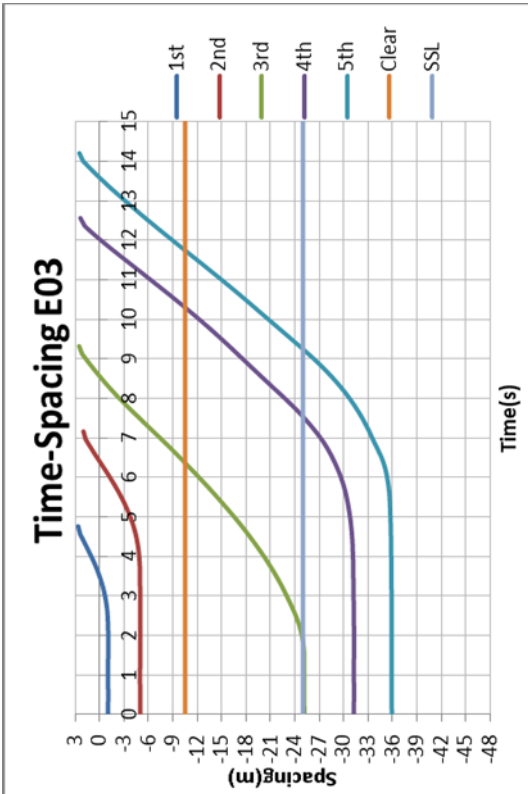
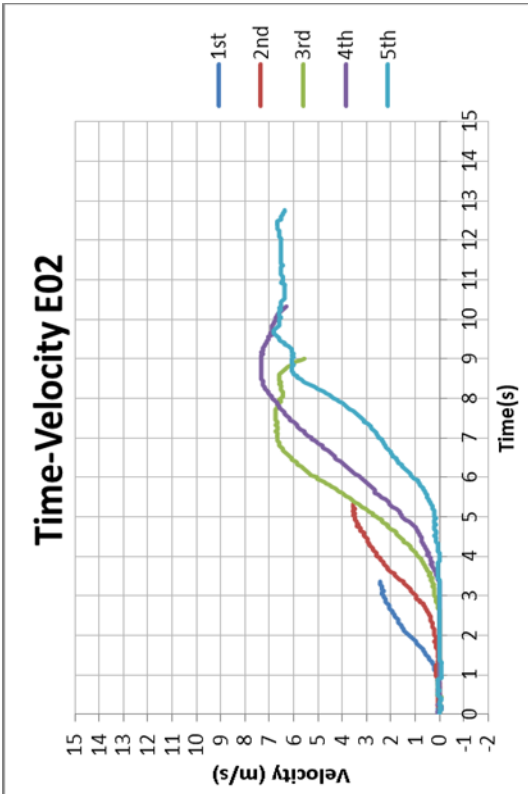
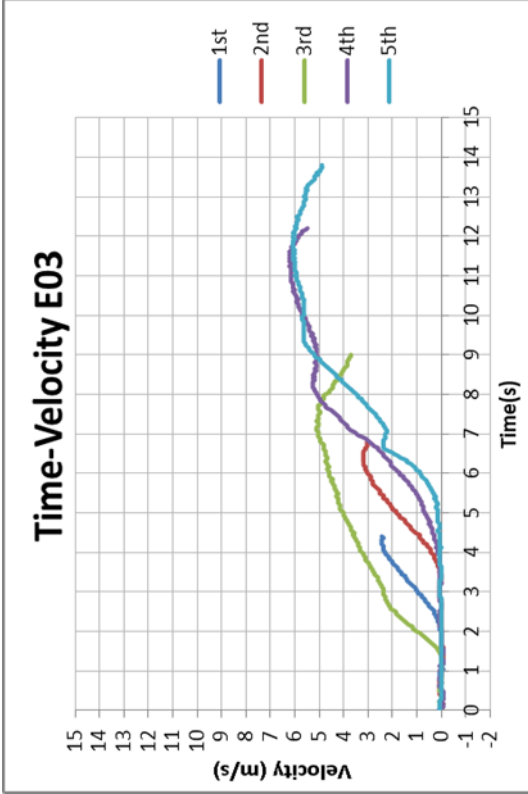
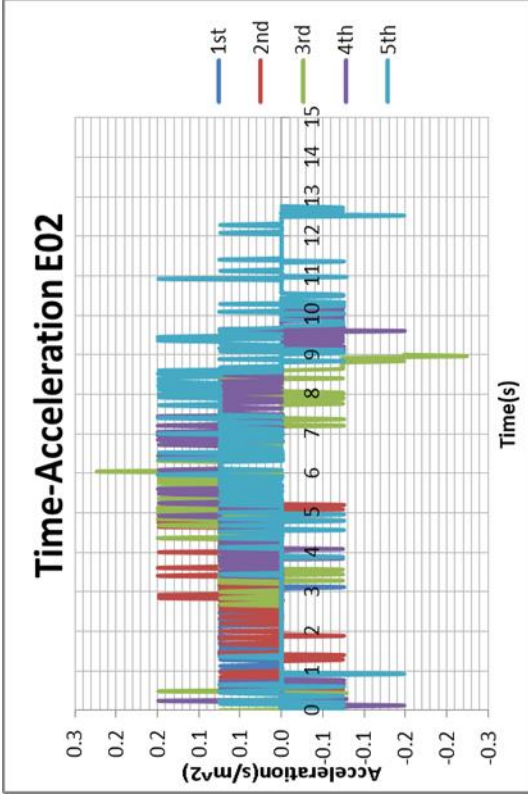


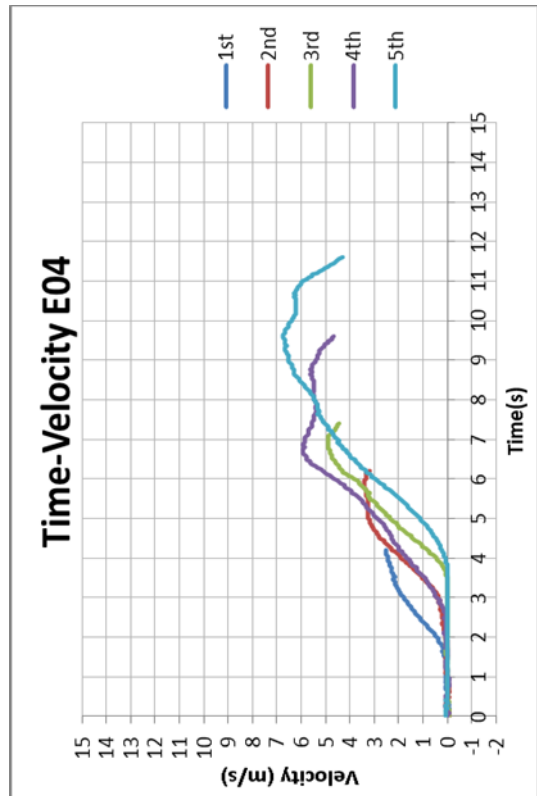
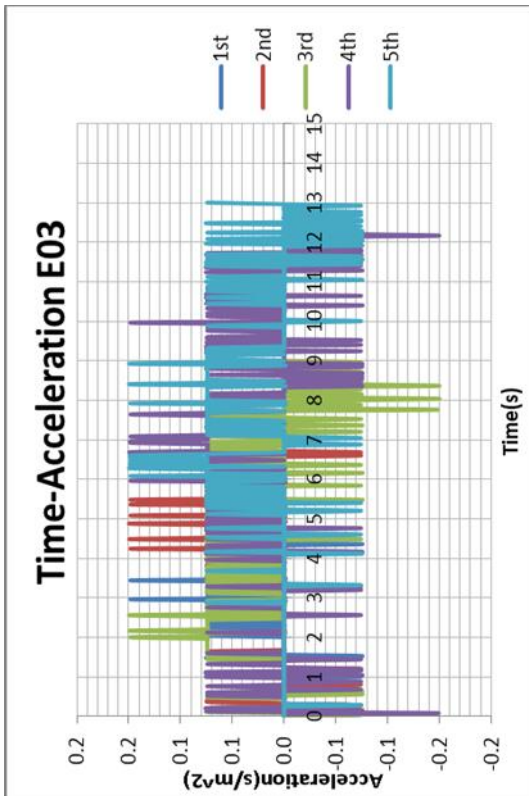
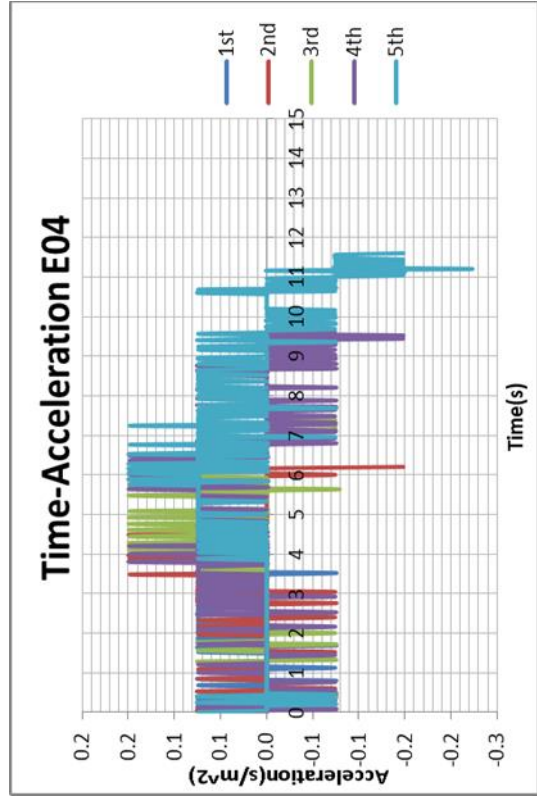
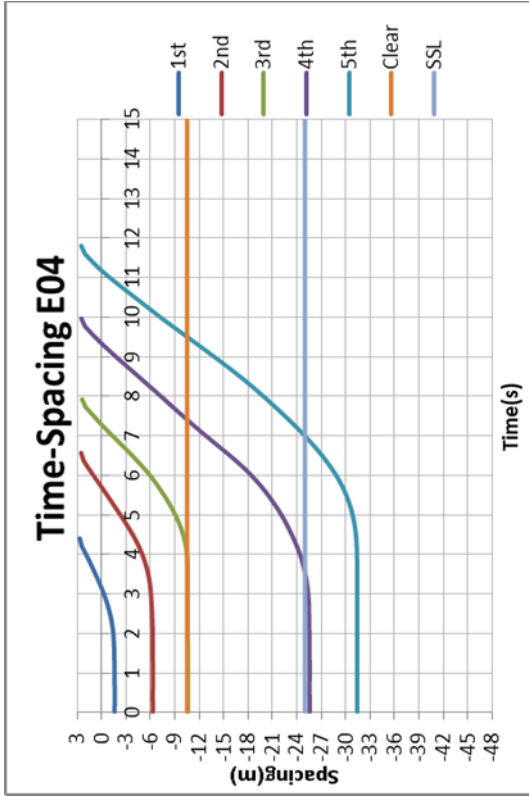


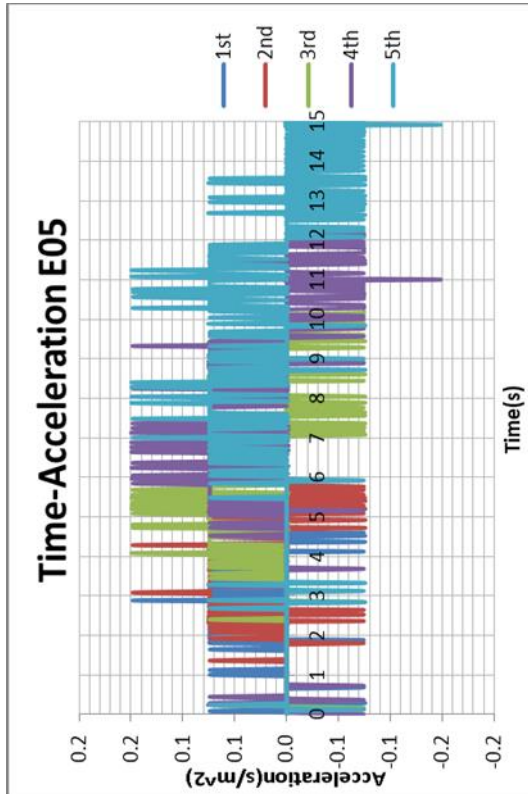
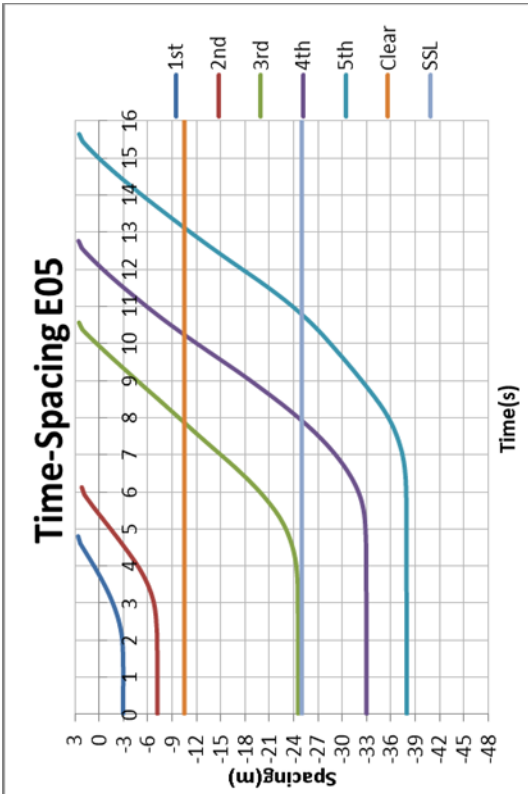
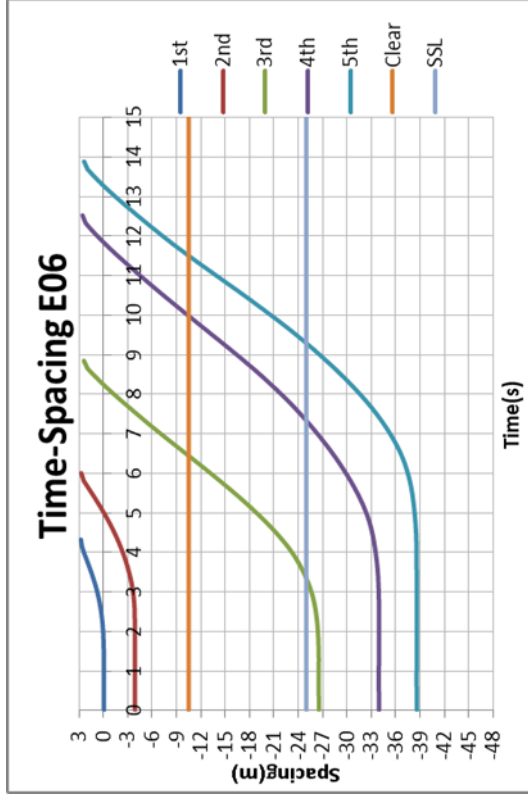
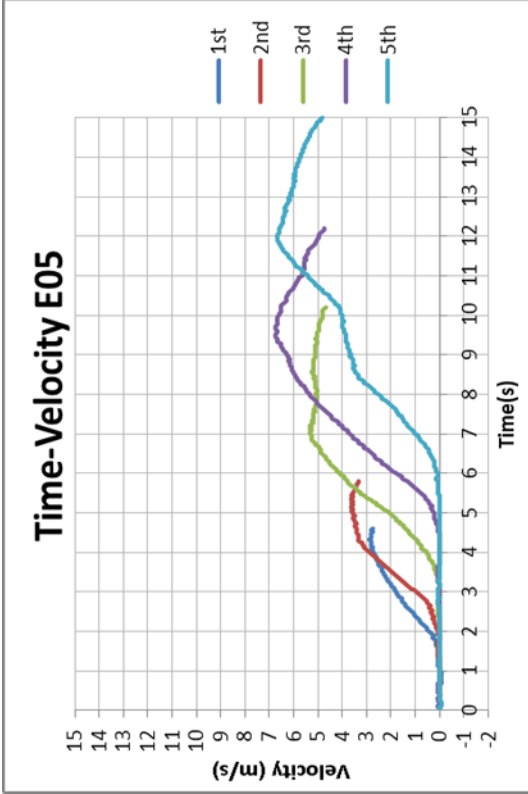


Appendix D: Nerang Data site II raw trajectory velocity & acceleration samples

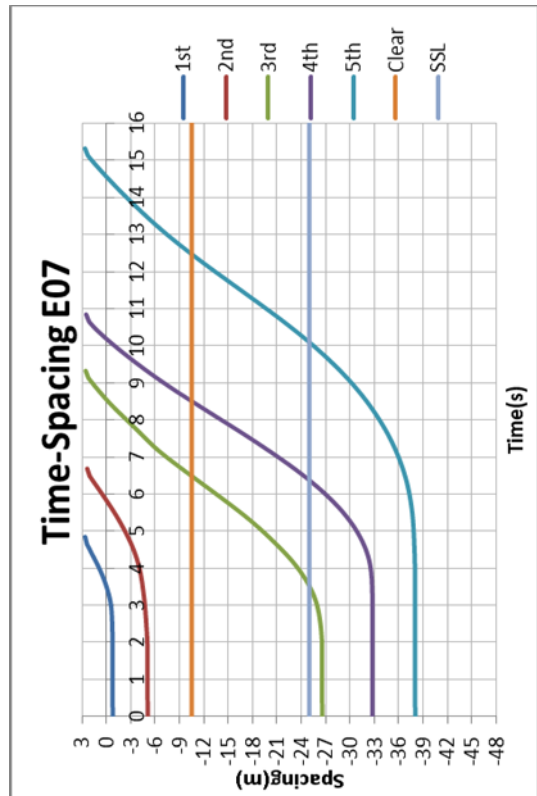
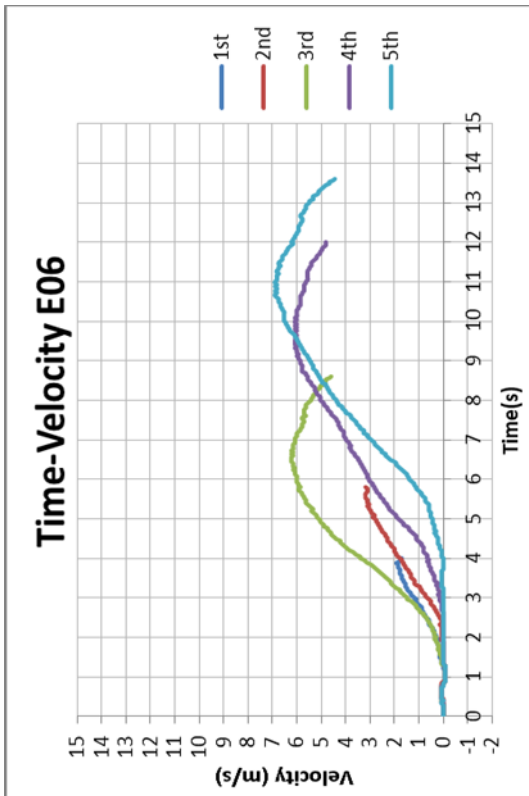
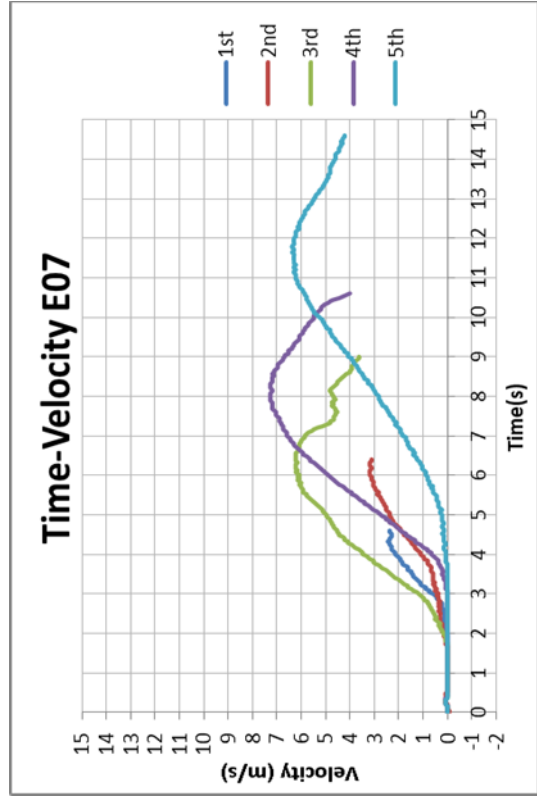
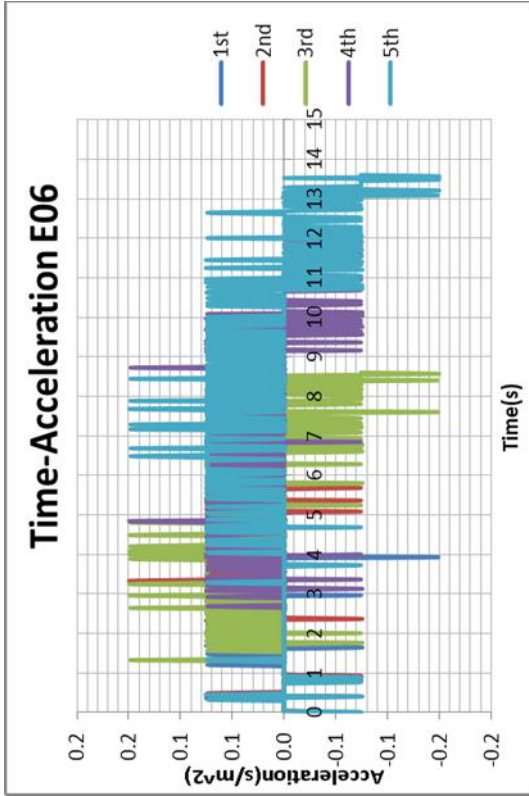


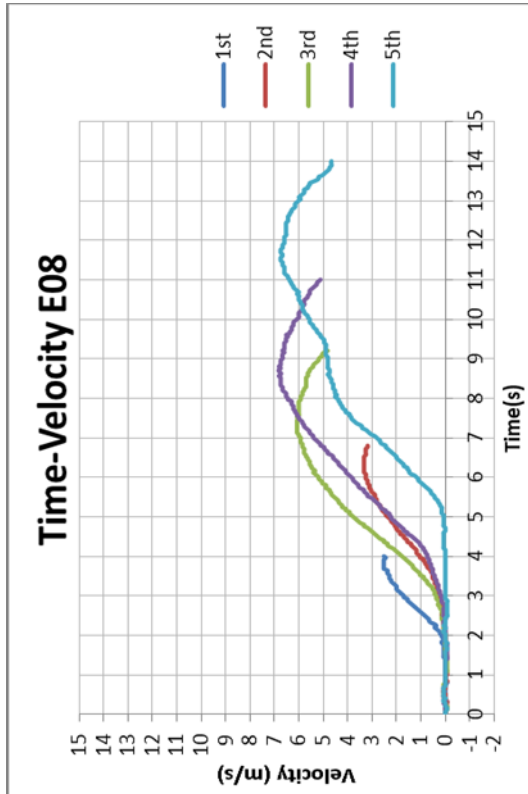
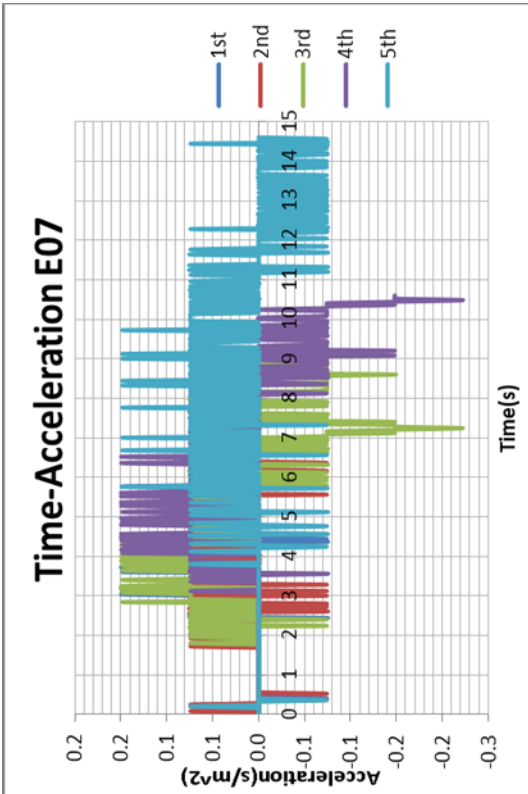
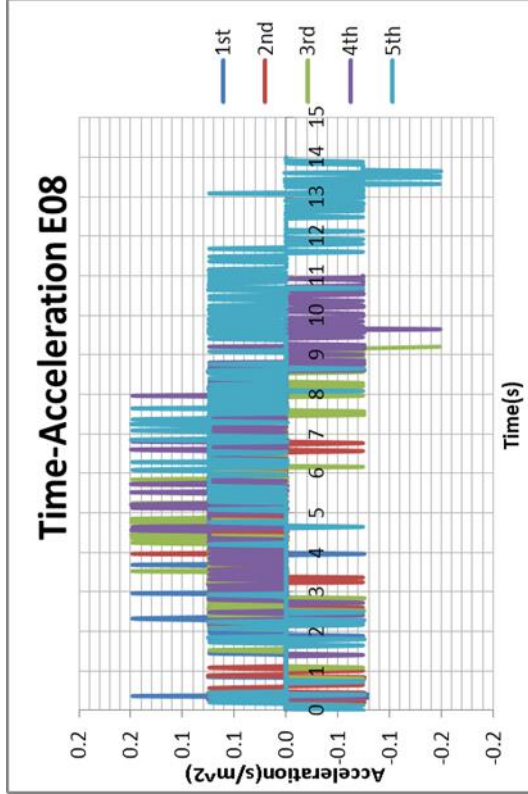
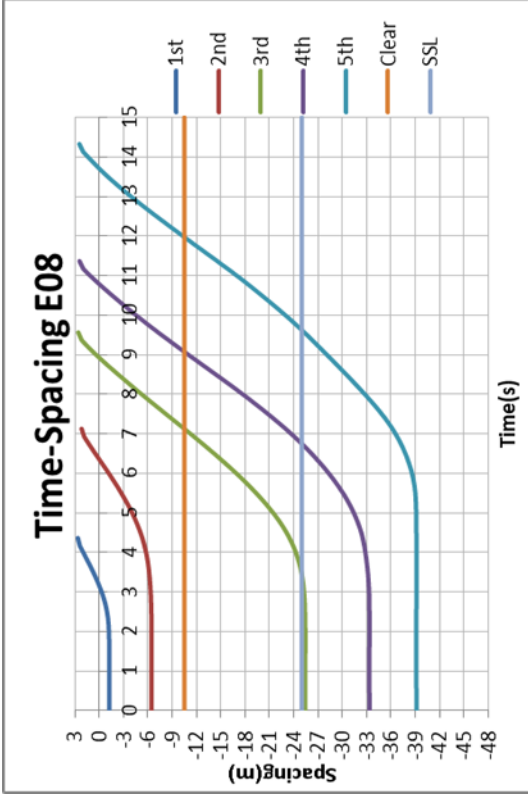


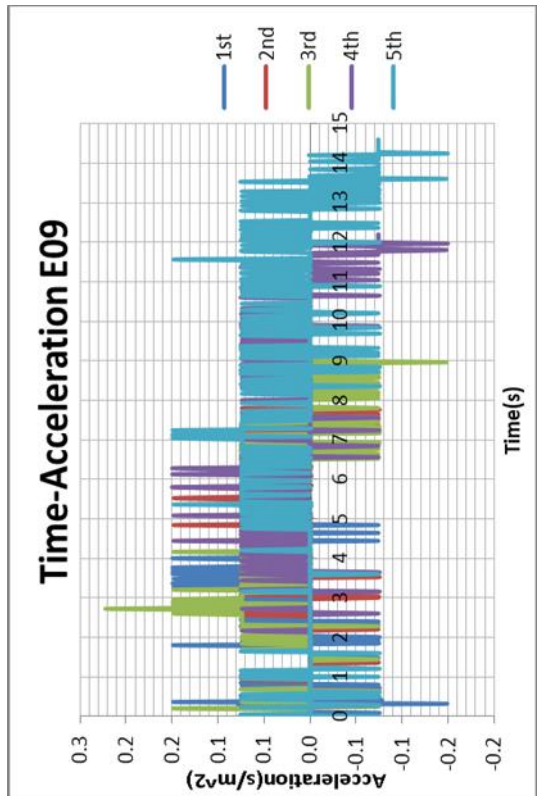
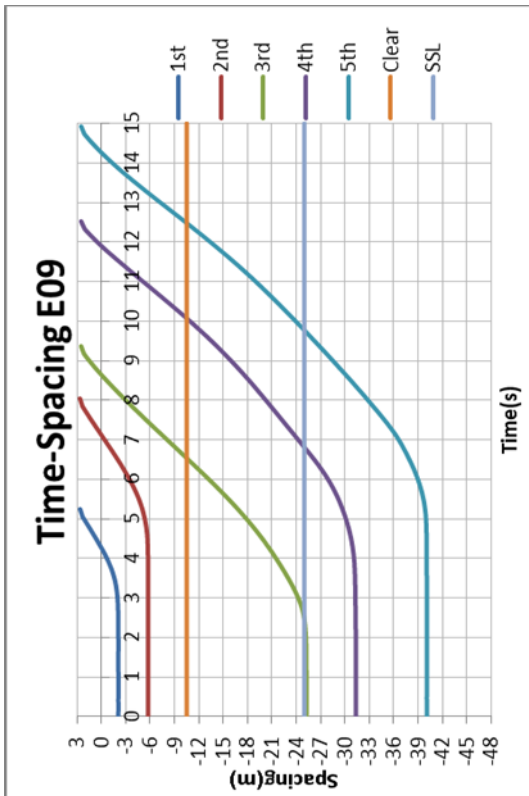
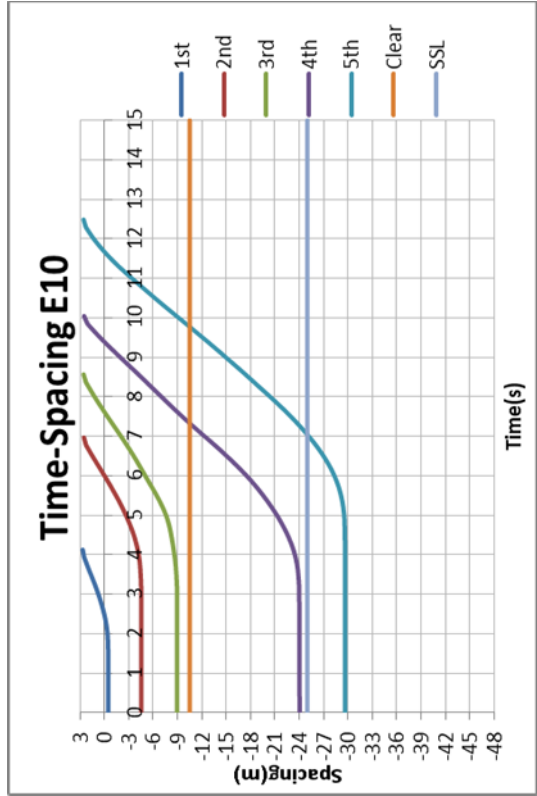
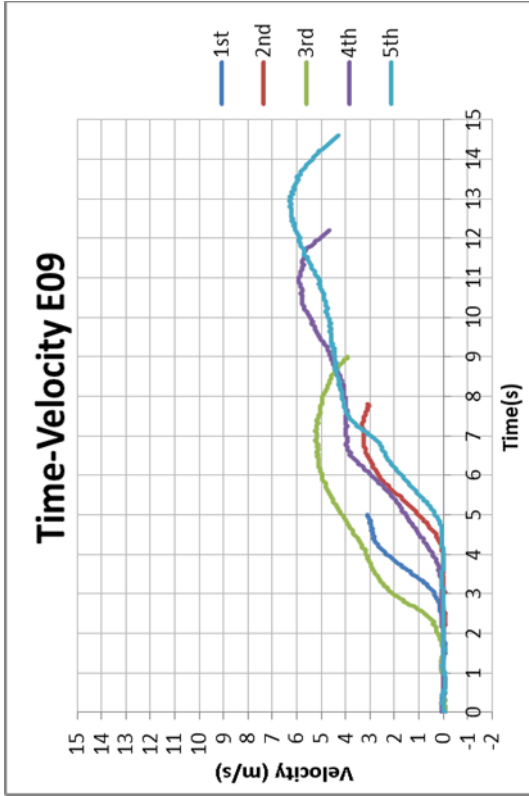


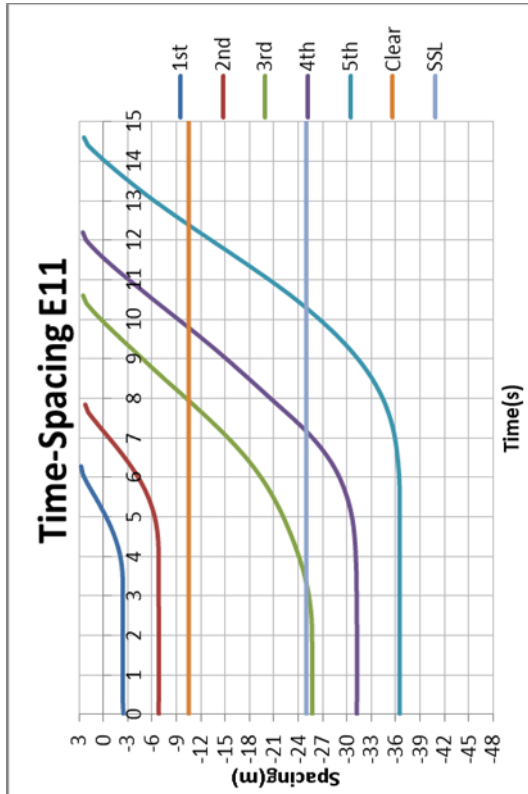
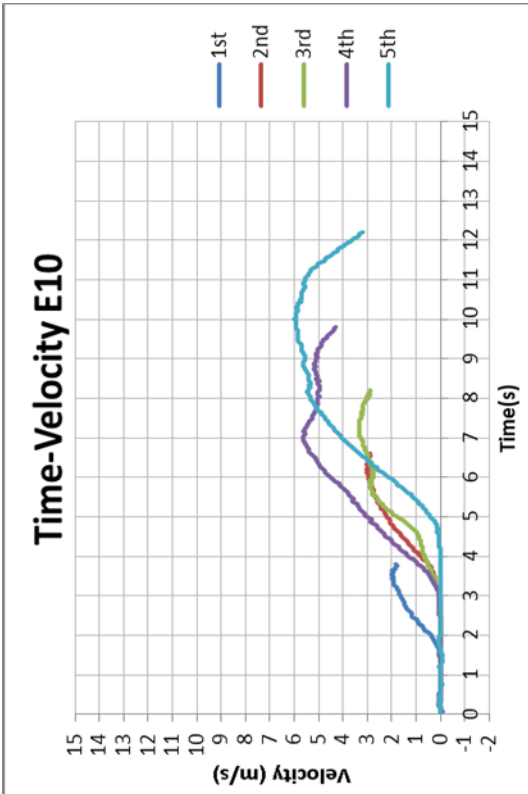
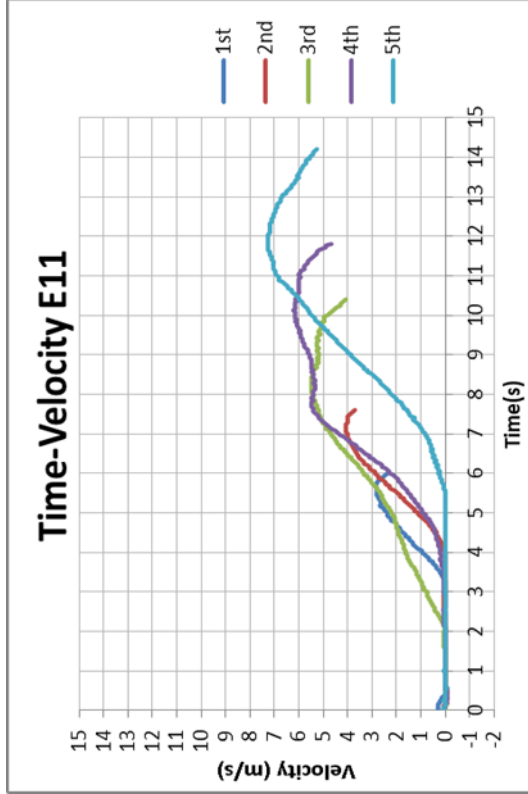
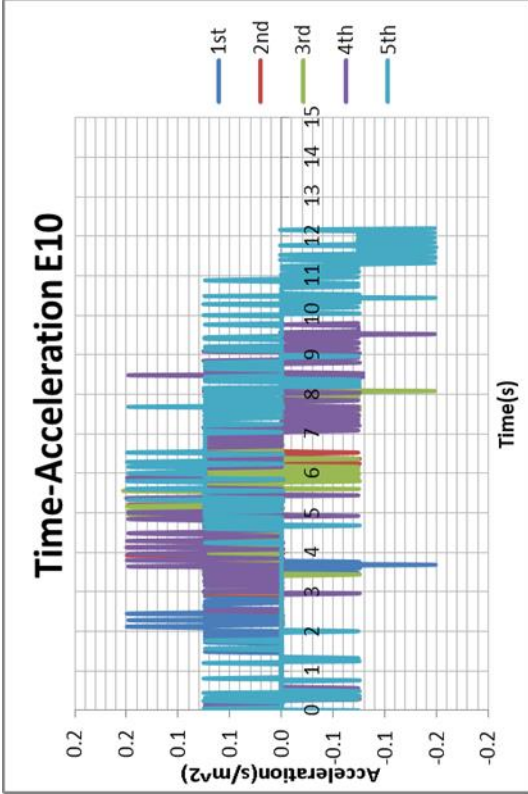


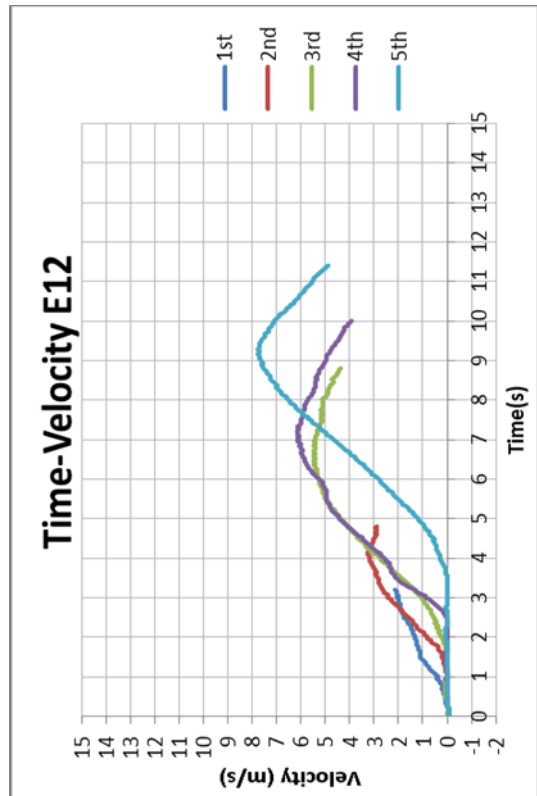
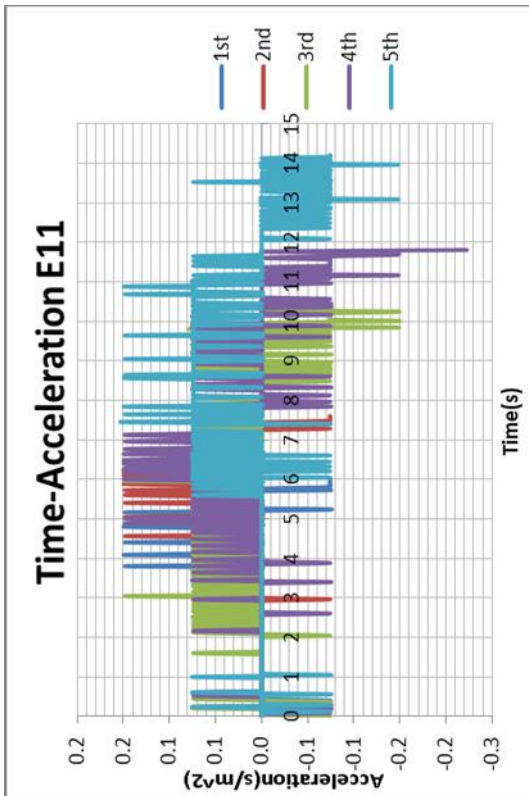
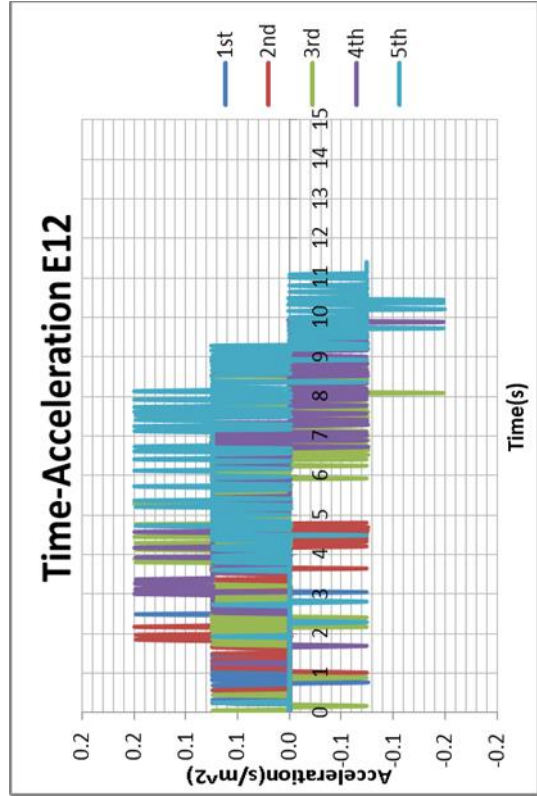
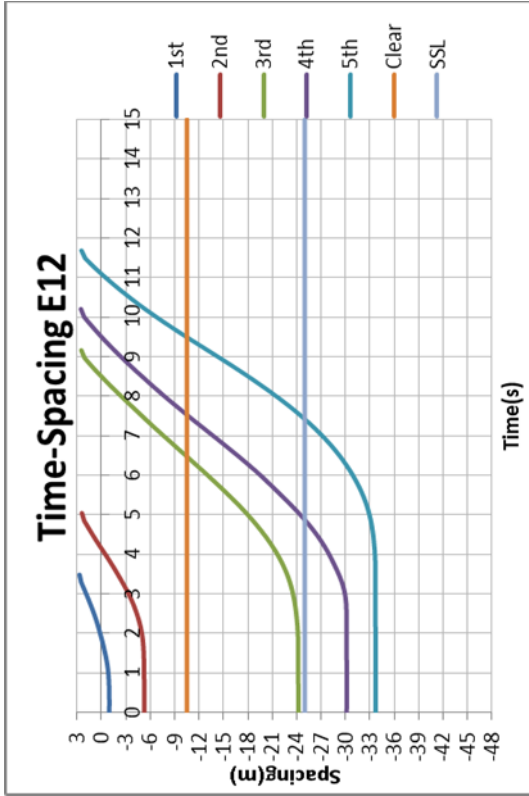


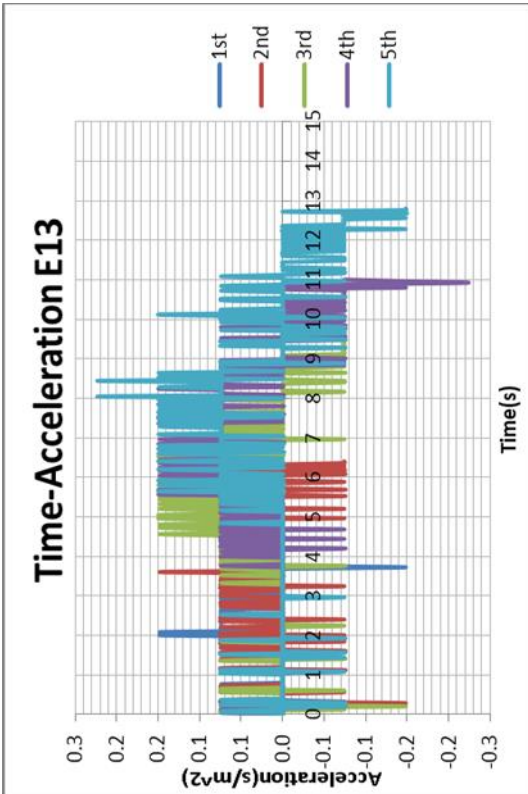
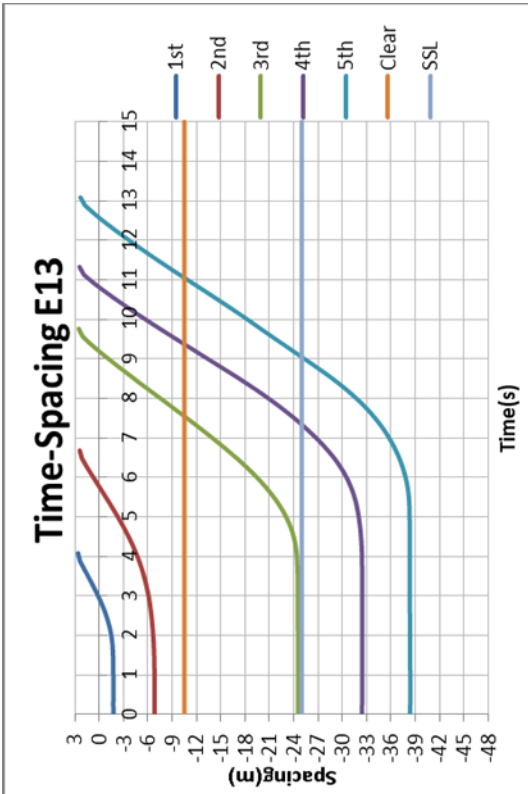
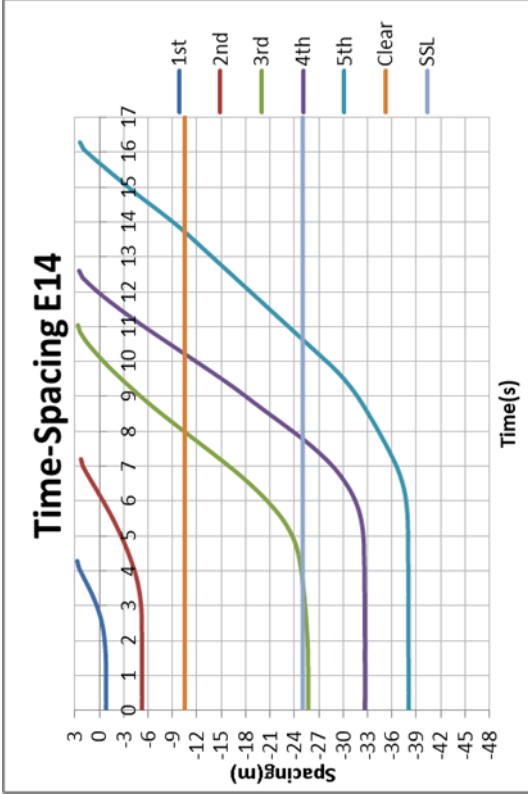
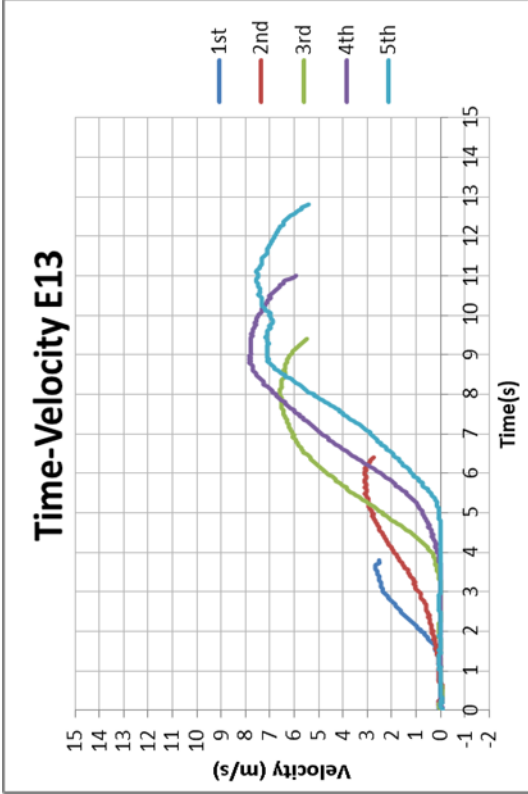


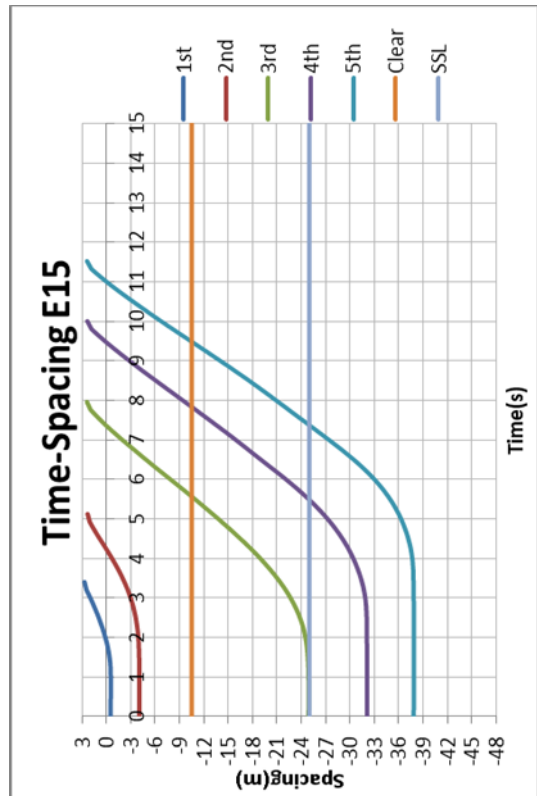
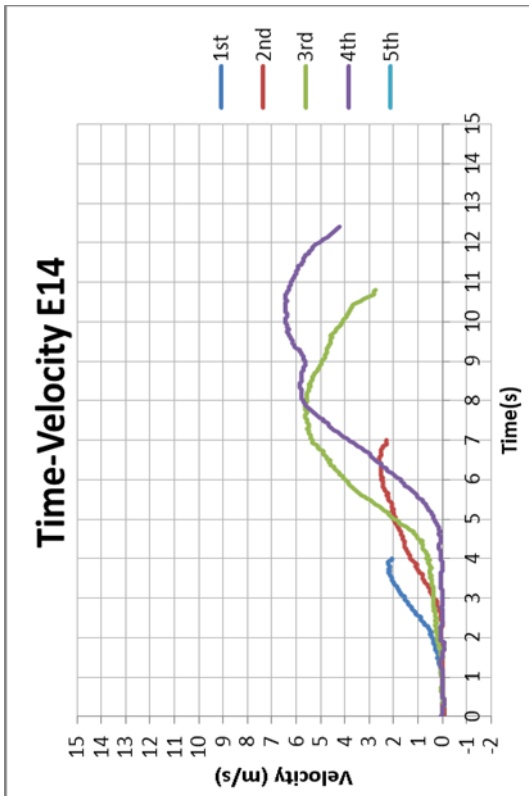
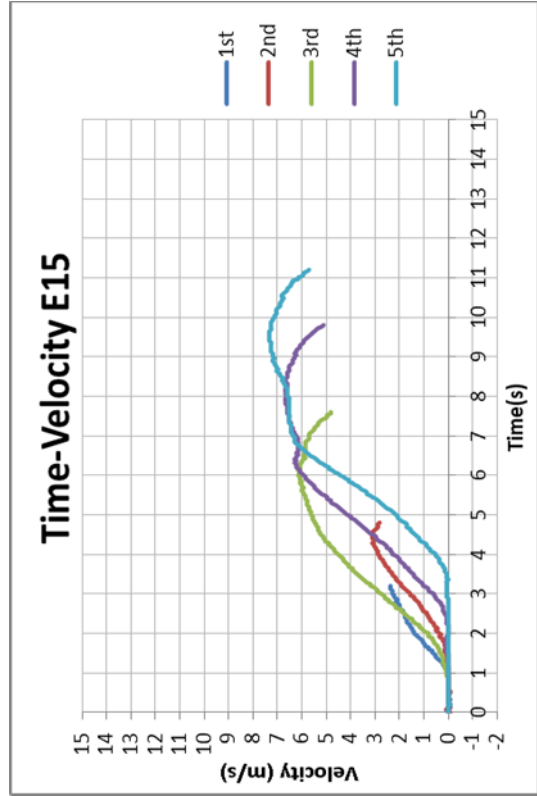
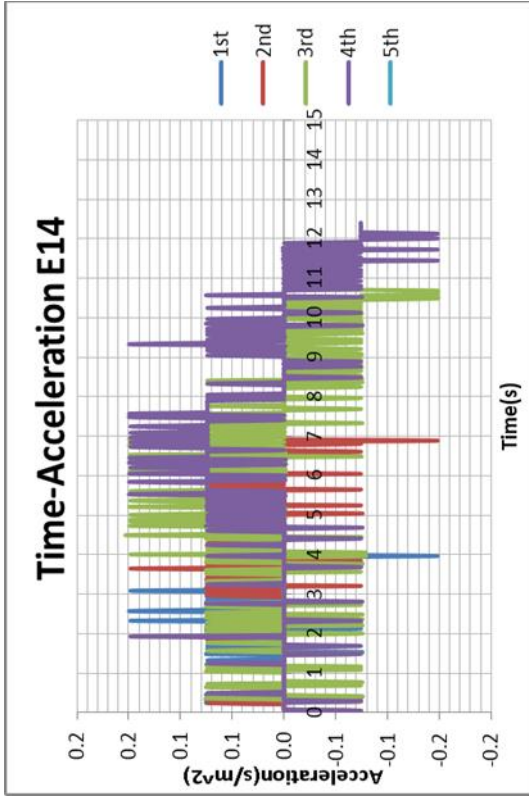


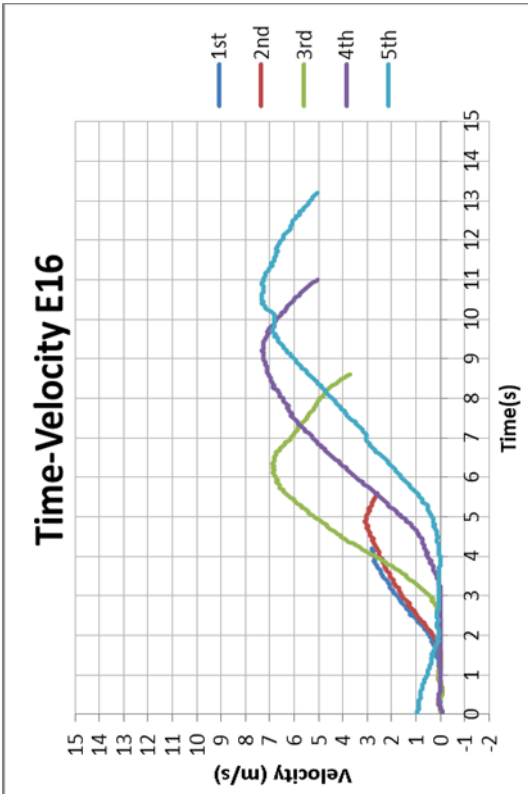
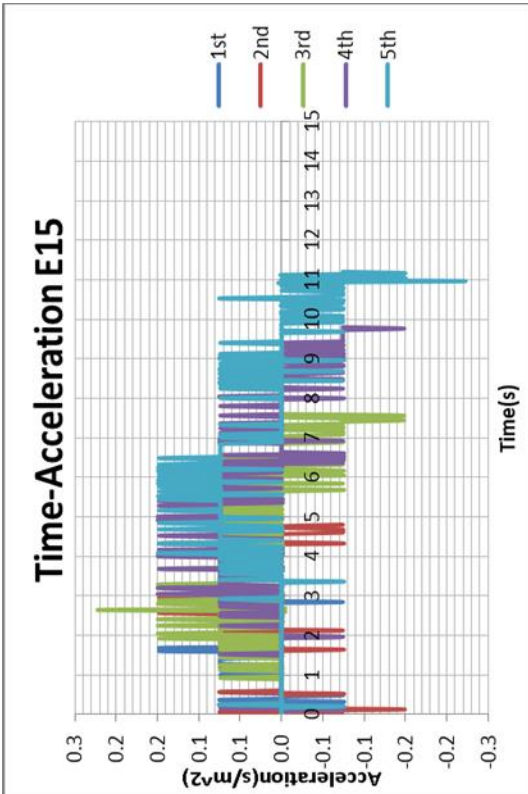
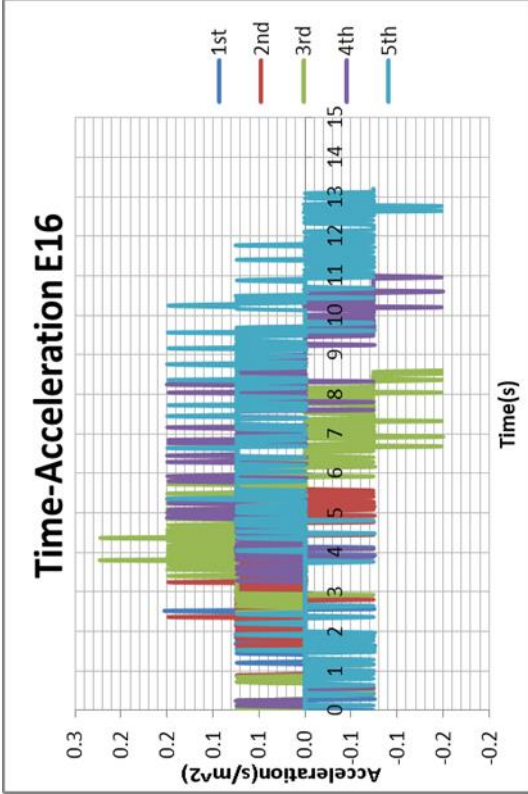
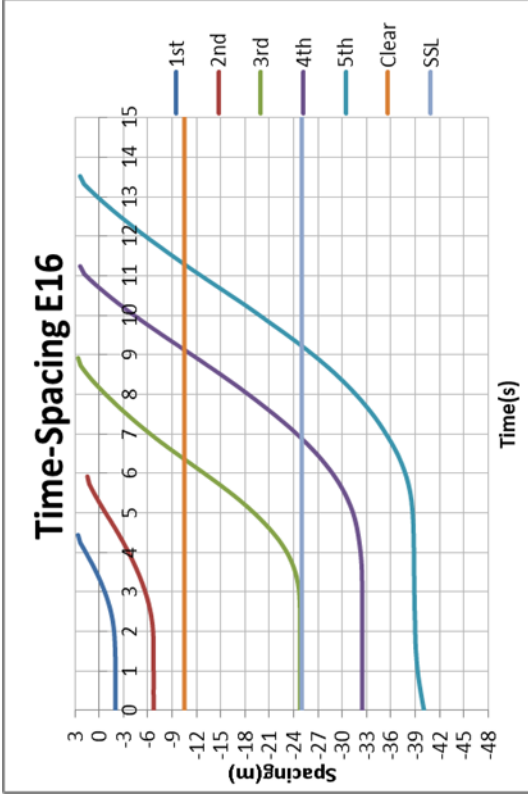




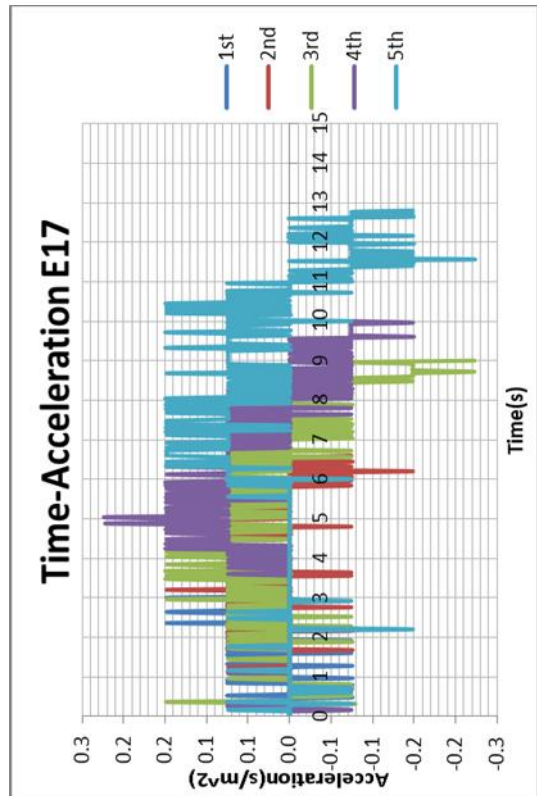
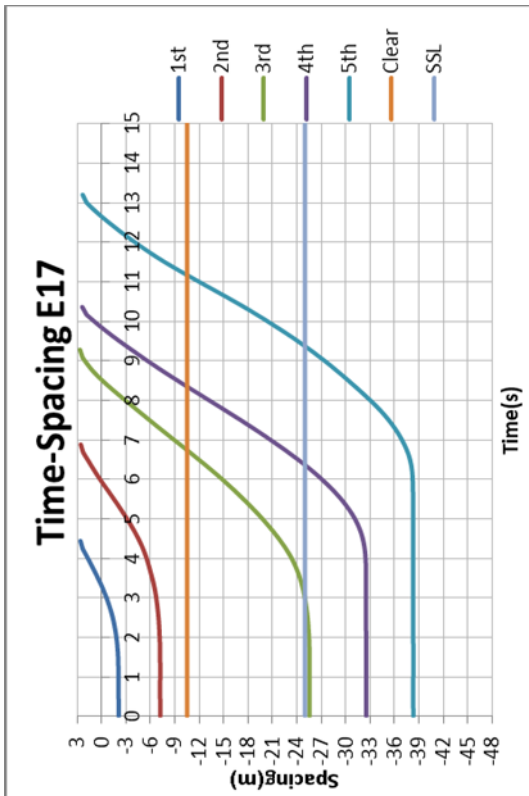
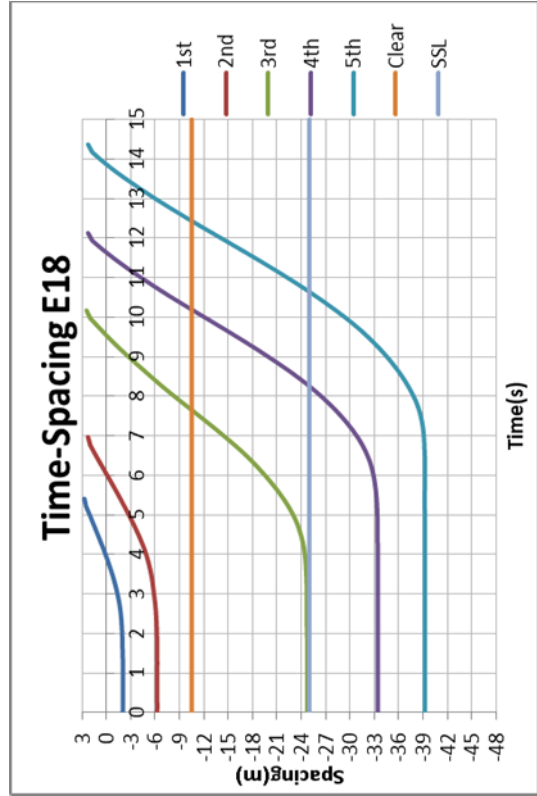
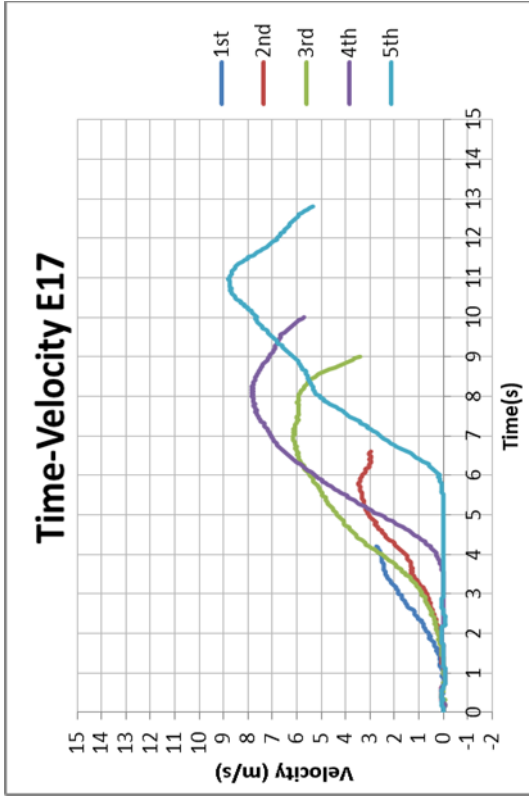


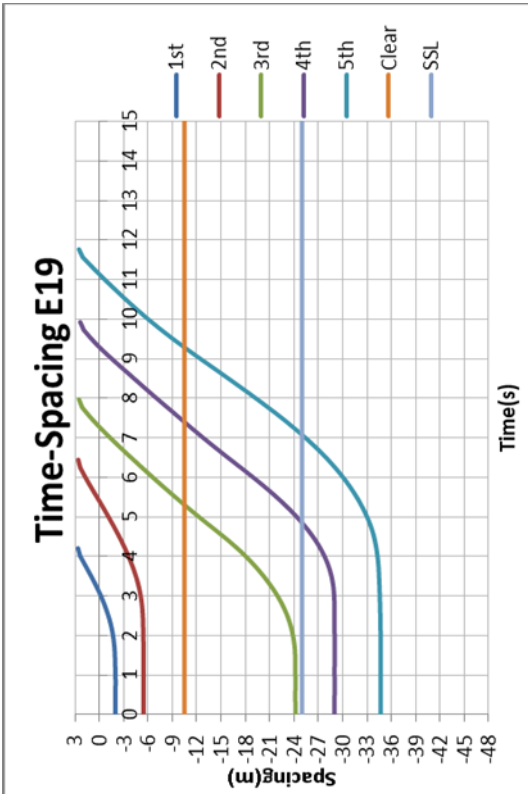
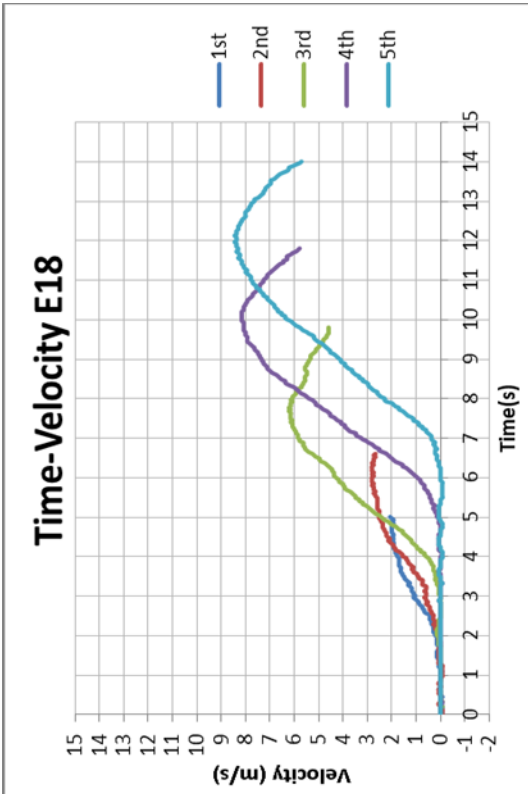
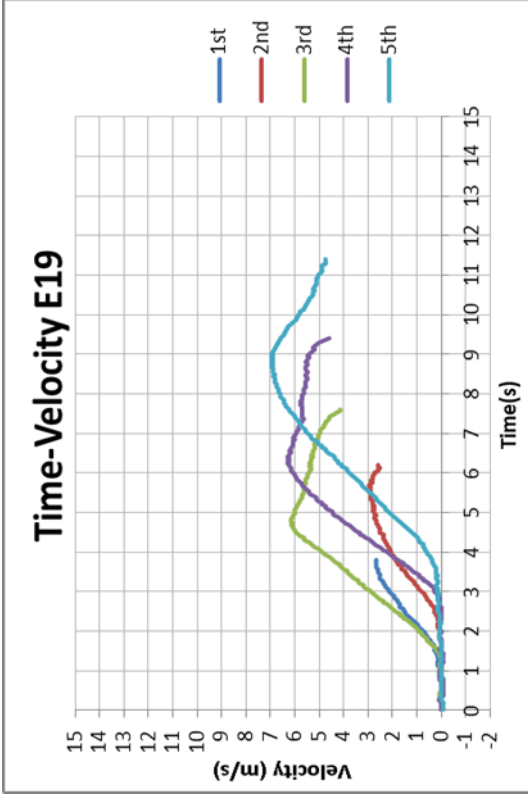
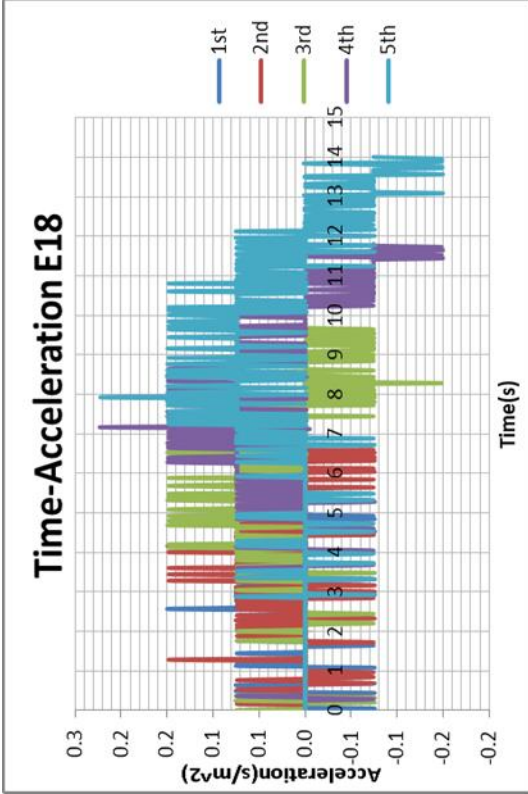


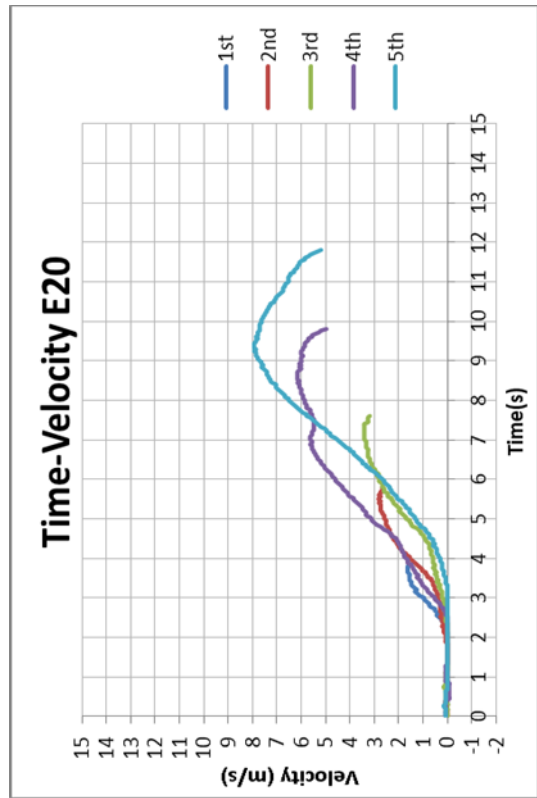
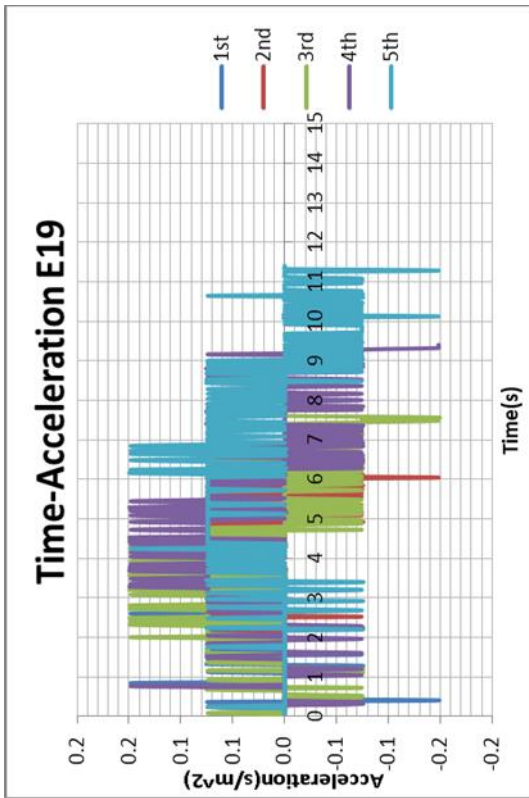
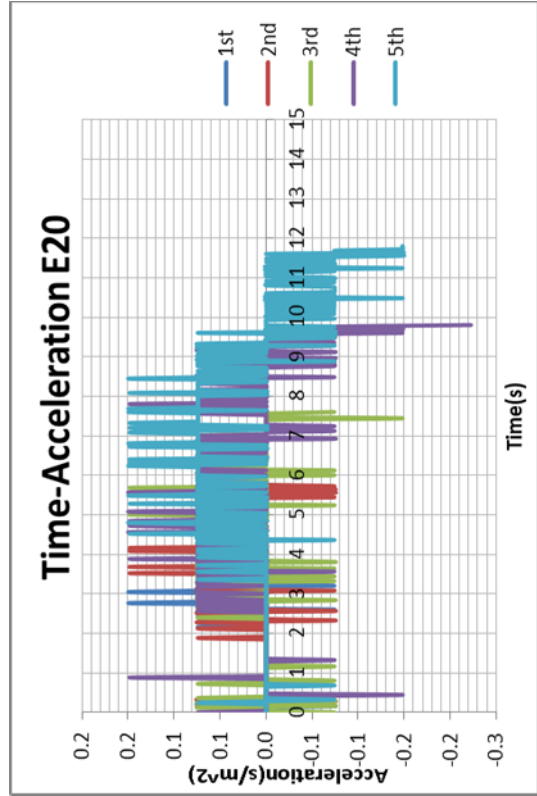
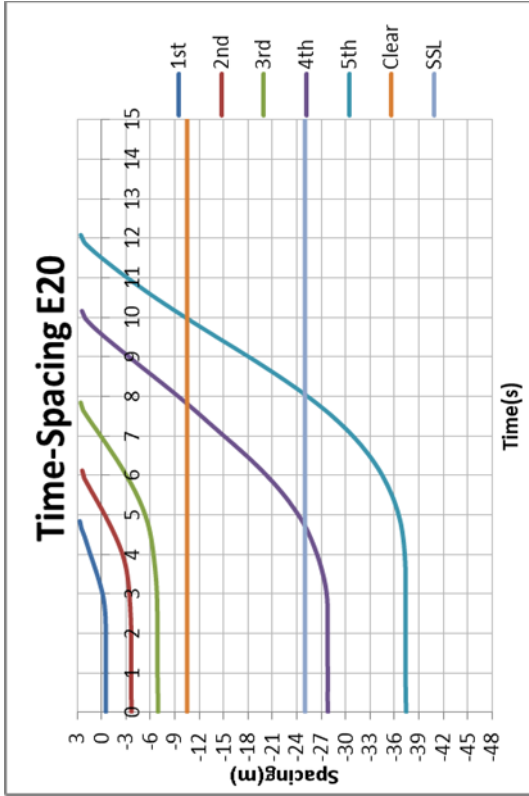


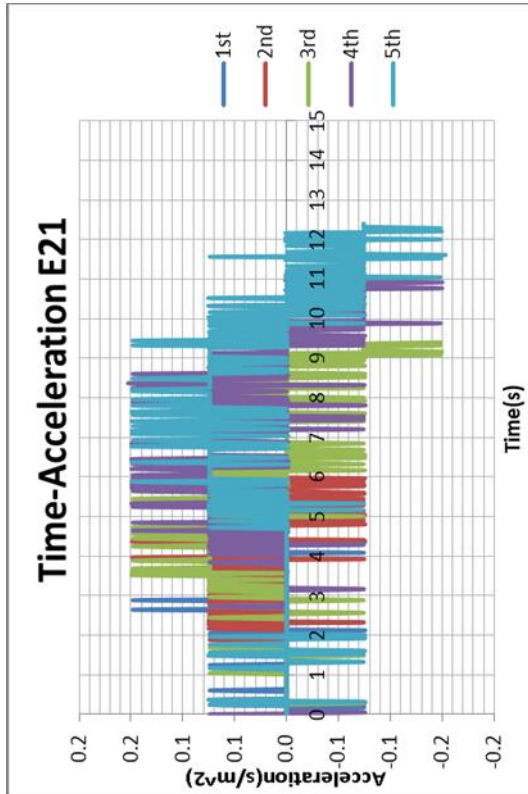
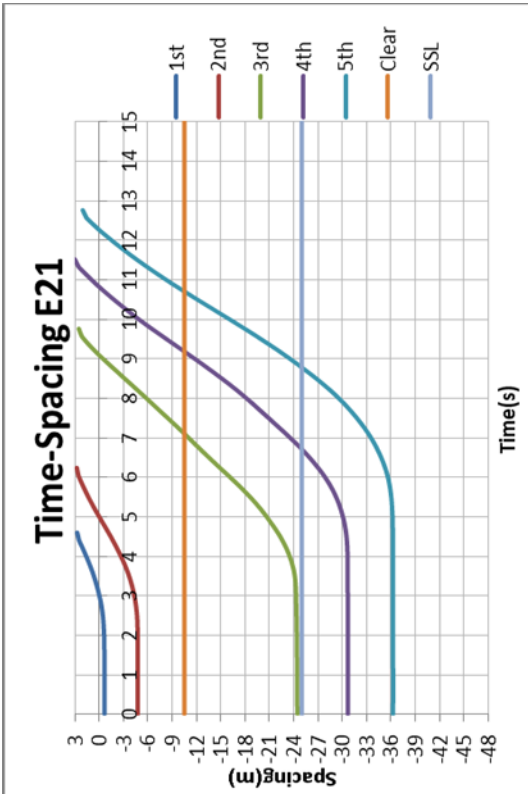
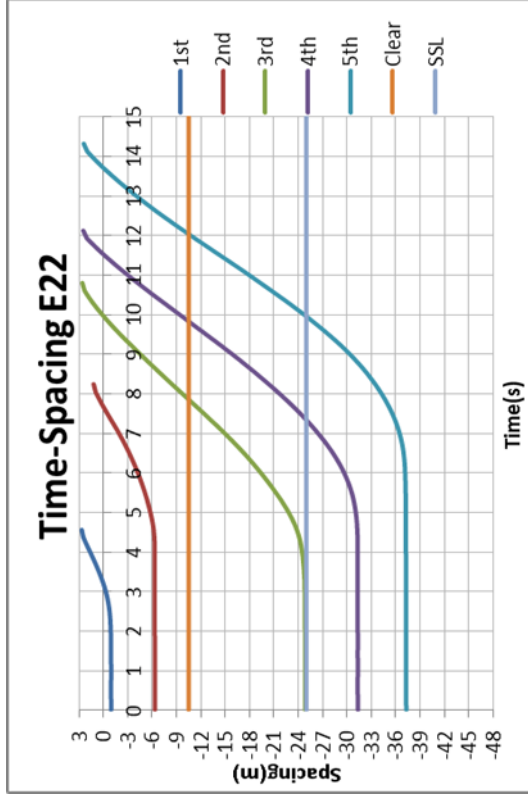
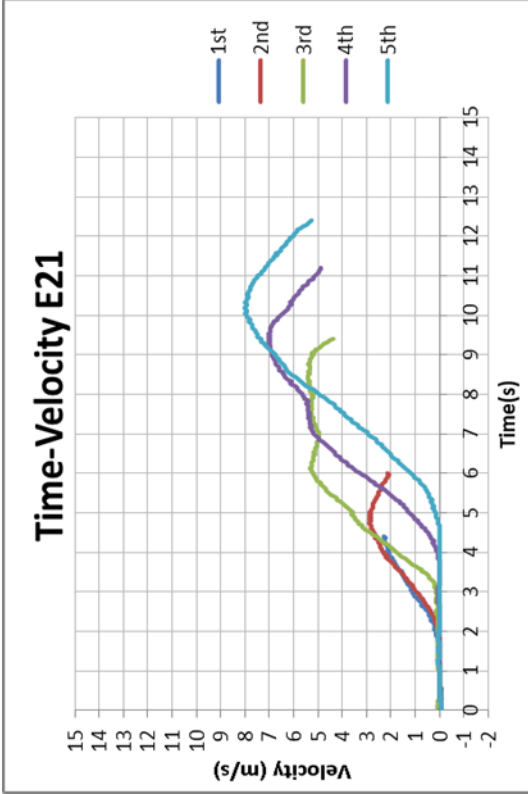


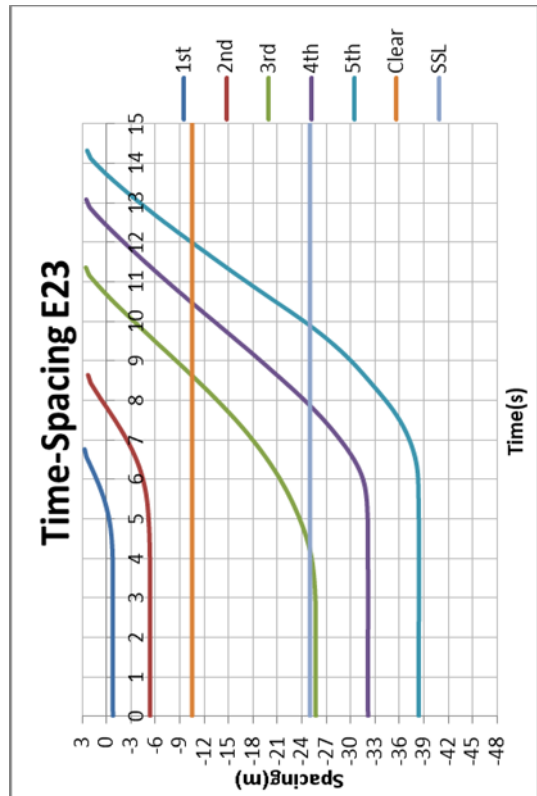
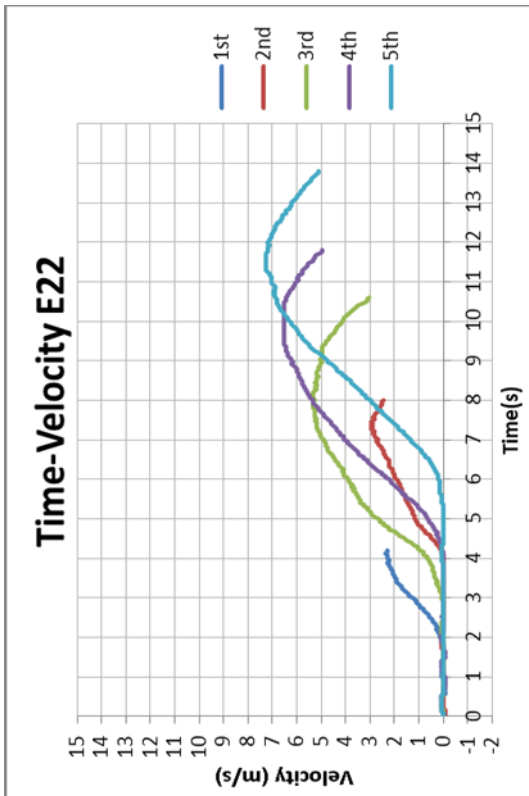
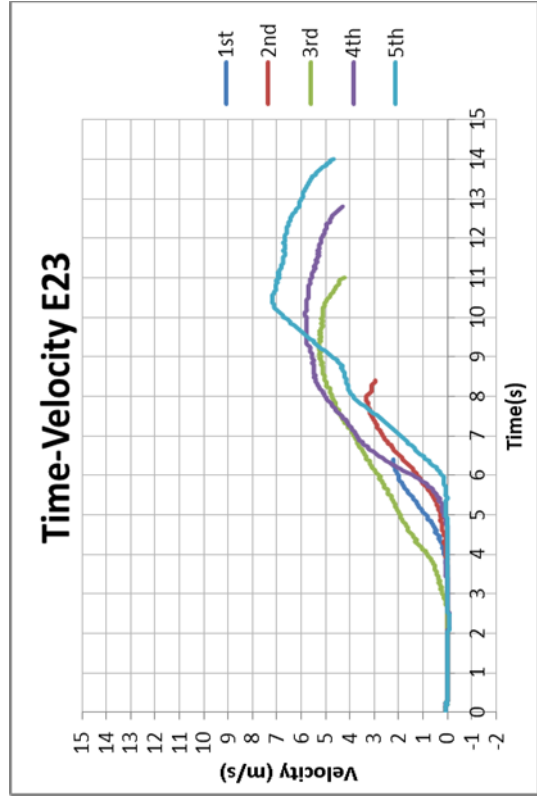
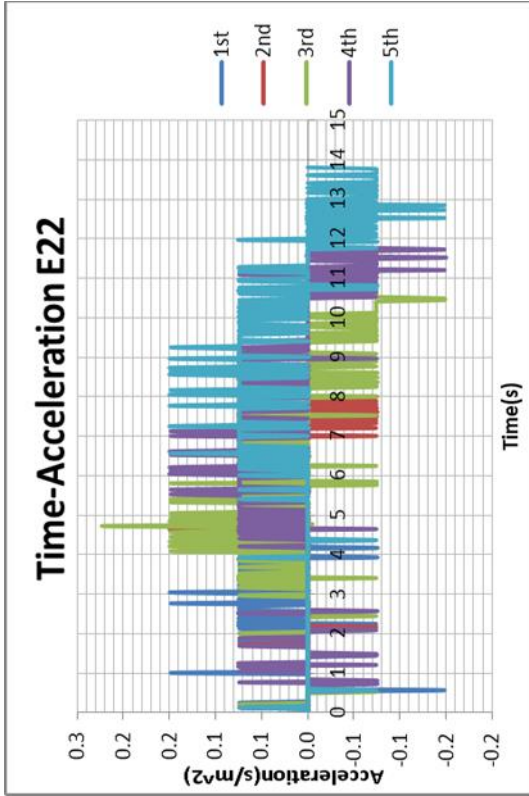


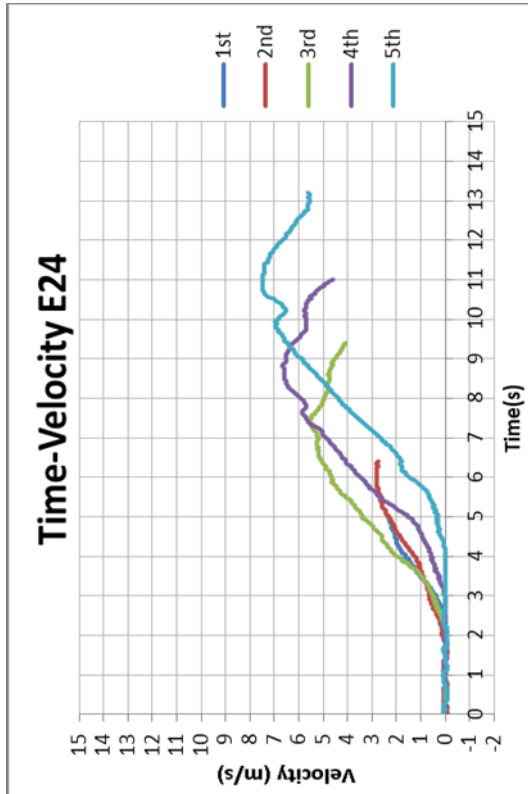
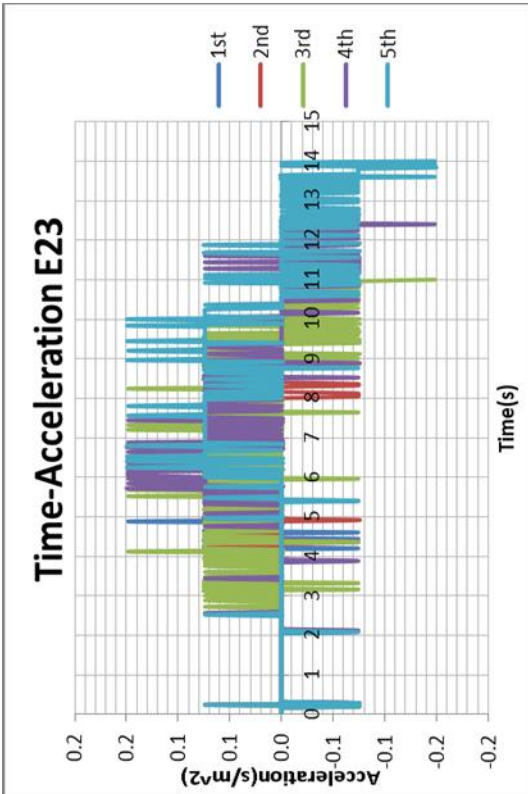
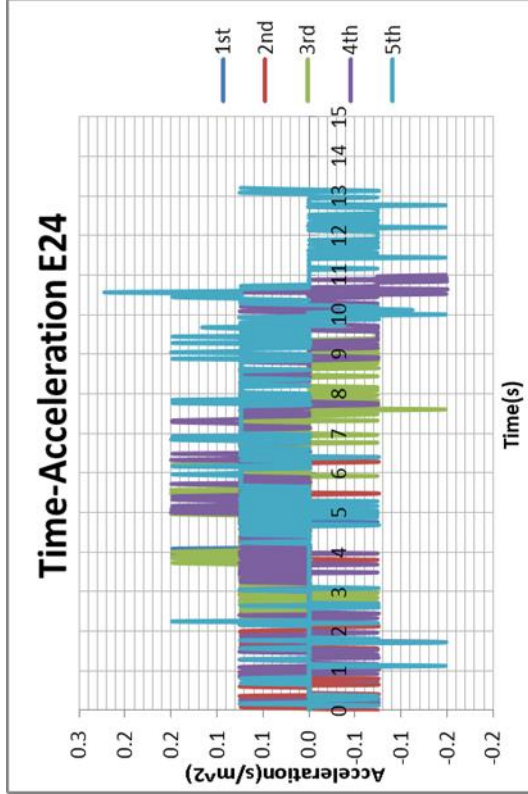
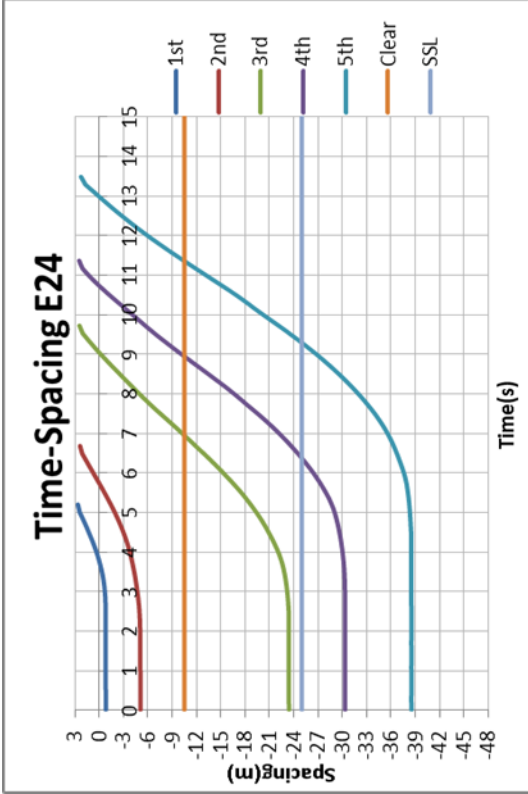


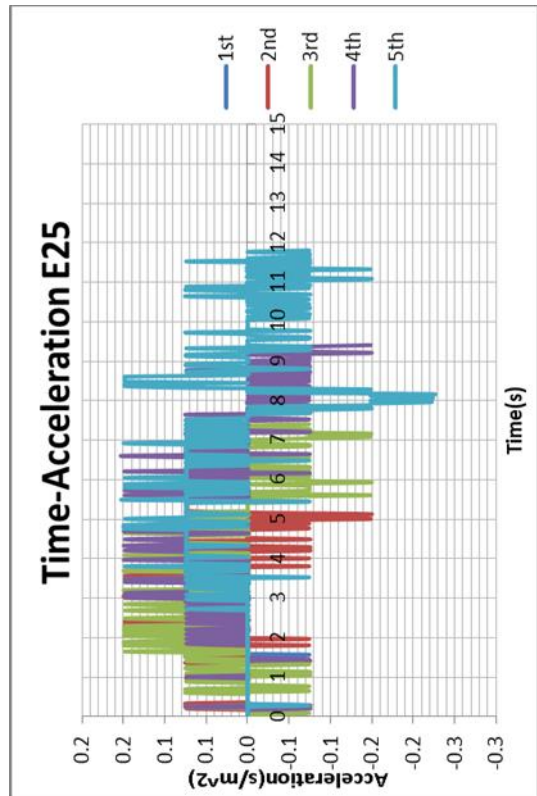
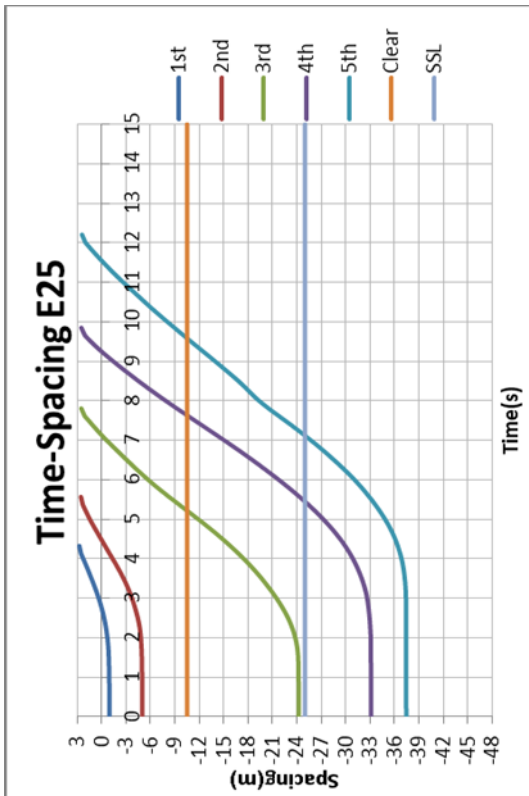
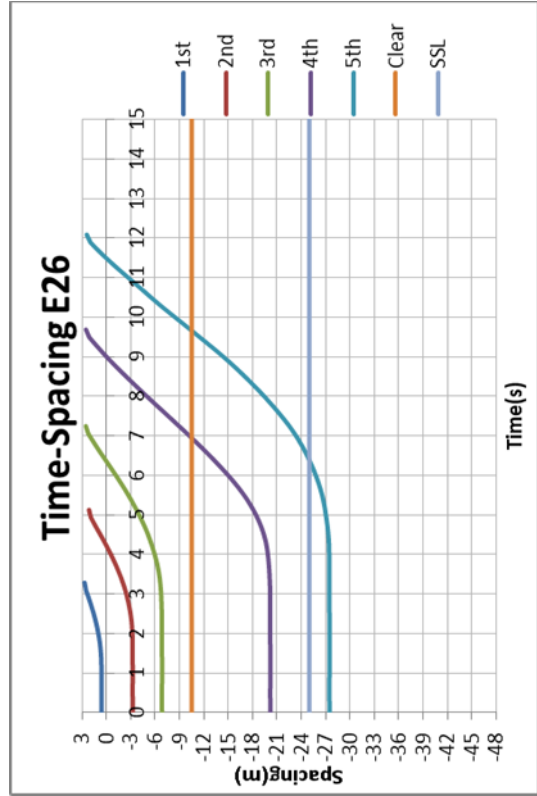
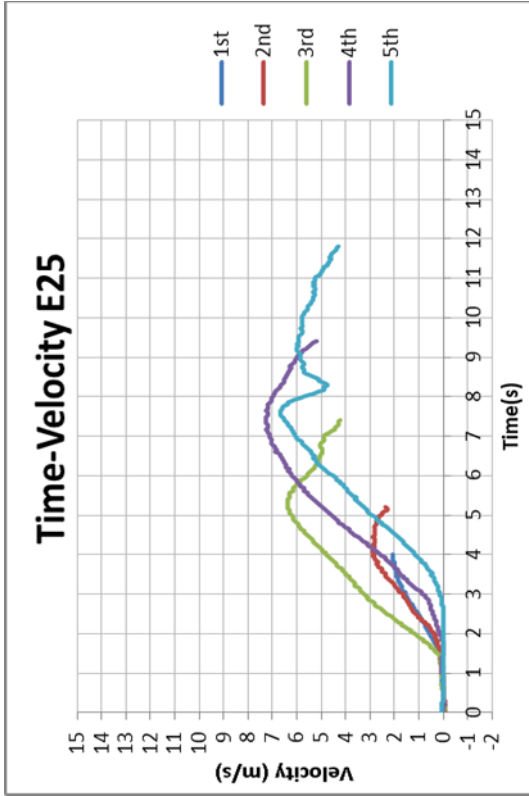


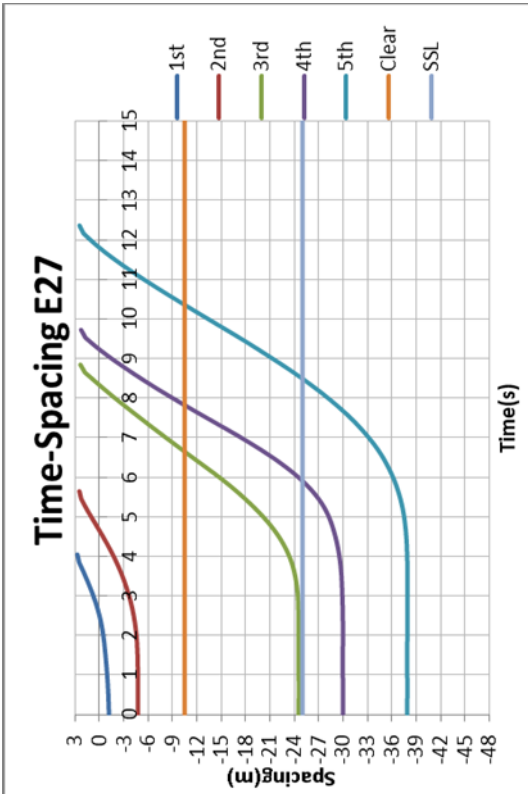
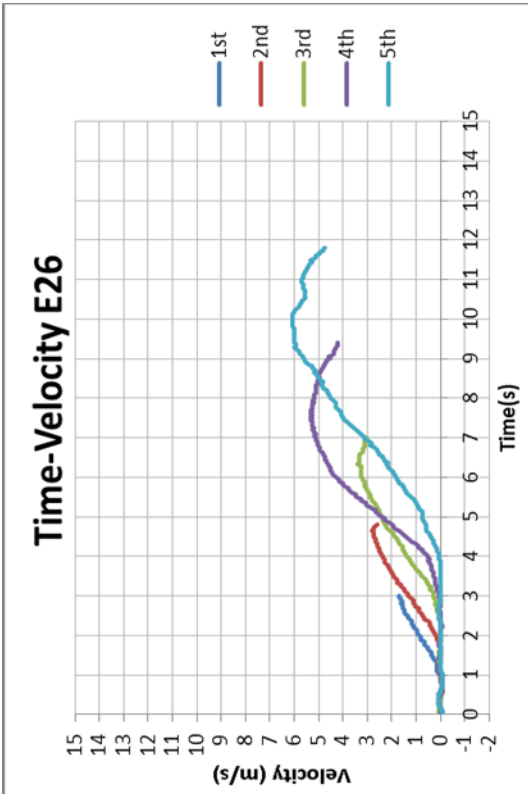
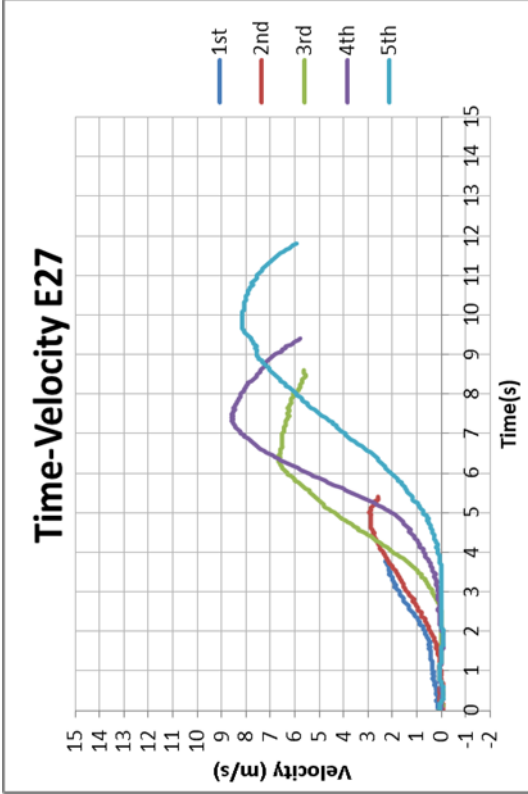
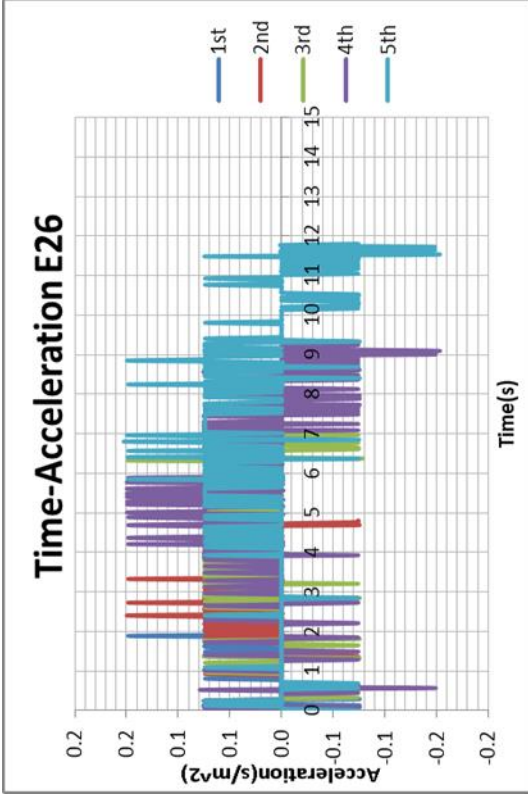




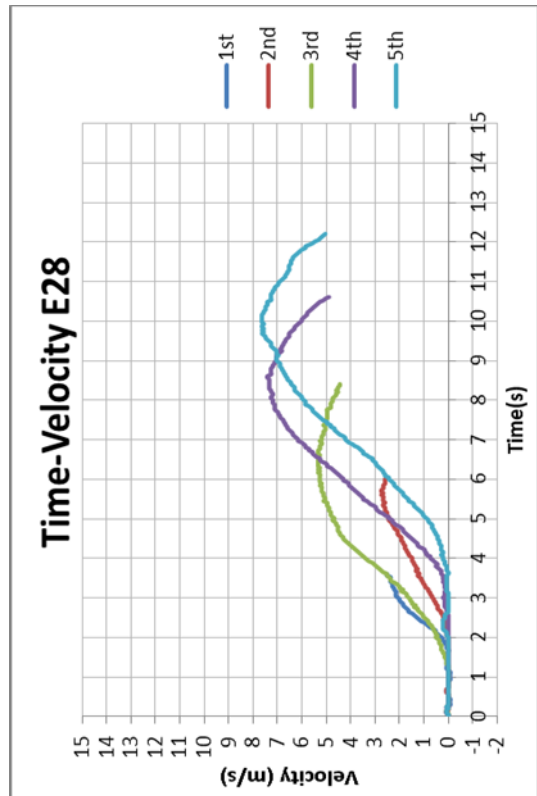
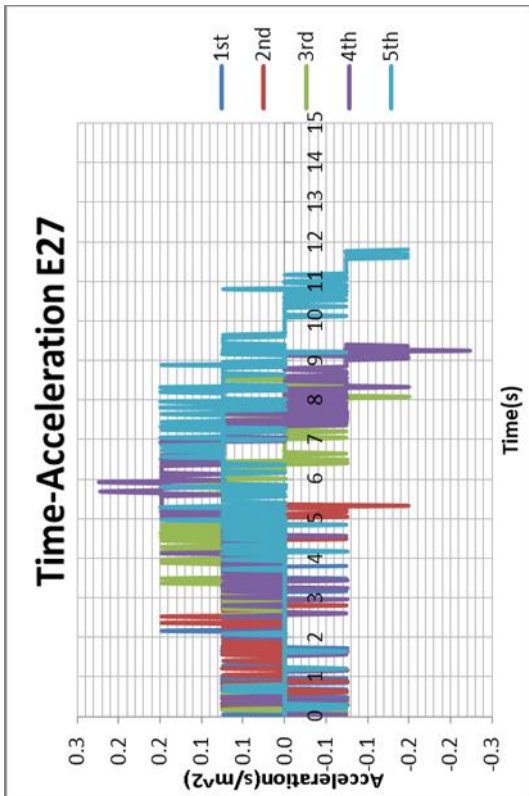
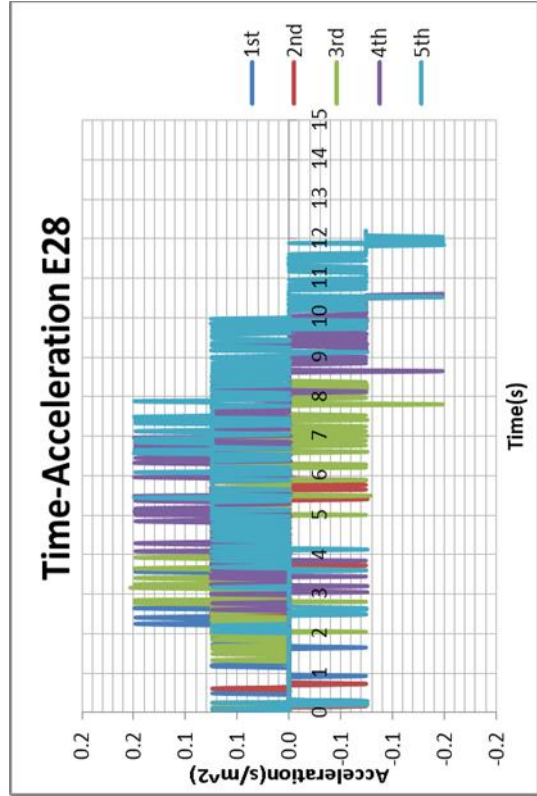
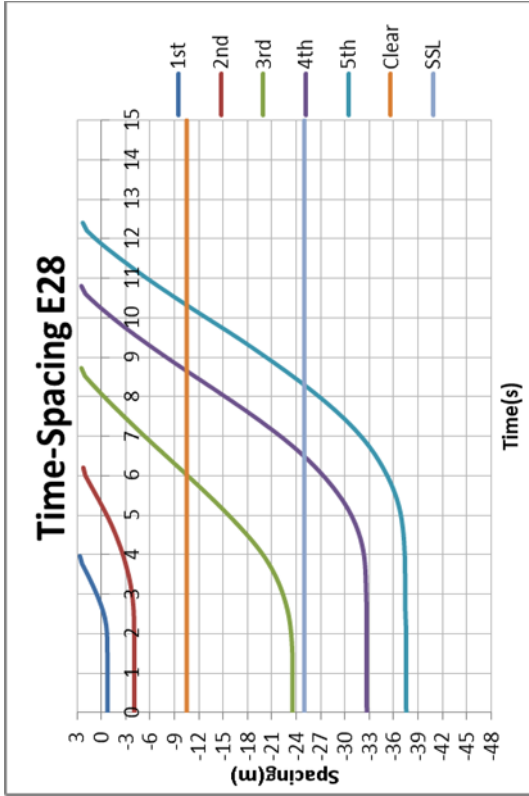


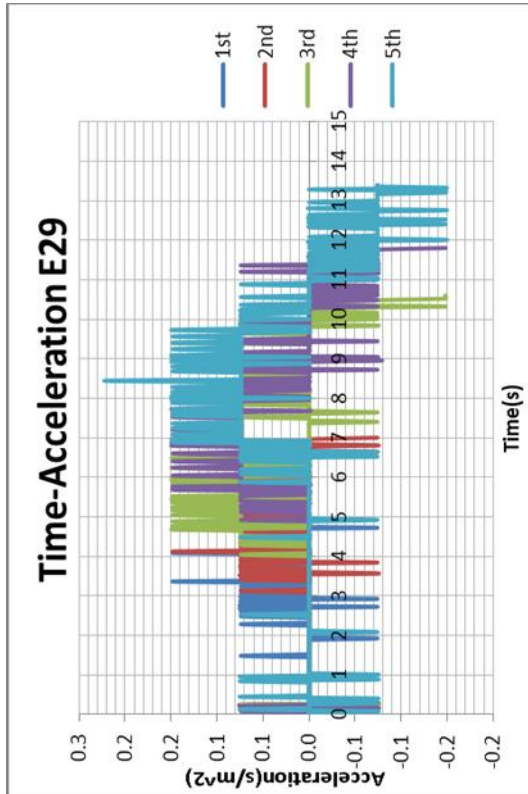
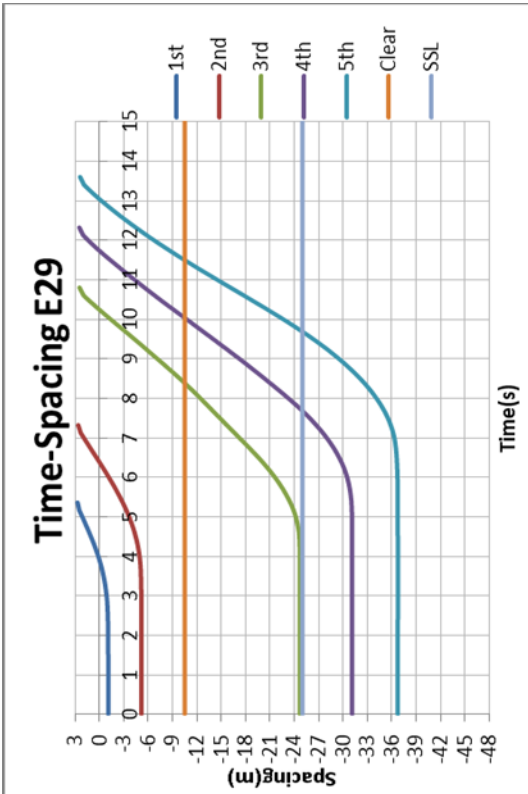
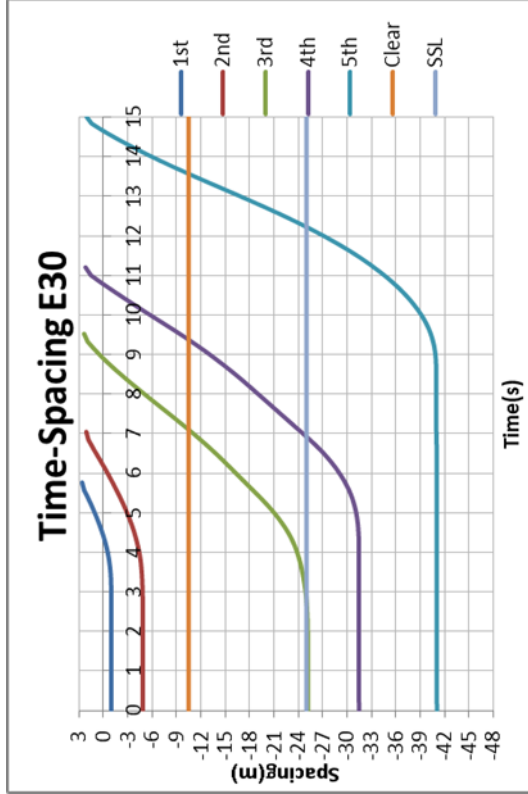
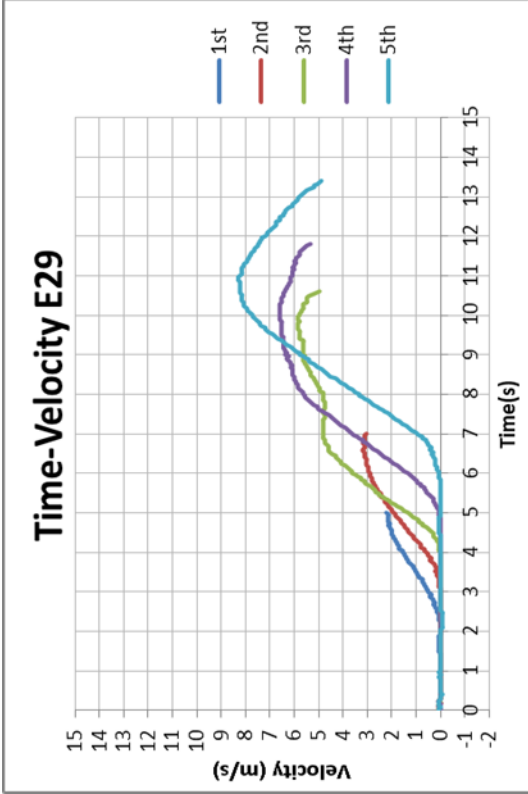


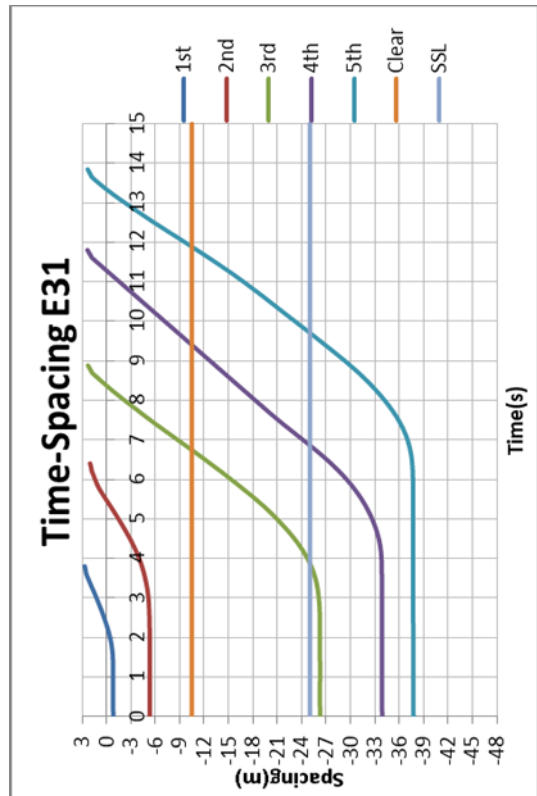
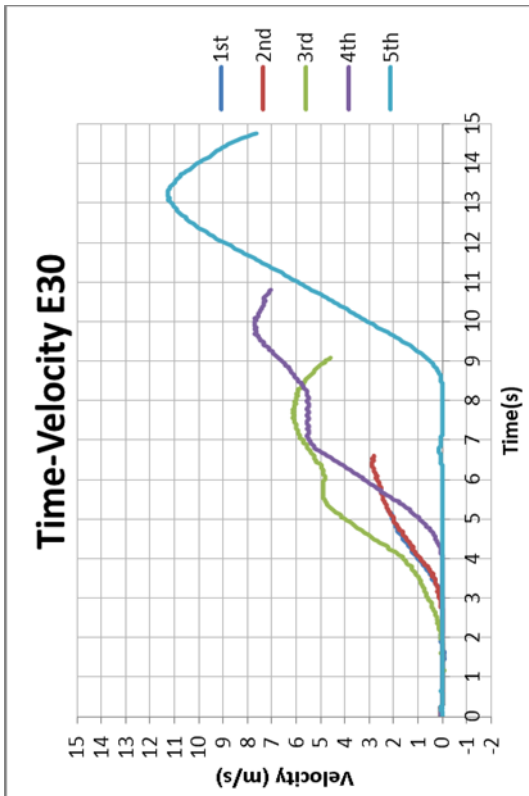
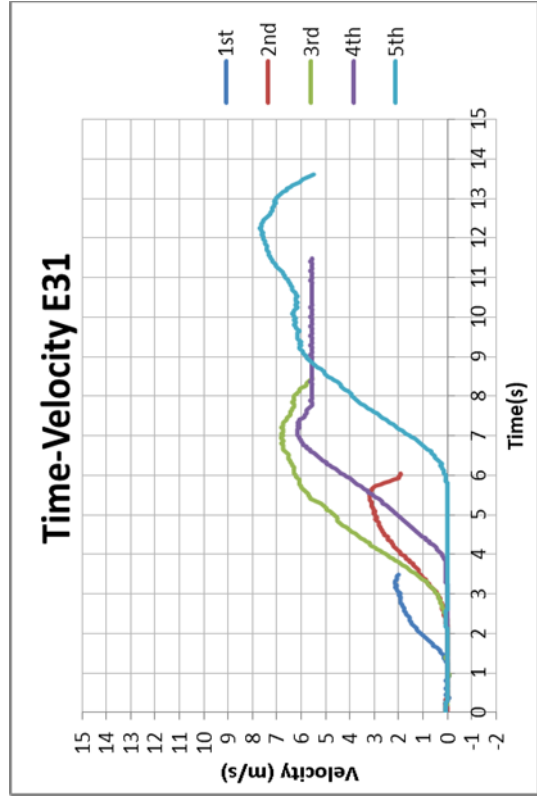
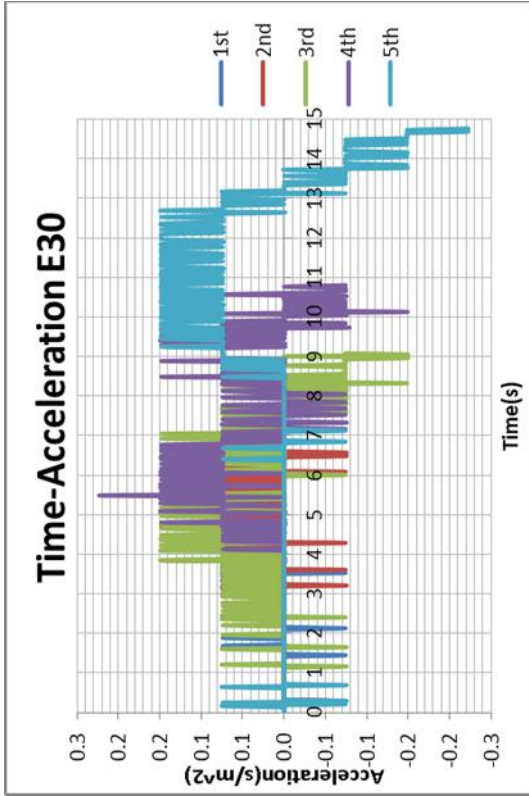


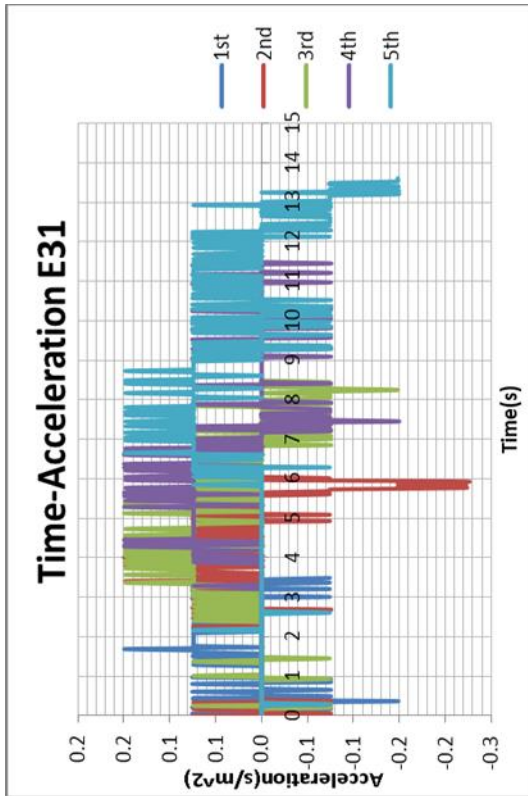










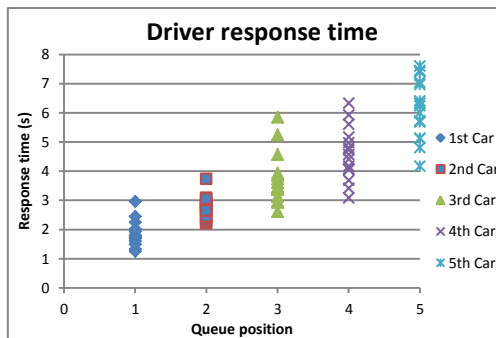
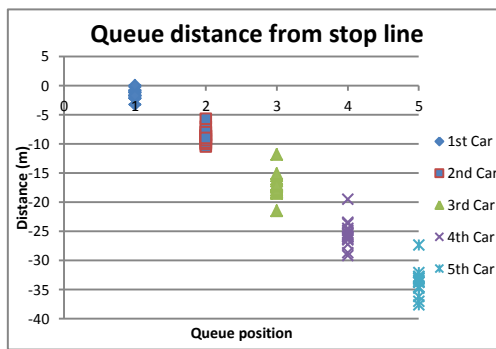


**Appendix E: Nerang Site I data parameters**

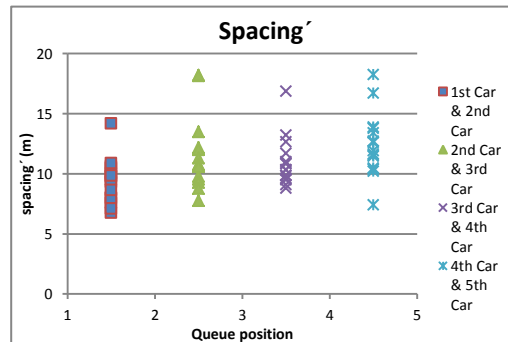
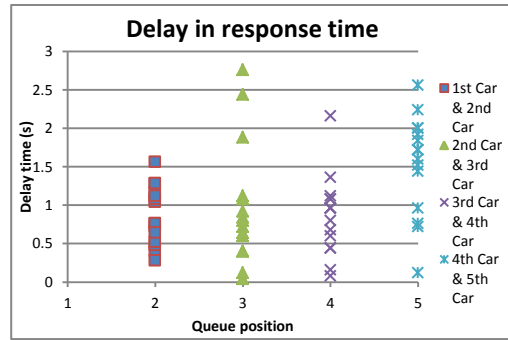
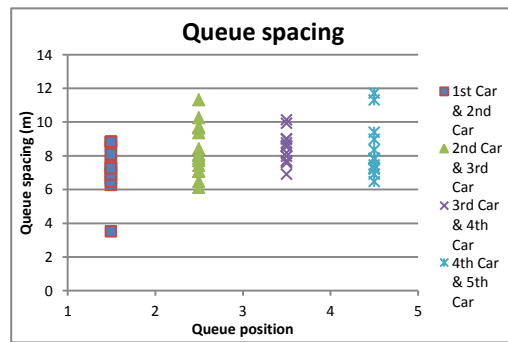
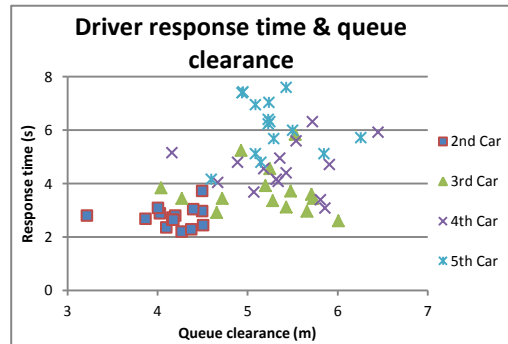
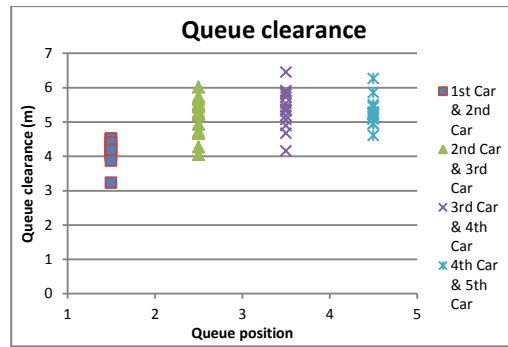
Queuing vehicles distance from the stop line (m)					
Sample	1 <sup>st</sup> Car	2 <sup>nd</sup> Car	3 <sup>rd</sup> Car	4 <sup>th</sup> Car	5 <sup>th</sup> Car
E01	-1.24	-7.85	-17.49	-26.02	-33.81
E02	-1.66	-10.18	-21.49	-29.16	-37.02
E03	-0.81	-7.06	-17.3	-24.87	-32.07
E04	-2.21	-8.66	-16.37	-24.54	-36.24
E06	-3.24	-10.48	-18.54	-28.68	-37.65
E07	-1.23	-10.03	-17.08	-25.84	-32.74
E08	-1.64	-8.64	-18.35	-25.26	-33.07
E10	-1.03	-9.86	-18.27	-27.24	-33.70
E11	-1.73	-8.62	-16.03	-25.96	-33.41
E12	-0.8	-8.55	-17.91	-26.5	-33.70
E13	-0.23	-9.06	-15.52	-23.48	-34.79
E15	-2.23	-5.74	-11.84	-19.54	-27.36
E16	0.03	-8.05	-15.12	-23.68	-33.07
E17	-2	-9.4	-17.23	-26.25	-34.59
E18	-1.75	-9	-16.98	-25.52	-32.80

Note: A negative value indicates vehicle's queue position is behind the stop line and the stop line at zero. A positive value means vehicle stop over the stop line.

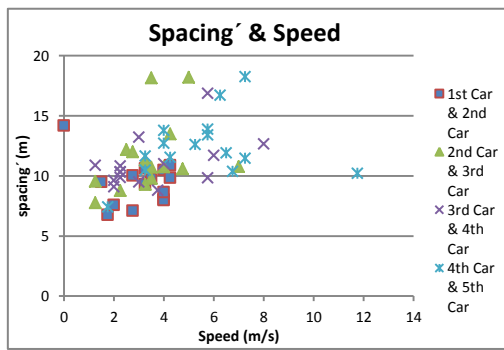
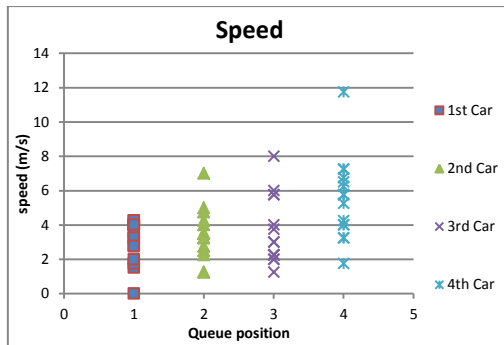
Driver response time (s)					
Sample	1 <sup>st</sup> Car	2 <sup>nd</sup> Car	3 <sup>rd</sup> Car	4 <sup>th</sup> Car	5 <sup>th</sup> Car
E01	1.6	2.88	2.92	3.08	4.8
E02	1.8	2.2	2.6	3.68	5.68
E03	2	2.28	3.12	4.08	6
E04	2.96	3.72	3.84	4.96	5.72
E06	2.24	2.72	3.44	4.8	6.24
E07	1.32	2.36	2.96	3.4	5.12
E08	2.44	2.96	3.6	4.56	6.4
E10	1.24	2.8	3.92	4.72	6.32
E11	2	3.08	5.84	5.92	7.44
E12	1.72	2.44	3.36	4.04	4.16
E13	1.48	2.64	3.72	4.16	5.12
E15	1.92	2.68	4.56	5.16	7.4



E16	1.68	2.8	5.24	6.32	7.04
E17	1.76	3.04	3.44	4.4	6.96
E18	2	2.64	3.44	5.6	7.6
Queue clearance (m)					
Sample	2 <sup>nd</sup> Car	3 <sup>rd</sup> Car	4 <sup>th</sup> Car	5 <sup>th</sup> Car	
E01	4.03	4.66	5.86	5.15	
E02	4.27	6.01	5.07	5.29	
E03	4.38	5.43	5.34	5.5	
E04	4.5	4.04	5.36	6.26	
E06	4.17	4.27	4.89	5.23	
E07	4.1	5.66	5.81	5.09	
E08	4.5	5.71	5.18	5.23	
E10	4.2	5.2	5.91	5.25	
E11	4.01	5.53	6.45	4.95	
E12	4.51	5.28	4.67	4.6	
E13	4.17	5.48	5.32	5.85	
E15	3.87	5.25	4.16	4.94	
E16	3.22	4.93	5.72	5.24	
E17	4.4	5.73	5.43	5.09	
E18	4.18	4.72	5.54	5.43	
Queue spacing (m)					
Sample	2 <sup>nd</sup> Car	3 <sup>rd</sup> Car	4 <sup>th</sup> Car	5 <sup>th</sup> Car	
E01	6.61	9.64	8.53	7.79	
E02	8.52	11.31	7.67	7.86	
E03	6.25	10.24	7.57	7.20	
E04	6.45	7.71	8.17	11.70	
E06	7.24	8.06	10.14	8.97	
E07	8.80	7.05	8.76	6.90	
E08	7.00	9.71	6.91	7.81	
E10	8.83	8.41	8.97	6.46	
E11	6.89	7.41	9.93	7.45	
E12	7.75	9.36	8.59	7.20	
E13	8.83	6.46	7.96	11.31	
E15	3.51	6.10	7.70	7.82	
E16	8.08	7.07	8.56	9.39	
E17	7.40	7.83	9.02	8.34	
E18	7.25	7.98	8.54	7.28	
Delay in response time (s)					
Sample	2 <sup>nd</sup> Car	3 <sup>rd</sup> Car	4 <sup>th</sup> Car	5 <sup>th</sup> Car	
E01	1.28	0.04	0.16	1.72	
E02	0.4	0.4	1.08	2	
E03	0.28	0.84	0.96	1.92	
E04	0.76	0.12	1.12	0.76	
E06	0.48	0.72	1.36	1.44	
E07	1.04	0.6	0.44	1.72	
E08	0.52	0.64	0.96	1.84	
E10	1.56	1.12	0.8	1.6	
E11	1.08	2.76	0.08	1.52	
E12	0.72	0.92	0.68	0.12	
E13	1.16	1.08	0.44	0.96	
E15	0.76	1.88	0.6	2.24	
E16	1.12	2.44	1.08	0.72	
E17	1.28	0.4	0.96	2.56	
E18	0.64	0.8	2.16	2	
Spacing ' (m)					
Sample	2 <sup>nd</sup> Car	3 <sup>rd</sup> Car	4 <sup>th</sup> Car	5 <sup>th</sup> Car	
E01	10.48	9.56	9.11	11.66	
E02	9.51	12.2	9.5	13.42	
E03	6.76	12.02	9.65	11.55	
E04	8.05	7.78	11.72	13.78	
E06	7.59	9.81	13.23	11.94	
E07	10.62	9.29	9.88	10.23	
E08	8	10.72	9.85	13.9	
E10	14.18	10.76	10.37	10.38	
E11	9.78	18.17	10.89	11.48	

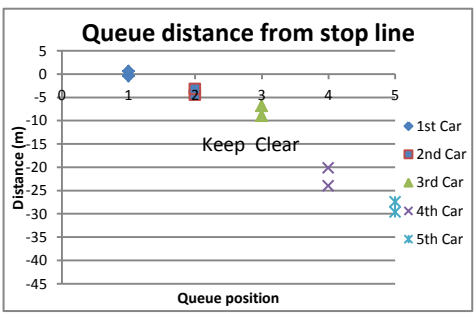
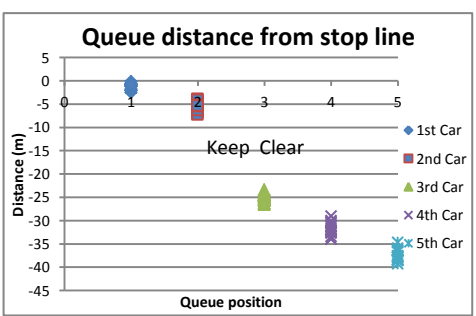


E12	9.31	11.31	11.02	7.42
E13	10.04	10.78	8.81	12.73
E15	7.1	13.51	10.32	16.73
E16	9.85	18.21	12.68	10.5
E17	10.89	8.79	10.83	18.27
E18	8.64	10.59	16.88	12.63
Speed (m/s)				
Sample	1 <sup>st</sup> Car	2 <sup>nd</sup> Car	3 <sup>rd</sup> Car	4 <sup>th</sup> Car
E01	4	1.25	2	3.25
E02	1.5	2.5	3	5.75
E03	1.75	2.75	2	4.25
E04	4	1.25	6	4
E06	2	3.5	3	6.5
E07	3.25	3.25	2.25	11.75
E08	4	3.5	5.75	5.75
E10	0	4	2.25	6.75
E11	3.5	3.5	1.25	7.25
E12	3.25	3.25	4	1.75
E13	2.75	7	3.75	4
E15	2.75	4.25	2.25	6.25
E16	4.25	5	8	3.25
E17	4.25	2.25	2.25	7.25
E18	4	4.75	5.75	5.25
Note: These two parameters indicate two successive vehicles' spacing and the lead vehicle's speed at the time when the following vehicle makes response to the green signal.				

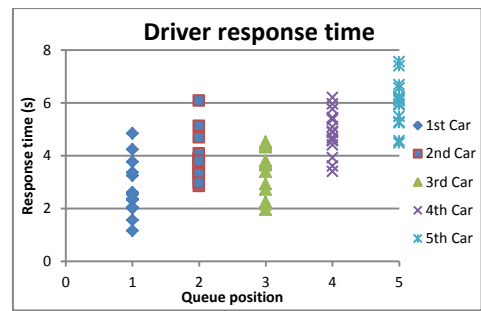


## Appendix F: Nerang Site II data parameters

Nerang Site II Data					
Queuing vehicles distance from the stop line (m)					
Sample	1 <sup>st</sup> Car	2 <sup>nd</sup> Car	3 <sup>rd</sup> Car	4 <sup>th</sup> Car	5 <sup>th</sup> Car
E01	-1.18	-5.36	-25.32	-31.71	-37.56
E02	-0.91	-4.98	-24.38	-30.33	-36.47
E03	-1.04	-4.99	-25.15	-31.25	-35.92
E06	-0.08	-3.90	-26.54	-33.94	-38.60
E11	-2.48	-6.82	-25.71	-31.22	-36.49
E13	-1.76	-6.84	-24.53	-32.43	-38.37
E15	-0.53	-4.05	-24.90	-32.11	-37.85
E17	-2.10	-7.21	-25.55	-32.53	-38.31
E18	-2.02	-6.25	-24.74	-33.41	-39.23
E19	-1.98	-5.45	-24.17	-28.99	-34.68
E21	-0.65	-4.76	-24.47	-30.68	-36.24
E23	-0.78	-5.35	-25.7	-32.13	-38.36
E24	-0.82	-5.08	-23.42	-30.33	-38.52
E27	-1.18	-4.75	-24.53	-29.98	-37.91
E28	-0.75	-4.06	-23.54	-32.68	-37.54
E29	-1.1	-5.17	-24.69	-31.11	-36.73
E31	-0.83	-5.31	-26.26	-33.89	-37.74
Driver response time (s)					
Sample	1 <sup>st</sup> Car	2 <sup>nd</sup> Car	3 <sup>rd</sup> Car	4 <sup>th</sup> Car	5 <sup>th</sup> Car
E01	2.36	3.88	1.96	3.92	5.24
E02	2.04	3.24	4.32	4.88	6.16
E03	3.24	4.68	2.16	5.76	6.24
E06	1.16	3.6	2.92	4.68	5.96
E11	4.24	5.12	3.64	5.36	7.4



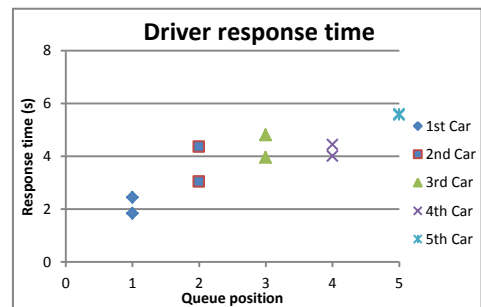
E13	2.32	3.56	4.52	5.44	6.12
E15	1.56	2.84	2.24	3.4	4.48
E17	2.6	3.8	3.4	4.56	6.56
E18	3.36	3.88	4.48	6.2	7.56
E19	2.36	3.36	2.24	3.6	4.56
E21	2.6	3.32	3.8	5.08	6.08
E23	4.84	6.08	4.4	5.96	6.68
E24	3.76	4.08	3.68	4.92	5.92
E27	2	2.96	3.72	4.6	5.48
E28	2.52	3.8	2.72	4.4	5.28
E29	3.8	4.56	5	6	7.16
E31	2.16	3.68	3.52	4.6	6.92



Queuing vehicles distance from the stop line (m)						
Sample	1 <sup>st</sup> Car	2 <sup>nd</sup> Car	3 <sup>rd</sup> Car	Clear	4 <sup>th</sup> Car	5 <sup>th</sup> Car
E10	-0.48	-4.55	-8.96			-24.04
E26	0.6	-3.25	-6.85		-20.19	-27.47

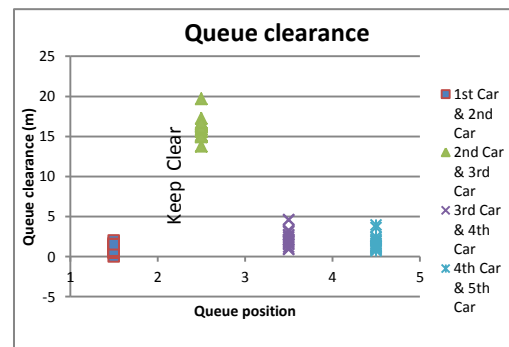
  

Driver response time (s)						
Sample	1 <sup>st</sup> Car	2 <sup>nd</sup> Car	3 <sup>rd</sup> Car	Keep	4 <sup>th</sup> Car	5 <sup>th</sup> Car
E10	2.44	4.36	4.8			4
E26	1.84	3.04	3.96		4.44	5.56

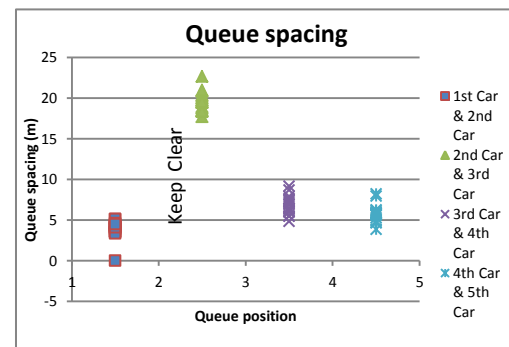
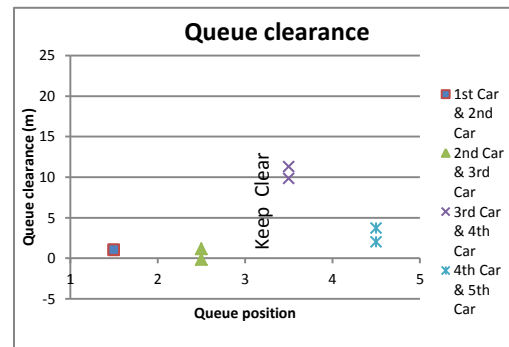


Note: There are 3 cars queuing in front of the Keep Clear road mark in Sample 10 and Sample 26.

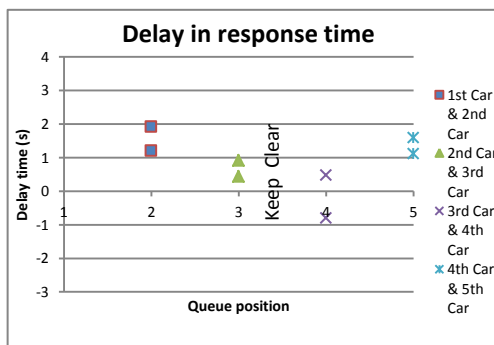
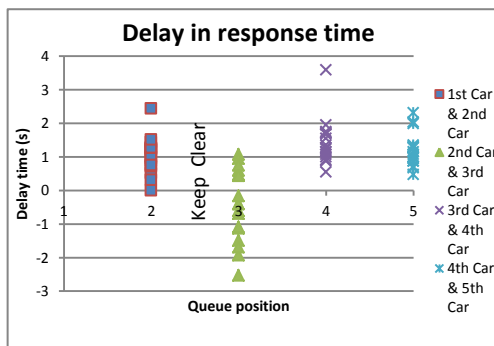
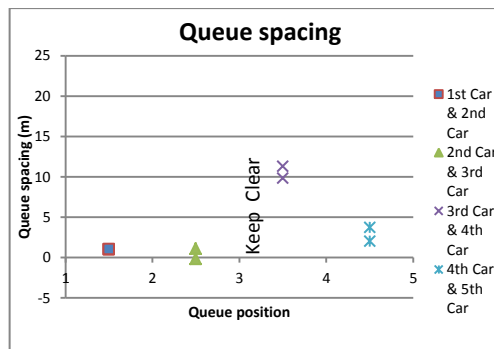
Queue clearance (m)				
Sample	2 <sup>nd</sup> Car	3 <sup>rd</sup> Car	4 <sup>th</sup> Car	5 <sup>th</sup> Car
E01	0.20	16.37	1.73	1.58
E02	0.64	15.62	1.19	1.41
E03	1.31	16.34	1.86	1.21
E06	0.49	19.70	2.74	0.94
E11	1.05	14.94	1.50	1.91
E13	1.72	13.78	3.10	1.34
E15	0.65	17.26	2.61	1.27
E17	1.98	14.98	3.29	2.00
E18	1.56	15.13	4.63	2.17
E19	0.47	15.62	0.87	1.65
E21	0.82	16.58	1.58	0.86
E23	1.31	16.57	2.03	2.48
E24	1.42	15.01	2.15	3.95
E27	0.47	16.26	0.95	3.62
E28	0.67	15.89	4.54	1.08
E29	0.71	16.13	2.41	1.15
E31	1.51	16.74	3.16	0.69



Queue spacing (m)				
Sample	2 <sup>nd</sup> Car	3 <sup>rd</sup> Car	4 <sup>th</sup> Car	5 <sup>th</sup> Car
E01	4.18	19.96	6.39	5.85
E02	4.07	19.40	5.95	6.14
E03	3.95	20.16	6.10	4.67
E06	3.82	22.64	7.40	4.66
E11	4.34	18.89	5.51	5.27
E13	5.08	17.69	7.90	5.94
E15	3.52	20.85	7.21	5.74
E17	5.11	18.34	6.98	5.78
E18	4.23	18.49	8.67	5.82
E19	3.47	18.72	4.82	5.69
E21	4.11	19.71	6.21	5.56
E23	4.57	20.35	6.43	6.23
E24	4.26	18.34	6.91	8.19
E27	3.57	19.78	5.45	7.93
E28	3.31	19.48	9.14	4.86
E29	4.07	19.52	6.42	5.62



E31	4.48		20.95	7.63	3.85
Queue clearance (m)					
Sample	2 <sup>nd</sup> Car	3 <sup>rd</sup> Car	Clear	4 <sup>th</sup> Car	5 <sup>th</sup> Car
E10	0.97	1.12		11.30	2.01
E26	1.04	-0.15		9.82	3.72
Queue spacing (m)					
Sample	2 <sup>nd</sup> Car	3 <sup>rd</sup> Car	Keep	4 <sup>th</sup> Car	5 <sup>th</sup> Car
E10	4.07	4.41		15.08	5.60
E26	3.85	3.60		13.34	7.28
Note: There are 3 cars queuing in front of the Keep Clear road mark in Sample 10 and Sample 26.					
Delay in response time (s)					
Sample	2 <sup>nd</sup> Car	Keep Clear	3 <sup>rd</sup> Car	4 <sup>th</sup> Car	5 <sup>th</sup> Car
E01	1.52		-1.92	1.96	1.32
E02	1.2		1.08	0.56	1.28
E03	1.44		-2.52	3.6	0.48
E06	2.44		-0.68	1.76	1.28
E11	0.88		-1.48	1.72	2.04
E13	1.24		0.96	0.92	0.68
E15	1.28		-0.6	1.16	1.08
E17	1.2		-0.4	1.16	2
E18	0.52		0.6	1.72	1.36
E19	1		-1.12	1.36	0.96
E21	0.72		0.48	1.28	1
E23	1.24		-1.68	1.56	0.72
E24	0.32		-0.4	1.24	1
E27	0.96		0.76	0.88	0.88
E28	1.28		-1.08	1.68	0.88
E29	0.76		0.44	1	1.16
E31	1.52	-0.16	1.08	2.32	
Delay in response time (s)					
Sample	2 <sup>nd</sup> Car	3 <sup>rd</sup> Car	Clear	4 <sup>th</sup> Car	5 <sup>th</sup> Car
E10	1.92	0.44		-0.8	1.6
E26	1.2	0.92		0.48	1.12
Note: There are 3 cars queuing in front of the Keep Clear road mark in Sample 10 and Sample 26.					



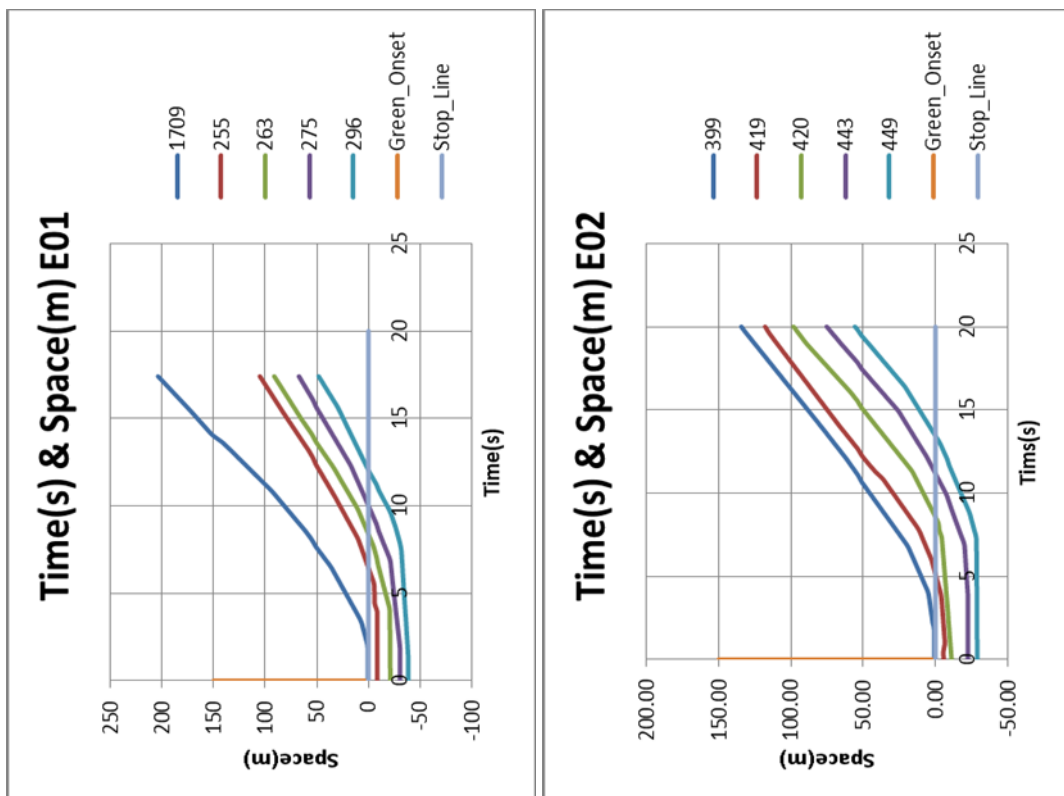
## Appendix G: Nerang Data average vehicle length

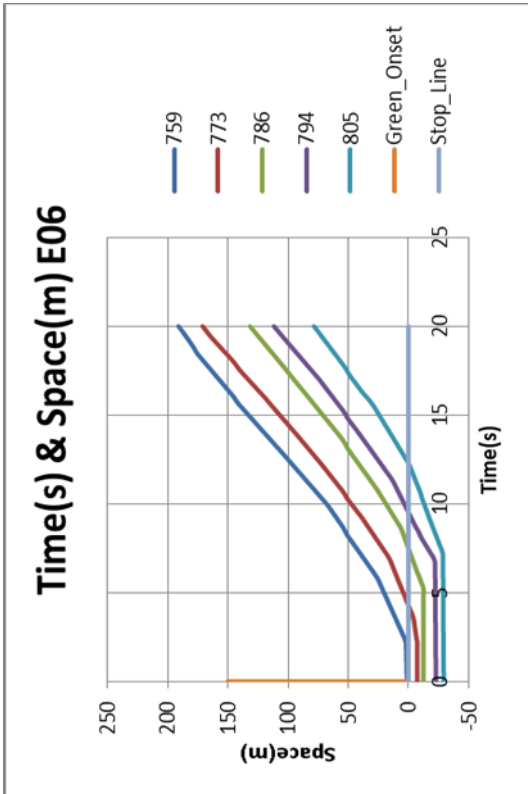
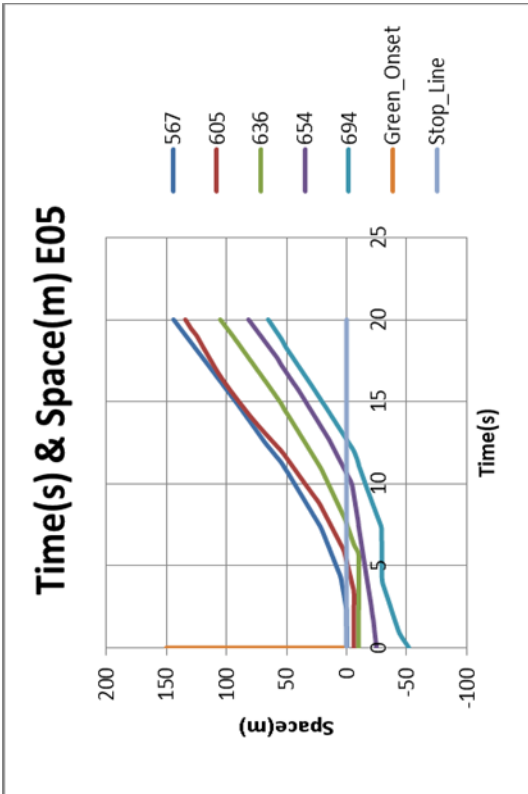
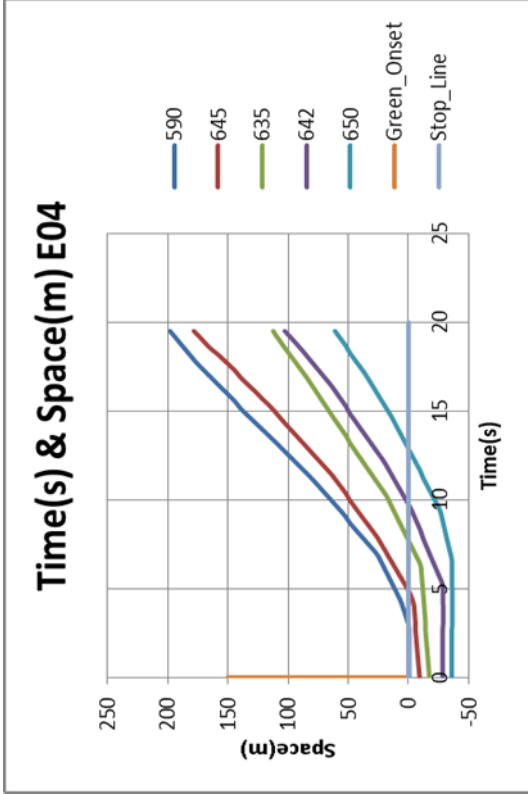
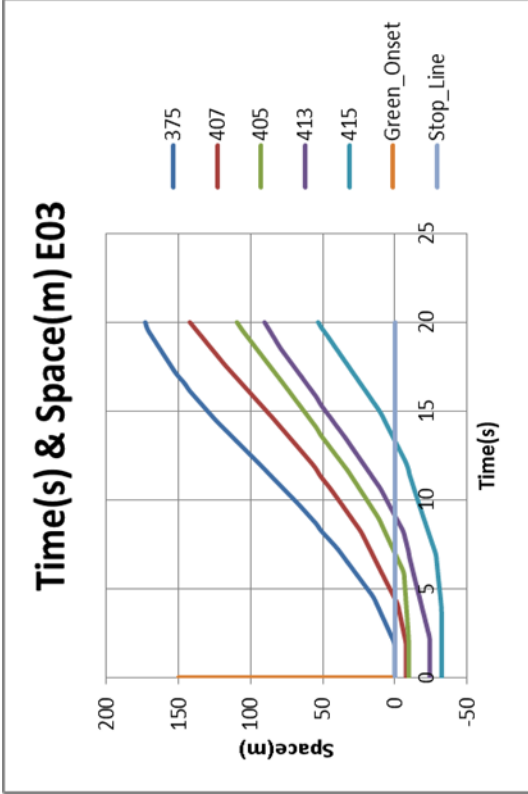
Site I				Site II					
Vehicle ID	Vehicle Length	Vehicle ID	Vehicle Length	Vehicle ID	Vehicle Length	Vehicle ID	Vehicle Length	Vehicle ID	Vehicle Length
93	4.03	1174	5.25	2	3.98	126	4.01	224	3.62
94	4.66	1175	4.37	3	3.59	127	3.36	225	3.33
96	5.85	1222	4.01	4	4.66	128	3.95	227	4.27
97	5.15	1228	5.53	5	4.27	130	3.59	228	4.73
98	4.05	1232	6.45	6	3.46	131	4.04	229	3.62
125	4.27	1234	4.95	17	3.43	132	4.4	239	3.26
126	6.01	1236	3.64	18	3.78	134	4.21	240	3.78
127	5.07	1476	4.51	19	4.76	136	3.36	241	4.4
130	5.29	1477	5.28	20	4.73	137	3.91	242	3.75
132	3.96	1478	4.67	21	3.33	138	4.8	243	3.59
404	4.38	1480	4.6	33	2.64	139	4.6	281	2.84
406	5.43	1482	4.78	34	3.82	140	3.29	282	3.33
409	5.34	1682	4.17	35	4.24	144	3.36	283	4.76
411	5.5	1683	5.48	36	3.46	146	4.24	284	4.24
412	4.74	1684	5.32	37	3.85	147	4.7	285	2.84
748	4.5	1686	5.85	39	3.43	161	2.87	302	3.07
750	4.04	1691	4.96	40	3.69	162	3.59	303	3.29
752	5.36	405	4.36	42	3.62	163	4.6	305	3.65
753	6.26	412	5.28	43	3.85	164	4.47	306	3.75

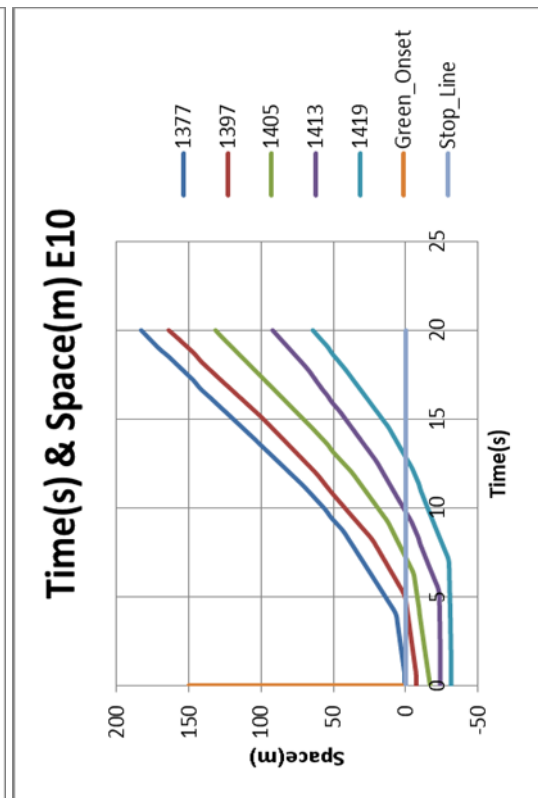
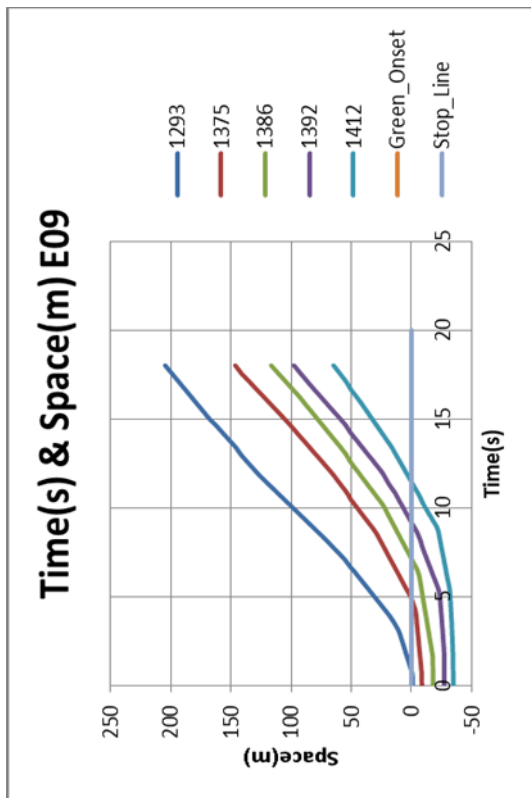
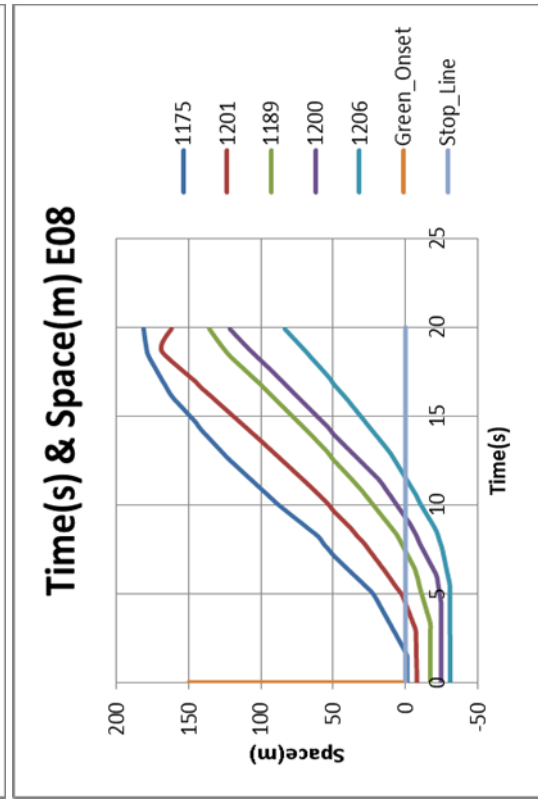
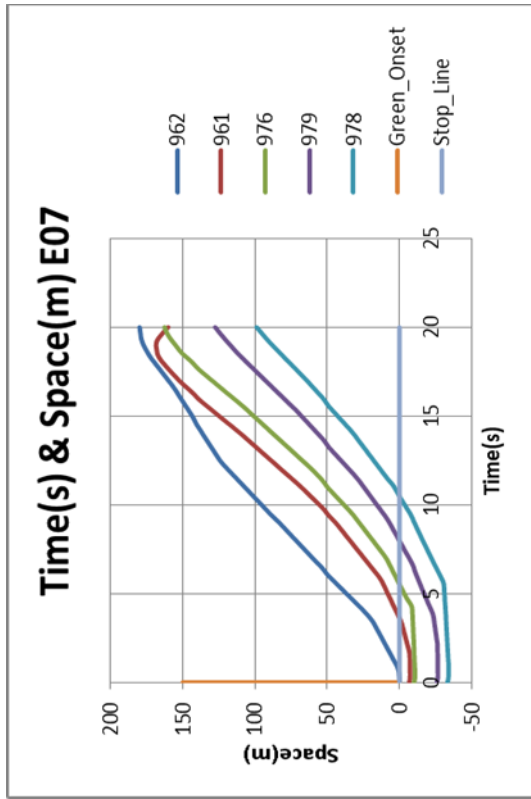


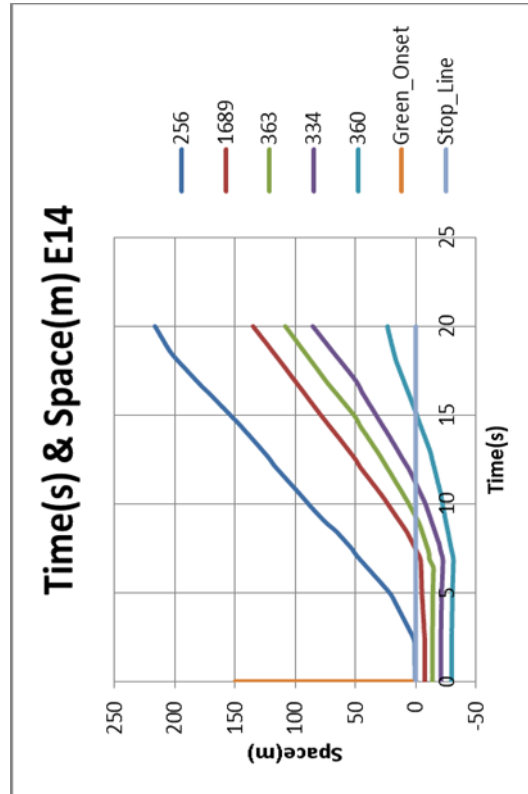
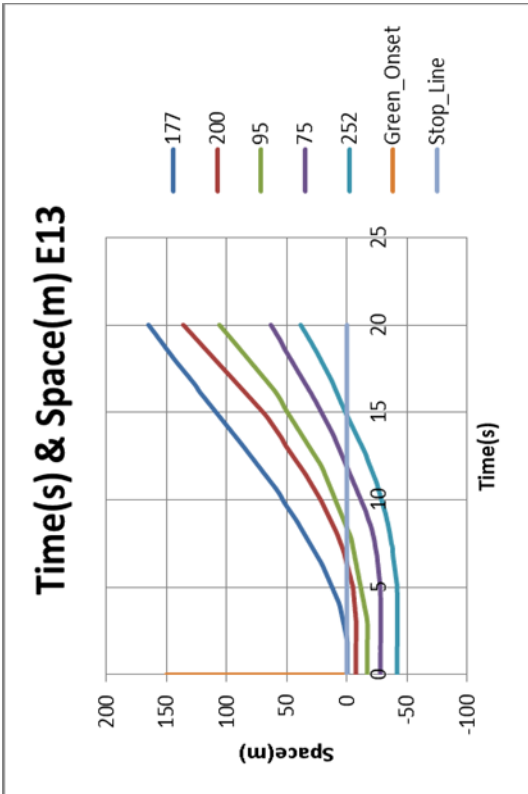
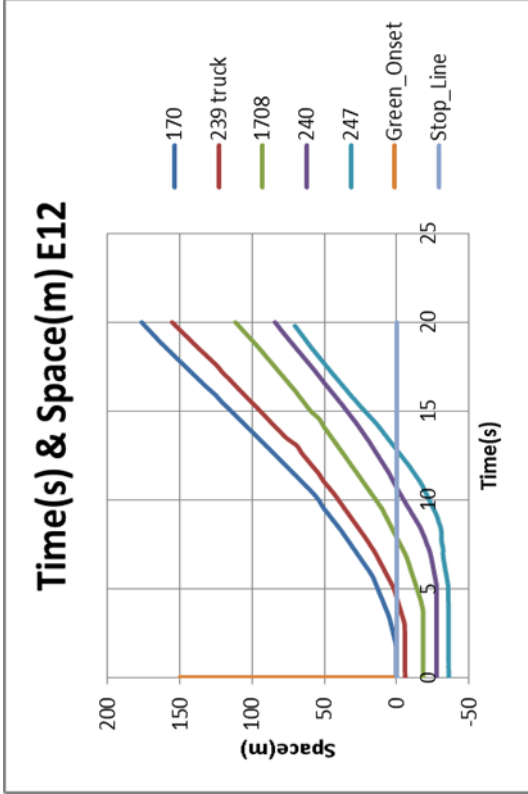
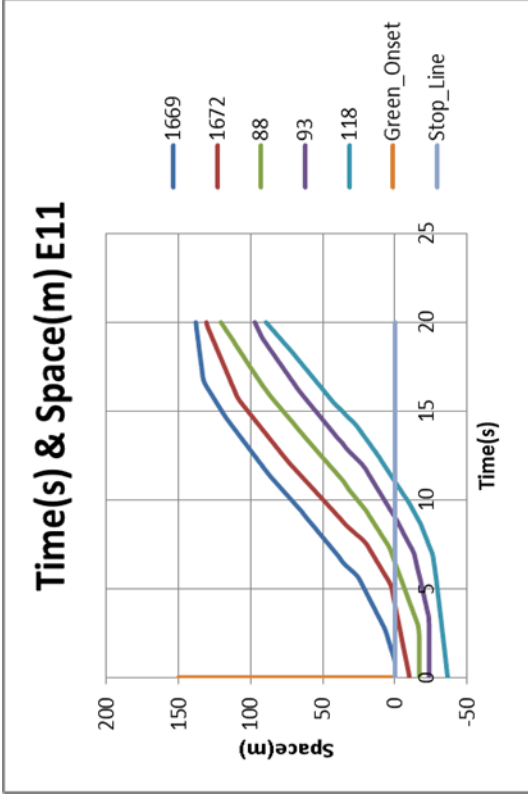
762	3.89	414	4.91	63	3.1	165	3.07	312	2.81
944	4.21	416	4.06	64	4.01	178	3.23	313	3.75
945	6.01	551	3.87	65	4.96	180	4.93	314	3.52
948	5.33	553	5.25	66	3.75	181	4.11	315	3.56
949	4.75	554	4.16	71	3.33	812	3.33	316	4.83
950	3.2	558	4.94	72	2.94	183	3.13	324	3.1
1033	4.17	560	4.45	73	4.66	184	3.36	325	3.52
1034	4.27	727	3.22	74	3.72	185	3.69	326	4.5
1036	4.89	728	4.93	75	3.75	186	3.78	327	4.31
1038	5.23	732	5.72	92	3.29	187	3.13	328	3.0
1047	3.06	735	5.24	93	3.88	189	2.67	361	2.64
1136	4.1	736	4.46	94	4.47	190	3.36	362	3.59
1144	5.66	558	4.4	95	4.24	191	4.04	363	4.6
1145	5.81	562	5.73	104	2.97	192	3.65	364	3.78
1146	5.09	563	5.43	105	3.85	193	3.33	365	3.98
1148	4.05	565	5.09	106	4.57	194	3.0	377	3.36
1210	4.5	569	3.68	107	4.01	195	3.1	379	4.01
1214	5.71			109	3.43	196	3.95	380	4.47
1215	5.18			110	3.26	197	4.04	381	3.07
1217	5.23			111	4.6	198	5.19	383	2.74
1218	4.73			113	3.0	205	2.58	384	3.78
329	4.31			114	3.1	206	3.07	385	4.44
330	4.97			115	3.29	207	3.88	397	3.29
334	5.3			116	3.78	209	3.78	402	2.97
335	5.78			117	3.59	220	3.29	403	4.21
1168	4.2			118	3.95	221	3.13	404	4.47
1170	5.2			124	3.29	222	4.63	405	3.16
1173	5.91			125	3.95	223	4.7	406	3.95
Average Vehicle Length (m) (Total 224 cars)							4.15 metres		

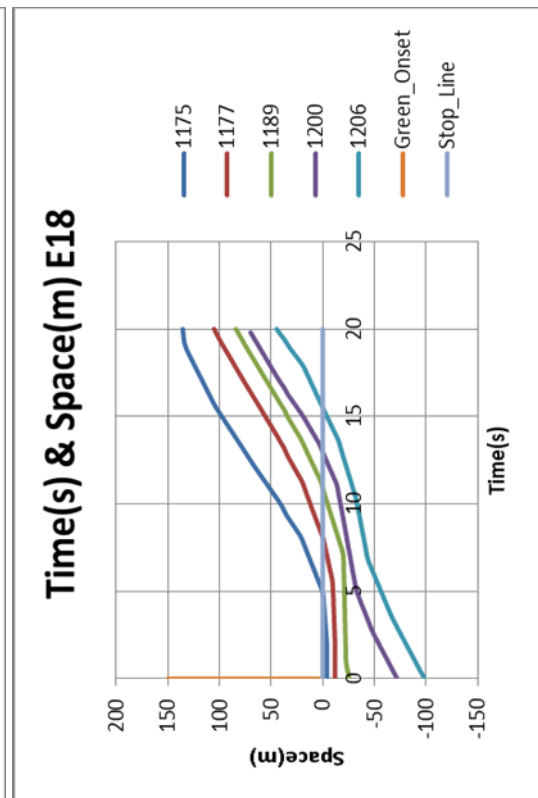
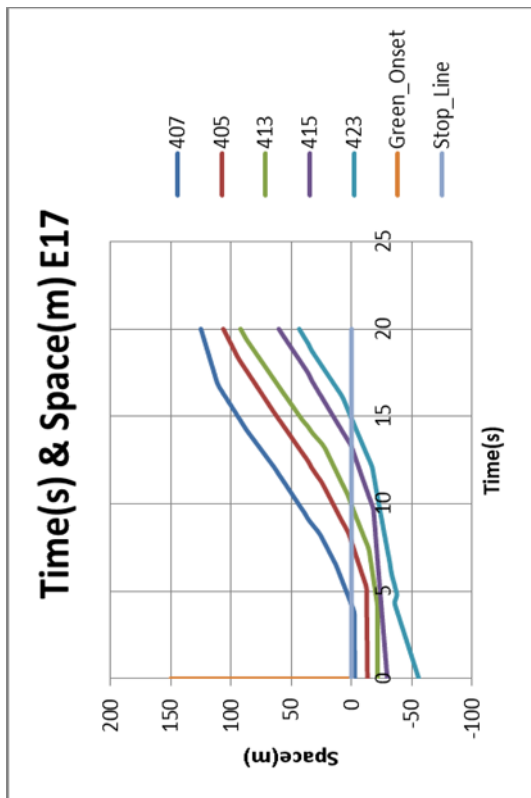
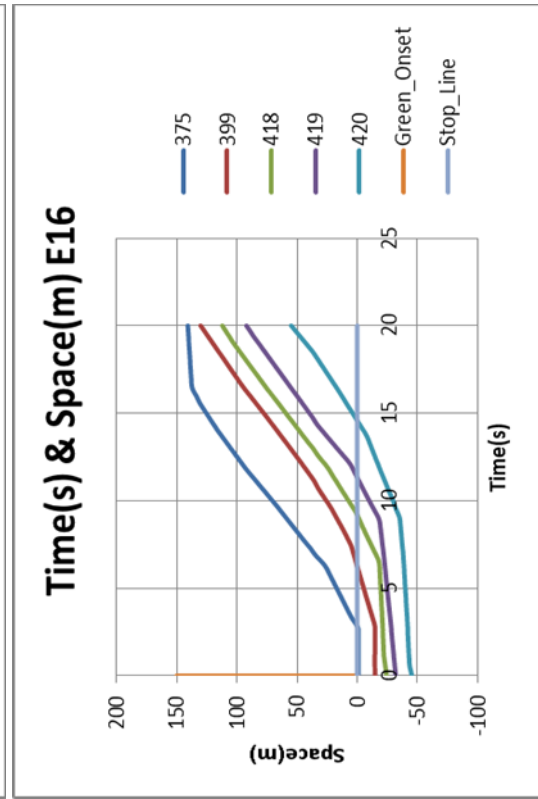
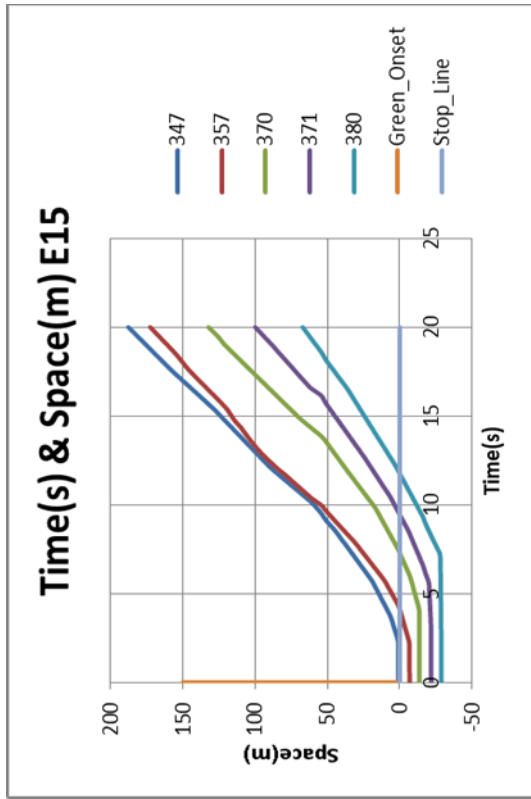
### Appendix H: NGSIM Peachtree Data 21 discharge samples

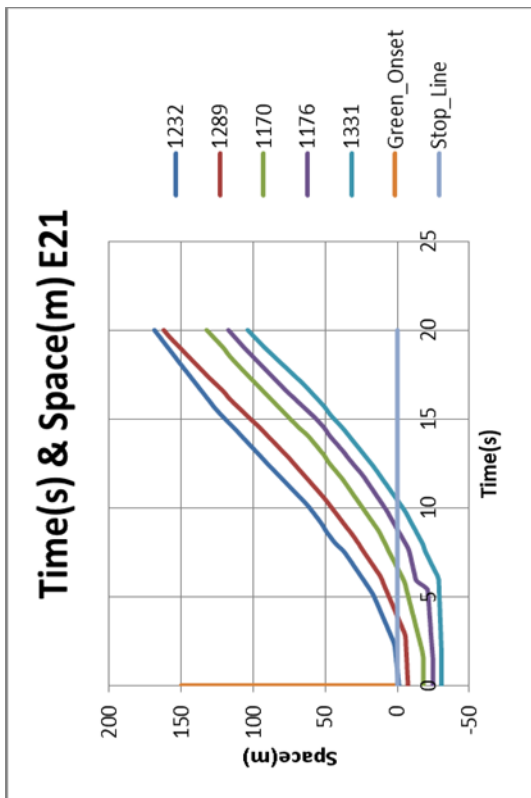
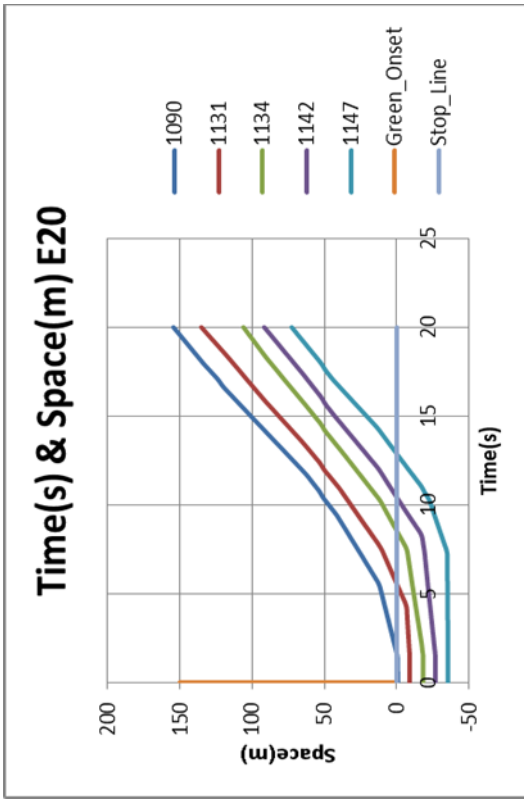
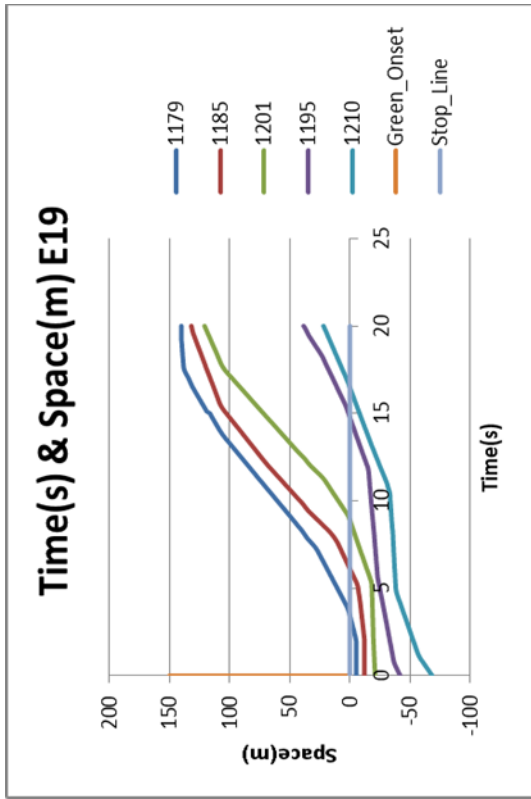












## Appendix I: Peachtree Data parameters

Queuing vehicles distance from the stop line (m)
--

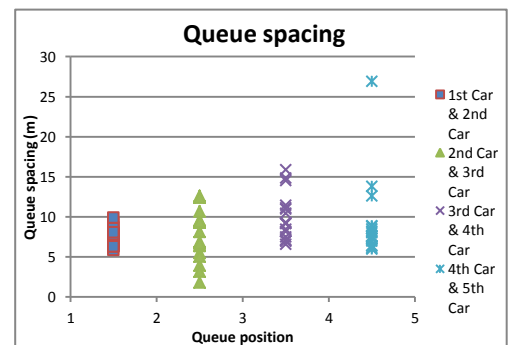
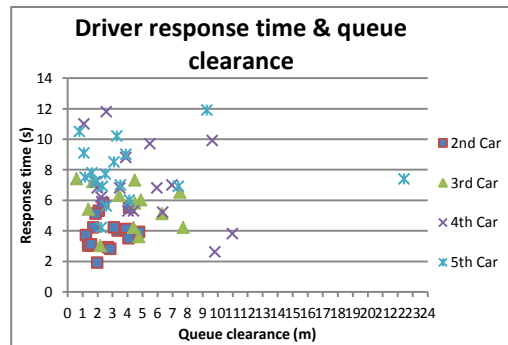
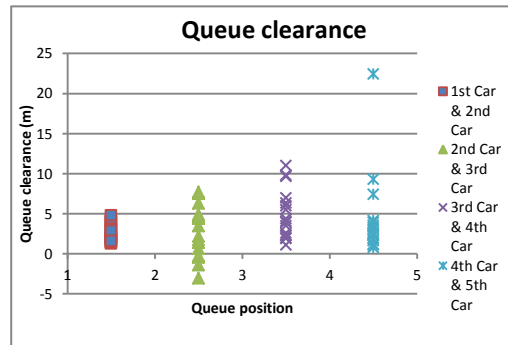
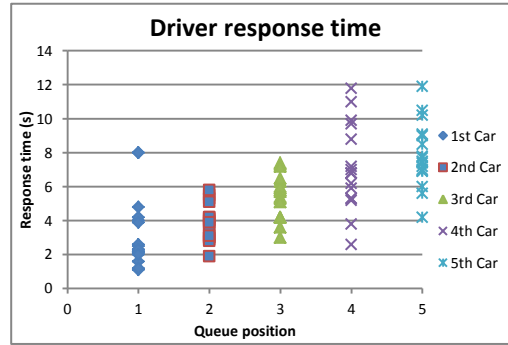
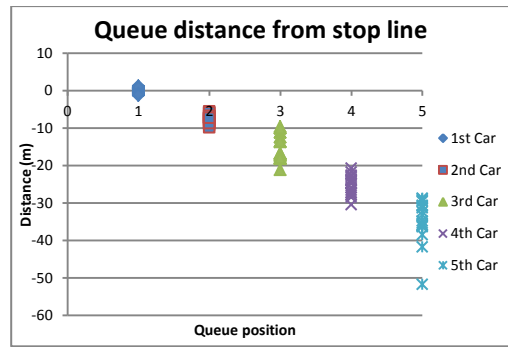
Sample	1 <sup>st</sup> Car	2 <sup>nd</sup> Car	3 <sup>rd</sup> Car	4 <sup>th</sup> Car	5 <sup>th</sup> Car
E01	0.7	-8.54	-21.15	-30.45	-38.48
E02	0.85	-5.59	-11.11	-22.58	-28.92
E03	0.25	-7.71	-9.55	-24.07	-32.31
E04	-0.49	-9.2	-17.35	-28.49	-36.04
E05	-0.14	-6	-9.94	-24.79	-51.71
E06	1.24	-7.35	-12.42	-22.89	-29.32
E07	0.1	-6.8	-10	-25.9	-33.2
E08	-1.3	-8	-17.3	-24.8	-30.9
E09	-0.9	-8.7	-18	-27.2	-34.8
E10	0.78	-7.15	-16.75	-23.9	-31.26
E11	0.1	-9.8	-16.7	-23.7	-36.3
E12	0.5	-5.8	-18.2	-27.4	-35.9
E13	-0.4	-7.4	-16.9	-27.9	-41.7
E14	0.6	-7.3	-13.7	-20.7	-29.6
E15	1	-6.8	-13.5	-21.7	-28.7
E20	-0.7	-8.77	-18.15	-26.6	-35.43
E21	-1	-7.3	-18	-24.6	-30.6

Note: A negative value indicates vehicle's queue position is behind the stop line and the stop line at zero. A positive value means vehicle stop over the stop line.

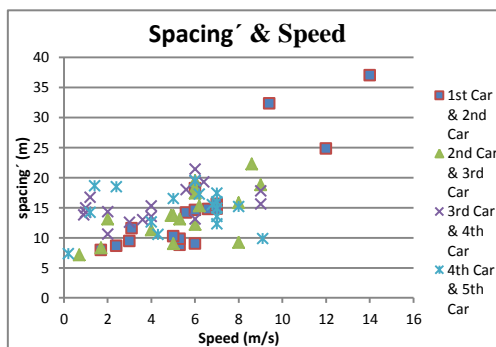
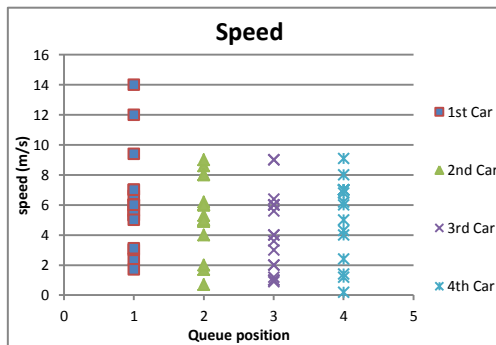
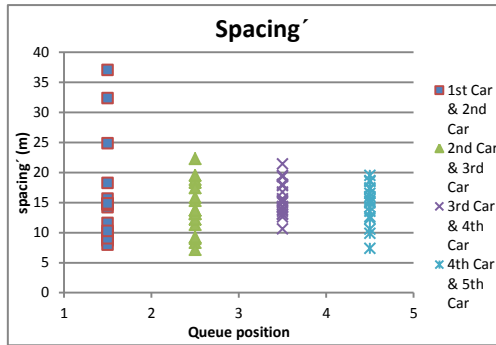
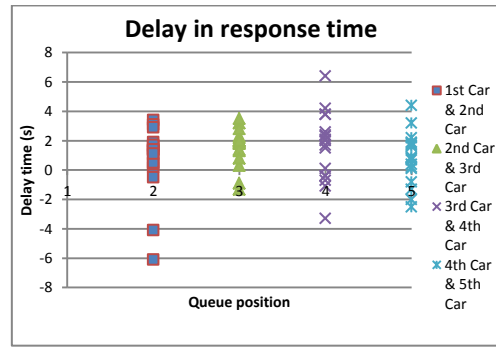
Driver response time (s)					
Sample	1 <sup>st</sup> Car	2 <sup>nd</sup> Car	3 <sup>rd</sup> Car	4 <sup>th</sup> Car	5 <sup>th</sup> Car
E01	2.1	5.5	4.2	6.8	7.7
E02	4	4.2	7.4	7	7.8
E03	2.1	4	5.9	2.6	7
E04	2.5	4.1	6.3	5.2	6.9
E05	4.2	3.7	5.7	9.9	7.4
E06	2.2	3.5	5.3	6.8	7.2
E07	8	1.9	4.2	3.8	5.6
E08	1.6	3	5.8	5.9	7.5
E09	1.1	4.2	6	5.3	8.5
E10	1.2	2.9	4.2	6.2	4.2
E11	8	3.9	3	6.8	6.9
E12	2.6	3	6.5	8.8	9
E13	3.9	5.3	7.3	9.7	11.9
E14	4.8	5.8	7.2	11	10.2
E15	2.2	5.1	5.4	11.8	10.5
E20	2.3	2.8	3.6	5.3	6
E21	2	3.1	5.1	7.2	9.1

Queue clearance (m)				
Sample	2 <sup>nd</sup> Car	3 <sup>rd</sup> Car	4 <sup>th</sup> Car	5 <sup>th</sup> Car
E01	4.14	7.71	3.5	2.53
E02	1.74	0.62	6.97	1.64
E03	3.36	-3.06	9.82	3.54
E04	3.91	3.45	6.34	2.35
E05	1.26	-0.46	9.65	22.42
E06	4.09	-0.23	5.97	1.83
E07	2	-1.4	11	2.6
E08	1.5	4.5	2.3	1.2
E09	3.1	4.9	4.4	3.1
E10	2.73	4.4	2.25	2.26
E11	4.8	2.2	2	7.4
E12	1.4	7.5	3.9	3.9
E13	2.1	4.5	5.5	9.3
E14	2.4	1.7	1.1	3.3
E15	1.9	1.4	2.6	0.8
E20	2.87	4.78	4.05	4.13
E21	1.6	6.3	1.9	1.1

Queue spacing (m)				
Sample	2 <sup>nd</sup> Car	3 <sup>rd</sup> Car	4 <sup>th</sup> Car	5 <sup>th</sup> Car
E01	9.24	12.61	9.3	8.03
E02	6.44	5.52	11.47	6.34
E03	7.96	1.84	14.52	8.24
E04	8.71	8.15	11.14	7.55
E05	5.86	3.94	14.85	26.92
E06	8.59	5.07	10.47	6.43
E07	6.9	3.2	15.9	7.3
E08	6.7	9.3	7.5	6.1
E09	7.8	9.3	9.2	7.6
E10	7.93	9.6	7.15	7.36
E11	9.9	6.9	7	12.6



E12	6.3	12.4	9.2	8.5
E13	7	9.5	11	13.8
E14	7.9	6.4	7	8.9
E15	7.8	6.7	8.2	7
E20	8.07	9.38	8.45	8.83
E21	6.3	10.7	6.6	6
Delay in response time (s)				
Sample	2 <sup>nd</sup> Car	3 <sup>rd</sup> Car	4 <sup>th</sup> Car	5 <sup>th</sup> Car
E01	3.4	-1.3	2.6	0.9
E02	0.2	3.2	-0.4	0.8
E03	1.9	1.9	-3.3	4.4
E04	1.6	2.2	-1.1	1.7
E05	-0.5	2	4.2	-2.5
E06	1.3	1.8	1.5	0.4
E07	-6.1	2.3	-0.4	1.8
E08	1.4	2.8	0.1	1.6
E09	3.1	1.8	-0.7	3.2
E10	1.7	1.3	2	-2
E11	-4.1	-0.9	3.8	0.1
E12	0.4	3.5	2.3	0.2
E13	1.4	2	2.4	2.2
E14	1	1.4	3.8	-0.8
E15	2.9	0.3	6.4	-1.3
E20	0.5	0.8	1.7	0.7
E21	1.1	2	2.1	1.9
Spacing ' (m)				
Sample	2 <sup>nd</sup> Car	3 <sup>rd</sup> Car	4 <sup>th</sup> Car	5 <sup>th</sup> Car
E01	32.31	13.11	12.59	15.51
E02	8.76	13.67	14.97	10.52
E03	14.14	15.29	13.77	18.46
E04	9.81	22.28	16.74	17.24
E05	8.63	11.31	19.28	18.62
E06	14.73	18.34	18.01	9.85
E07	14.6	12.2	14.2	16.5
E08	15.6	18.8	13.5	13.5
E09	24.8	15.8	14.3	17.4
E10	7.91	8.33	12.98	7.32
E11	14.8	13.1	15.3	12.6
E12	9.4	19.5	19.5	16
E13	18.2	9	21.4	19.5
E14	37	9.2	15.6	14.9
E15	9	17.4	17.8	15.2
E20	11.54	7.11	10.6	14.24
E21	10.2	13.7	13.1	12.3
Speed (m/s)				
Sample	1 <sup>st</sup> Car	2 <sup>nd</sup> Car	3 <sup>rd</sup> Car	4 <sup>th</sup> Car
E01	9.4	5.3	3	6.8
E02	5.3	4.9	1	4.3
E03	5.6	6.2	0.9	2.4
E04	5.3	8.6	1.2	6.2
E05	2.4	4	6.4	1.4
E06	6.6	6	5.6	9.1
E07	6	6	1	5
E08	7	9	4	7
E09	12	8	2	7
E10	1.7	1.7	3.6	0.2
E11	7	2	4	4
E12	3	6	6	7
E13	6	5	6	6
E14	14	8	9	7
E15	6	6	9	8
E20	3.1	0.7	2	1.2
E21	5	5	6	7



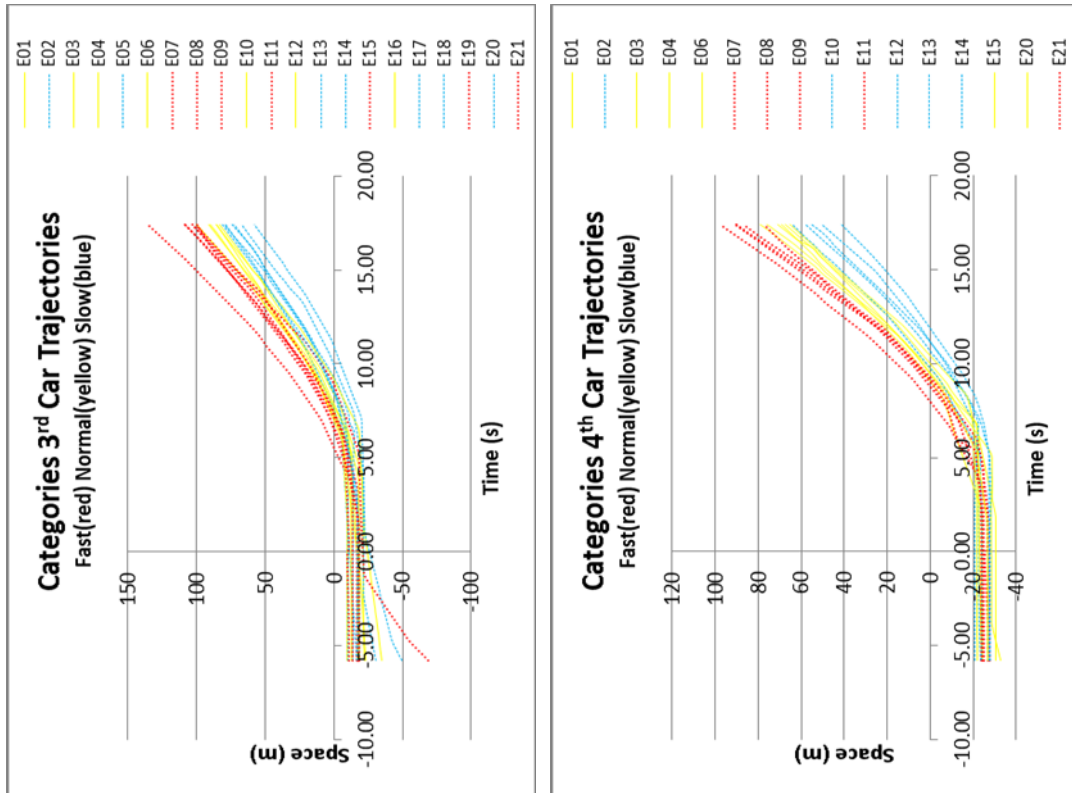


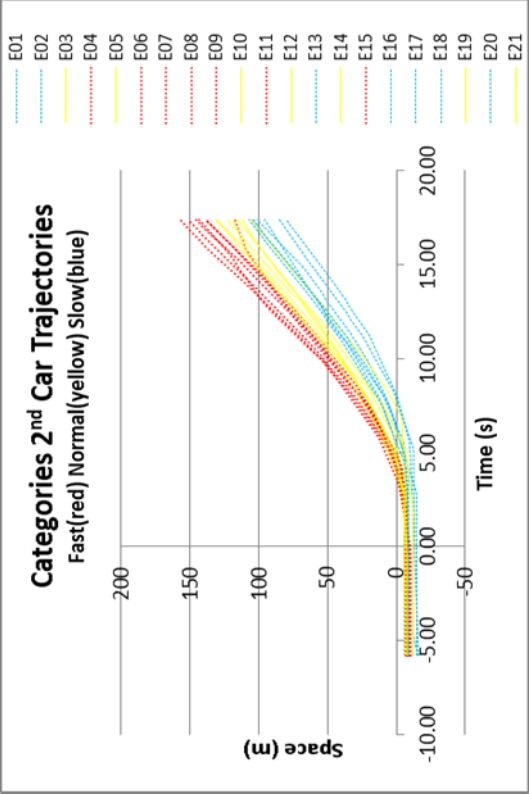
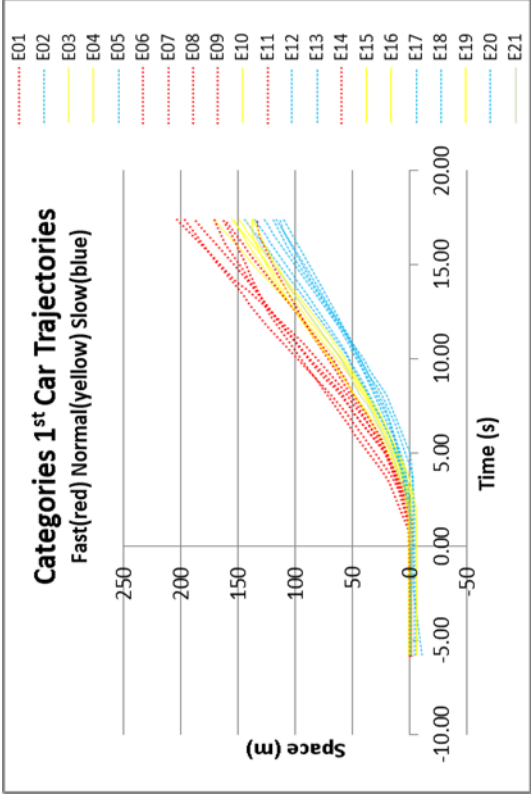
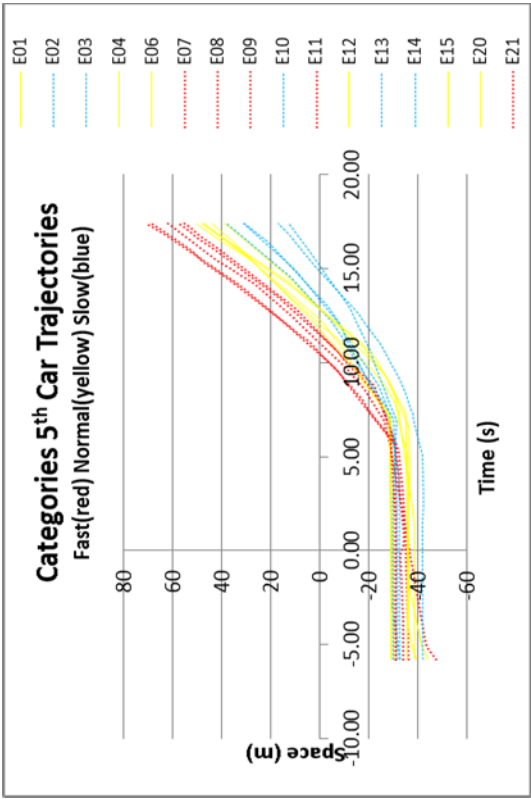
Note: These two parameters indicate two successive vehicles' spacing and the lead vehicle's speed at the time when the following vehicle makes response to the green signal.

### Appendix J: Peachtree Data raw vehicle length (m)

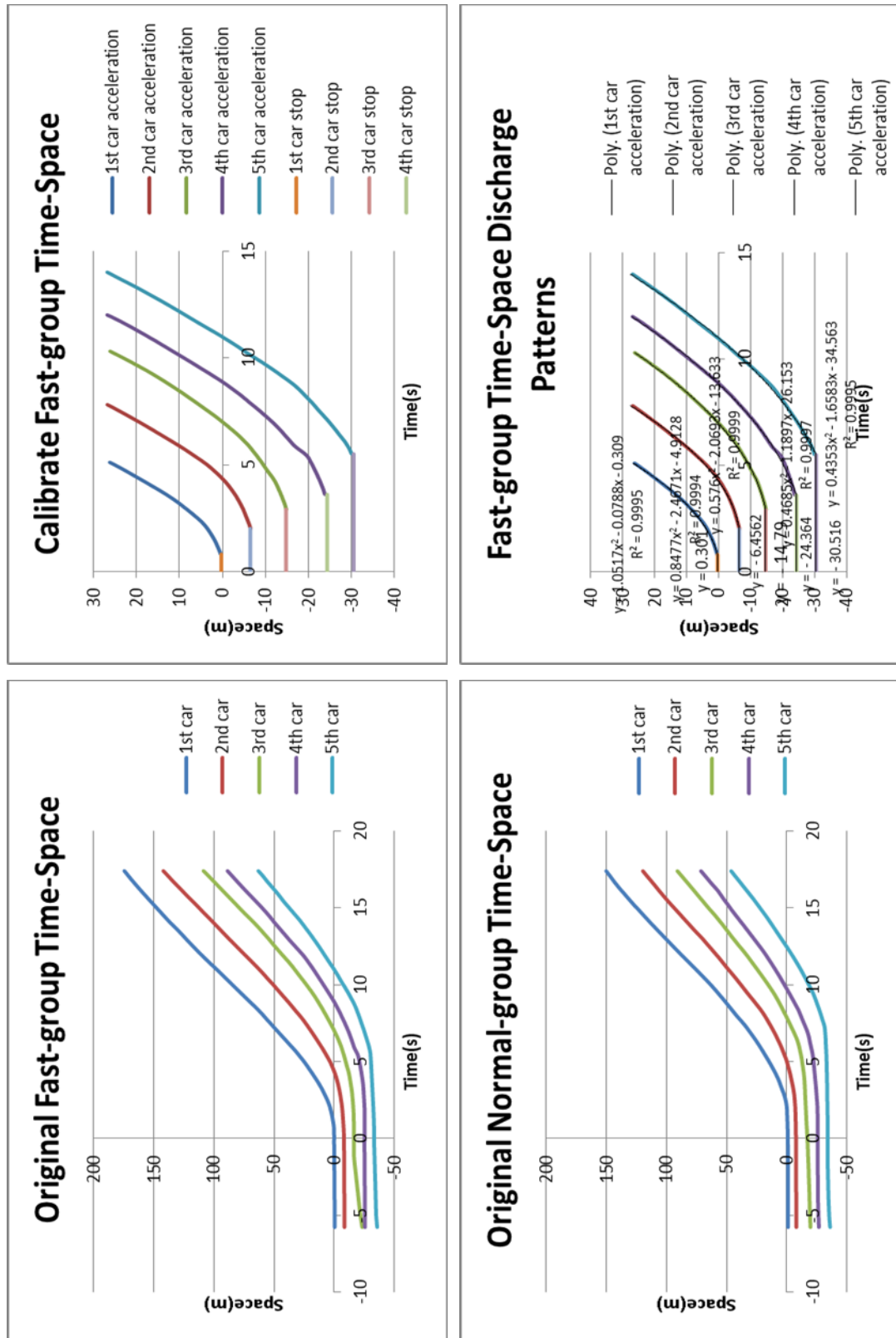
E01	E02	E03	E04	E05	E06	E07
4.9, 5.1, 5.5, 5.5, 5.8	4.5, 4.6, 4.7, 4.7, 4.9	4.6, 4.7, 4.7, 4.8, 4.9	4.8, 4.8, 4.7, 4.9, 5.2	4.4, 4.5, 4.6, 4.4, 5.2	4.5, 4.6, 4.5, 4.9, 5.3	4.6, 4.7, 4.9, 4.9, 4.6
E08	E09	E10	E11	E12	E13	E14
4.6, 4.8, 4.9, 5.2, 5.2	4.4, 4.5, 4.7, 4.8, 5.0	5.2, 4.7, 4.9, 5.1, 5.2	5.1, 4.7, 4.8, 5.0, 5.2	4.9, 5.5, 5.3, 4.6, 4.9	4.9, 5.0, 5.5, 6.4, 4.5	4.7, 5.6, 5.9, 5.6, 5.5
E15	E16	E17	E18	E19	E20	E21
5.3, 5.6, 5.9, 6.2, 5.9	4.9, 4.5, 4.7, 4.6, 4.5	4.7, 4.8, 4.7, 4.9, 5.2	5.2, 4.6, 4.9, 5.2, 4.9	4.6, 4.9, 5.2, 4.8, 4.6	4.6, 4.6, 4.7, 5.2, 4.4	4.4, 4.7, 4.9, 4.7, 4.9

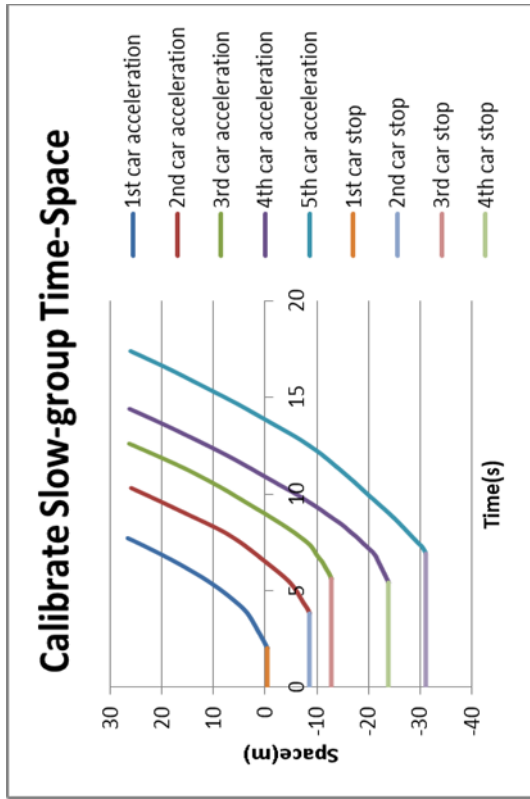
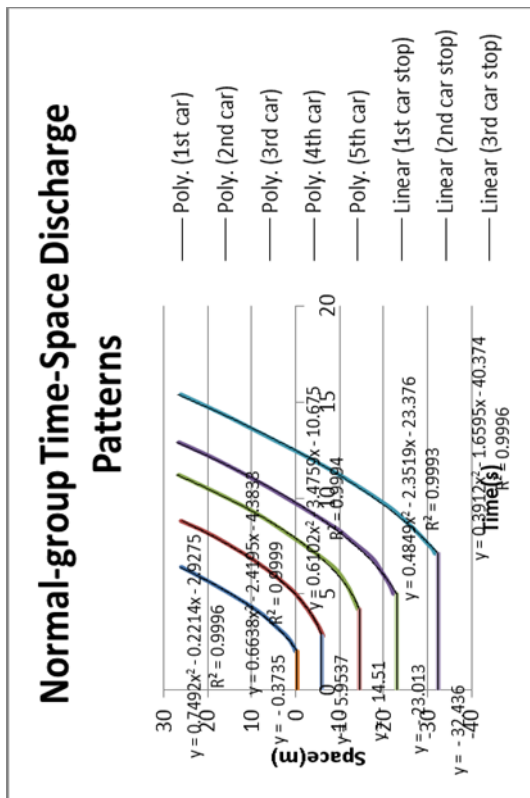
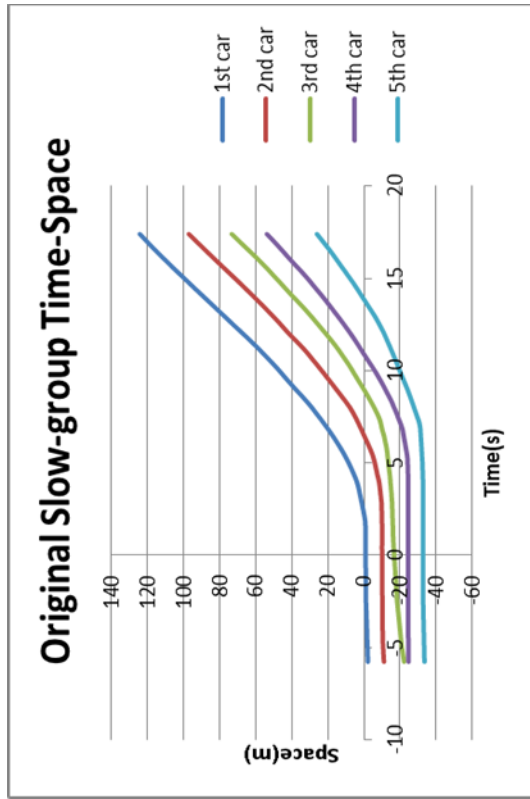
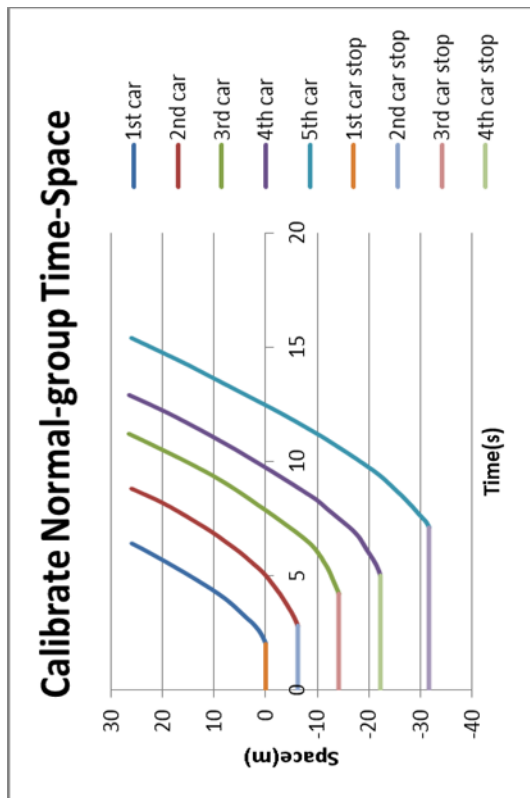
### Appendix K: Peachtree Data categories “Fast” “Normal” “Slow” trajectories

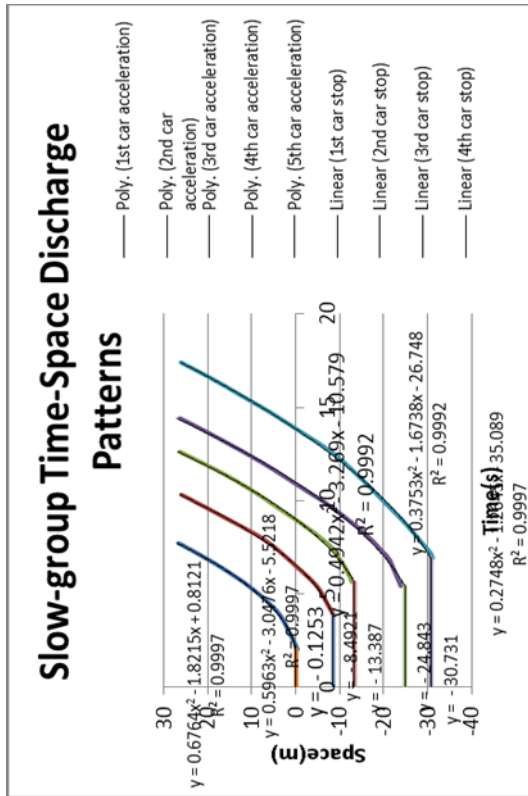




Appendix L: Peachtree data original & calibration of three group trajectories



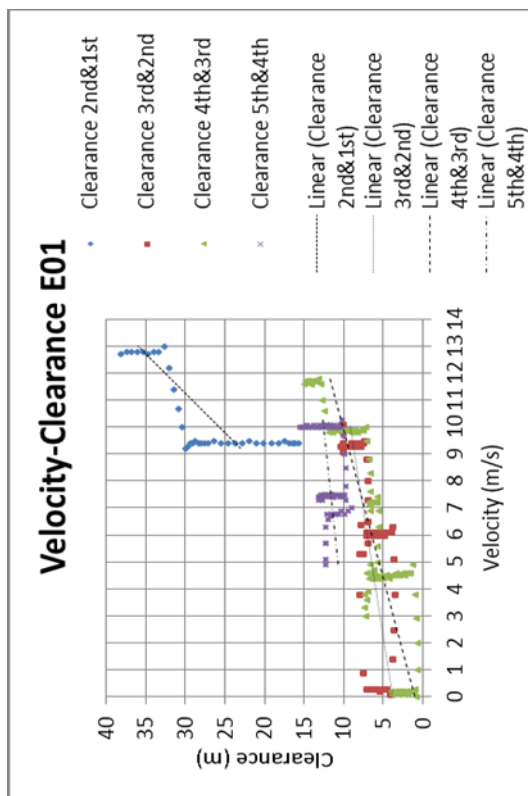
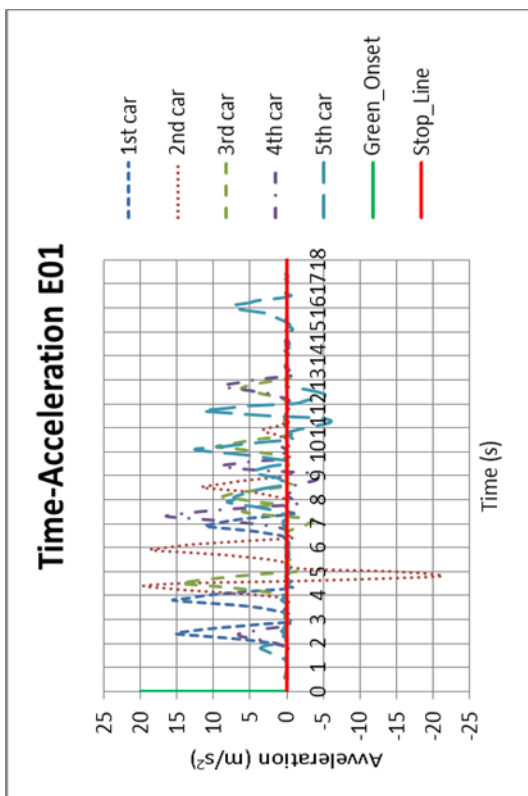
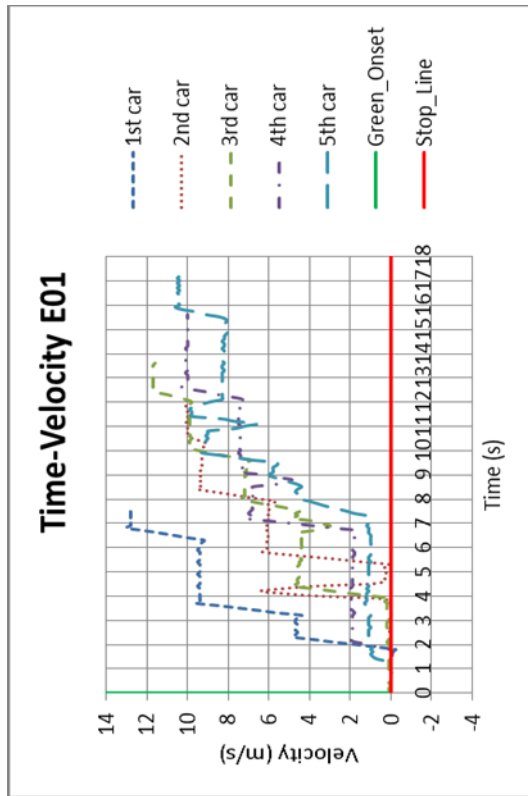
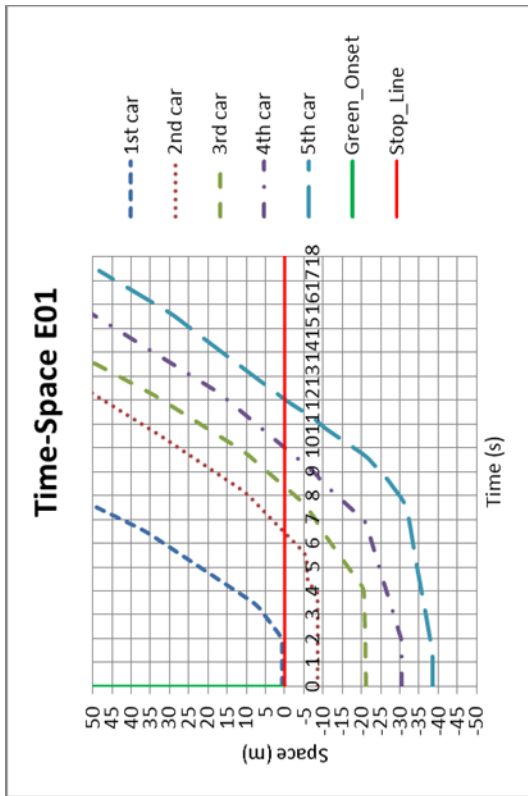


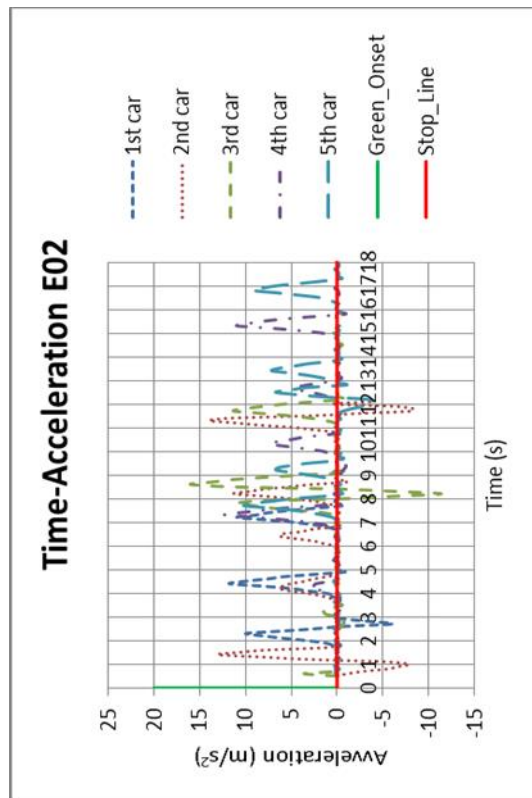
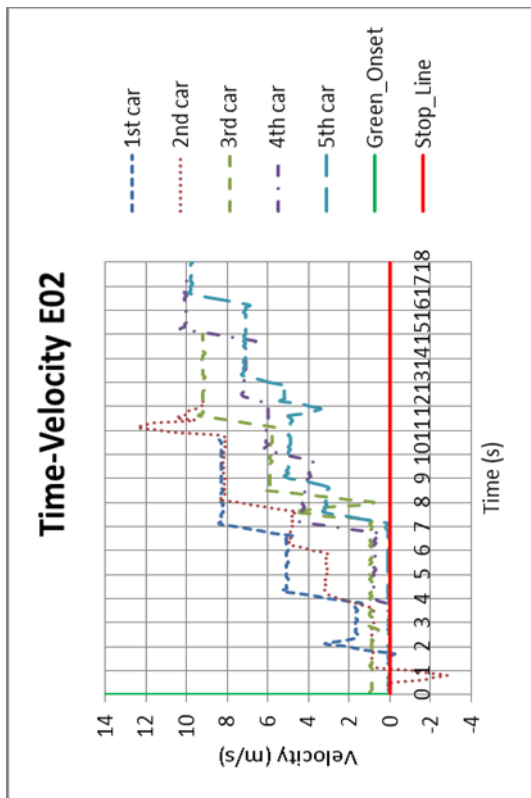
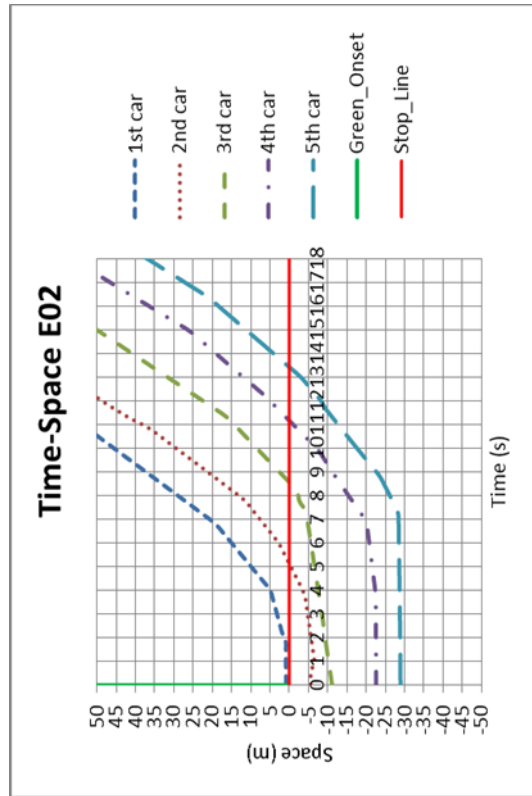
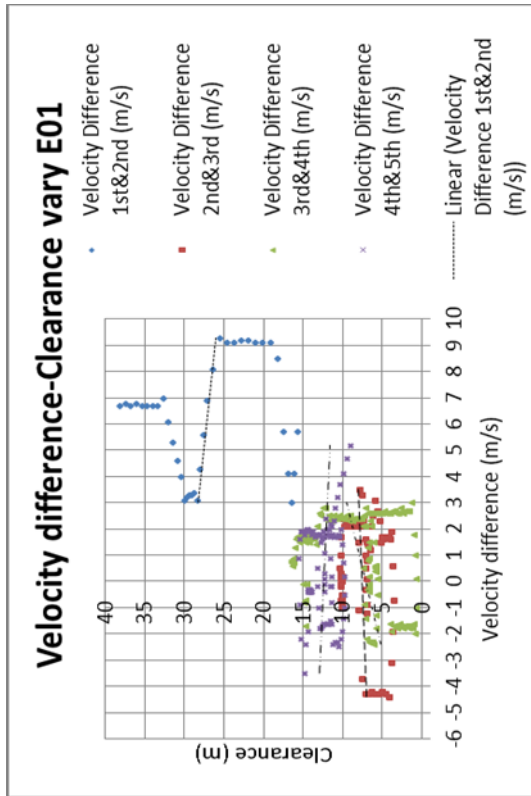


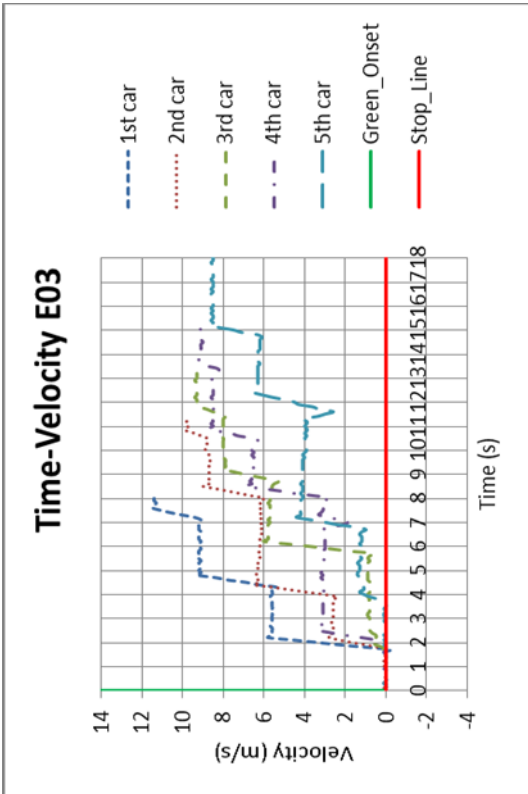
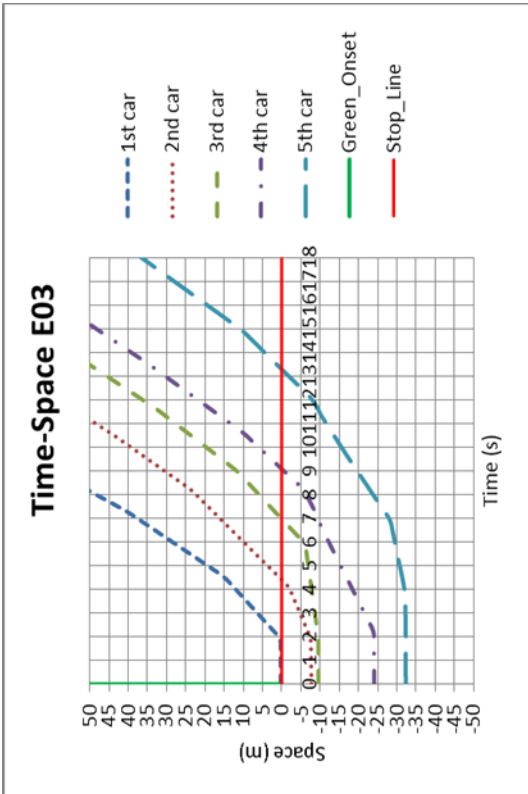
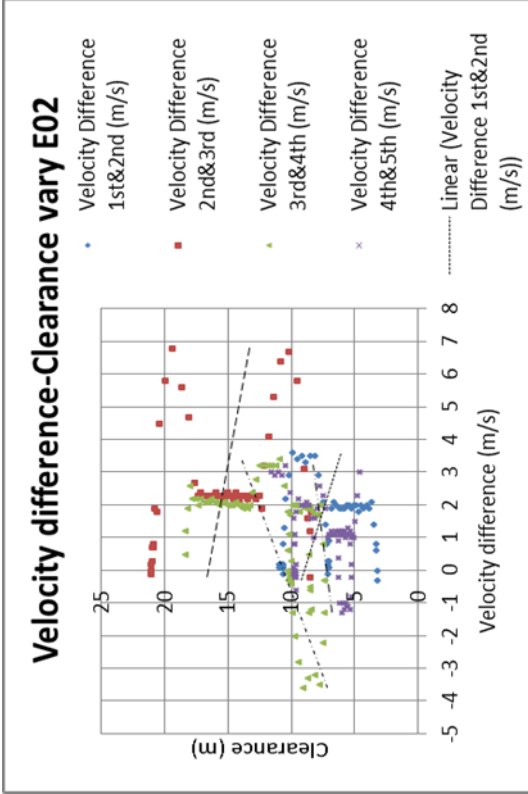
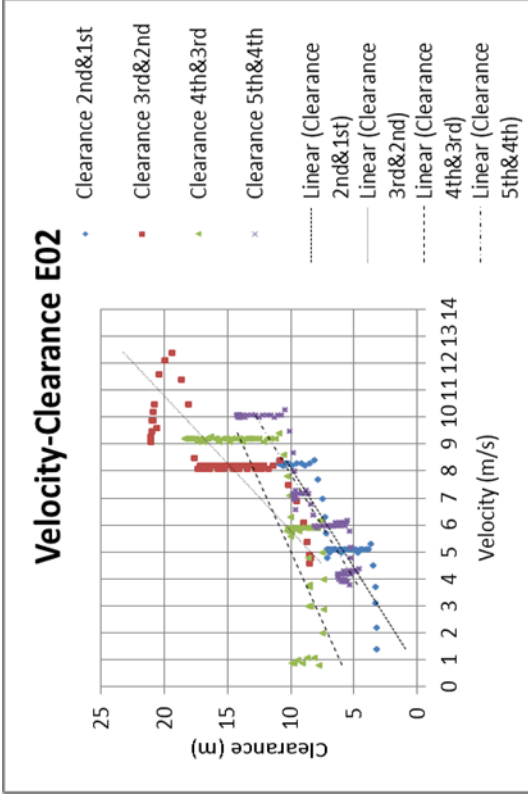
### Appendix M: The 20<sup>th</sup> percentile Clearance & Velocity

Patterns ID	Queue position	Velocity $S_v$ in m/s with clearance between two successive vehicles $f(S_v)$ in metres.	Conditions
D2	2 <sup>nd</sup> & 1 <sup>st</sup>	$f(S_v) = 1.3763 S_v - 1.1698$	$S_v$ is 1 <sup>st</sup> vehicle velocity, $f(S_v)$ is applicable to test the 2 <sup>nd</sup> vehicle
D3	3 <sup>rd</sup> & 2 <sup>nd</sup>	$f(S_v) = 1.5394 S_v - 1.1299$	$S_v$ is 2 <sup>nd</sup> vehicle velocity, $f(S_v)$ is applicable to test the 3 <sup>rd</sup> vehicle
D4	4 <sup>th</sup> & 3 <sup>rd</sup>	$f(S_v) = 0.8351 S_v + 2.767$	$S_v$ is 3 <sup>rd</sup> vehicle velocity, $f(S_v)$ is applicable to test the 4 <sup>th</sup> vehicle
D5	5 <sup>th</sup> & 4 <sup>th</sup>	$f(S_v) = 1.1218 S_v + 2.594$	$S_v$ is 4 <sup>th</sup> vehicle velocity, $f(S_v)$ is applicable to test the 5 <sup>th</sup> vehicle

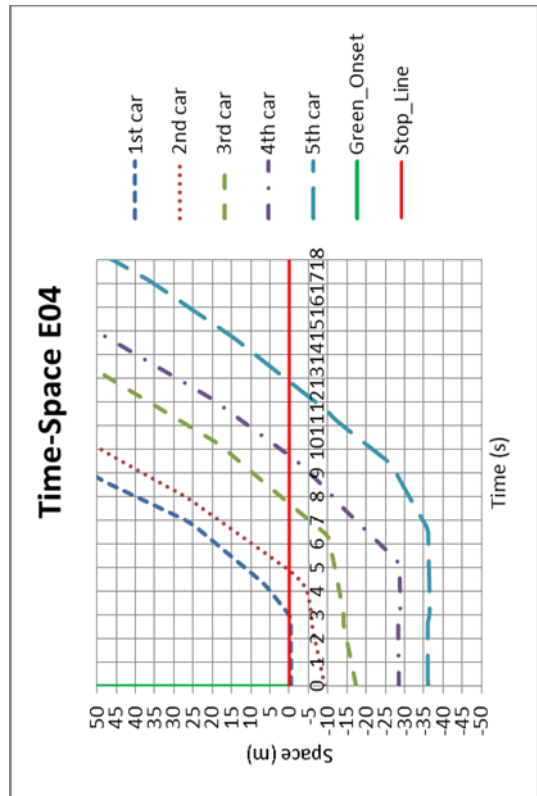
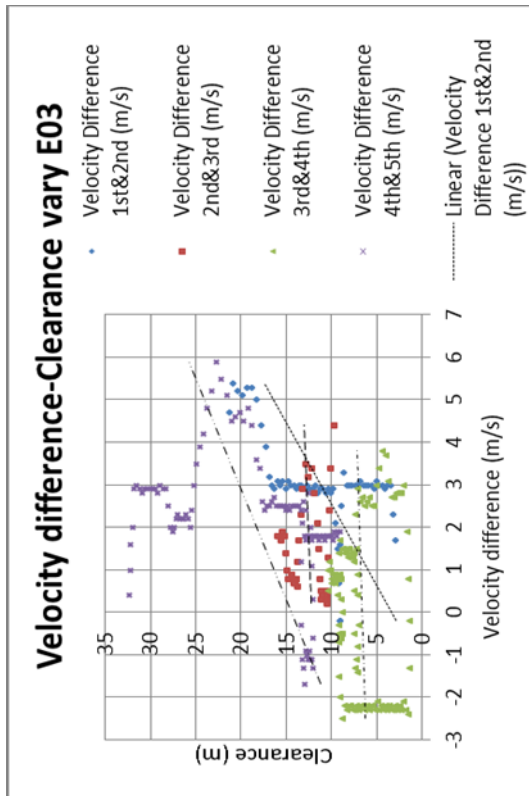
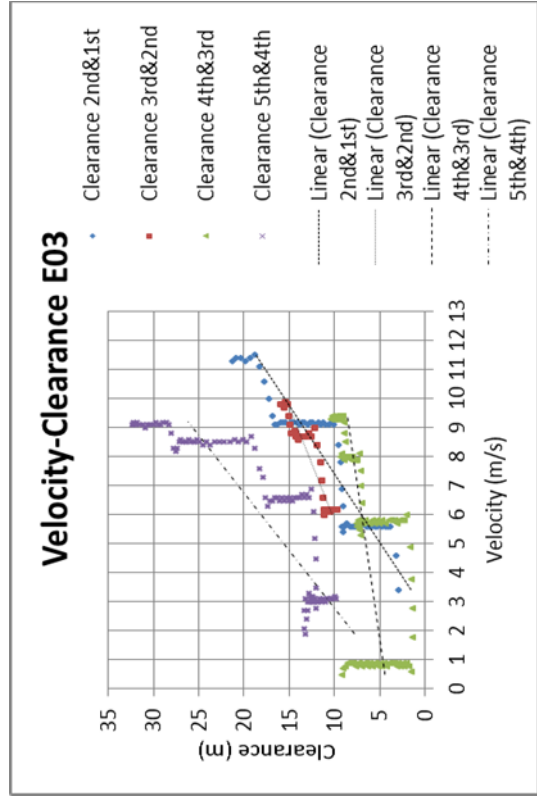
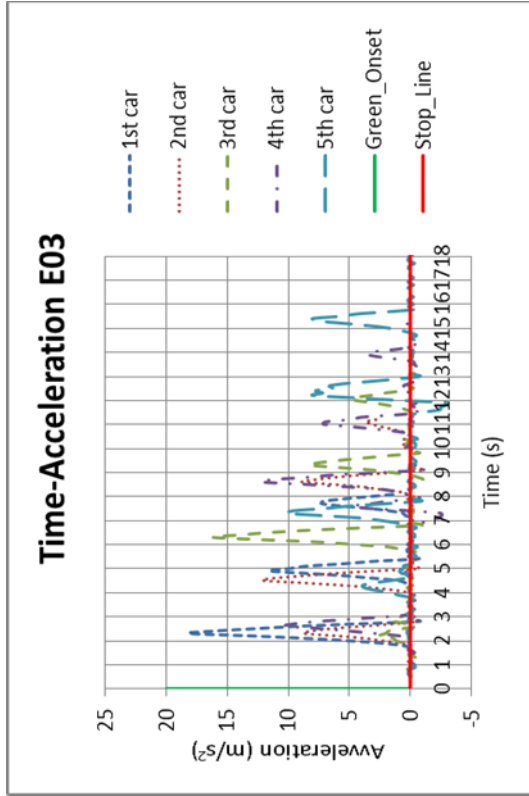
**Appendix N: Peachtree Data velocity acceleration & clearance analysis**

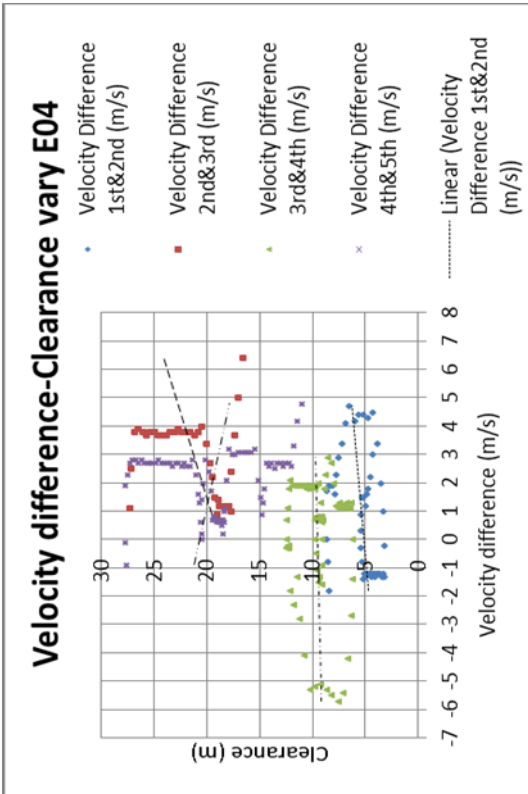
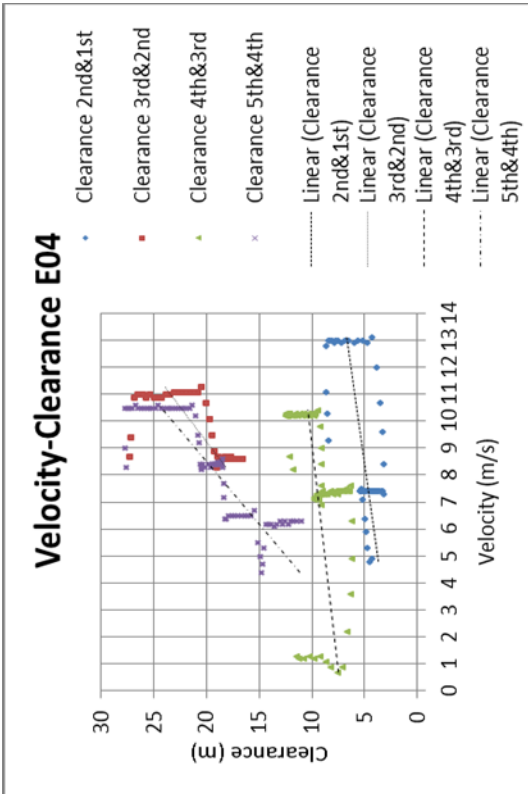
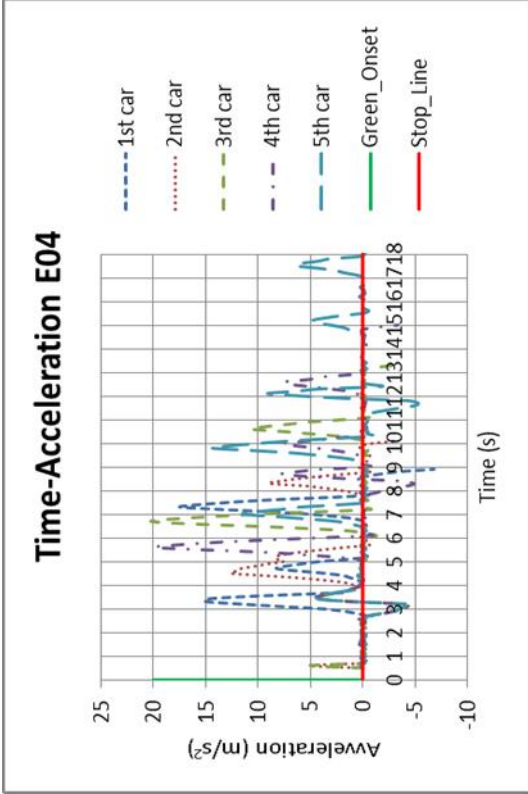
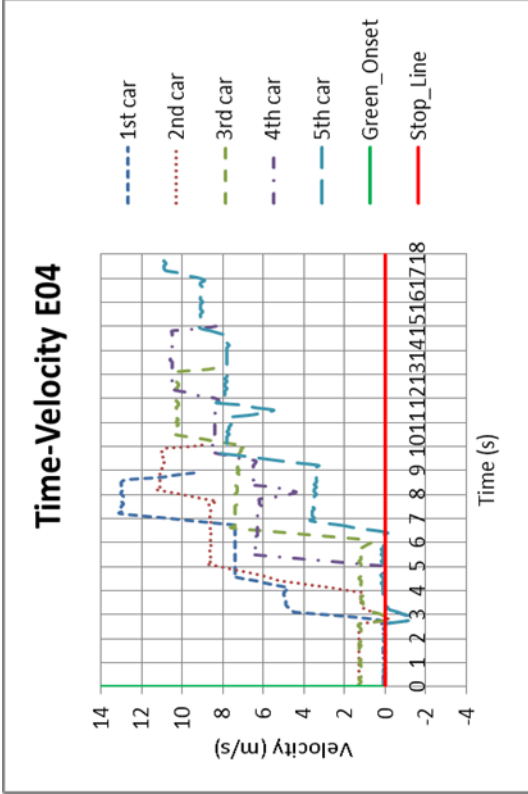


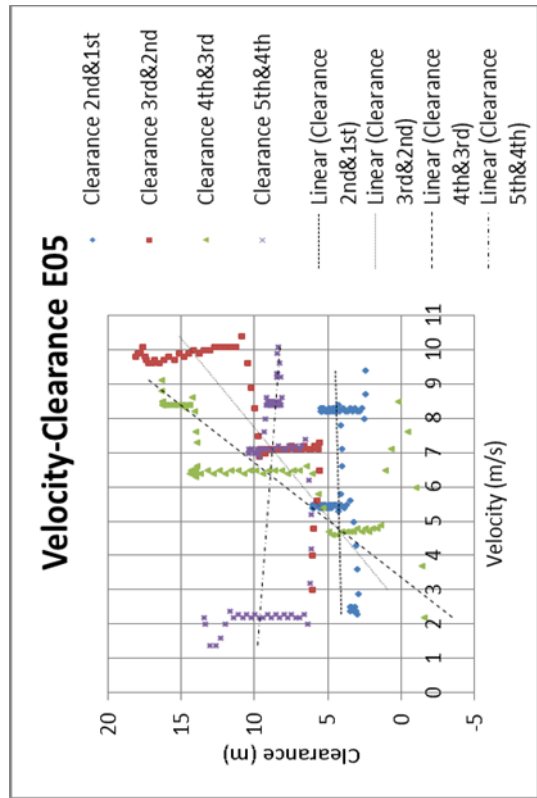
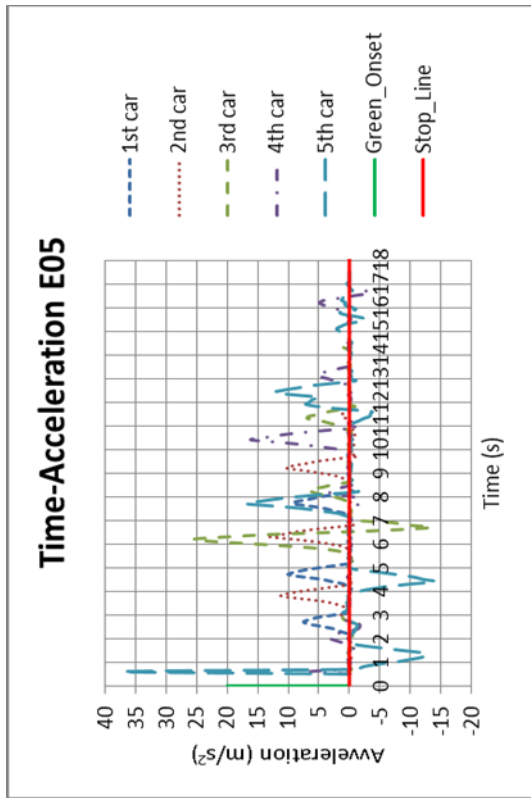
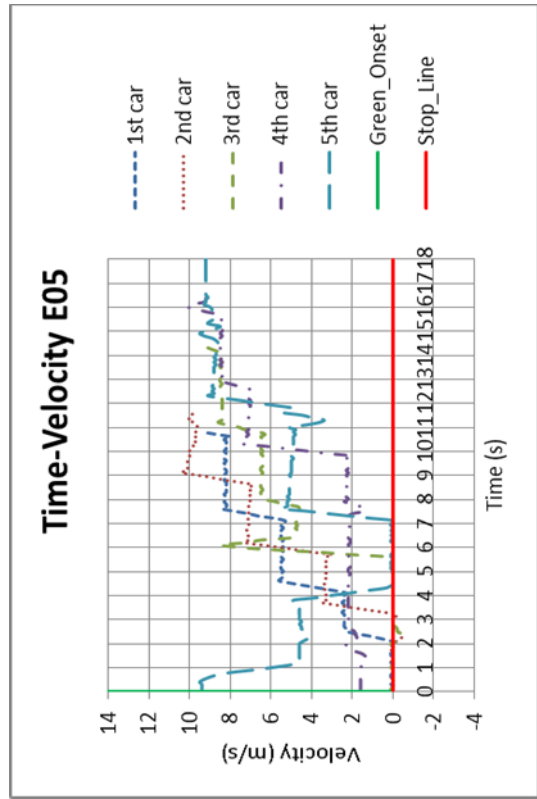
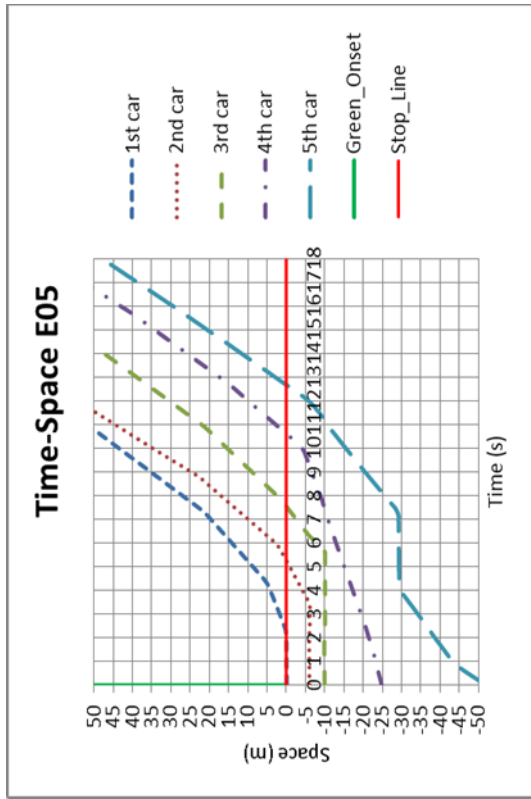


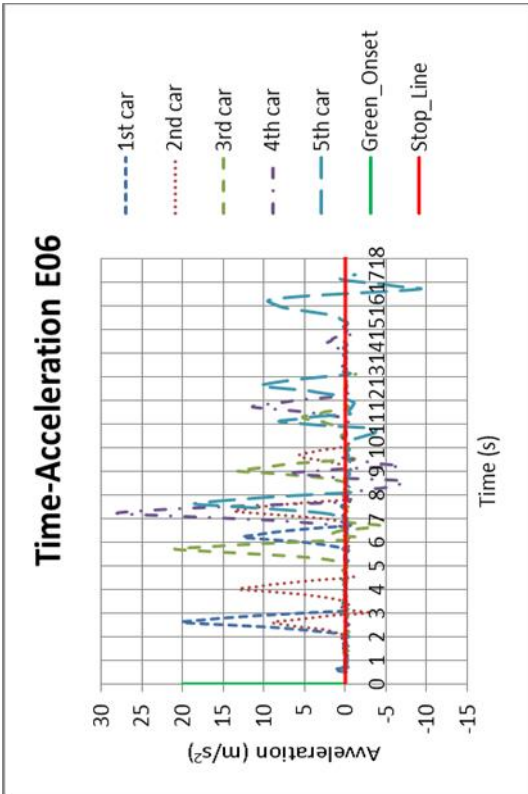
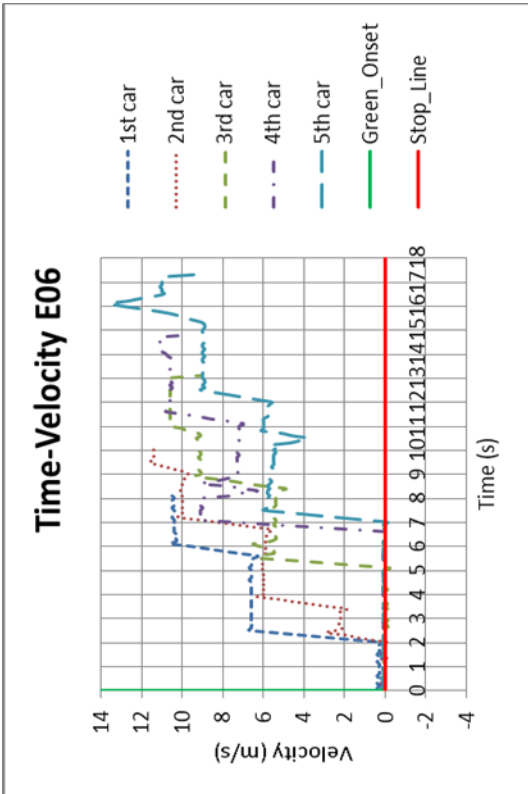
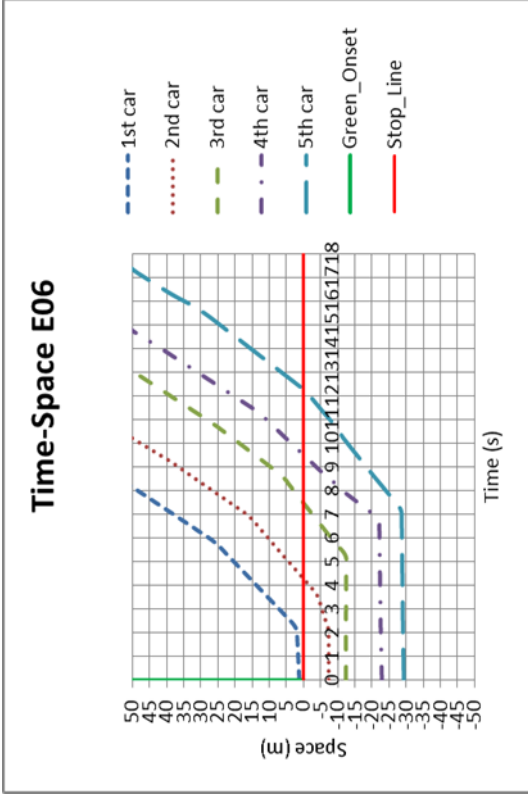
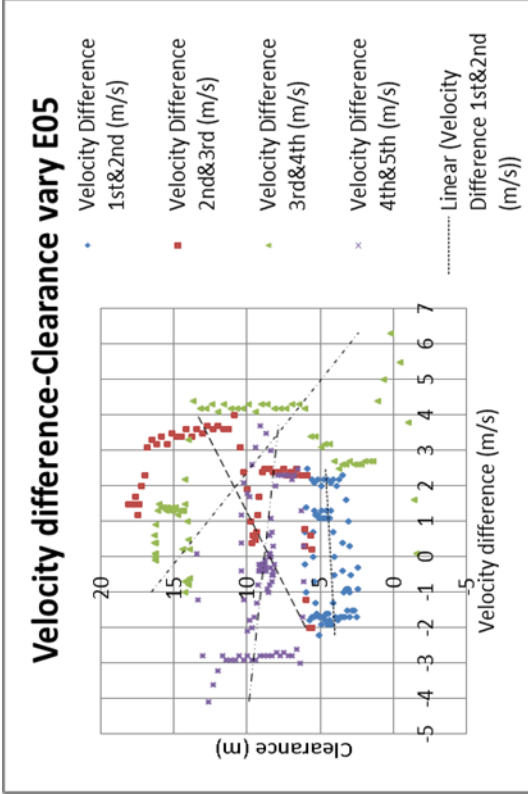


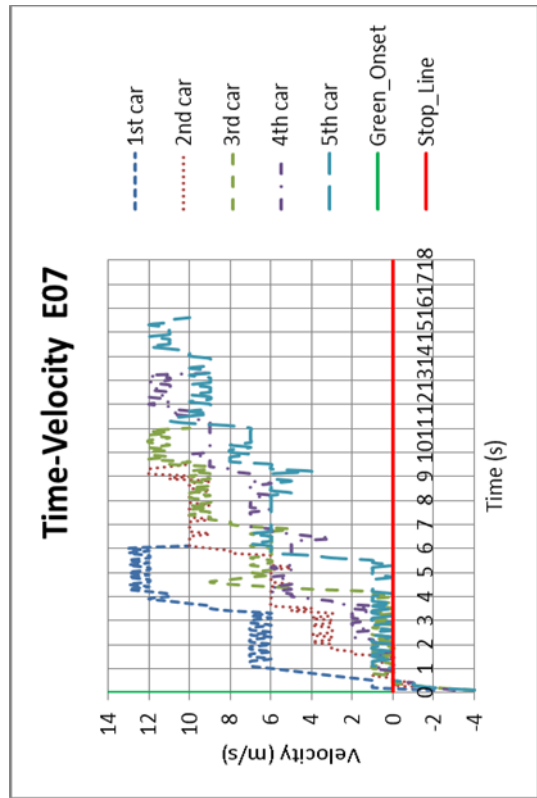
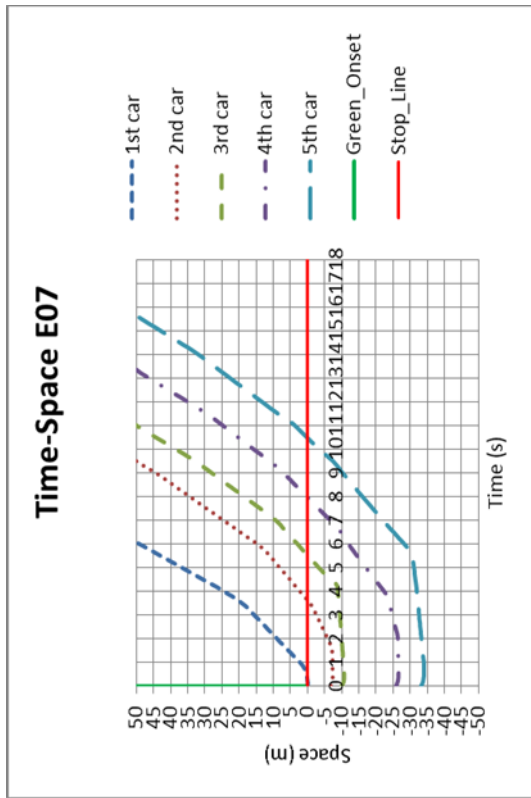
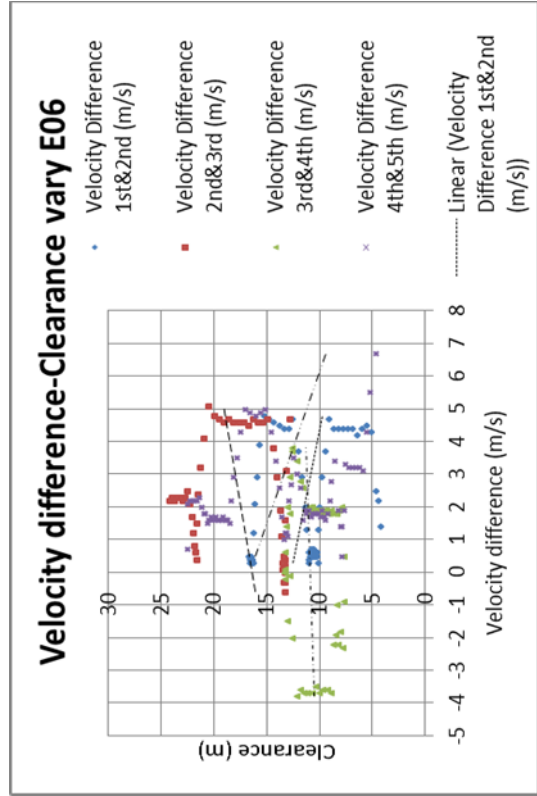
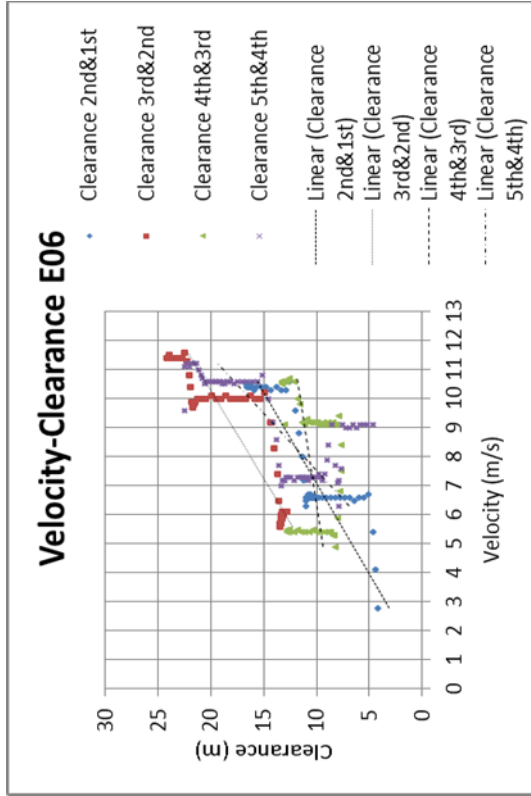


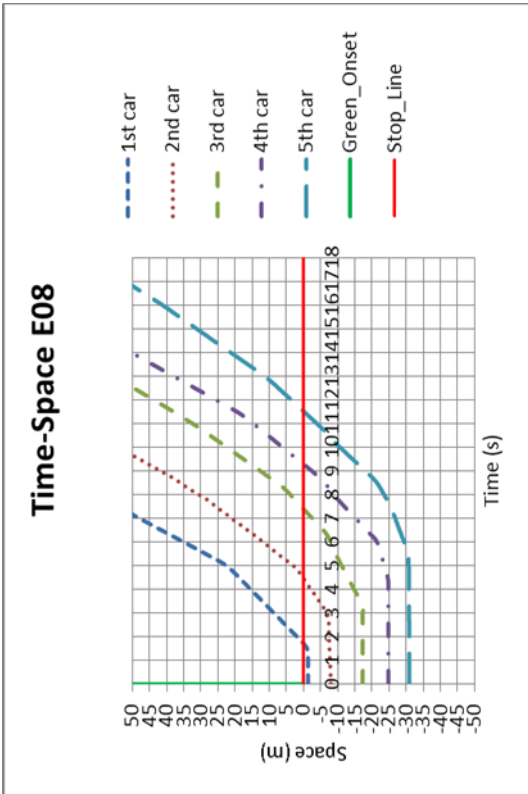
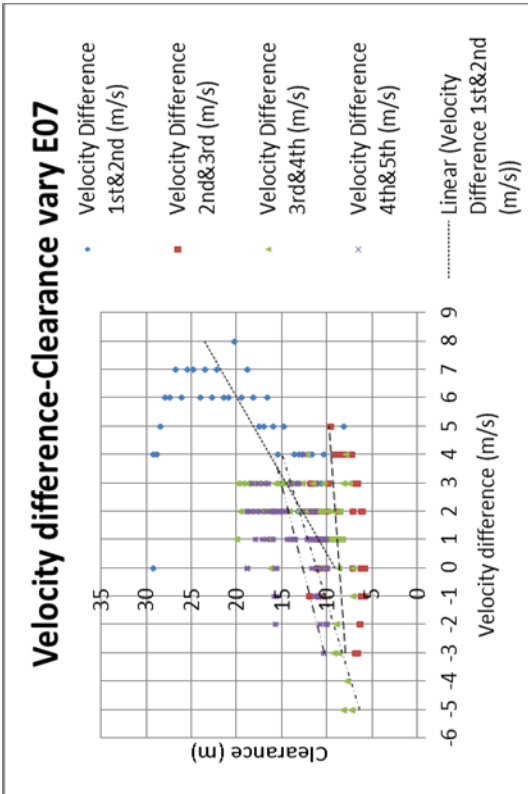
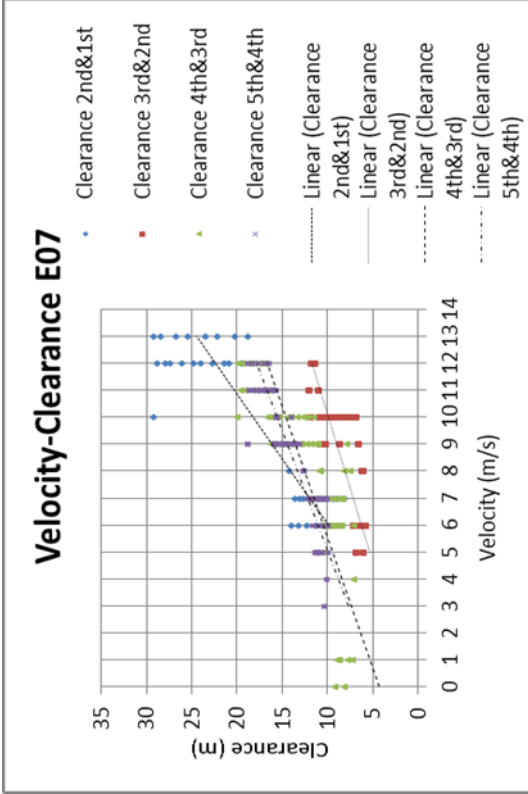
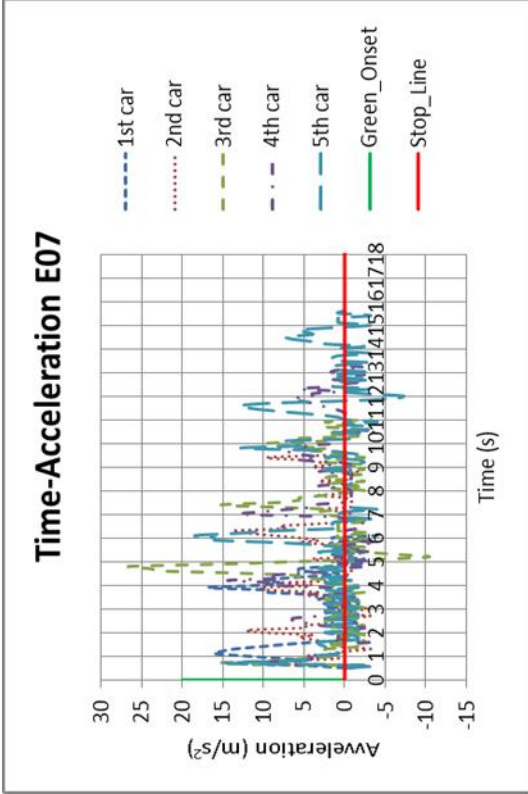


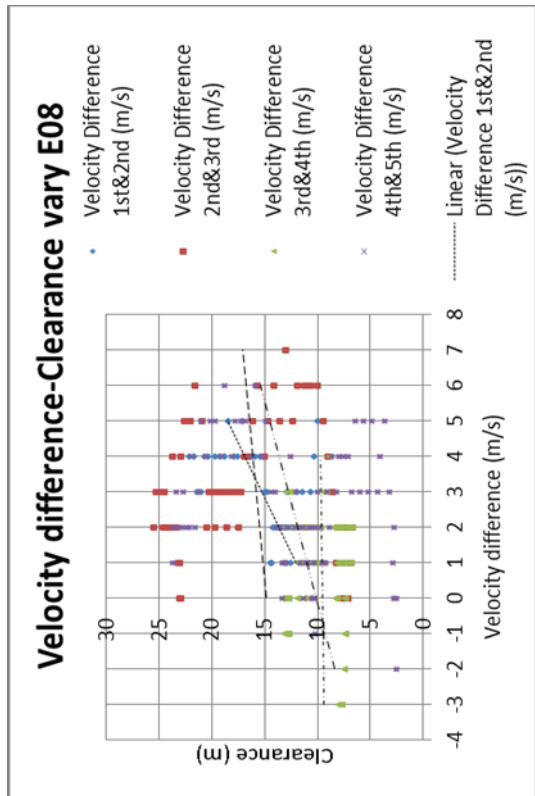
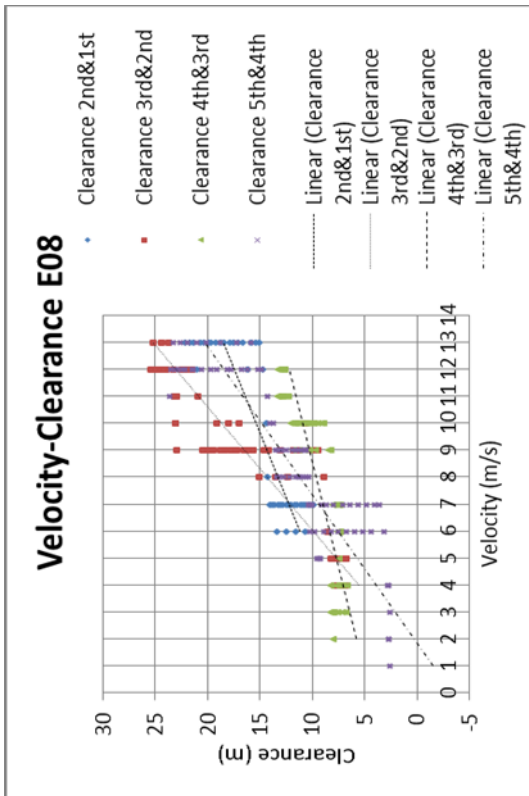
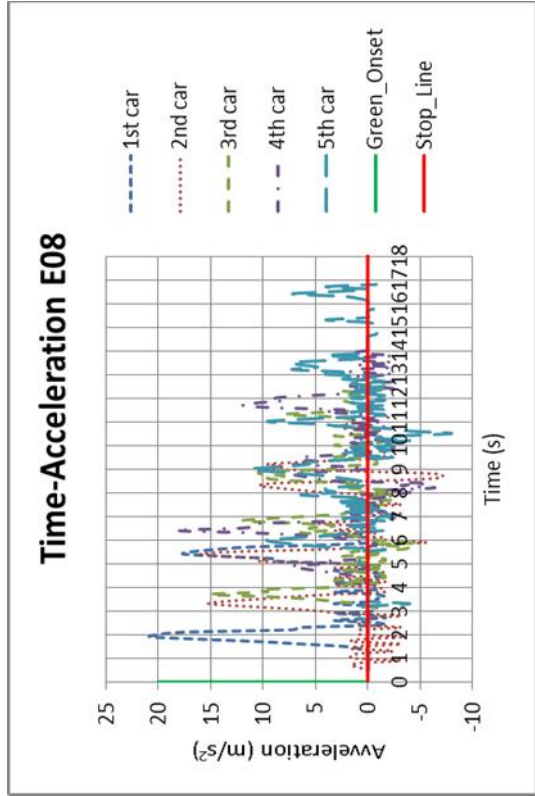
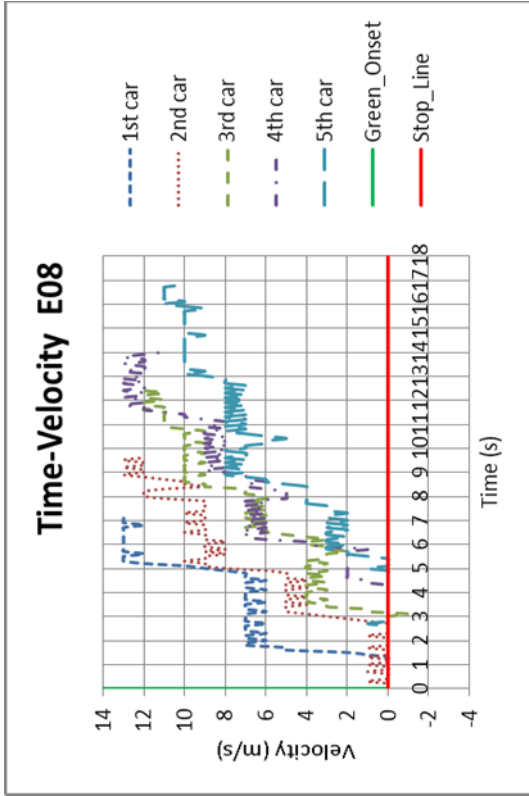


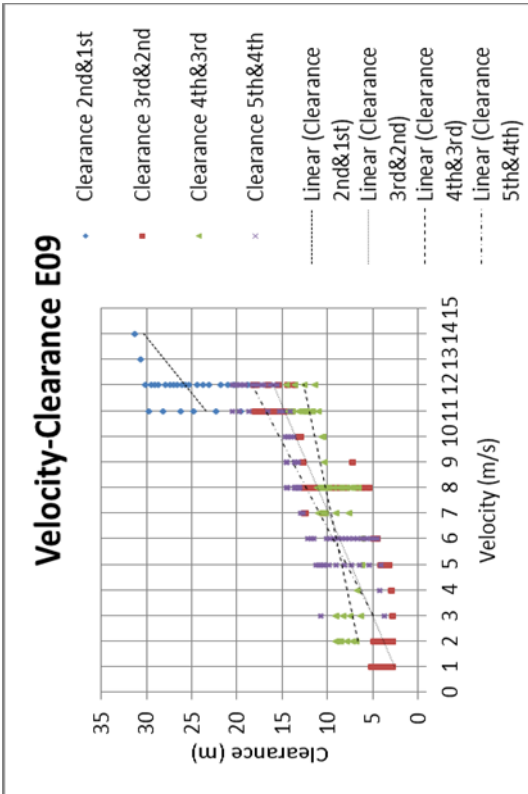
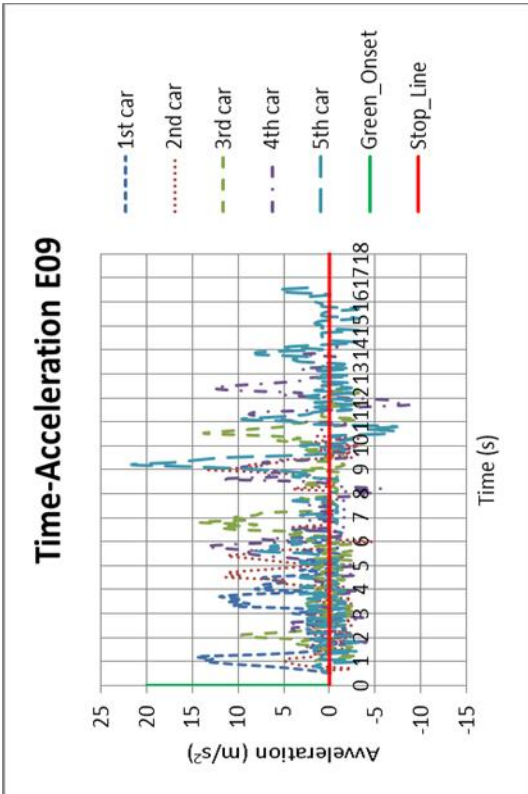
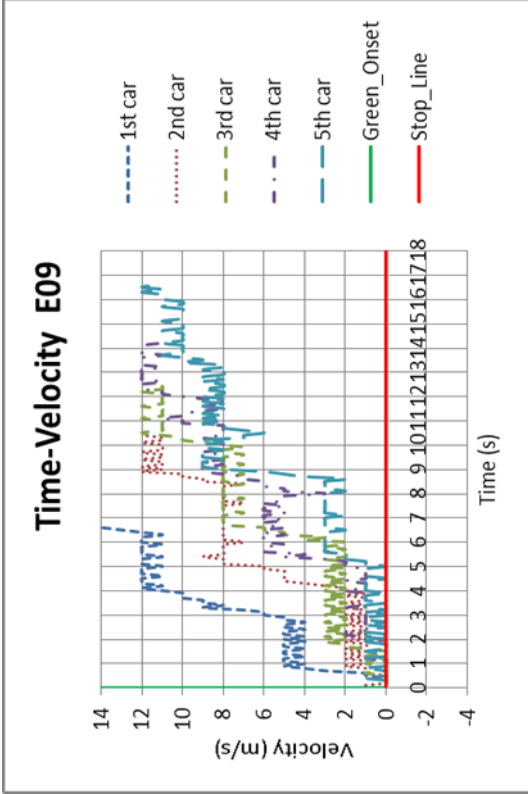
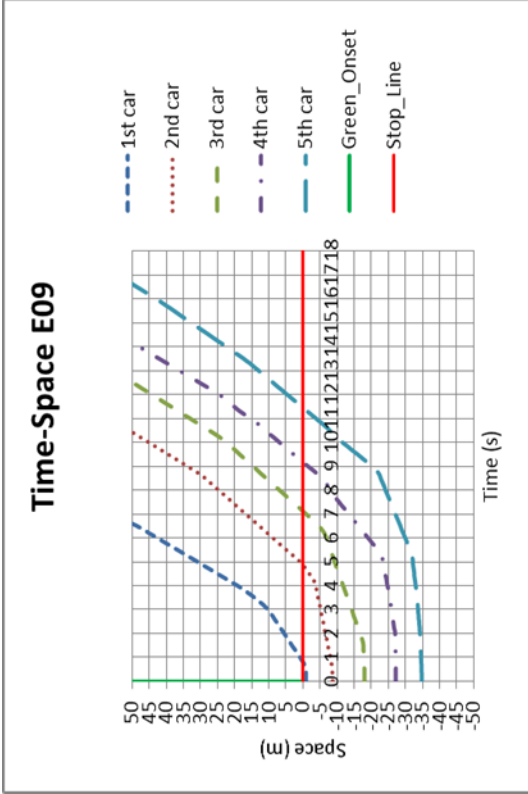




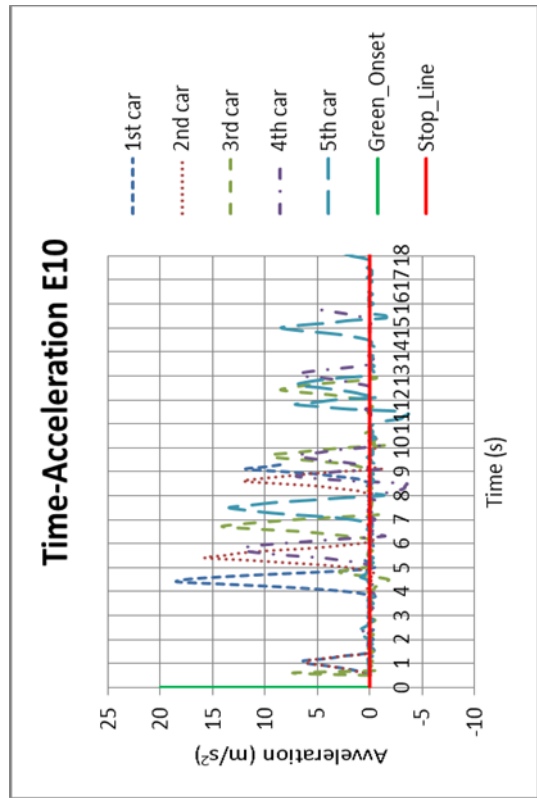
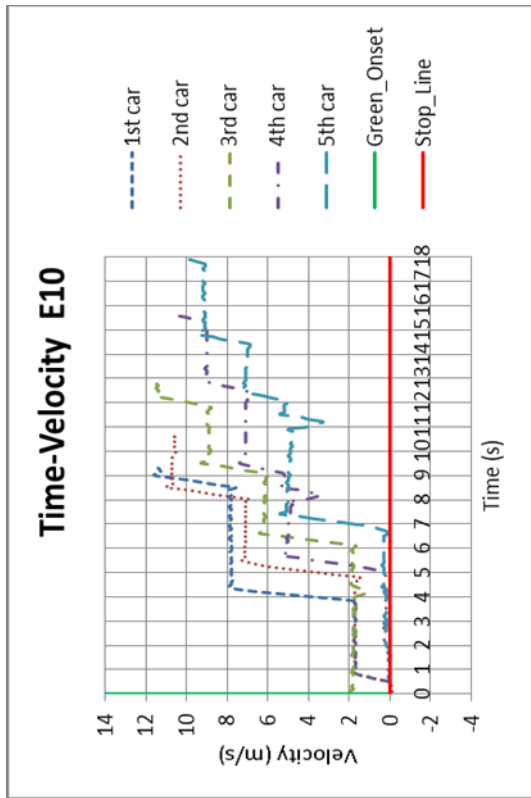
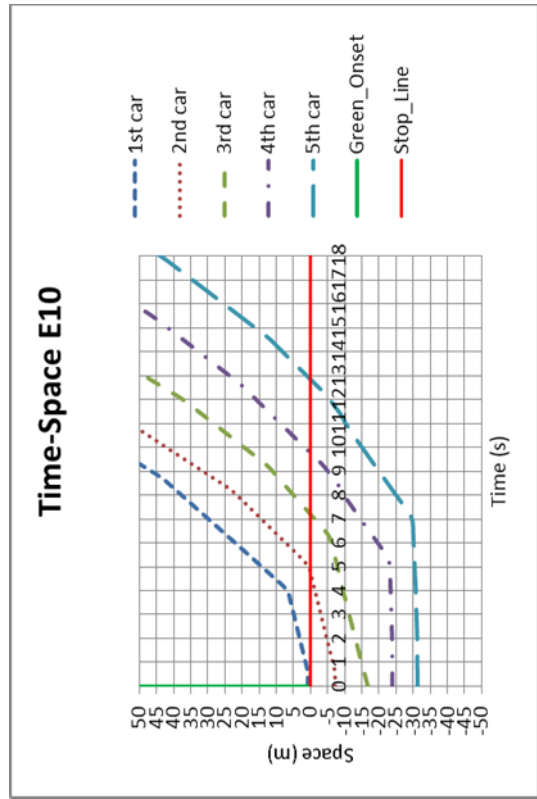
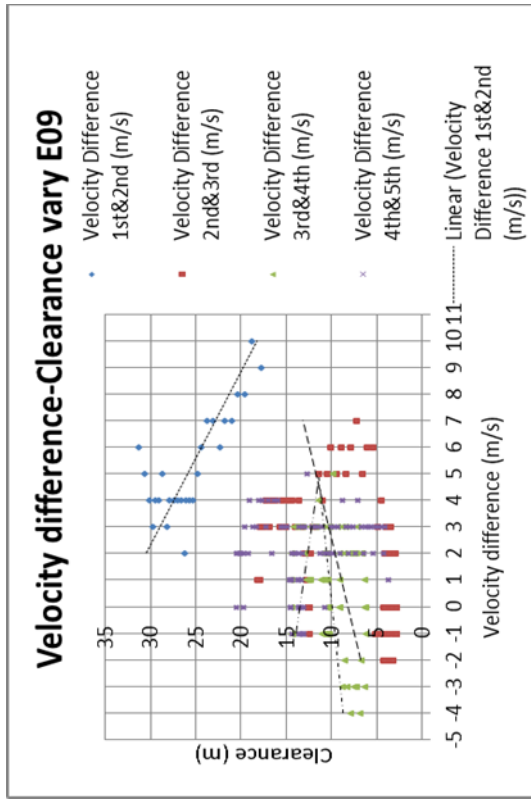


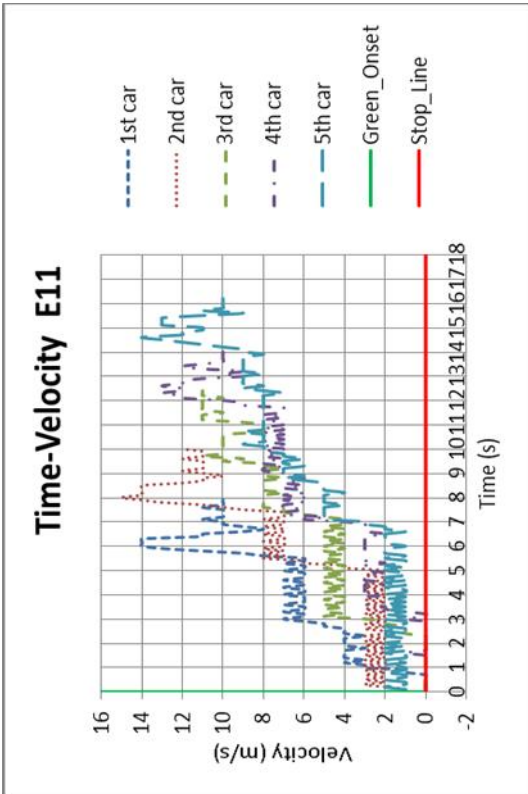
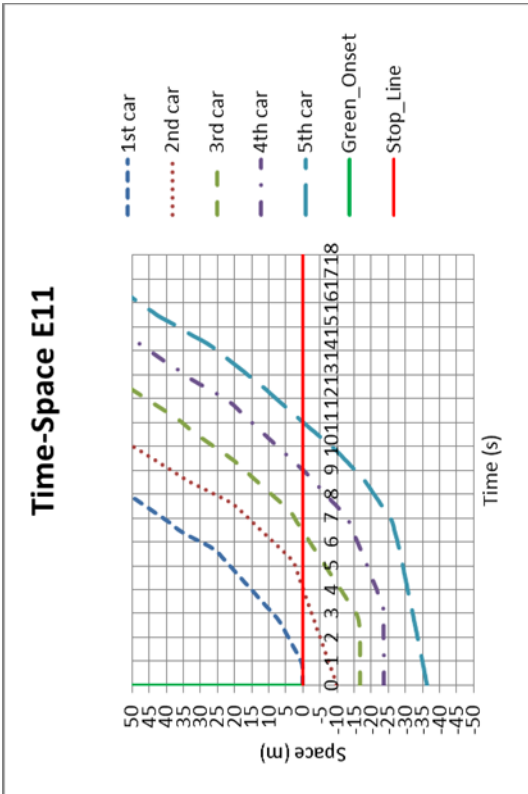
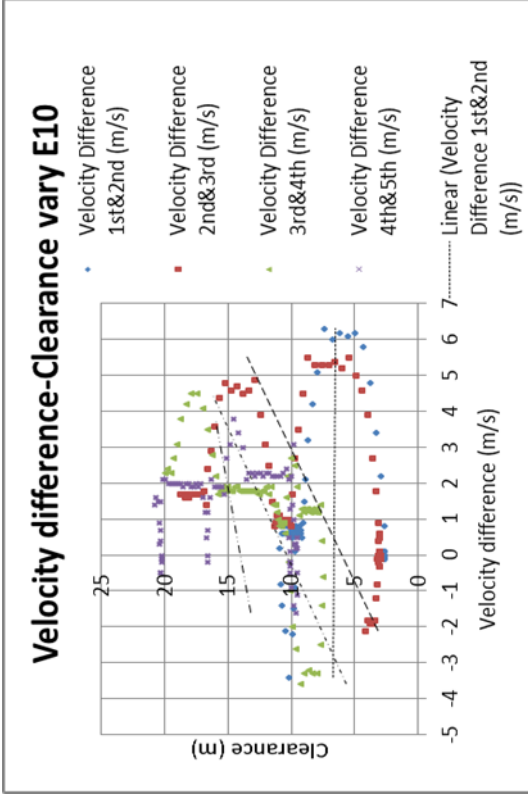
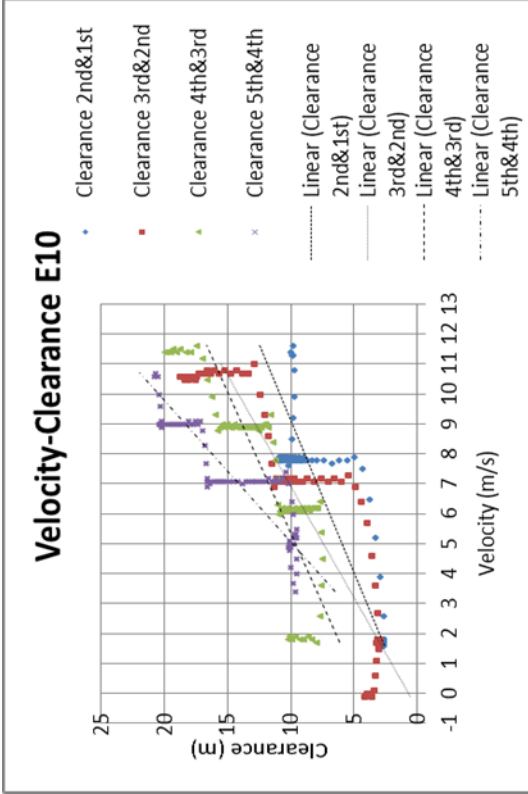


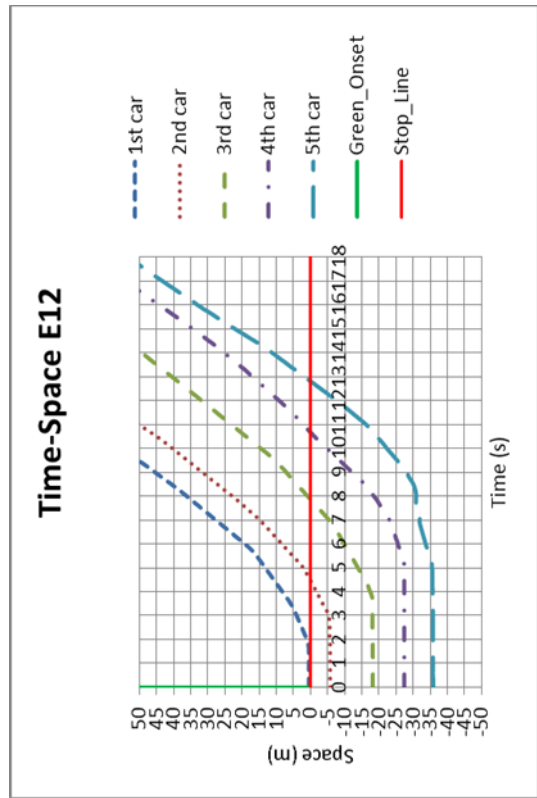
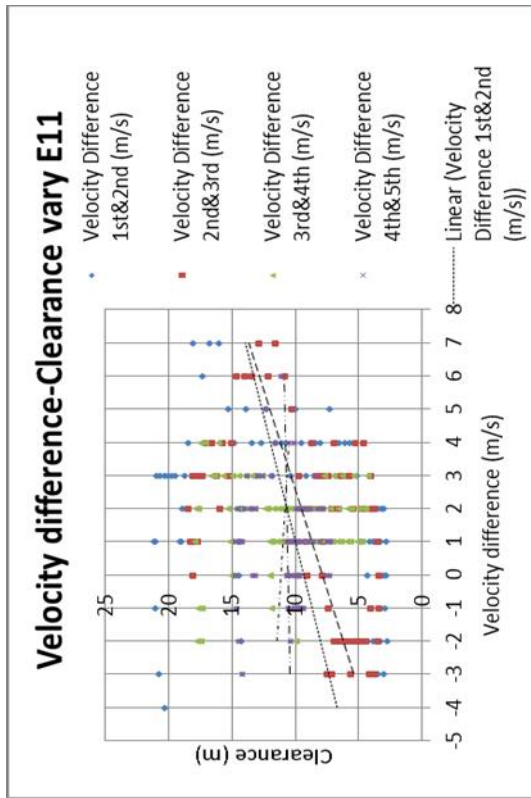
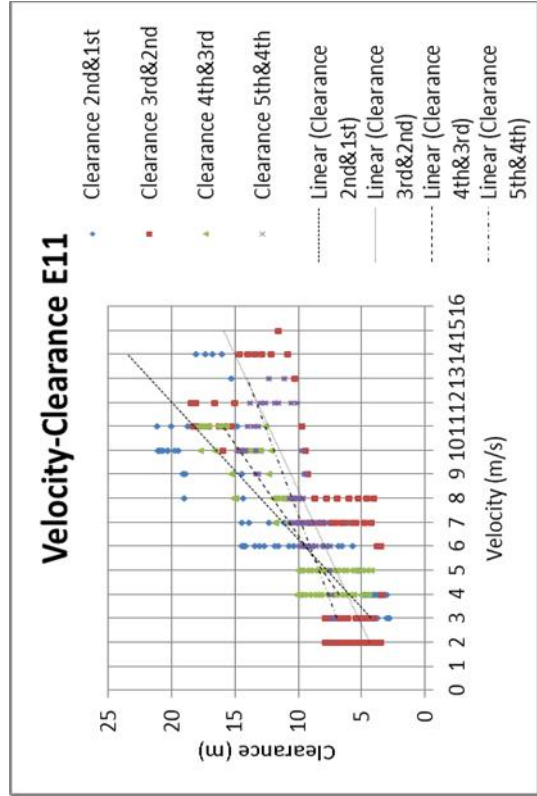
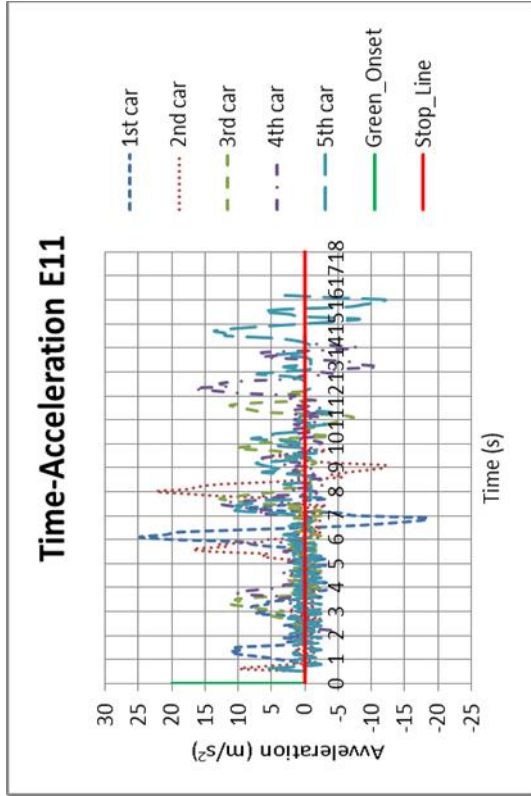


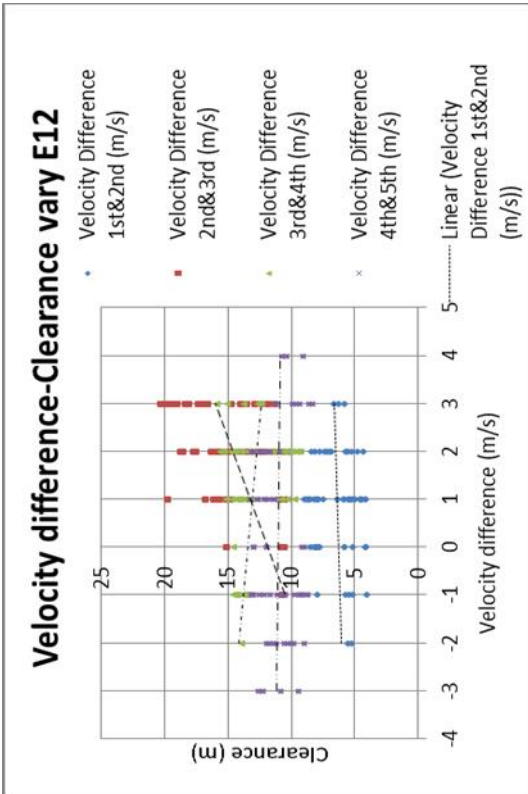
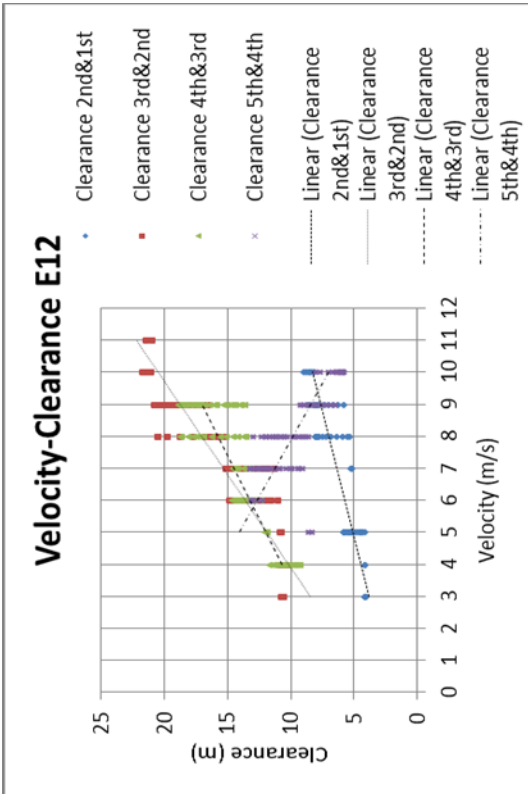
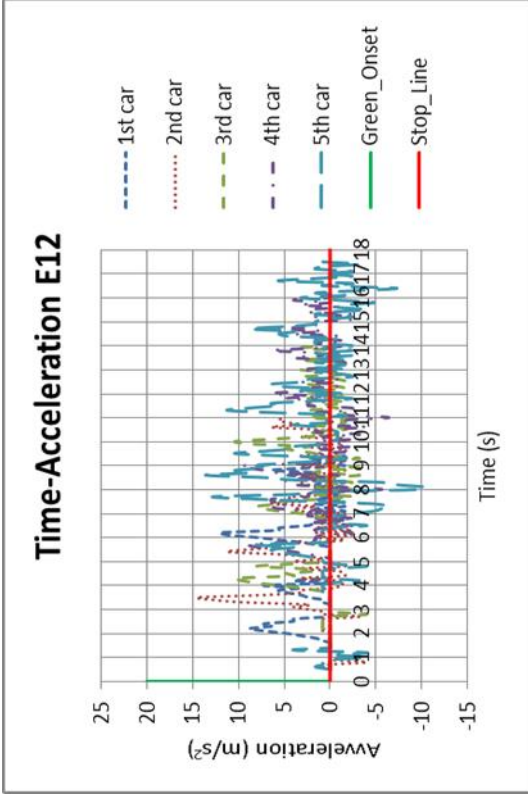
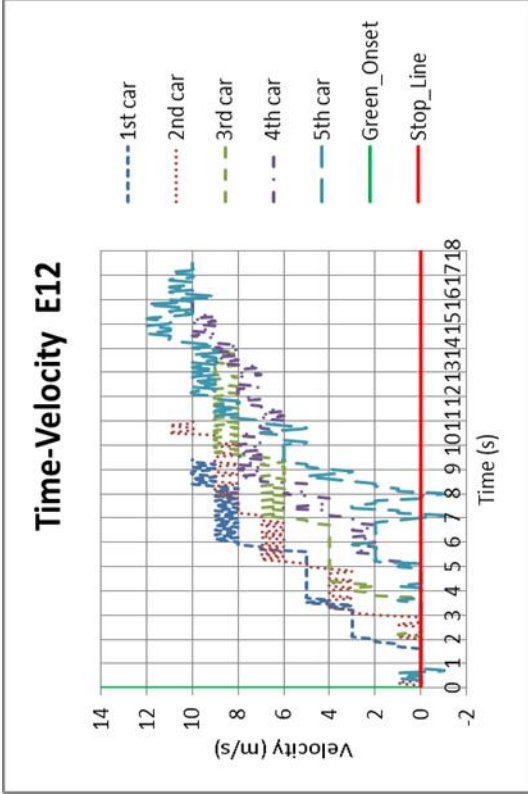


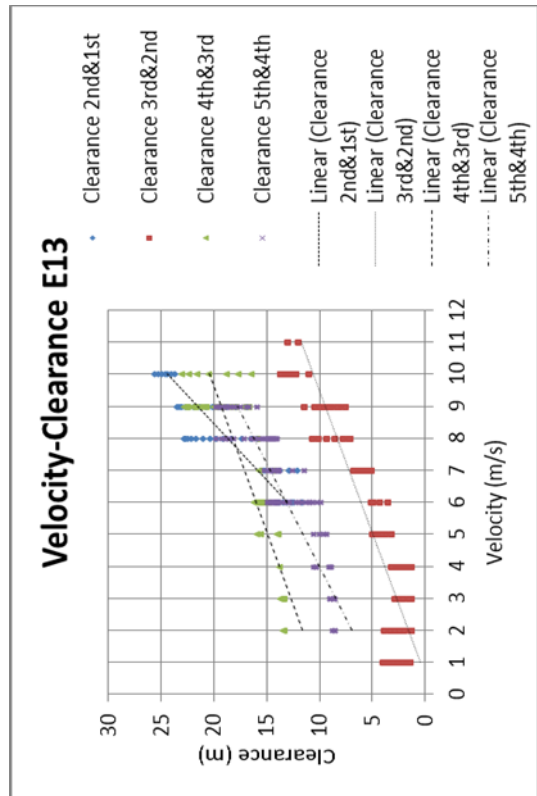
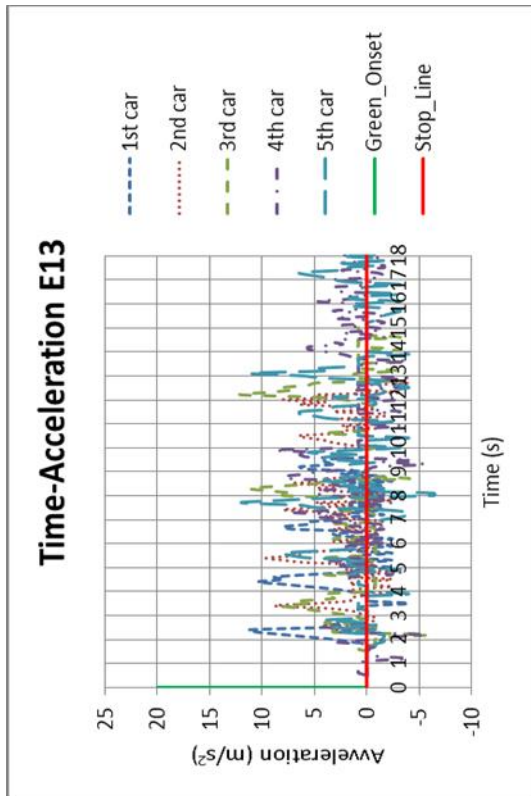
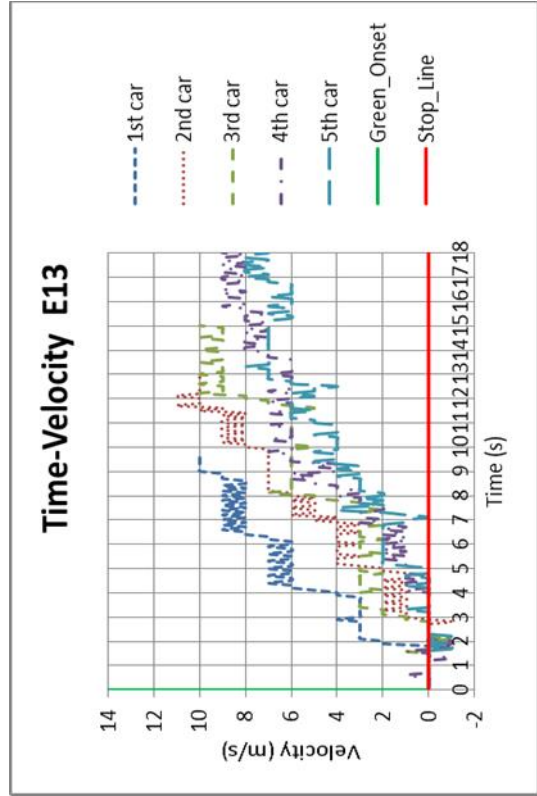
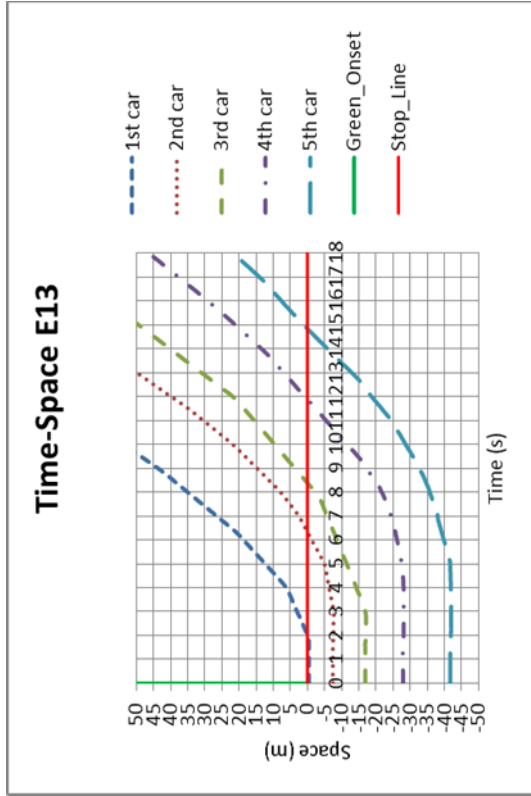


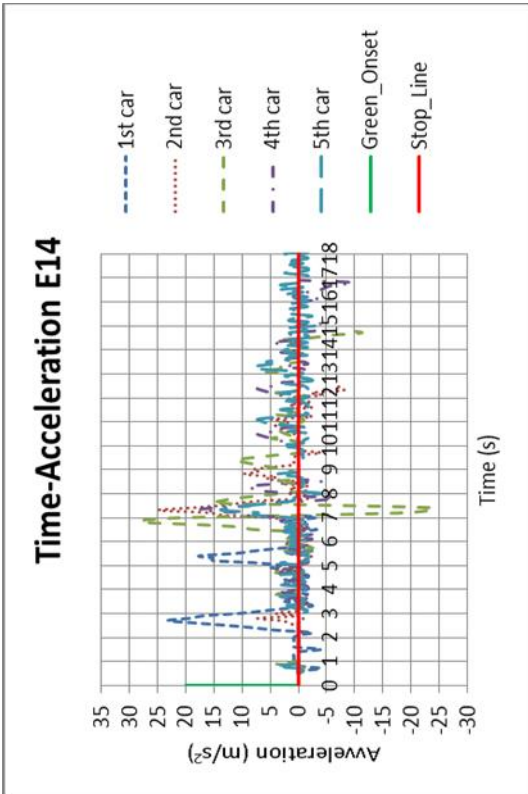
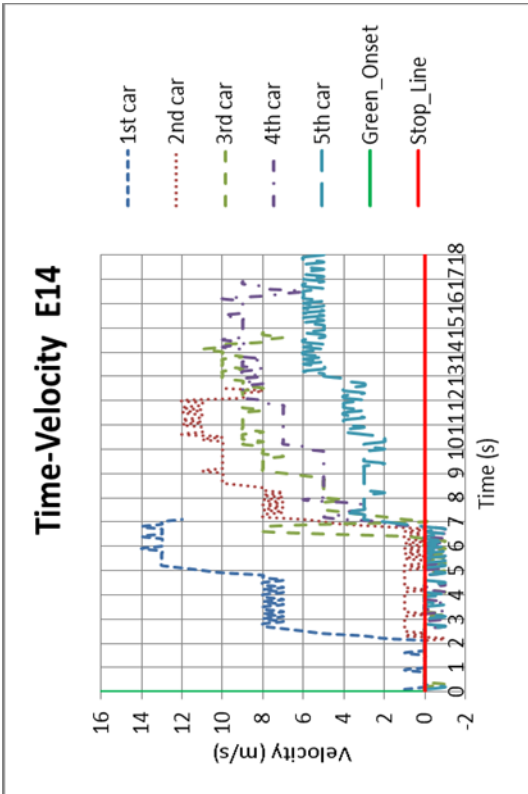
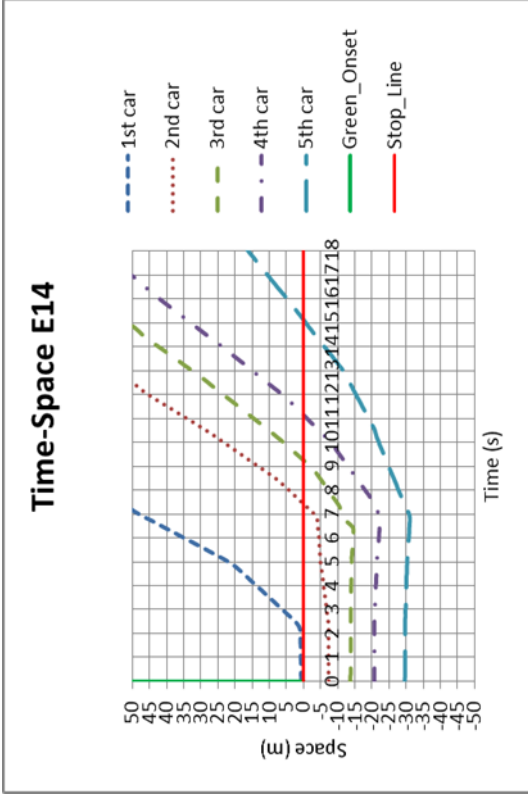
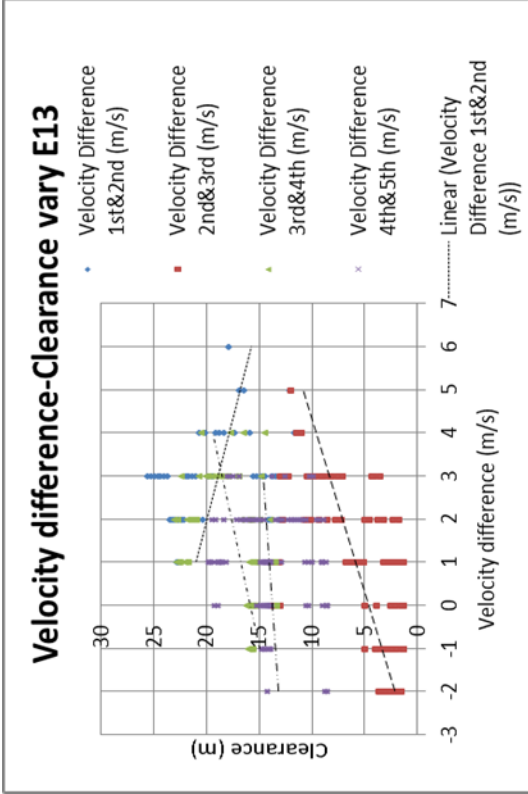


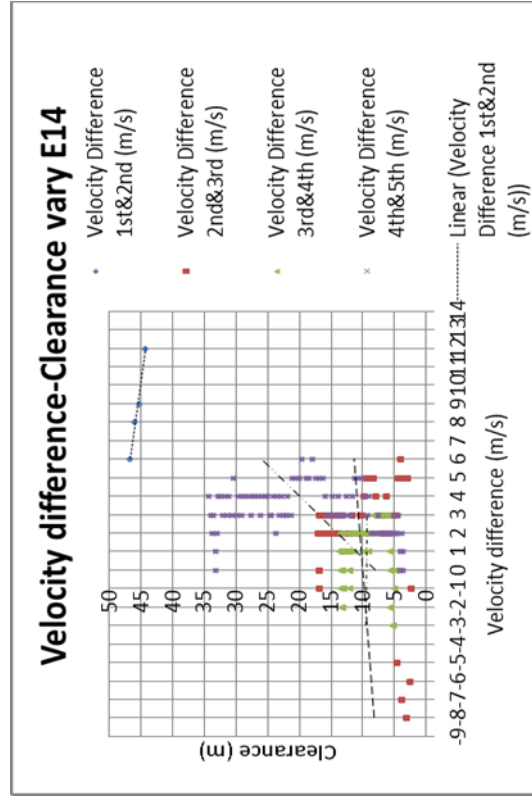
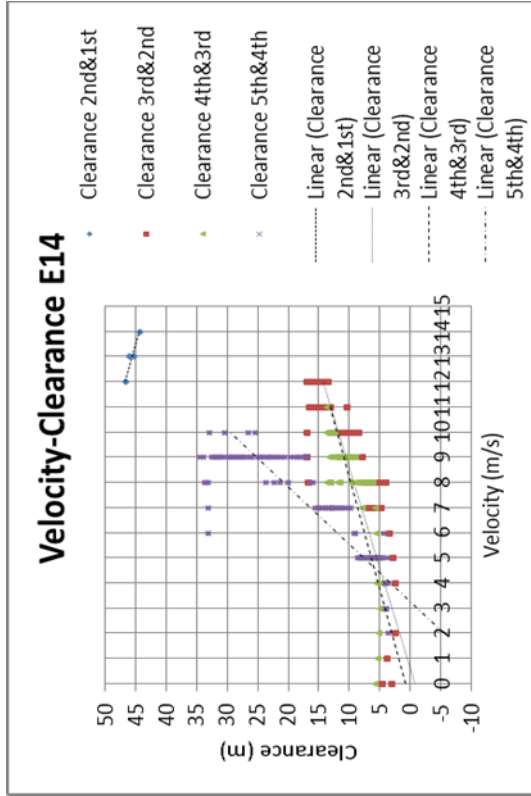
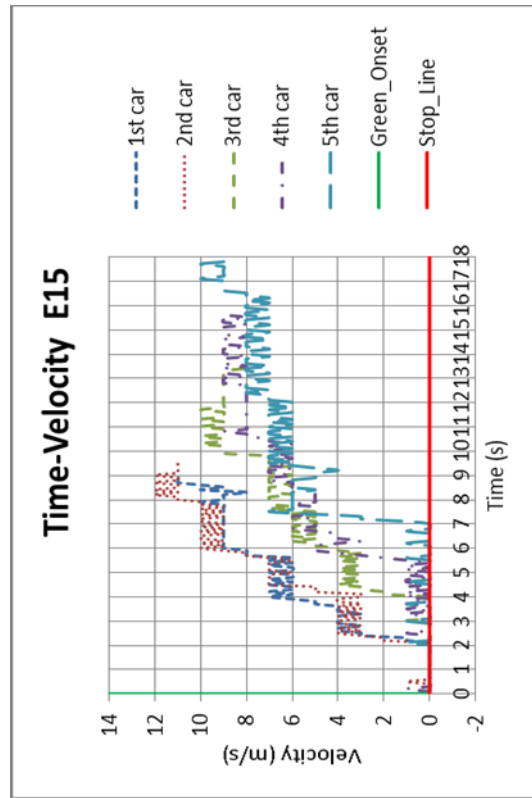
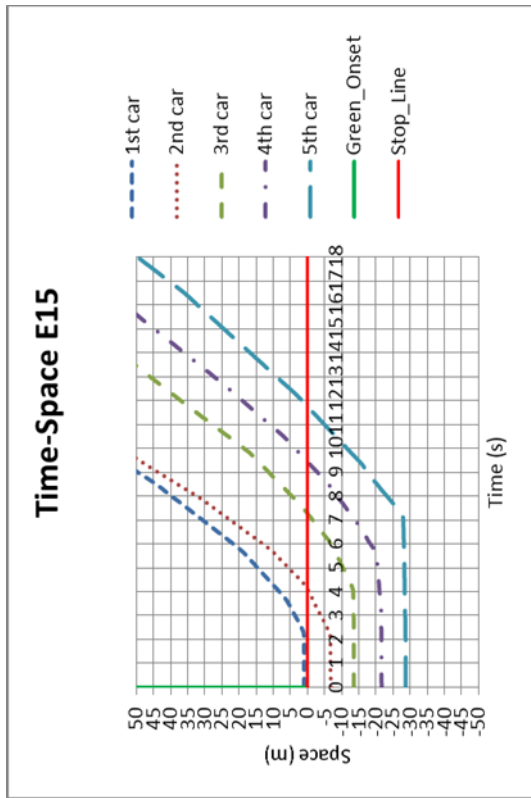


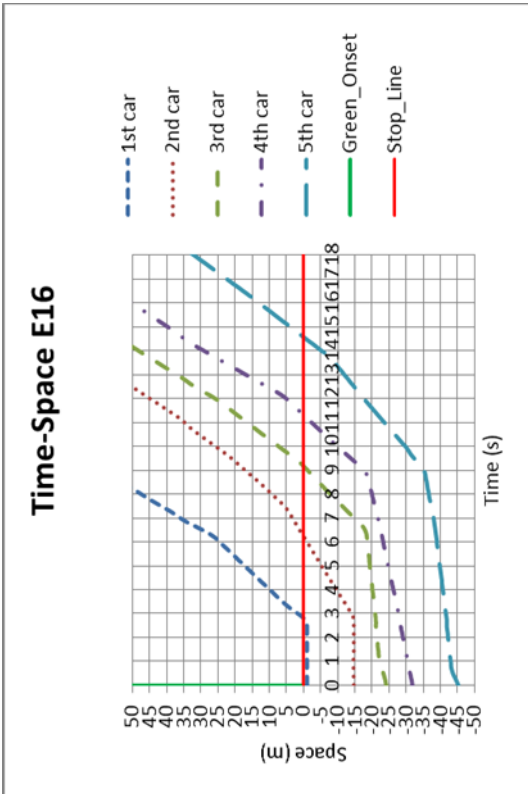
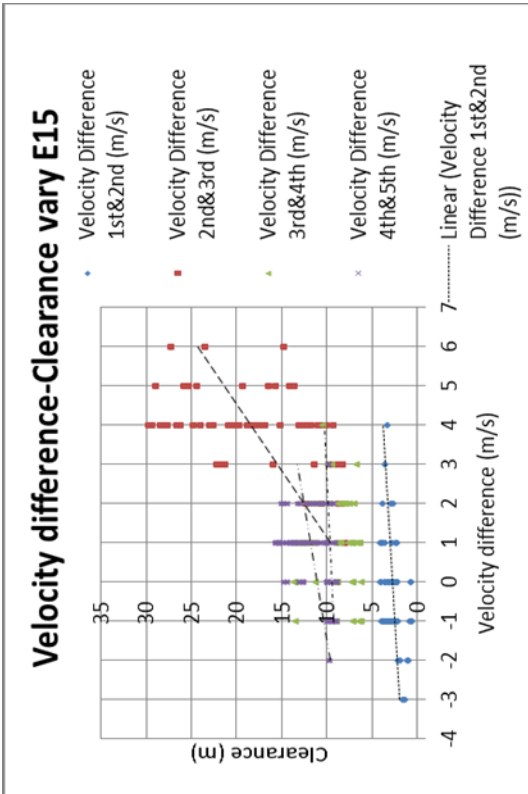
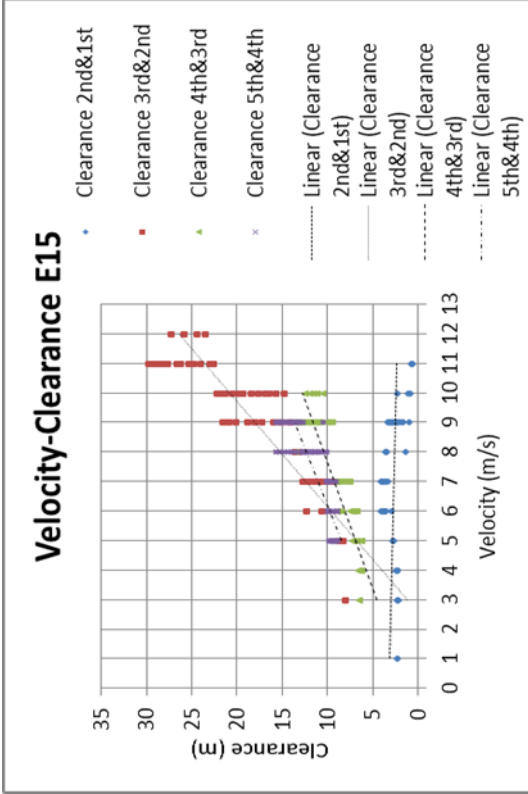
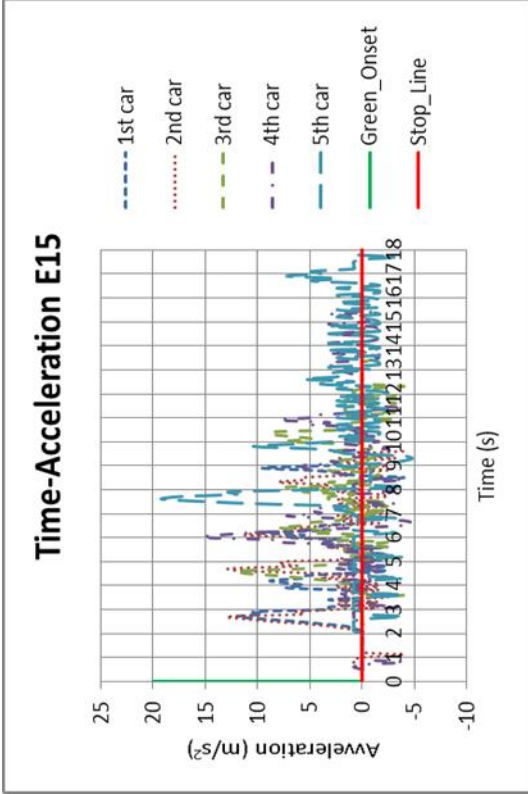




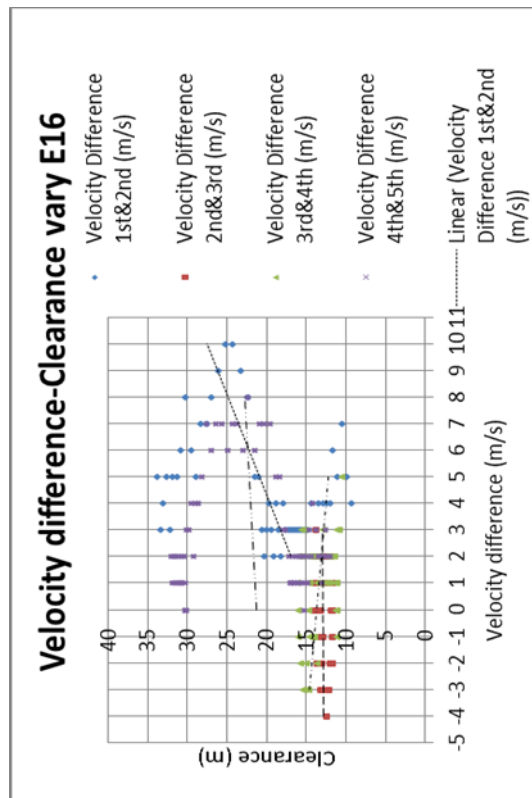
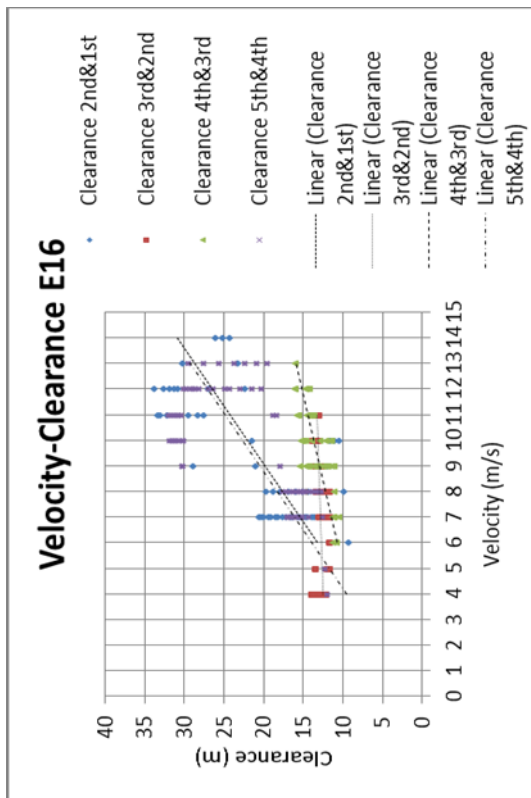
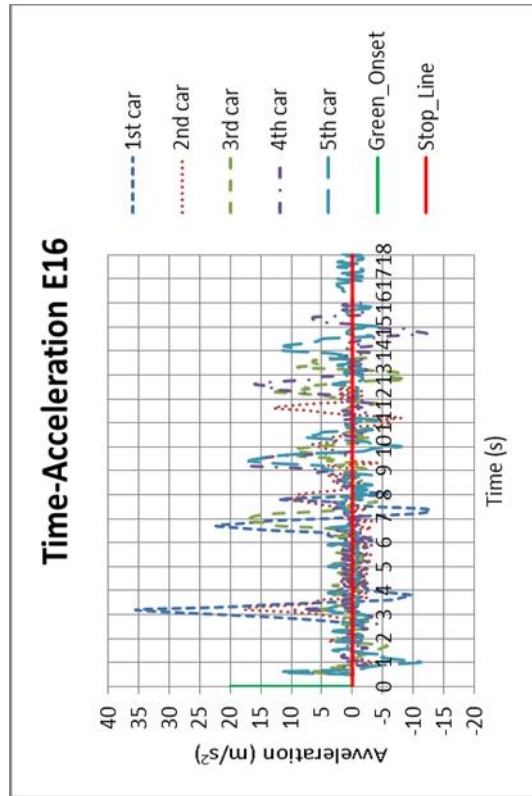
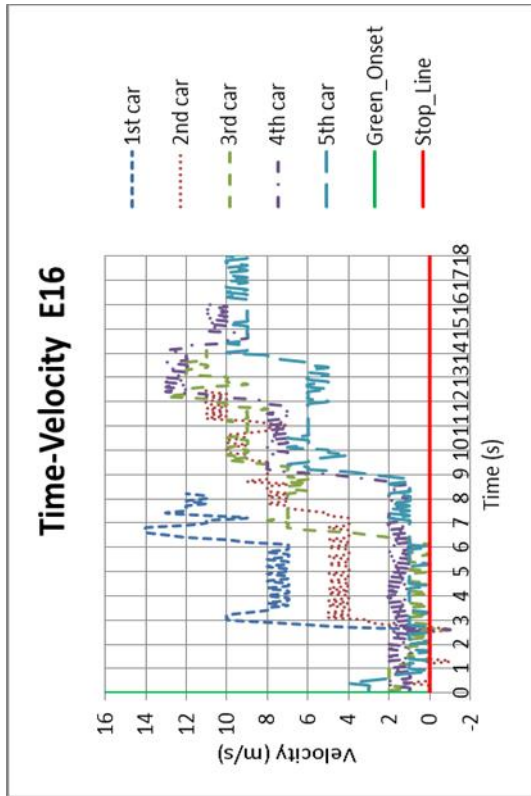


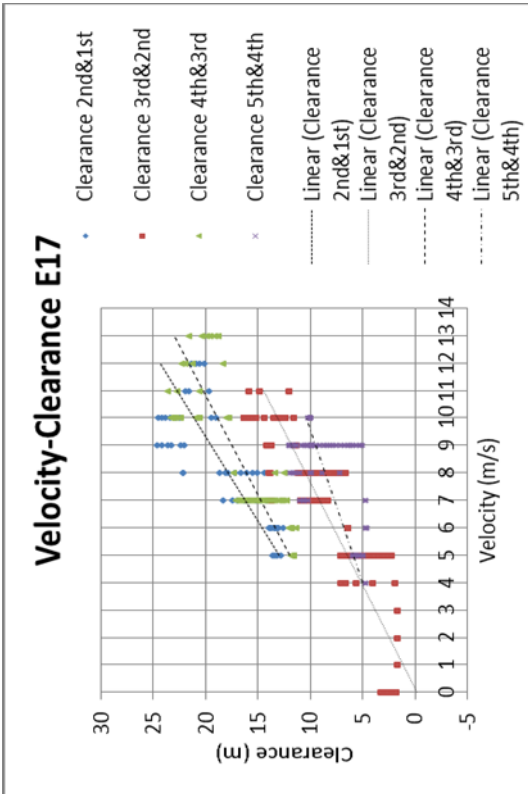
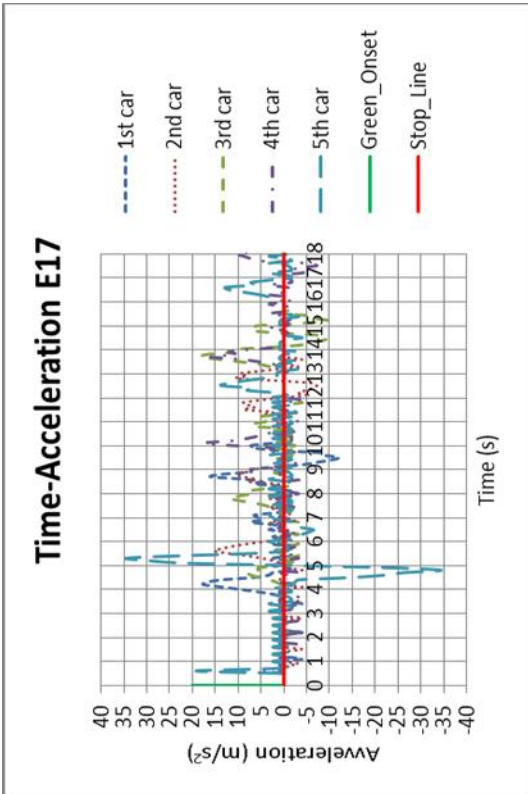
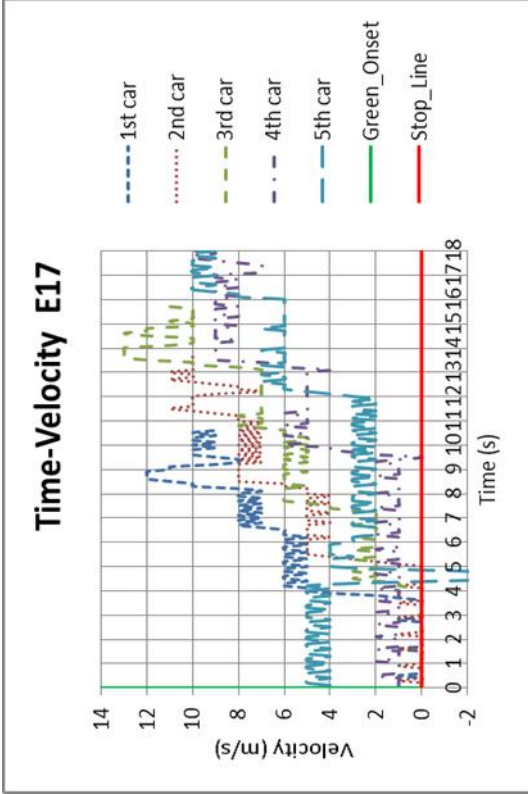
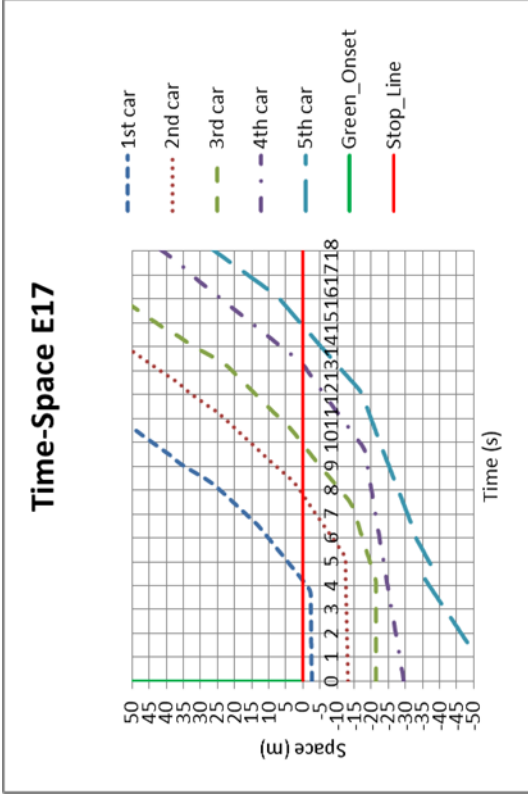


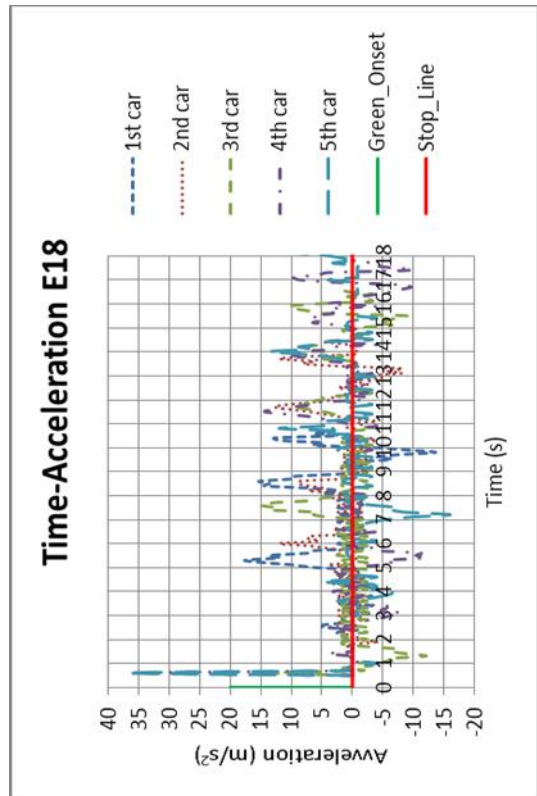
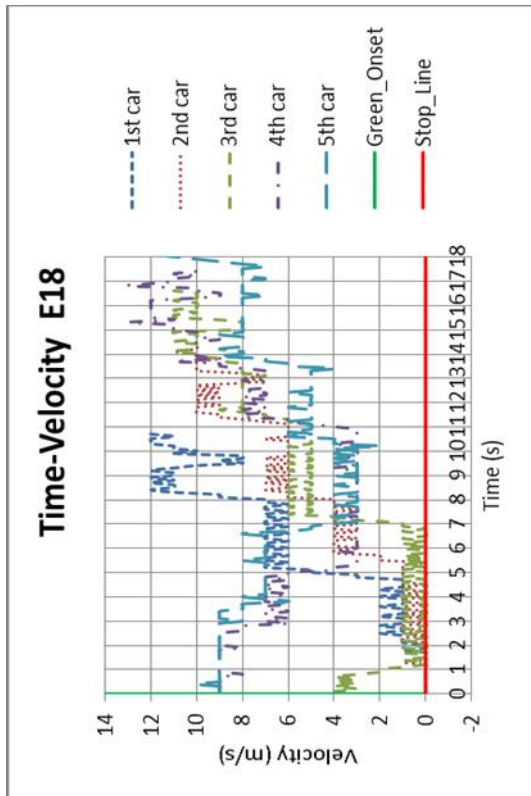
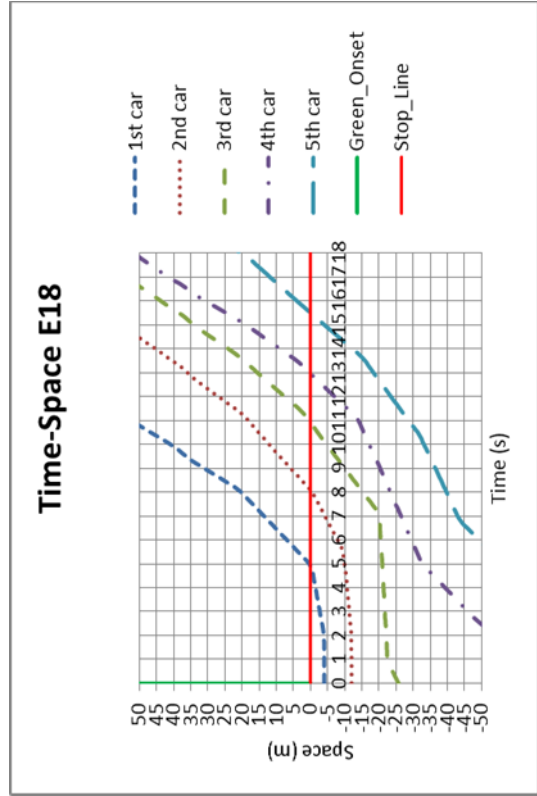
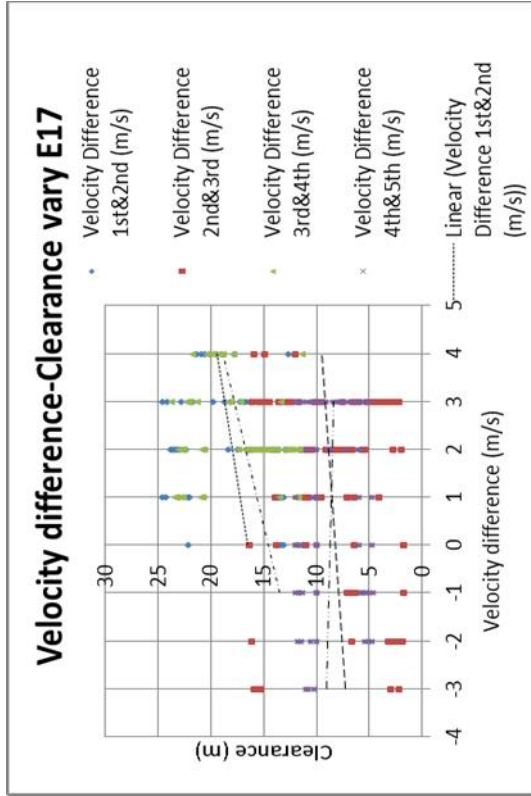


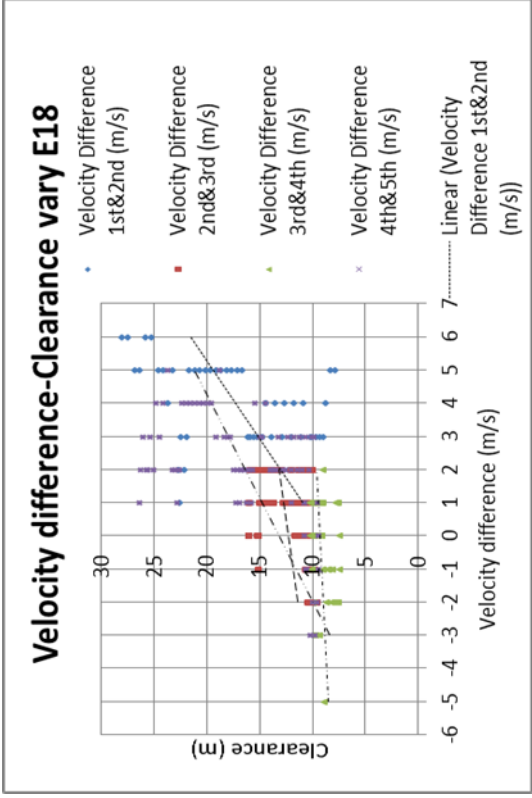
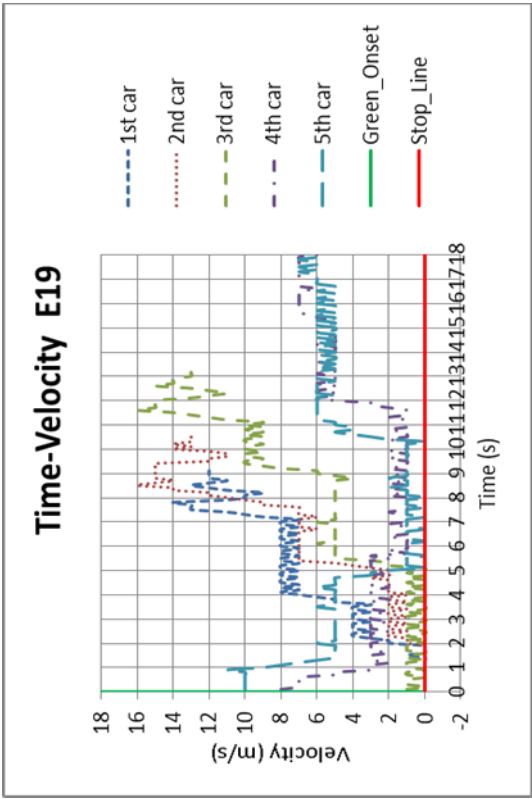
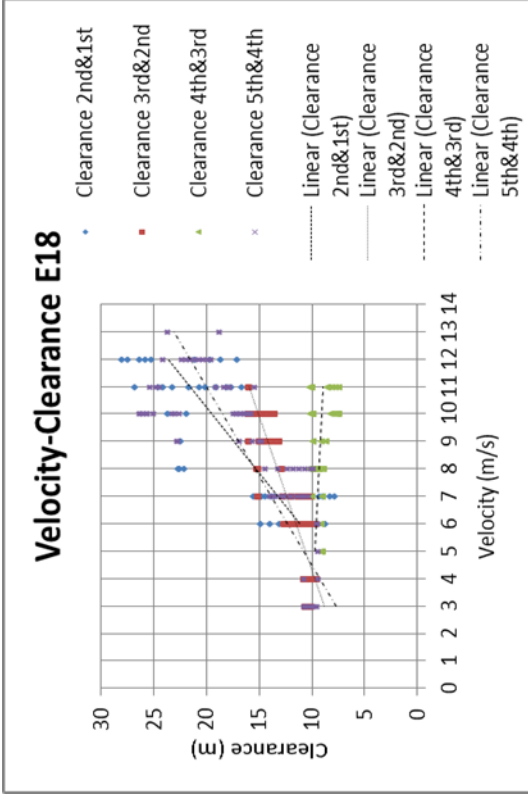
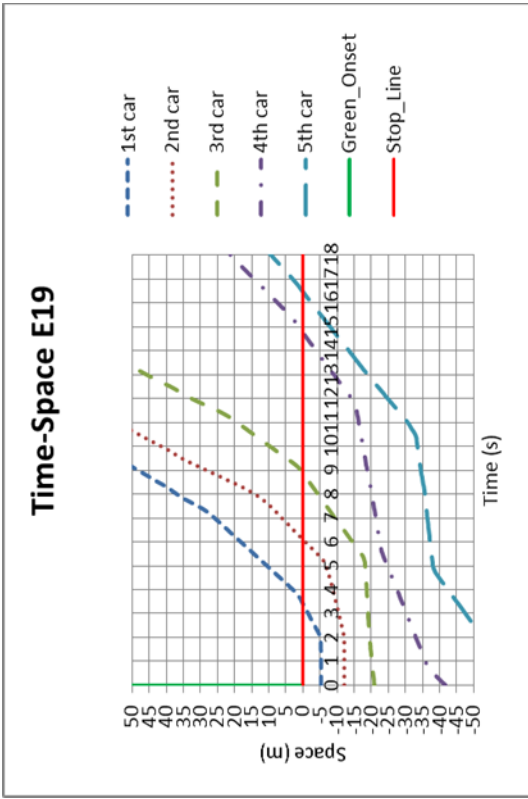


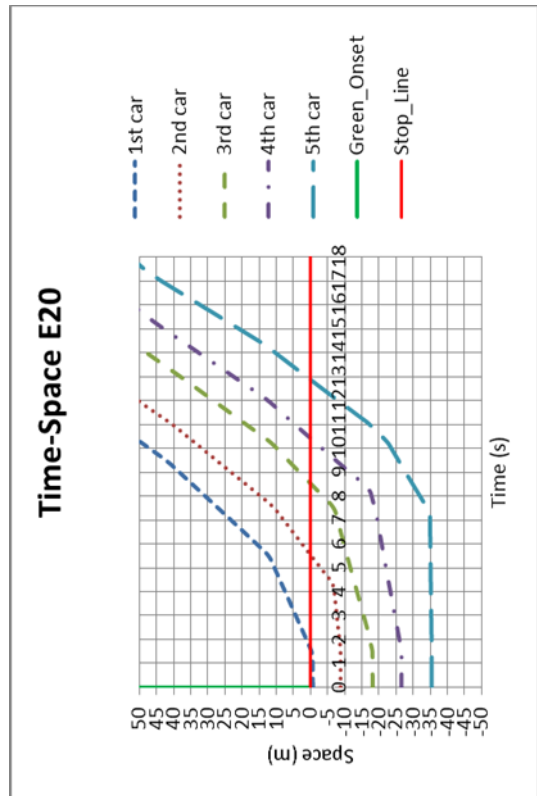
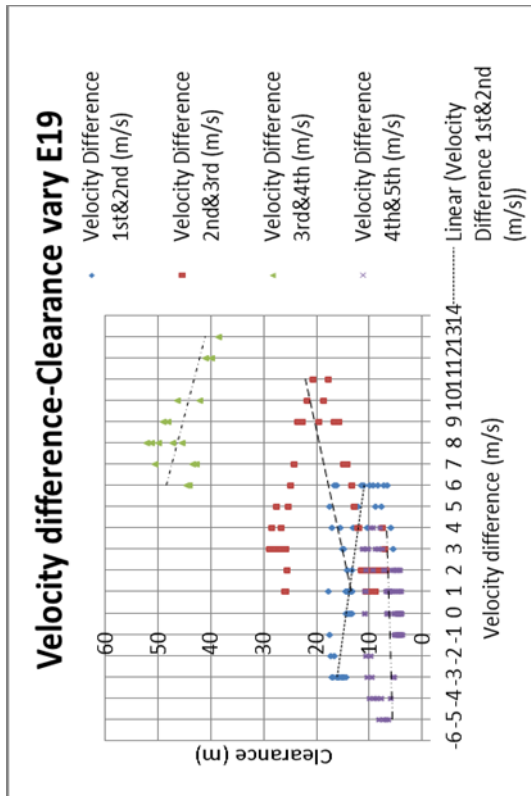
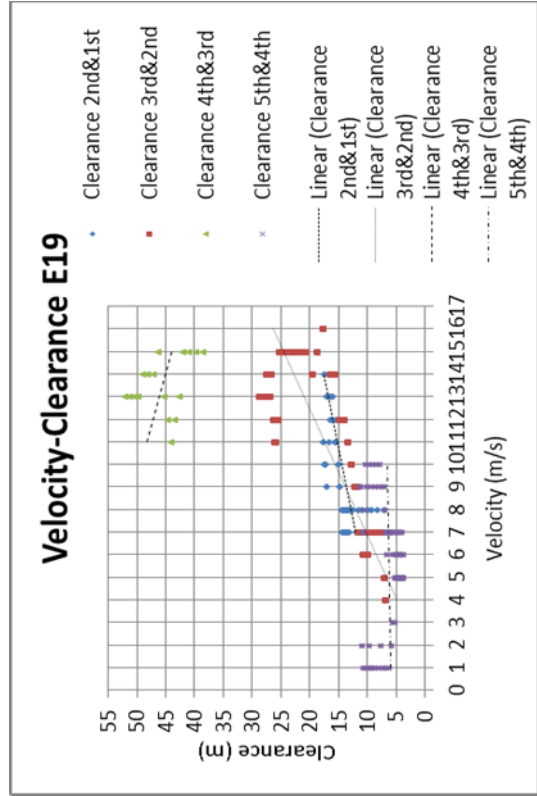
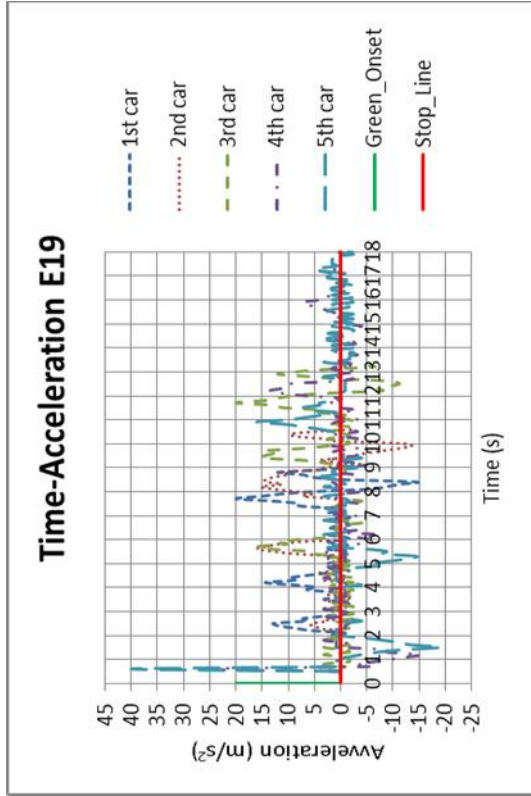


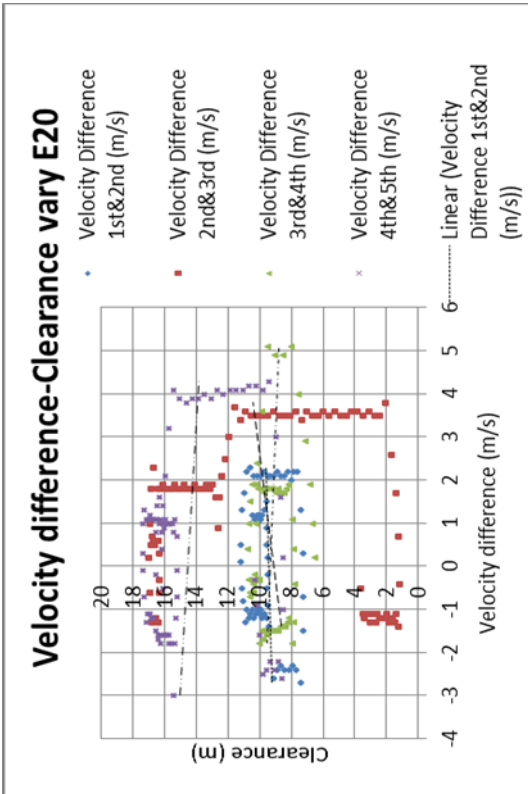
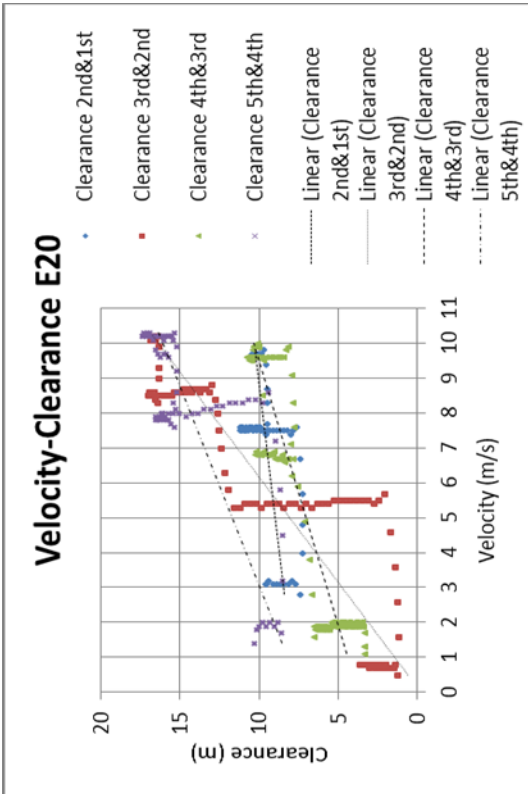
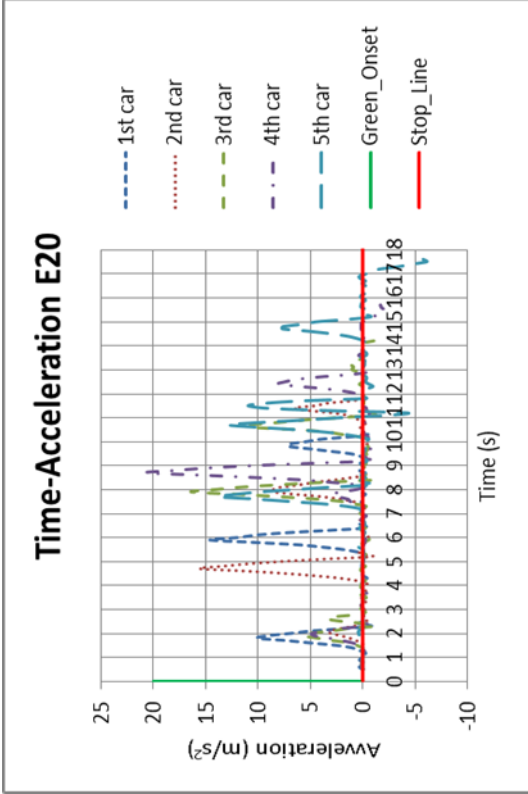
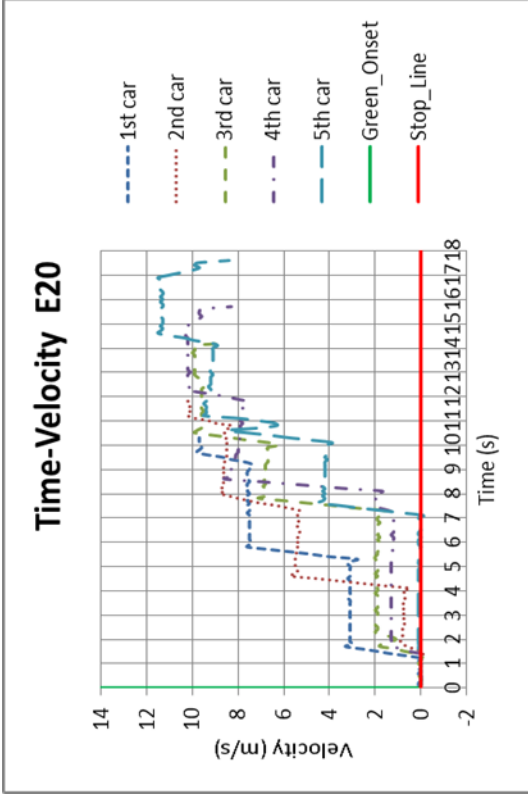


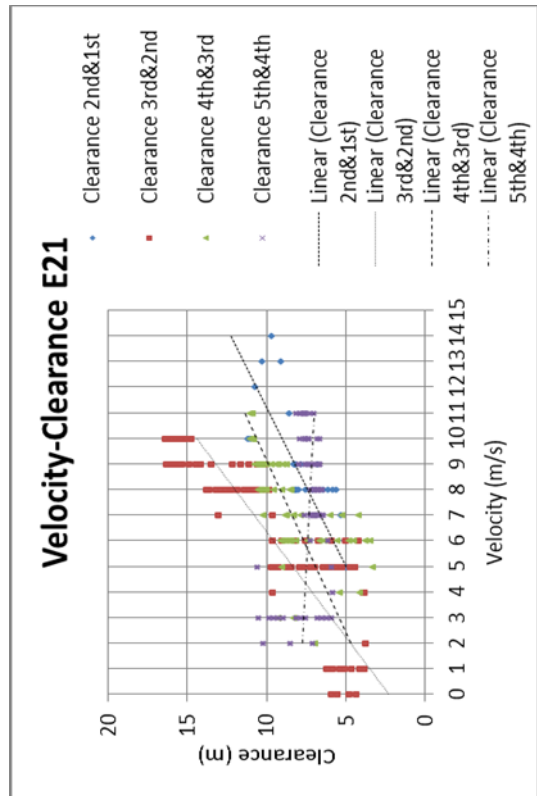
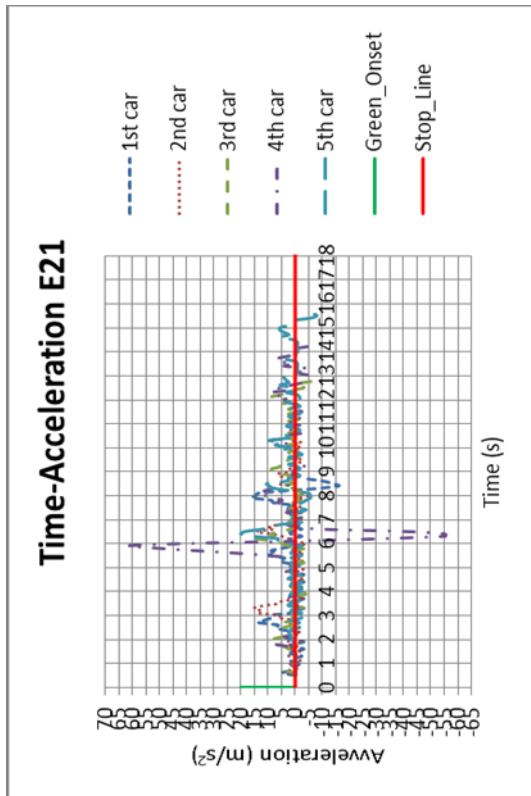
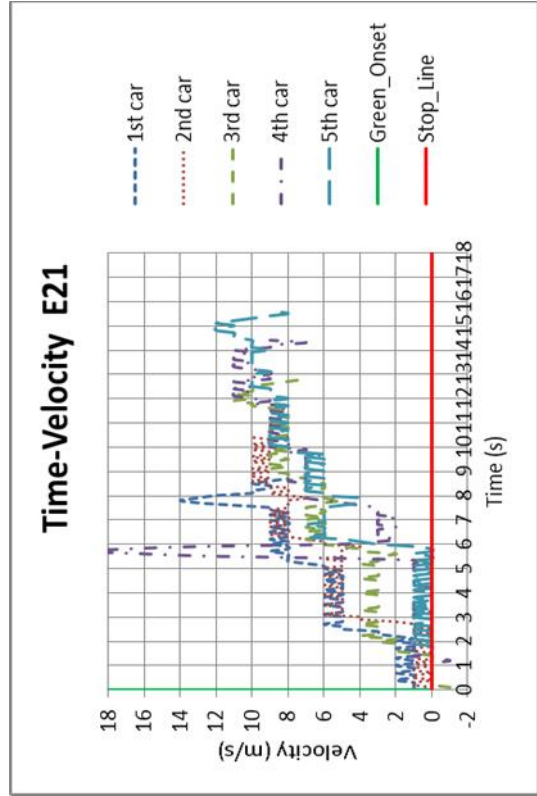
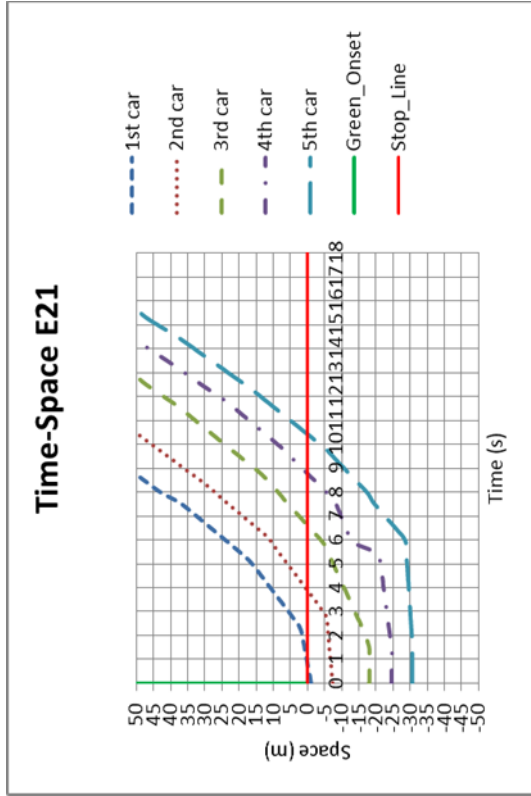


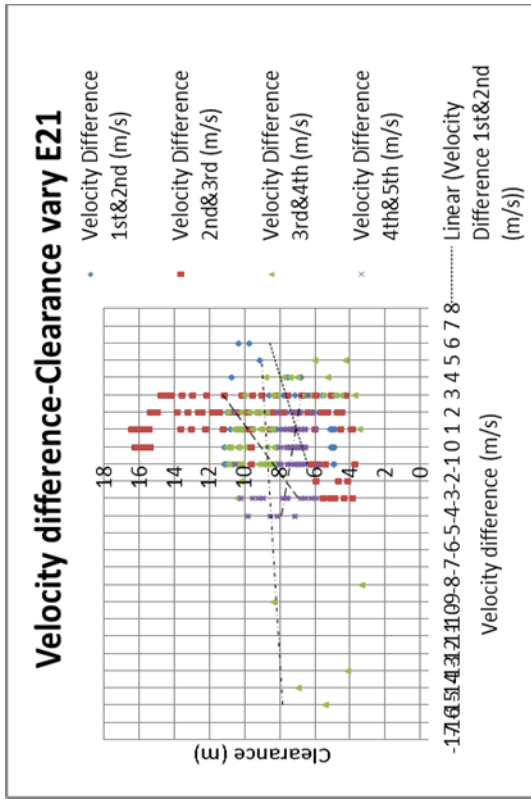




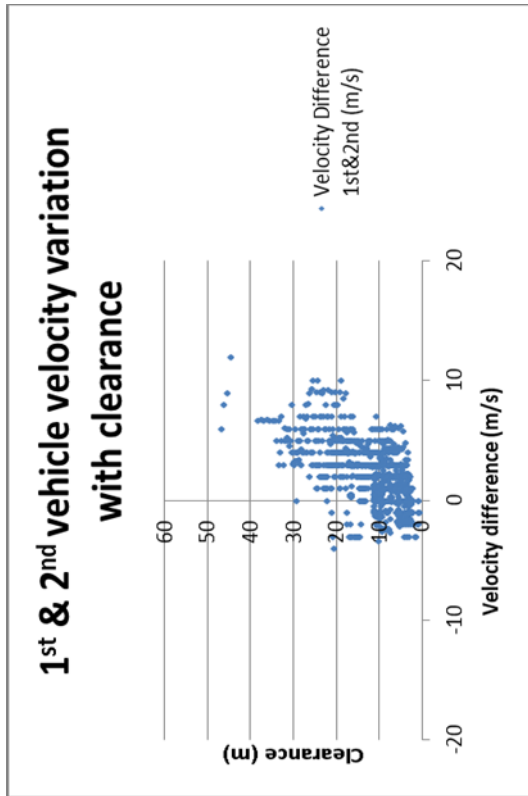
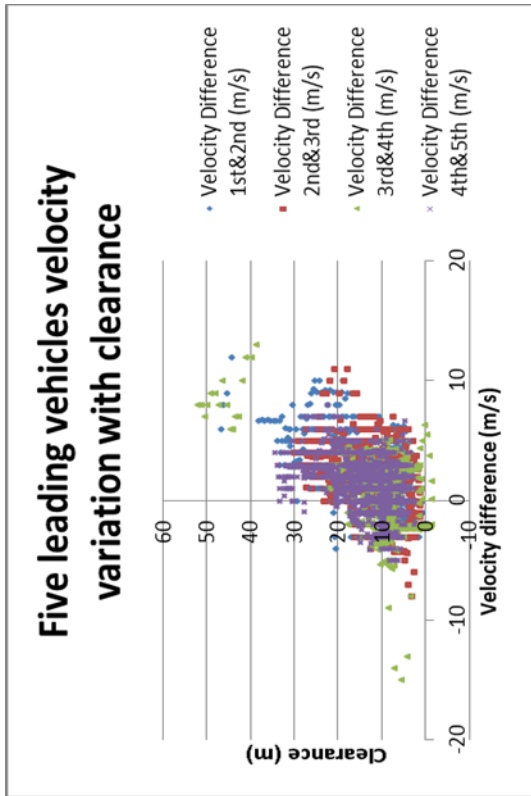




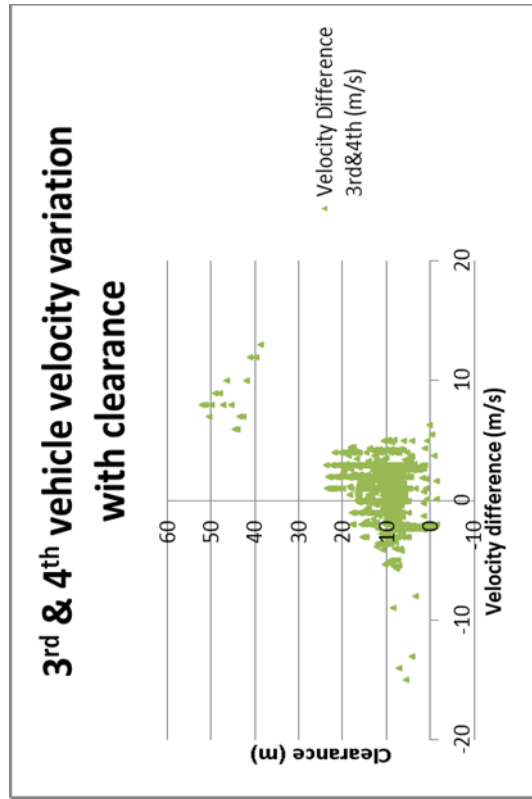
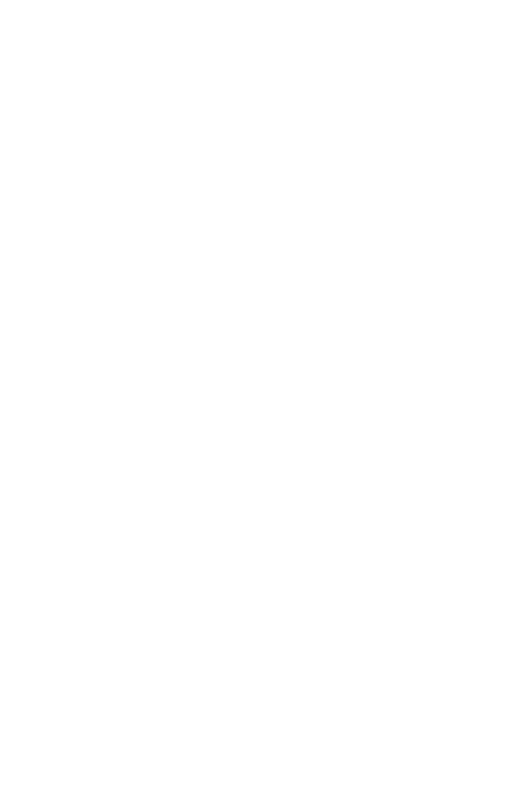
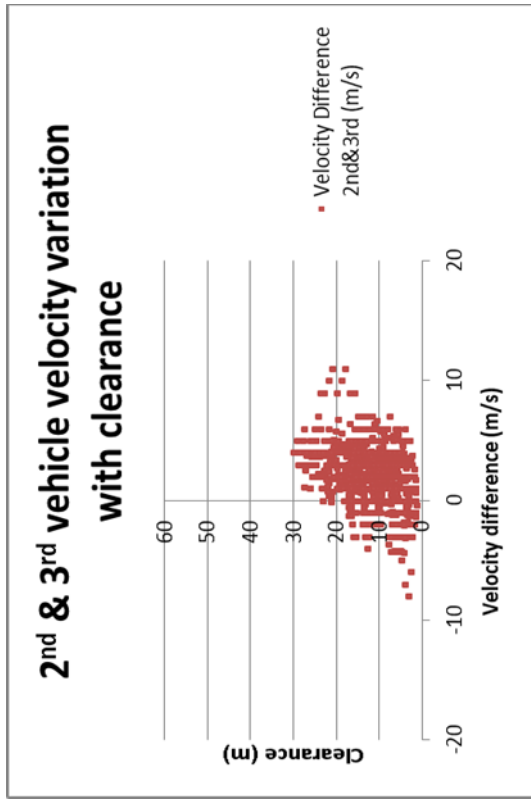
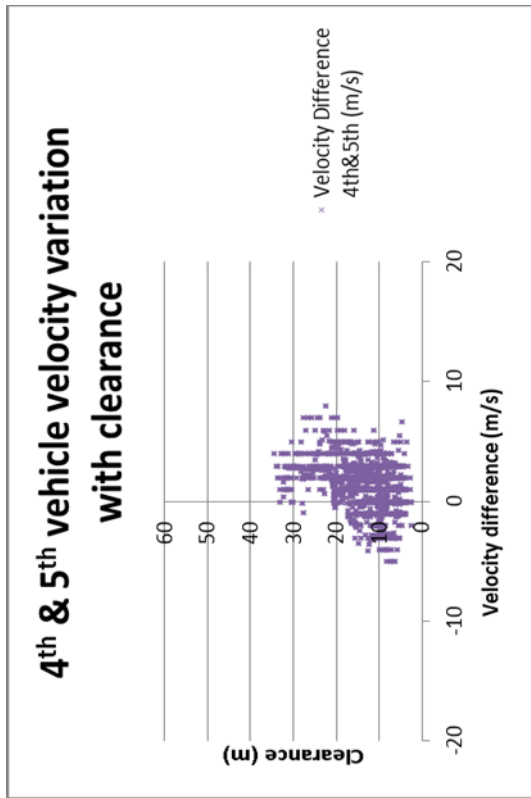




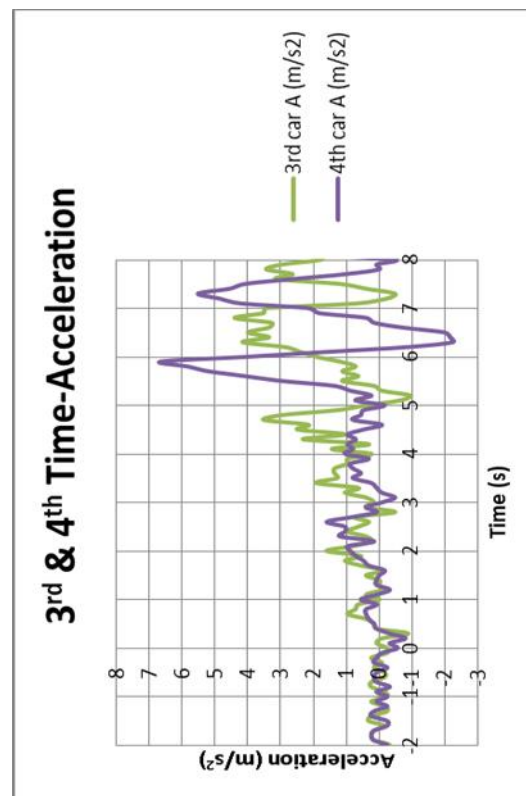
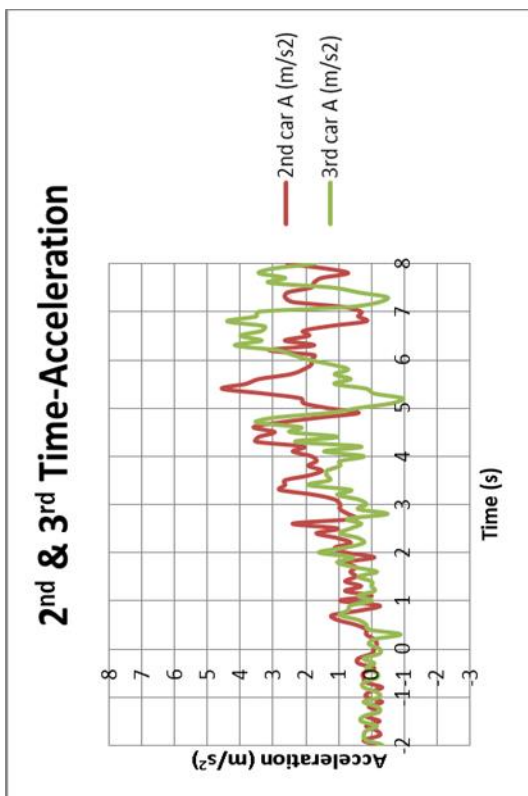
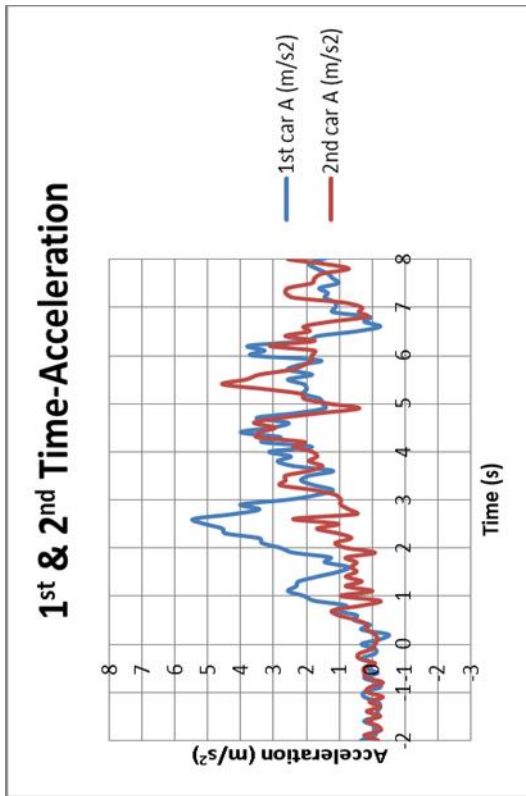
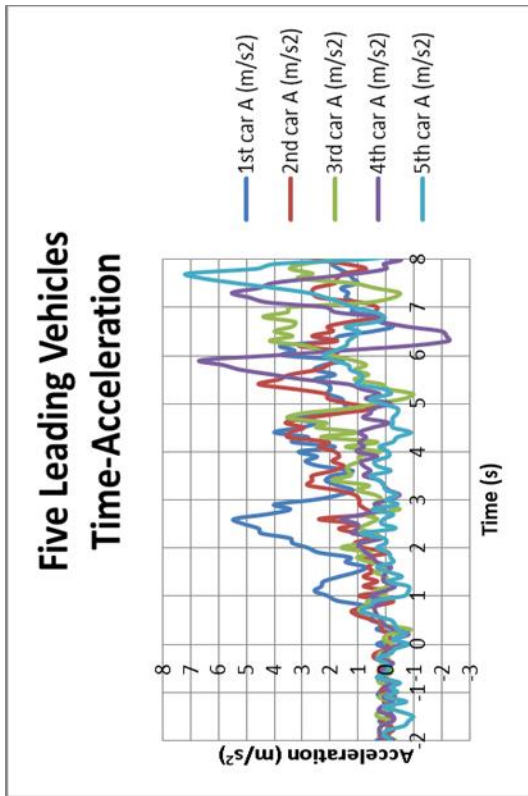
Appendix O: Peachtree data five leading vehicle velocity variation with clearance

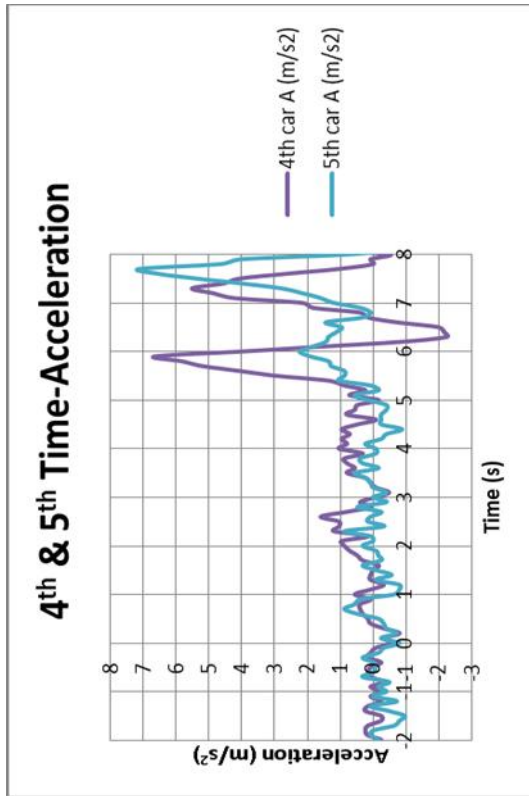




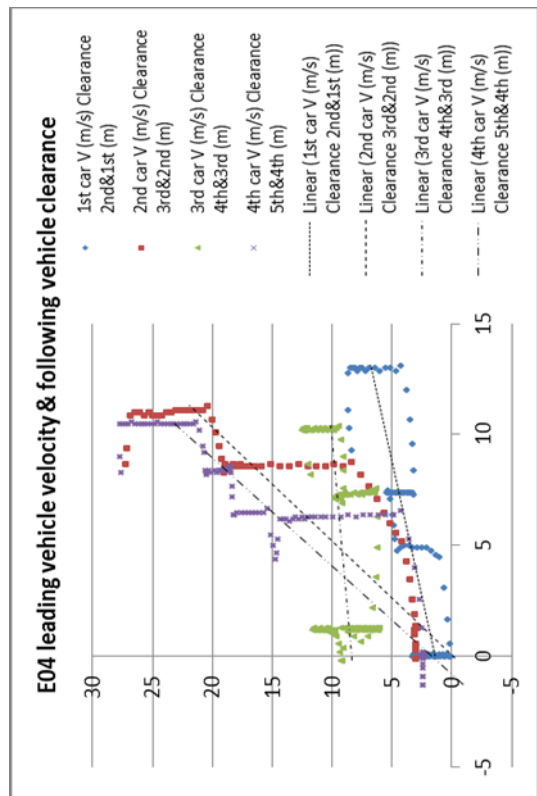
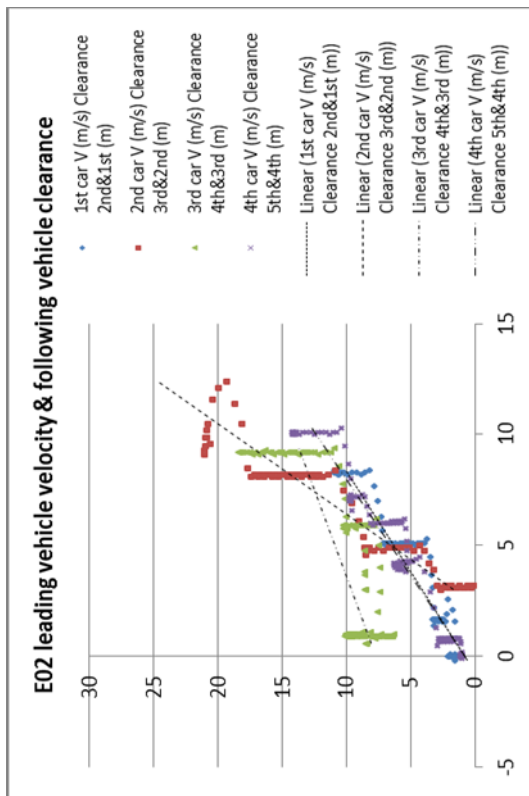


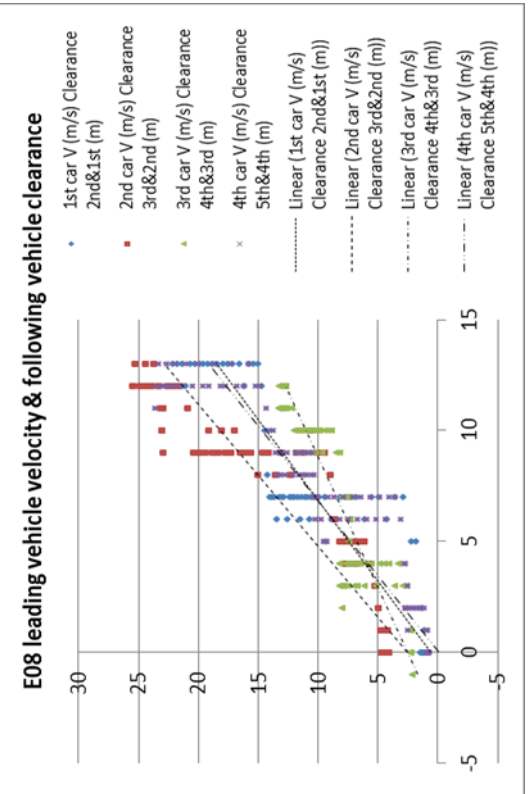
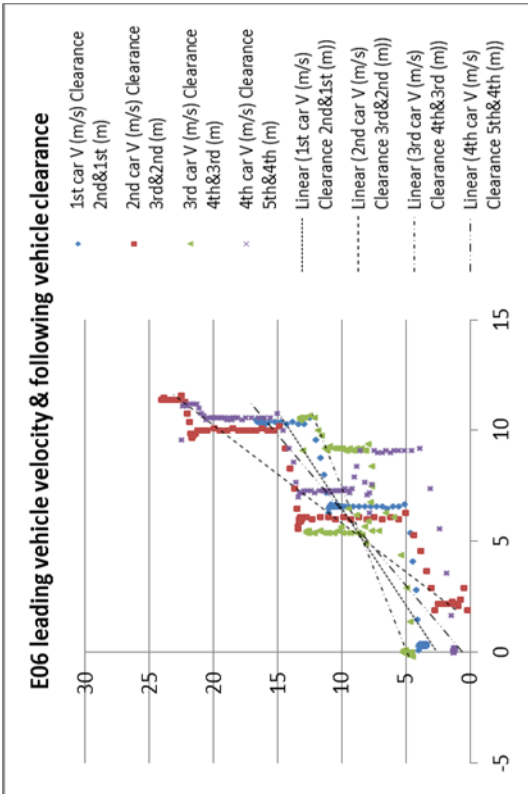
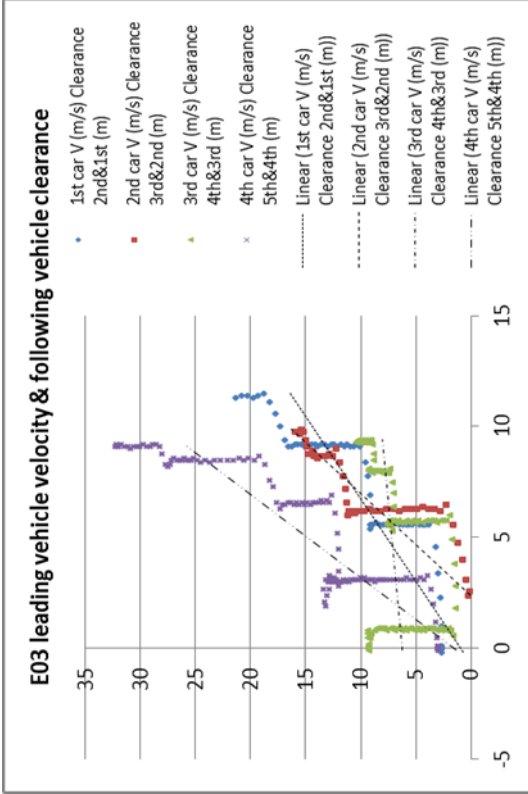
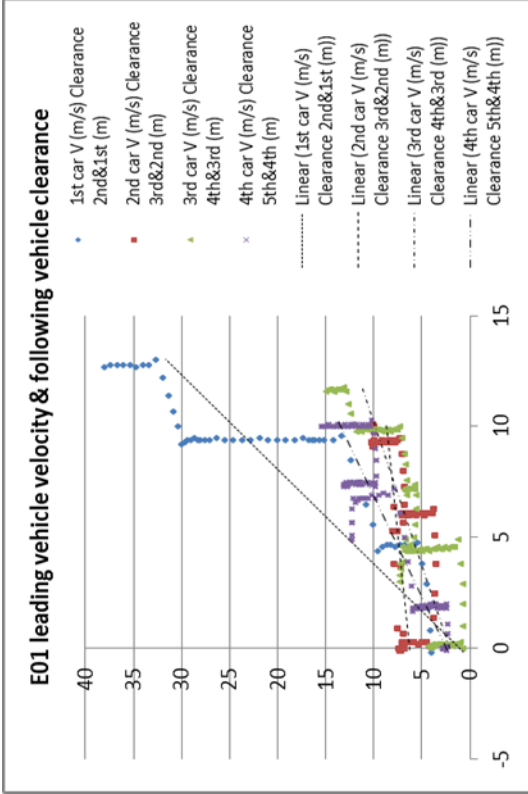
**Appendix P: Peachtree Data five leading vehicles's time & acceleration**

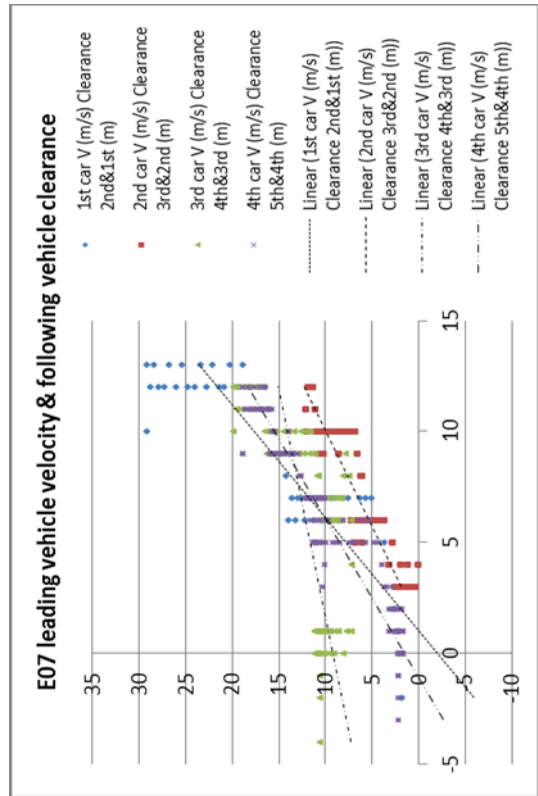
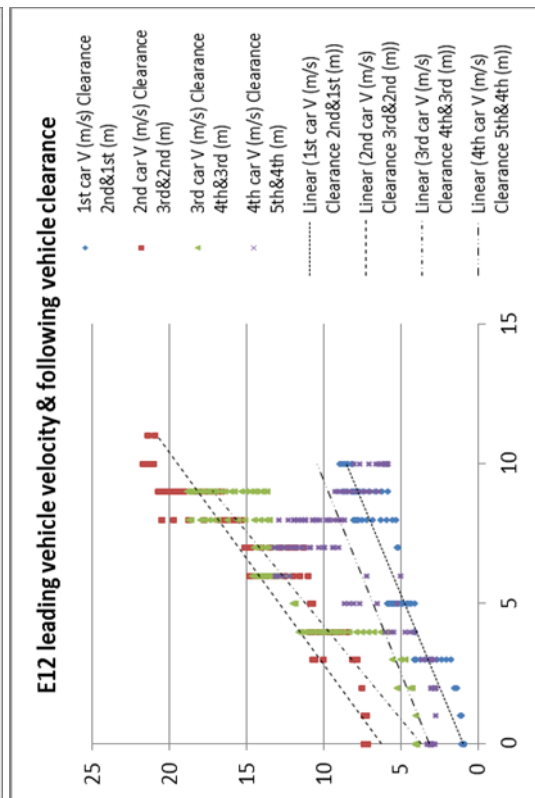
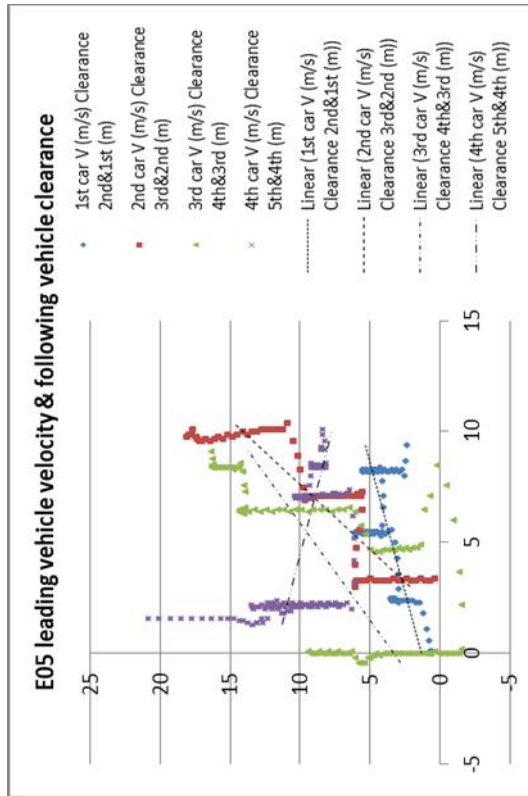
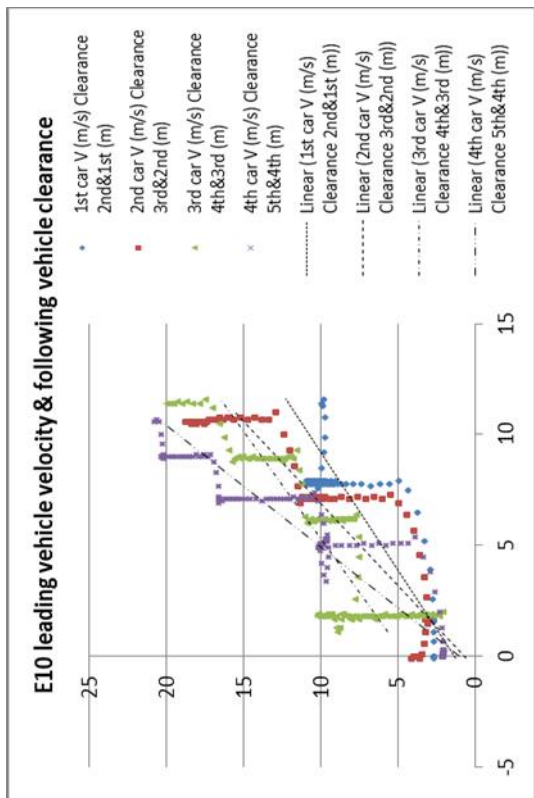


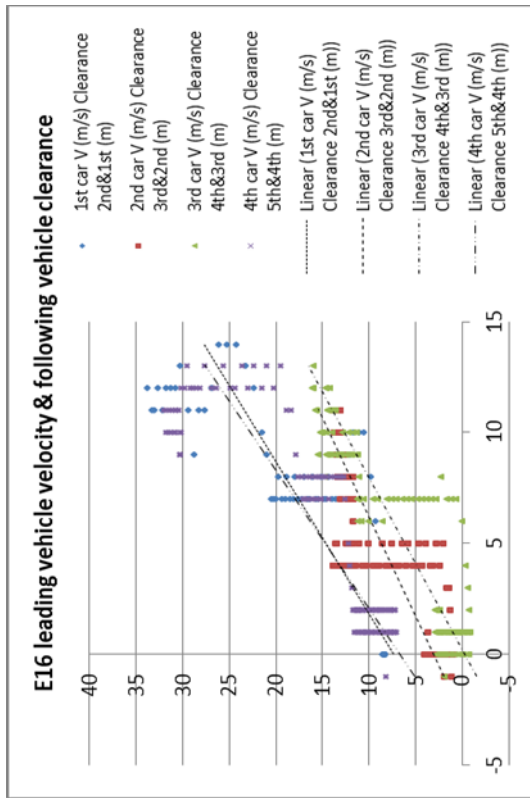
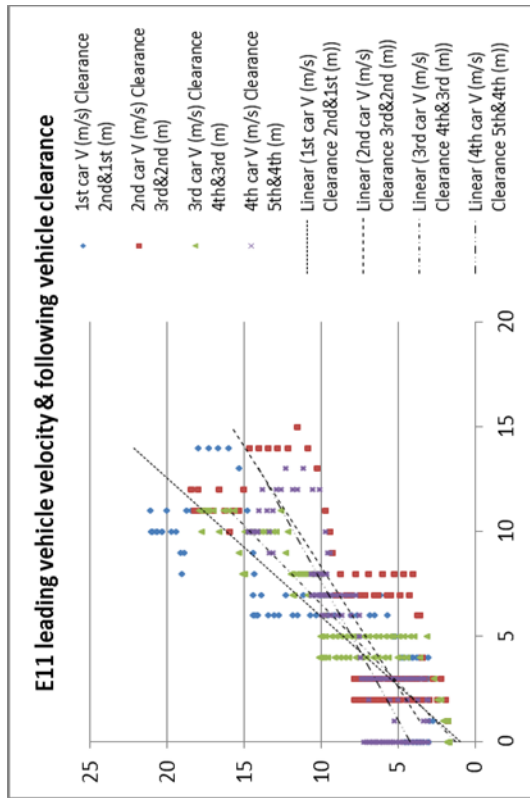
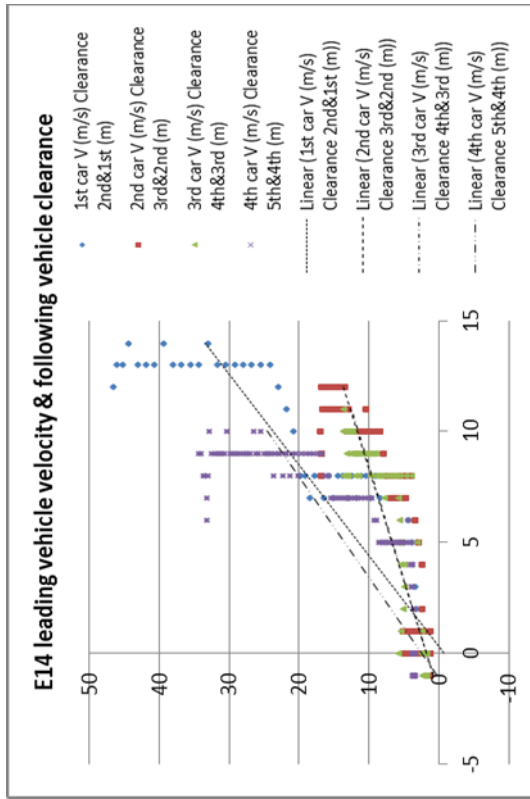
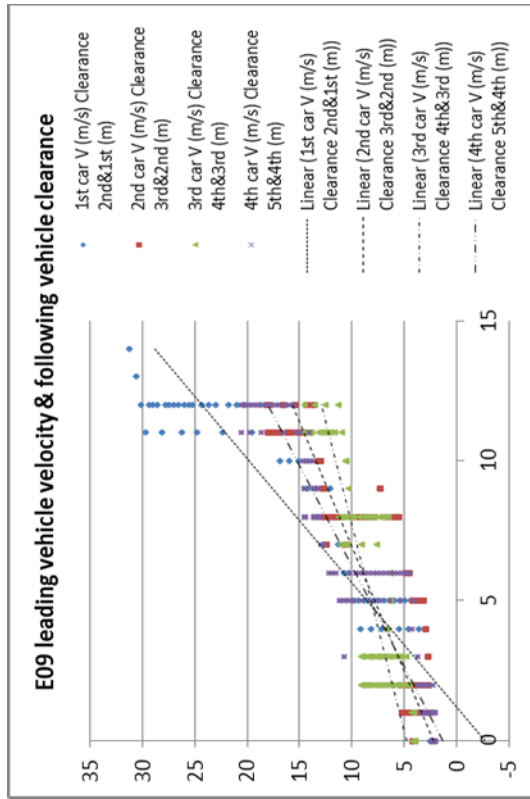


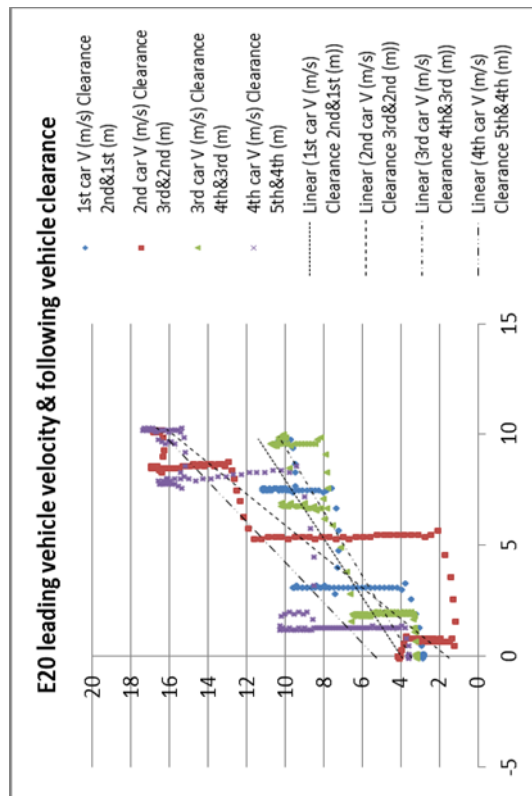
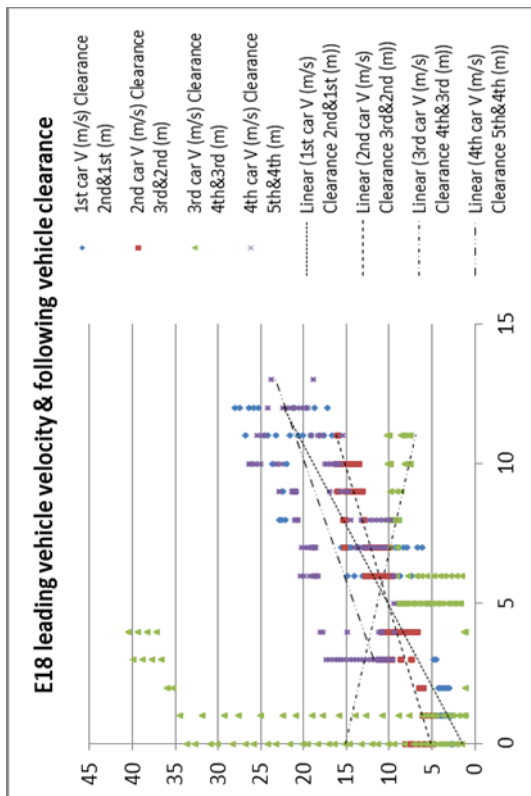
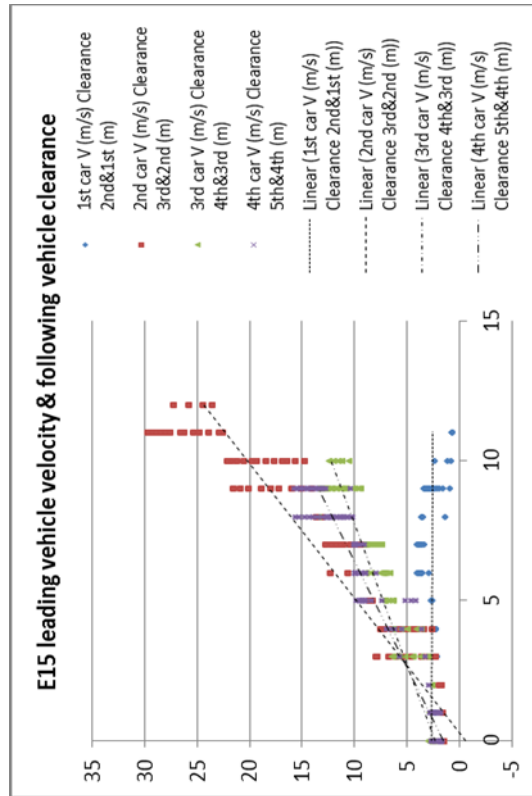
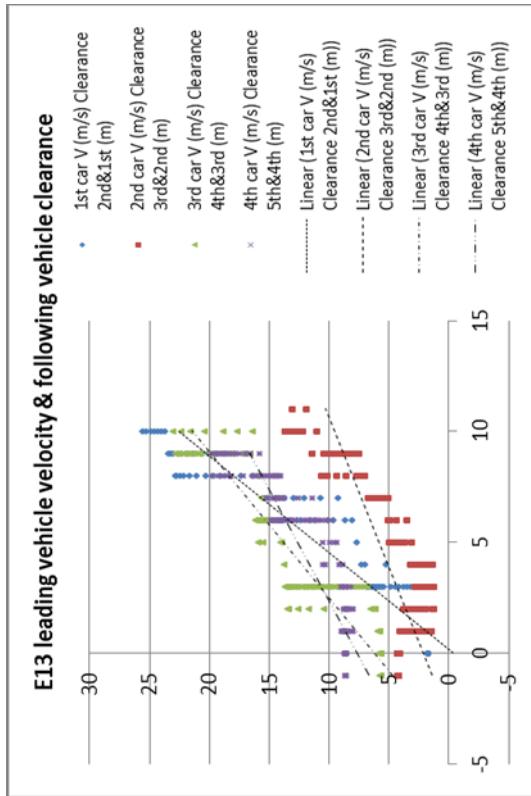
## Appendix Q: Peachtree Data each sample velocity & clearance

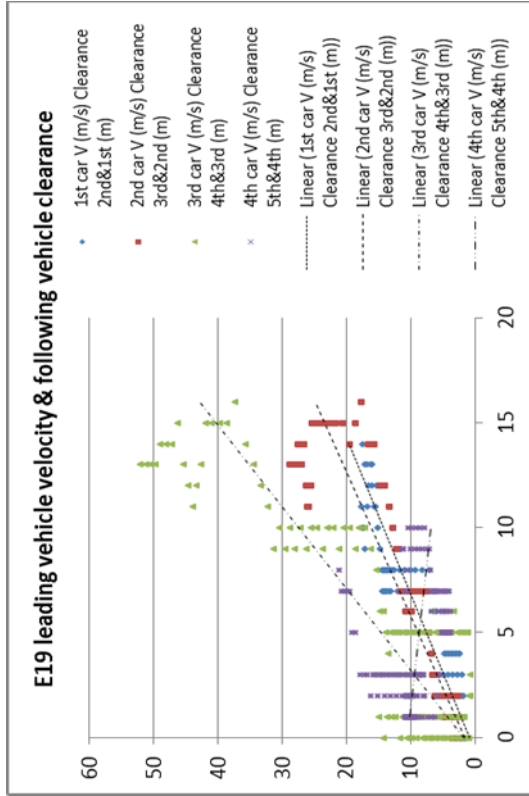
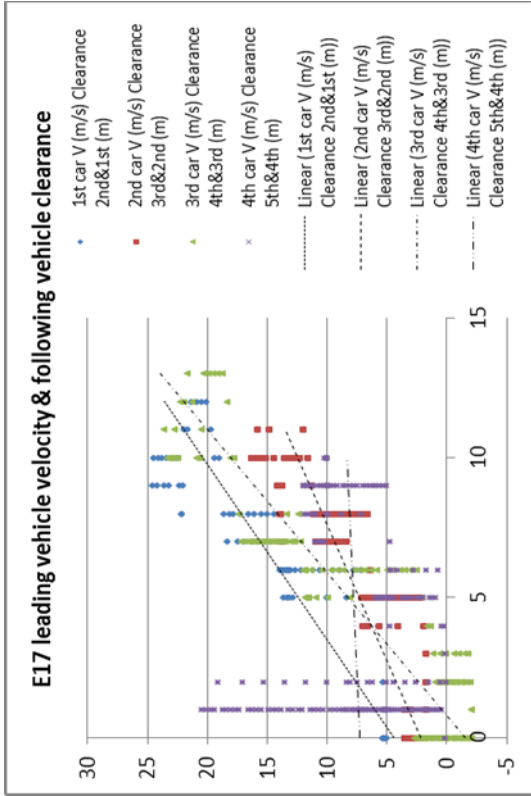
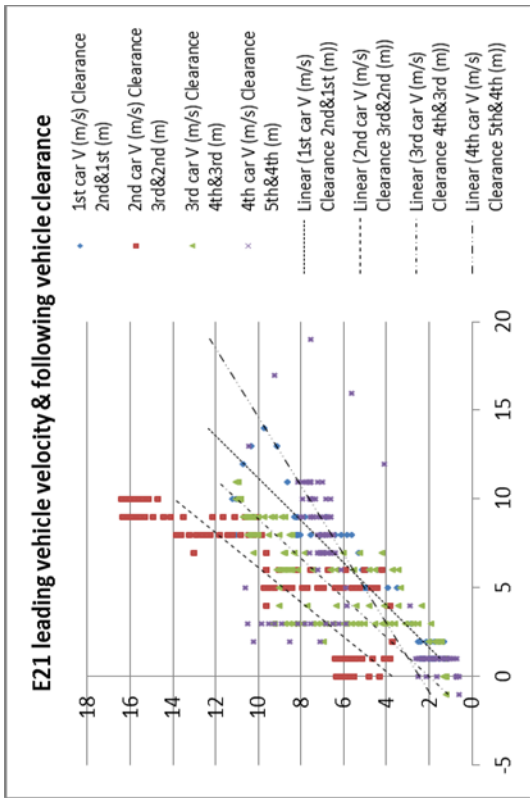






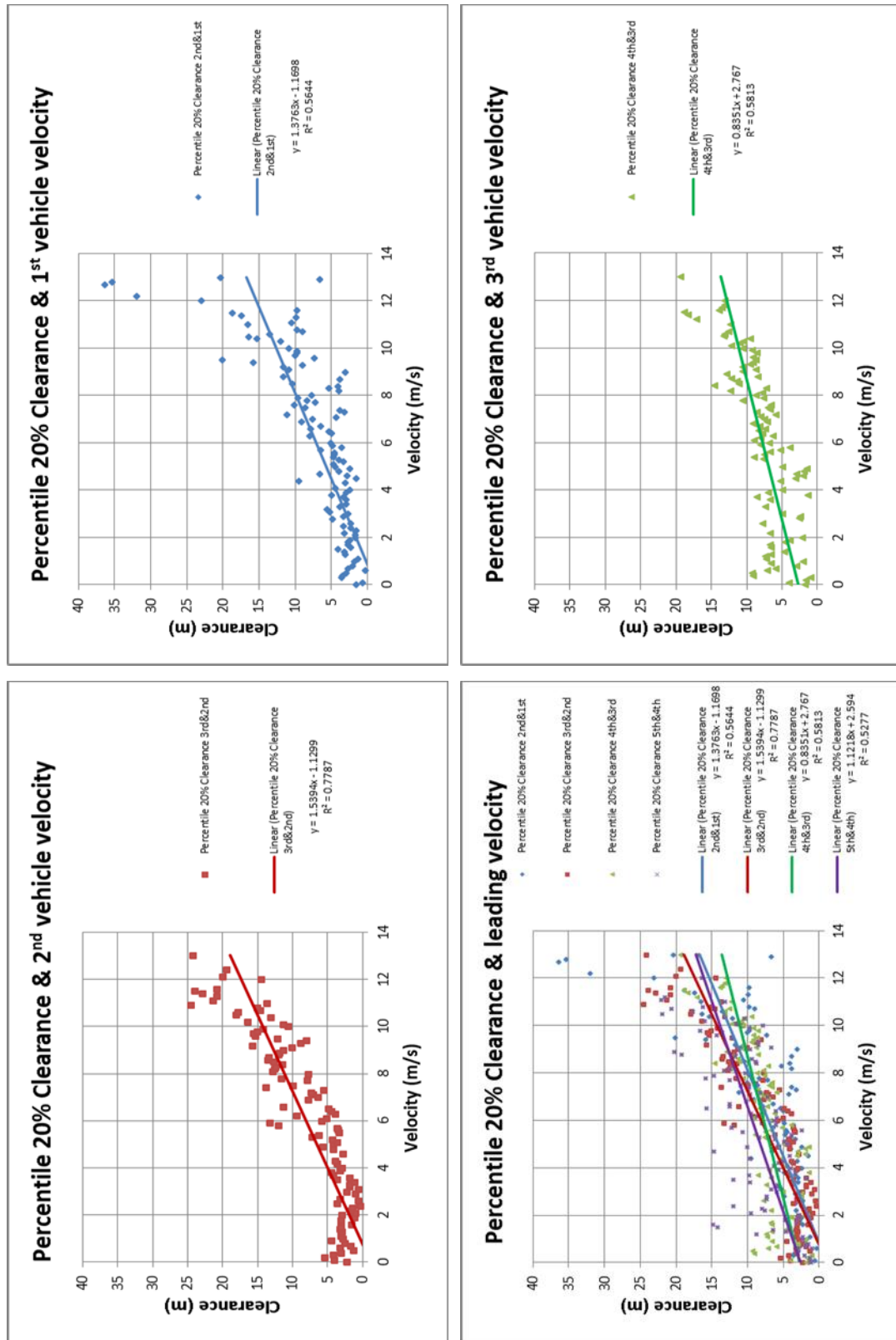


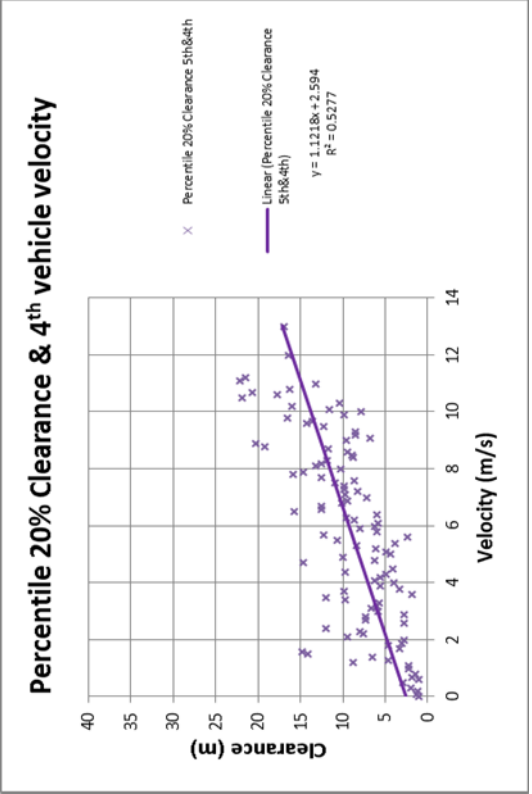
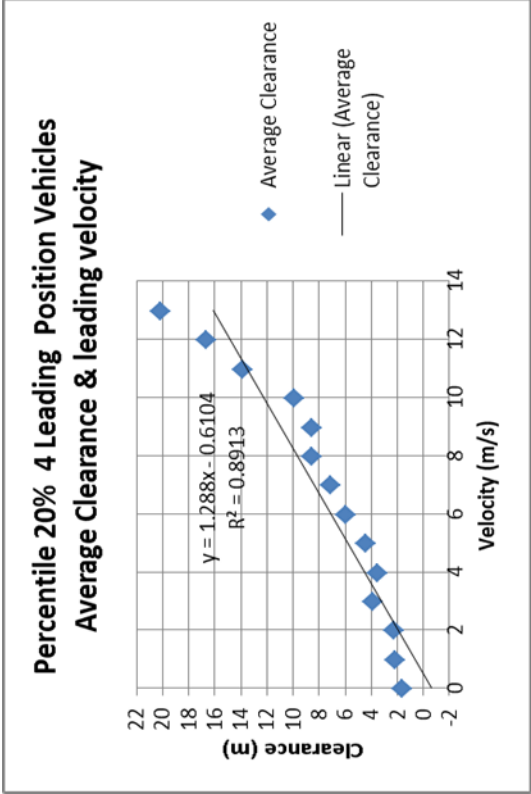




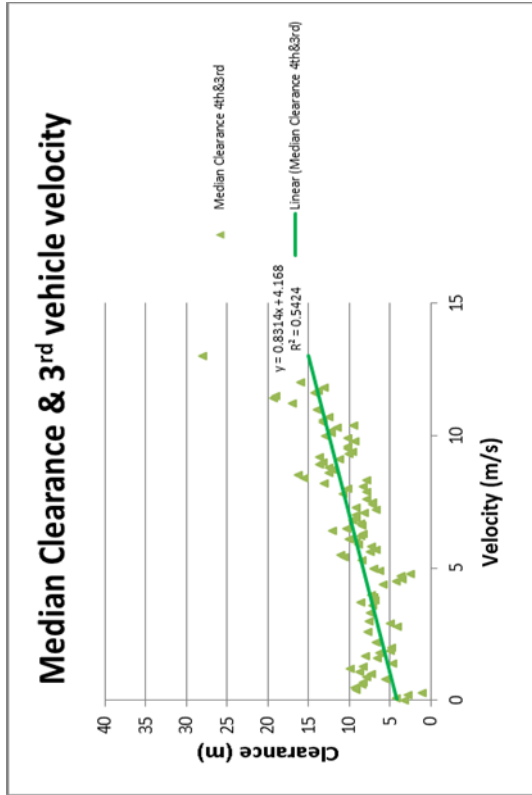
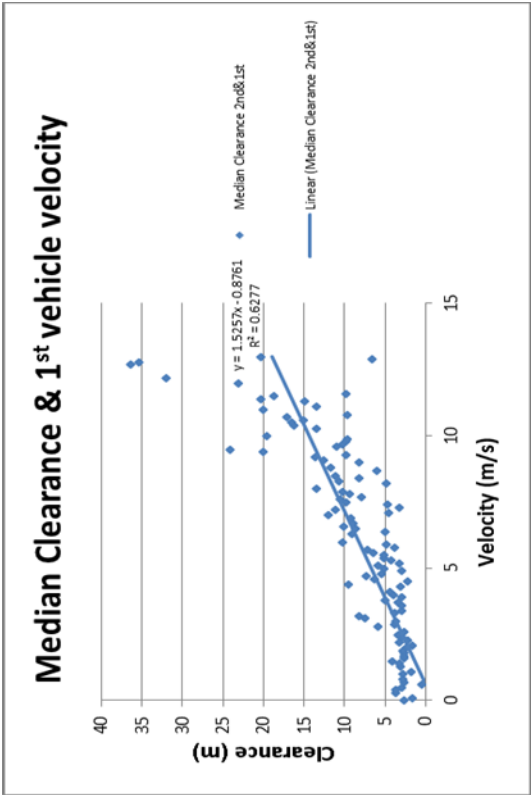


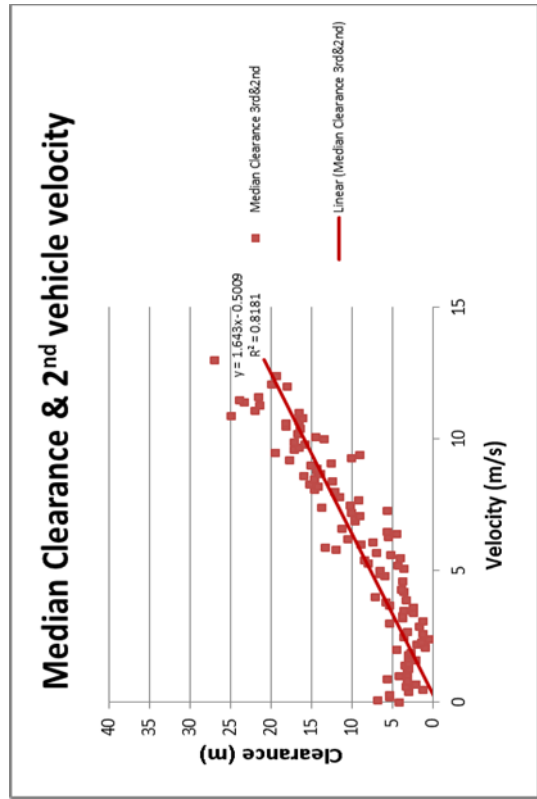
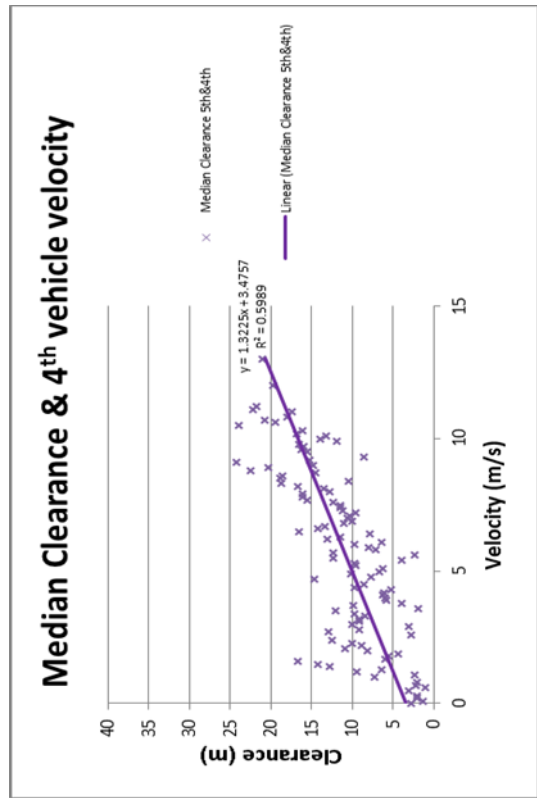
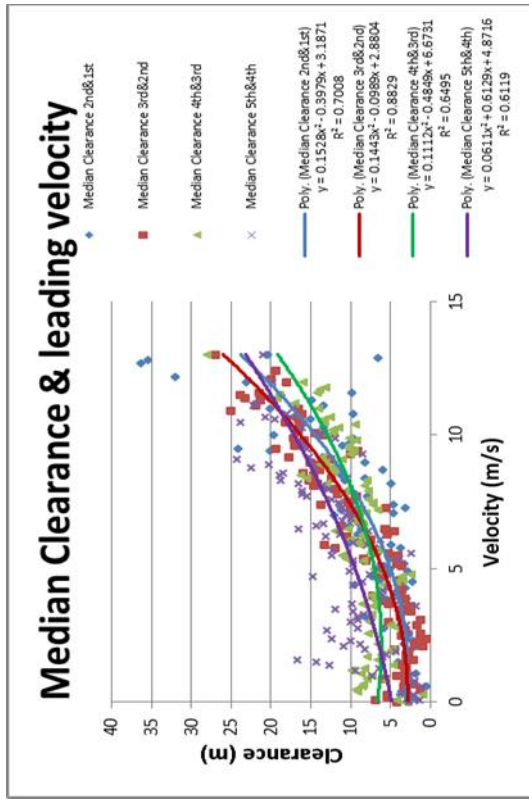
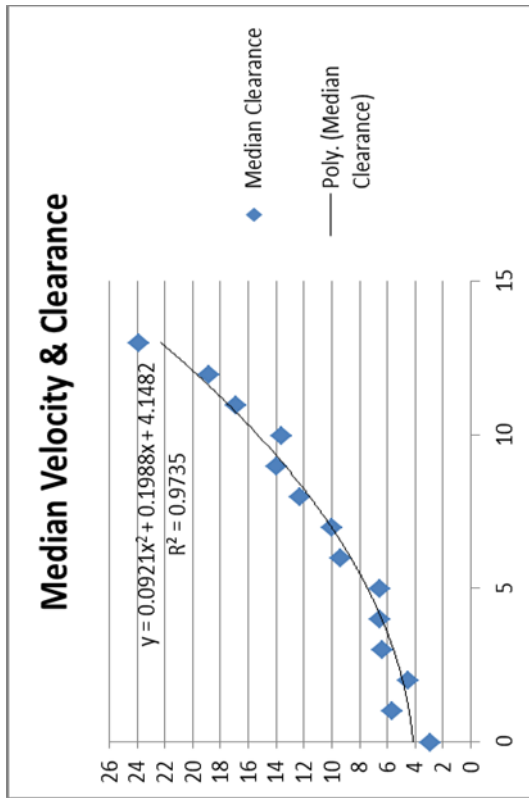
## Appendix R: Peachtree data 20 percentile safety distance



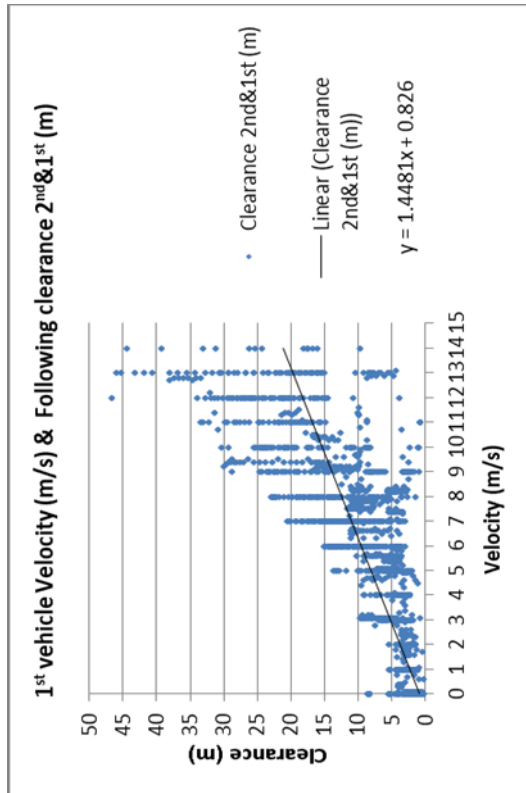
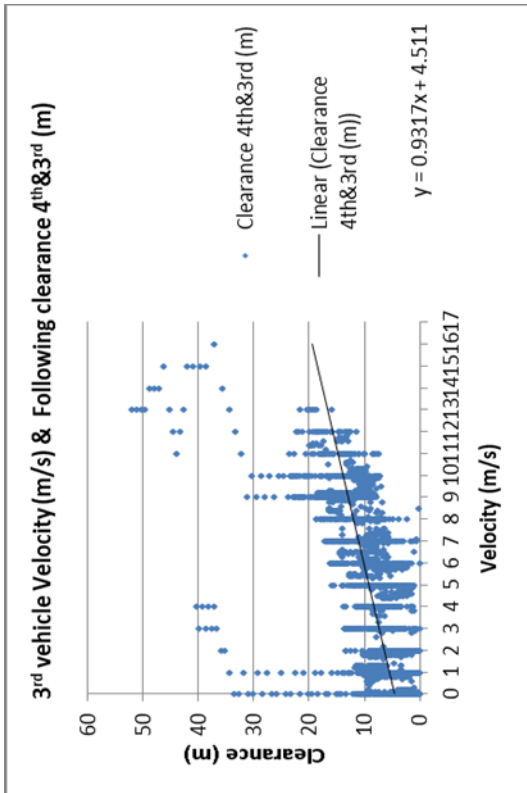
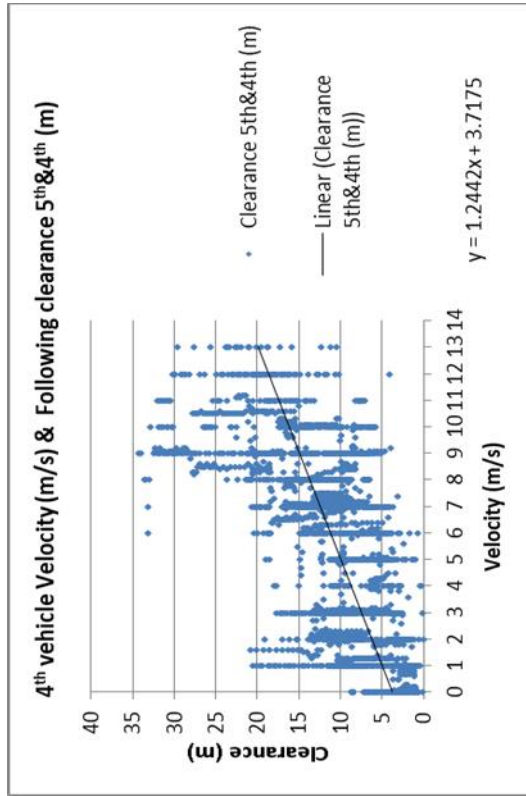
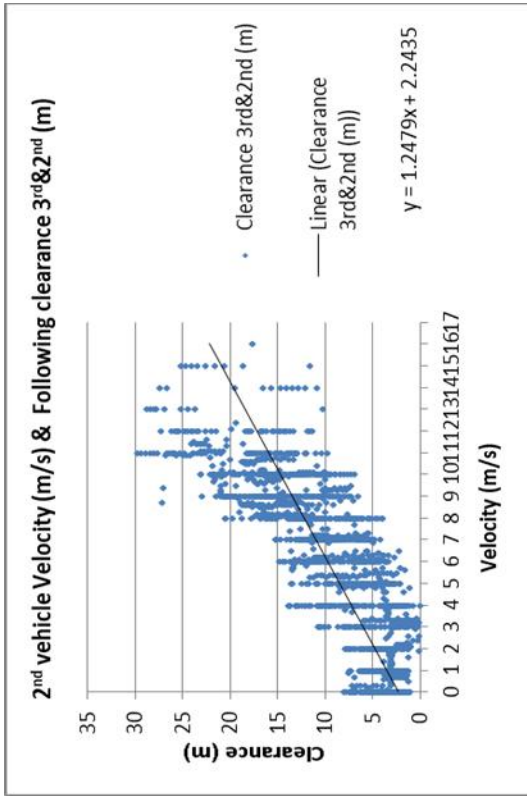


**Appendix S: Peachtree Data median safety distance**





**Appendix T: Peachtree Data average safety distance**



## Appendix U: Peachtree Data minimum safety distance

